PNNL-38071, Rev 0
EWG-RPT-045, Rev 0

Enhanced Hanford High-Aluminum Waste Glass Property Data Development

August 2025

RL Russell
V Gervasio
SM Baird
DL Bellofatto
DA Cutforth
JL George
JD Vienna

U.S. DEPARTMENT of ENERGY

Prepared for the U.S. Department of Energy
under Contract DE-AC05-76RL01830

DISCLAIMER

PACIFIC NORTHWEST NATIONAL LABORATORY
operated by
BATTELLE
for the
UNITED STATES DEPARTMENT OF ENERGY
under Contract DE-AC05-76RL01830

Printed in the United States of America

**Available to DOE and DOE contractors from
the Office of Scientific and Technical
Information,
P.O. Box 62, Oak Ridge, TN 37831-0062**
www.osti.gov
**ph: (865) 576-8401
fox: (865) 576-5728
email: reports@osti.gov**

**Available to the public from the National Technical Information Service
5301 Shawnee Rd., Alexandria, VA 22312
ph: (800) 553-NTIS (6847)
or (703) 605-6000
email: info@ntis.gov
Online ordering: http://www.ntis.gov**

PNNL-38071, Rev 0
EWG-RPT-045, Rev 0

Enhanced Hanford High-Aluminum Waste Glass Property Data Development

August 2025

RL Russell
V Gervasio
SM Baird
DL Bellofatto
DA Cutforth
JL George
JD Vienna

Prepared for
the U.S. Department of Energy
under Contract DE-AC05-76RL01830

Pacific Northwest National Laboratory
Richland, Washington 99354

Abstract

This study investigated the effects of aluminum concentration on simulated high-level waste glass properties to eventually establish an aluminum limit (as single-component or multiple-component constraints) for glass formulations for high-aluminum Hanford wastes. A test matrix of 25 high-aluminum glasses ($20 \leq Al_2O_3 \leq 28.57$ wt%) was generated, and the chemical compositions were measured. The following properties were measured: crystal formation after centerline canister cooling, crystallinity as a function of temperature, density, viscosity, electrical conductivity, toxic leaching characteristics using the Toxicity Characteristic Leaching Procedure, product consistency using the Product Consistency Test, and SO_3 solubility. These results are reported here.

Acknowledgments

The authors gratefully acknowledge the financial support provided by the U.S. Department of Energy Hanford Field Office, Waste Treatment and Immobilization Plant Project, with technical oversight by Albert Kruger. The following Pacific Northwest National Laboratory staff members are acknowledged for their contributions: Xiaonan Lu for technical review of the report, David MacPherson for quality assurance, Chrissy Charron and Cassie Martin for programmatic support during the work, Will Eaton for project management, and Matt Wilburn for his editorial support.

The authors thank Madison Hsieh of Savannah River National Laboratory for her help in the analysis and testing of the glasses.

Acronyms and Abbreviations

ARG-1	Analytical Reference Glass-1
CCC	canister centerline cooling (heat treatment)
CF	crystal fraction
DFHLW	Direct Feed High-Level Waste
DFLAW	Direct Feed Low-Activity Waste
DOE	U.S. Department of Energy
EC	electrical conductivity
EPA	U.S. Environmental Protection Agency
η_{1150}	viscosity at 1150 °C
HLW	high-level waste
IC	ion chromatography
ICP-OES	inductively coupled plasma – optical emissions spectroscopy
KH	potassium hydroxide digestion
LAW	low-activity waste
LM	lithium metaborate/tetraborate fusion
NIST	National Institute of Standards and Technology
NQAP	Nuclear Quality Assurance Program
PCT	Product Consistency Test
PF	sodium peroxide fusion
PNNL	Pacific Northwest National Laboratory
QA	quality assurance
RCRA	Resource Conservation and Recovery Act
rTCLP	normalized release of toxicity characteristic leaching procedure
SRNL	Savannah River National Laboratory
SSM	sulfur saturated melt
T_L	liquidus temperature
T_M	melting temperature
TCLP	Toxicity Characteristic Leaching Procedure
UTS	Universal Treatment Standards
VFT	Vogel-Fulcher-Tamman
WTP	Waste Treatment and Immobilization Plant
XRD	X-ray diffraction

Contents

Figures

Tables

1.0 Introduction

The U.S. Department of Energy (DOE) Hanford Field Office requested that Pacific Northwest National Laboratory (PNNL) provide expert evaluation and experimental work in support of the River Protection Project vitrification technology development (DOE 2012). The long-term objective of this work is to expand the Hanford Site waste glass database and property-composition models to cover the balance of the Hanford tank waste treatment and immobilization mission.

This report presents the glass compositions and glass property data developed in the Hanford high-aluminum waste glass property data development effort. When the data development effort for enhanced Hanford waste glasses is complete, enhanced waste glass property models will be developed. Section 1.1 summarizes the background of high-aluminum waste and glass. Section 1.2 summarizes the high-aluminum waste glass composition region and test matrix tested in this study. Section 1.3 documents the quality assurance (QA) program used in performing the work discussed in this report.

1.1 Background

To begin the treatment of the nuclear waste as soon as possible, the Hanford Field Office is considering implementing a sequenced approach for vitrification of low-activity waste (LAW) and high-level waste (HLW) at the Hanford Site. The sequenced approach is called Direct Feed Low-Activity Waste (DFLAW) and Direct Feed High-Level Waste (DFHLW). If brought into practice for DFHLW, the Pretreatment Facility at the Hanford Waste Treatment and Immobilization Plant (WTP) could be bypassed, meaning that the ultrafiltration and caustic leaching operations either would not be performed or would be replaced by an interim pretreatment function (Parsons 2023; Bergmann et al. 2022). This has an added benefit of significantly reducing the inventory of soda reporting to LAW (Goel et al. 2019).

However, the proposed changes in the processing of both LAW and HLW streams are likely to have impacts on the downstream vitrification operations. One potential major challenge during vitrification of DFHLW is high concentration of aluminum if the waste is not properly leached before sending it to the melter. However, simultaneous advances in glass waste loading of aluminum can avoid the need for caustic leaching of HLW.

According to the 2008 HLW feed vector reported by Vienna et al. (2013), many HLW compositions contain high concentrations of Al_2O_3. The Al_2O_3 fraction is projected to range from roughly 10 to 70 mass% on a calcined oxide basis after caustic leaching and even more without caustic leaching. The efficiency of WTP operation will be strongly influenced by the loading of high Al_2O_3 wastes in HLW glass and the chemical form of Al that impacts the melter processing rate.

A major effort is underway to optimize waste loading in glass. The focus of this effort is increasing the loading of high-Al_2O_3 HLW in glass. Increasing the loading of high-aluminum wastes in glass may shorten the tank waste treatment mission and/or reduce or eliminate the need for caustic leaching of the waste. However, waste glasses with high concentrations of Al_2O_3 are prone to nepheline ($NaAlSiO_4$) precipitation upon slow cooling (Vienna et al. 2017; Kroll et al. 2019; Lu et al. 2021). If nepheline forms upon cooling, it will likely reduce the durability of the resulting glass by removing three moles of glass formers (1 mole of Al_2O_3 and 2 moles of SiO_2) for every mole of Na_2O (Vienna et al. 2017; Kim et al. 1995). Nepheline formation will also make it difficult to predict the Product Consistency Test (PCT) response (ASTM C1285), which must be controlled and reported for HLW canisters to be qualified for disposal (DOE 1996). For high-Al_2O_3 glasses to be approved for disposal, nepheline formation must be avoided, or the amount formed and its impact on glass durability predicted. Being able to predict the amount of nepheline formed and the PCT response would provide a basis for specifying a constraint to avoid HLW glass compositions that would yield unacceptable PCT and Toxicity Characteristic Leaching Procedure (TCLP) responses.

1.2 Waste Glass Composition Region and Test Matrix

This section discusses the development of the experimental glass composition region and test matrix for the high-aluminum concentration waste glasses that were tested.

Glass formulation calculations were performed using the existing glass property models given in Vienna et al. (2016) for spinel liquidus temperature (T_L) and viscosity at 1150 °C (η_{1150}) and in Piepel et al. (2008) for PCT responses. Table 1.1 summarizes the lower and upper bounds of component concentrations in the glasses resulting from the glass formulation efforts. The components listed in Table 1.1 include those that are high in waste and/or are expected to limit the waste loading in glass (Al_2O_3, F, K_2O, Na_2O, ZnO, ZrO_2, and others) and the glass forming additive components (B_2O_3, CaO, Li_2O, and SiO_2).

Table 1.1. Lower and Upper Bound of Component Concentrations (wt%) in the High-Aluminum Waste Glasses

Component	Variable	Wt% in “others”	Lower Bound (wt%)	Upper Bound (wt%)
Al_2O_3	Y	--	20	30
B_2O_3	Y	--	8	22
Bi_2O_3	In Others	8.60	0.08	0.75
CaO	In Others	17.19	0.17	1.50
CdO	In Others	1.72	0.02	0.15
Cr_2O_3	Y	--	0	2
F	In Others	9.87	0.10	0.86
Fe_2O_3	Y	--	0	12
K_2O	In Others	25.26	0.24	2.2
Li_2O	Y	--	0	6
MgO	In Others	8.60	0.08	0.75
MnO	In Others	1.05	0.01	0.09
Na_2O	Y	--	5	20
NiO	In Others	13.76	0.13	1.2
P_2O_5	Y	--	0	4.5
SiO_2	Y	--	22	40.6
SO_3	In Others	5.85	0.06	0.51
SrO	In Others	1.77	0.02	0.15
TiO_2	In Others	3.44	0.03	0.30
ZnO	In Others	2.91	0.03	0.25
ZrO_2	Y	--	0	6

A space-filling technique was used with JMP version 13.0 (SAS Institute Inc.) software to generate a test matrix of 23 glasses with one repeat (HAlG-25 is a repeat of HAlG-08) and one centroid glass (HAlG-24) for a total of 25 glasses. This experimental design was chosen to spread the selected components as evenly as possible throughout the Hanford high-aluminum waste composition region. Table 1.2 lists the 25 high-aluminum waste glasses comprising the test matrix.

This report summarizes the experimental methods used to fabricate, heat treat, and test the 25-glass high-aluminum waste test matrix prepared at PNNL. Measured properties related to glass performance and processing are described in this report and are provided in appendices.

Table 1.2. Targeted Compositions (mass fractions) for the High-Aluminum Waste Glasses

Component	Glass ID									
	HAlG-01	HAlG-02	HAlG-03	HAlG-04	HAlG-05	HAlG-06	HAlG-07	HAlG-08	HAlG-09	HAlG-10
Ag_2O	0.0000	0.0000	0.0000	0.0000	0.0000	0.0000	0.0000	0.0000	0.0000	0.0000
Al_2O_3	0.2024	0.2389	0.2011	0.2067	0.2004	0.2786	0.2373	0.2433	0.2112	0.2017
B_2O_3	0.0950	0.1974	0.1572	0.1021	0.2120	0.1958	0.1133	0.1482	0.2179	0.1766
Bi_2O_3	0.0071	0.0014	0.0021	0.0062	0.0043	0.0018	0.0060	0.0010	0.0016	0.0012
CaO	0.0143	0.0029	0.0043	0.0124	0.0086	0.0037	0.0119	0.0019	0.0031	0.0024
CdO	0.0014	0.0003	0.0004	0.0012	0.0009	0.0004	0.0012	0.0002	0.0003	0.0002
Cr_2O_3	0.0002	0.0160	0.0017	0.0113	0.0066	0.0119	0.0007	0.0065	0.0106	0.0188
F	0.0082	0.0016	0.0024	0.0071	0.0049	0.0021	0.0069	0.0011	0.0018	0.0014
Fe_2O_3	0.0136	0.0478	0.0569	0.0689	0.1109	0.0147	0.0908	0.1065	0.0481	0.0749
K_2O	0.0210	0.0042	0.0063	0.0182	0.0126	0.0054	0.0175	0.0028	0.0046	0.0035
Li_2O	0.0050	0.0107	0.0093	0.0038	0.0045	0.0032	0.0018	0.0180	0.0562	0.0494
MgO	0.0071	0.0014	0.0021	0.0062	0.0043	0.0018	0.0060	0.0010	0.0016	0.0012
MnO	0.0009	0.0002	0.0003	0.0008	0.0005	0.0002	0.0007	0.0001	0.0002	0.0002
Na_2O	0.1999	0.1922	0.1675	0.1952	0.1572	0.1966	0.1984	0.1748	0.1362	0.1544
NiO	0.0114	0.0023	0.0034	0.0099	0.0069	0.0029	0.0095	0.0015	0.0025	0.0019
P_2O_5	0.0421	0.0371	0.0337	0.0037	0.0078	0.0232	0.0210	0.0436	0.0136	0.0408
PbO	0.0000	0.0000	0.0000	0.0000	0.0000	0.0000	0.0000	0.0000	0.0000	0.0000
RuO_2	0.0000	0.0000	0.0000	0.0000	0.0000	0.0000	0.0000	0.0000	0.0000	0.0000
SiO_2	0.3147	0.2227	0.3277	0.3300	0.2202	0.2523	0.2484	0.2476	0.2322	0.2265
SO_3	0.0049	0.0010	0.0015	0.0042	0.0029	0.0012	0.0041	0.0007	0.0011	0.0008
SrO	0.0015	0.0003	0.0004	0.0013	0.0009	0.0004	0.0012	0.0002	0.0003	0.0003
TiO_2	0.0029	0.0006	0.0009	0.0025	0.0017	0.0007	0.0024	0.0004	0.0006	0.0005
ZnO	0.0024	0.0005	0.0007	0.0021	0.0015	0.0006	0.0020	0.0003	0.0005	0.0004
ZrO_2	0.0441	0.0207	0.0202	0.0060	0.0306	0.0025	0.0190	0.0004	0.0560	0.0431
Total	1.00000	1.00000	1.00000	1.00000	1.00000	1.00000	1.00000	1.00000	1.00000	1.00000

Table 1.2. (cont.)

Component	Glass ID									
	HAlG-11	HAlG-12	HAlG-13	HAlG-14	HAlG-15	HAlG-16	HAlG-17	HAlG-18	HAlG-19	HAlG-20
Ag_2O	0.0000	0.0000	0.0000	0.0000	0.0000	0.0000	0.0000	0.0000	0.0000	0.0000
Al_2O_3	0.2452	0.2107	0.2042	0.2289	0.2243	0.2159	0.2062	0.2857	0.2763	0.2092
B_2O_3	0.0884	0.1613	0.0824	0.1677	0.0865	0.1039	0.1313	0.1116	0.0802	0.2002
Bi_2O_3	0.0032	0.0046	0.0057	0.0009	0.0030	0.0022	0.0031	0.0037	0.0014	0.0022
CaO	0.0063	0.0091	0.0115	0.0017	0.0060	0.0045	0.0061	0.0073	0.0027	0.0043
CdO	0.0006	0.0009	0.0012	0.0002	0.0006	0.0005	0.0006	0.0007	0.0003	0.0004
Cr_2O_3	0.0181	0.0165	0.0025	0.0176	0.0195	0.0200	0.0013	0.0075	0.0085	0.0127
F	0.0036	0.0052	0.0066	0.0010	0.0034	0.0026	0.0035	0.0042	0.0016	0.0025
Fe_2O_3	0.0173	0.0017	0.0861	0.0998	0.0129	0.0421	0.0076	0.0052	0.0614	0.0074
K_2O	0.0093	0.0134	0.0169	0.0026	0.0087	0.0065	0.0090	0.0108	0.0040	0.0064
Li_2O	0.0459	0.0071	0.0481	0.0534	0.0593	0.0254	0.0263	0.0587	0.0550	0.0353
MgO	0.0032	0.0046	0.0057	0.0009	0.0030	0.0022	0.0031	0.0037	0.0014	0.0022
MnO	0.0004	0.0006	0.0007	0.0001	0.0004	0.0003	0.0004	0.0005	0.0002	0.0003
Na_2O	0.1994	0.1936	0.1685	0.1863	0.1489	0.1904	0.1752	0.1873	0.1979	0.1414
NiO	0.0051	0.0073	0.0092	0.0014	0.0048	0.0036	0.0049	0.0059	0.0022	0.0035
P_2O_5	0.0370	0.0106	0.0064	0.0080	0.0018	0.0221	0.0105	0.0397	0.0169	0.0448
PbO	0.0000	0.0000	0.0000	0.0000	0.0000	0.0000	0.0000	0.0000	0.0000	0.0000
RuO_2	0.0000	0.0000	0.0000	0.0000	0.0000	0.0000	0.0000	0.0000	0.0000	0.0000
SiO_2	0.2578	0.2859	0.2813	0.2223	0.4015	0.3050	0.3648	0.2287	0.2612	0.2926
SO_3	0.0022	0.0031	0.0039	0.0006	0.0020	0.0015	0.0021	0.0025	0.0009	0.0015
SrO	0.0007	0.0009	0.0012	0.0002	0.0006	0.0005	0.0006	0.0008	0.0003	0.0004
TiO_2	0.0013	0.0018	0.0023	0.0004	0.0012	0.0009	0.0012	0.0015	0.0005	0.0009
ZnO	0.0011	0.0015	0.0019	0.0003	0.0010	0.0008	0.0010	0.0012	0.0005	0.0007
ZrO_2	0.0543	0.0596	0.0537	0.0061	0.0110	0.0493	0.0413	0.0331	0.0269	0.0313
Total	1.00000	1.00000	1.00000	1.00000	1.00000	1.00000	1.00000	1.00000	1.00000	1.00000

Table 1.2. (cont.)

Component	Glass ID				
	HAlG-21	HAlG-22	HAlG-23	HAlG-24	HAlG-25
Ag_2O	0.0000	0.0000	0.0000	0.0002	0.0000
Al_2O_3	0.2274	0.2065	0.2090	0.2200	0.2433
B_2O_3	0.1178	0.0929	0.1749	0.1550	0.1482
Bi_2O_3	0.0047	0.0068	0.0040	0.0100	0.0010
CaO	0.0093	0.0135	0.0080	0.0350	0.0019
CdO	0.0009	0.0014	0.0008	0.0010	0.0002
Cr_2O_3	0.0045	0.0172	0.0088	0.0075	0.0065
F	0.0054	0.0078	0.0046	0.0030	0.0011
Fe_2O_3	0.0815	0.0118	0.0019	0.0550	0.1065
K_2O	0.0137	0.0198	0.0118	0.0070	0.0028
Li_2O	0.0464	0.0432	0.0573	0.0300	0.0180
MgO	0.0047	0.0068	0.0040	0.0100	0.0010
MnO	0.0006	0.0008	0.0005	0.0100	0.0001
Na_2O	0.1586	0.1316	0.1108	0.1150	0.1748
NiO	0.0075	0.0108	0.0064	0.0040	0.0015
P_2O_5	0.0430	0.0258	0.0342	0.0100	0.0436
PbO	0.0000	0.0000	0.0000	0.0030	0.0000
RuO_2	0.0000	0.0000	0.0000	0.0001	0.0000
SiO_2	0.2548	0.3712	0.3354	0.3150	0.2476
SO_3	0.0032	0.0046	0.0027	0.0030	0.0007
SrO	0.0010	0.0014	0.0008	0.0012	0.0002
TiO_2	0.0019	0.0027	0.0016	0.0000	0.0004
ZnO	0.0016	0.0023	0.0014	0.0000	0.0003
ZrO_2	0.0118	0.0213	0.0210	0.0100	0.0004
Total	1.00000	1.00000	1.00000	1.00000	1.00000

1.3 Quality Assurance

This work was performed in accordance with the PNNL Nuclear Quality Assurance Program (NQAP). The NQAP complies with the DOE Order 414.1D, *Quality Assurance*, and 10 CFR 830 Subpart A, *Quality Assurance Requirements*. The NQAP uses NQA-1-2012, *Quality Assurance Requirements for Nuclear Facility Application,* as its consensus standard and NQA-1-2012, Subpart 4.2.1, as the basis for its graded approach to quality.

The NQAP works in conjunction with PNNL's laboratory-level Quality Management Program, which is based on the requirements as defined in DOE Order 414.1D and 10 CFR 830, Subpart A, *Quality Assurance Requirements*.

The work described in this report was performed to QA technology readiness level 4. This work was performed to support technology development. Data obtained may be used to support nuclear facility design input. Work and deliverables will comply with the PNNL NQAP for this grading level and any additional controls.

2.0 Test Methods

This section describes how the data were obtained for the 25 high-aluminum waste glasses described in Section 1.0. The descriptions include the methods for (1) glass fabrication, (2) chemical composition analysis, (3) density determination, (4) secondary phase identification from samples following canister centerline cooling (CCC), (5) viscosity measurement, (6) electrical conductivity (EC) measurement, (7) isothermal crystal fraction (CF), (8) PCT response, (9) TCLP response, and (10) sulfate solubility measurement for these matrix glasses.

2.1 Glass Fabrication

Glass fabrication was performed according to the PNNL procedure *Glass Batching and Melting* (WFDL-GBM-1, Rev 2).[1] Single metal oxides, single metal carbonates, boric acid, and sodium salts were weighed out in the appropriate masses to form the target glass composition for each glass and then placed in a plastic bag. After thorough mixing in the plastic bag for at least 30 s until uniform color developed, the powders were transferred into an agate milling chamber and milled for 2 min in the Angstrom vibratory mill. The powders were then transferred to a clean Pt-10%Rh (hereafter referred to as Pt-alloy) crucible for melting using a two-step melt process. The first melt was of the raw materials after mechanically mixing in an agate milling chamber. Initial melting was performed at a temperature of 1150 °C for 1 h for the compositions to melt and form glasses. After the first melt was air-quenched on a stainless-steel pouring plate, the glass was observed under an optical microscope to check for undissolved particles and/or salts. The glass was then ground for 5 min in a tungsten carbide vibratory mill (AngstromTE110) and turned into a fine powder.

A second melt of the glass for 1 h was performed at various temperatures based on observations for the first melt glass. Some glasses required three or four melts. The details of these melts are presented in Table 2.1. If more than two melts were required, the glass was again ground for 5 min in a tungsten carbide vibratory mill and turned into a fine powder before melting.

Most of the glasses were opaque and ranged in appearance from brown with swirls to green with crystals. The morphology and color of each quenched glass is shown in Appendix A. Because of this, these glasses were analyzed by X-ray diffraction (XRD) (as described in Section 2.4) to determine the phases present, and the results are shown in Appendix B. Two of the glasses were not analyzed as they melted as expected and appeared amorphous. Only one of the analyzed glasses was amorphous, with 22 showing crystals as presented in Table 2.2. However, this amorphous glass (HAlG-03) required four melts and an increase in temperature to 1250 °C to obtain a complete melt. Amorphous glass wasn't achievable in these compositions because spinel was primarily forming, which has a very high melting temperature (> 2000 °C).

Glass HAlG-10 formed ~2.8 wt% chromium-containing spinel and would not melt into a glass (Appendix A, Figure A.10). Therefore, this glass was not tested beyond this.

[1] Russell, RL. 2016. *Glass Batching and Melting.* WFDL-GBM-1, Rev. 2.

Table 2.1. Melting Temperatures and Times Used in Fabricating the 25 HAlG Glasses in the High Aluminum Study

	First Melt			Second Melt			Third and More Melts		
Glass ID	Date	Temp. (°C)	Time (h)	Date	Temp. (°C)	Time (h)	Date	Temp. (°C)	Time (h)
HAlG-01	11/9/21	1150	1	11/10/21	1250	1	11/10/21	1250	1
HAlG-02	11/11/21	1150	1	11/15/21	1150	1	11/15/21	1250	1
HAlG-03	11/16/21	1150	1	11/17/21	1150	1	11/18/21 11/19/21	1200 1250	1 1
HAlG-04	12/1/21	1150	1	12/6/21	1200	1	NA	NA	NA
HAlG-05	12/14/21	1150	1	12/15/21	1150	1	NA	NA	NA
HAlG-06	12/16/21	1150	1	12/20/21	1150	1	NA	NA	NA
HAlG-07-1	12/28/21	1150	1	12/29/21	1150	1	12/30/21 1/11/22	1200 1200	1 1
HAlG-08	1/17/22	1150	1	1/19/22	1150	1	NA	NA	NA
HAlG-09	1/17/22	1150	1	1/20/22	1150	1	1/24/22 1/26/22	1250 1400, stirred	1 1
HAlG-10	1/18/22	1300	1	1/24/22	1300	1	NA	NA	NA
HAlG-11	1/13/22	1250	1	1/17/22	1350	1	1/18/22	1350	1
HAlG-12	11/22/21	1150	1	11/23/21	1250	1	11/24/21 12/2/21	1200 1150	1 2
HAlG-13	1/25/22	1150	1	1/26/22	1400	1	NA	NA	NA
HAlG-14	1/26/22	1150	1	1/27/22	1150, stirred	1	NA	NA	NA
HAlG-15	12/13/21	1150	1	12/15/21	1150	1	1/14/22	1150	1
HAlG-16	1/27/22	1400, stirred	1	1/31/22	1400, stirred	1	NA	NA	NA
HAlG-17	1/28/22	1150	1	2/1/22	1150	1	2/2/22	1200	1
HAlG-18	12/7/21	1150	1	12/9/21	1200	1	1/11/22	1250	1
HAlG-19	2/1/22	1150, stirred	1	2/3/22	1300, stirred	1	NA	NA	NA
HAlG-20	1/12/22	1150	1	1/13/22	1150	1	NA	NA	NA
HAlG-21	12/30/21	1150	1	1/5/22	1150	1	NA	NA	NA
HAlG-22	12/29/21	1150	1	12/30/21	1150	1	1/13/22	1150	1
HAlG-23	12/21/21	1150	1	12/28/21	1150	1	1/13/22	1150	1
HAlG-24	2/3/22	1150, stirred	1	2/7/22	1150, stirred	1	NA	NA	NA
HAlG-25	2/4/22	1150, stirred	1	2/7/22	1150, stirred	1	NA	NA	NA

Table 2.2. Weight Percent Crystallinity and Identification of Crystals by XRD in Quenched Glasses

Glass ID	Wt% Crystallinity	Crystal Phase Identification
HAlG-01	1.13	$KAlSiO_4$
HAlG-02	0.96	Cr_2O_3
HAlG-03	< d.l.	Amorphous
HAlG-04	1.73	$NiCr_2O_4$ (spinel)
HAlG-05	2.10	$NiCr_2O_4$ (spinel)
HAlG-06	0.68	Cr_2O_3
HAlG-07-1	1.21	$NiCr_2O_4$ (spinel)
HAlG-08	1.61 0.62	$Cr_{0.75}Fe_{1.25}O_3$ $NiCr_2O_4$ (spinel)
HAlG-09	1.35	$NiCr_2O_4$ (spinel)
HAlG-10	2.99	$NiCr_2O_4$ (spinel)
HAlG-11	32.01 3.73	$KNaAlSiO_4$ (nepheline) Mg_2SiO_4
HAlG-12	0.56	Cr_2O_3
HAlG-13	2.98	$NiCr_2O_4$ (spinel)
HAlG-14	2.48	$NiCr_2O_4$ (spinel)
HAlG-15	1.48	$NiCr_2O_4$ (spinel)
HAlG-16	0.99 0.29 0.27	$NiCr_2O_4$ (spinel) Cr_2O_3 $KAlSiO_4$
HAlG-17	NA	NA
HAlG-18	37.27	$KAlSiO_4$
HAlG-19	1.45	$NiCr_2O_4$ (spinel)
HAlG-20	0.84 0.94	Cr_2O_3 $KAlSiO_4$
HAlG-21	NA	NA
HAlG-22	1.50	$NiCr_2O_4$ (spinel)
HAlG-23	0.68	Cr_2O_3
HAlG-24	1.14	$NiCr_2O_4$ (spinel)
HAlG-25	1.51 1.13 0.74	$Cr_{0.75}Fe_{1.25}O_3$ $KAlSiO_4$ $NiCr_2O_4$ (spinel)

NA=not analyzed
d.l. = XRD detection limit

2.2 Chemical Analysis of Glass Composition

To confirm that the "as-fabricated" glasses corresponded to the specified target compositions, a representative sample of each glass was chemically analyzed at Savannah River National Laboratory (SRNL). Three preparation techniques – sodium peroxide fusion (PF), lithium metaborate/tetraborate fusion (LM), and potassium hydroxide digestion (KH) – were used to prepare the glass samples, in duplicate, for analysis.

Each of the duplicate samples was analyzed twice for each element of interest by inductively coupled plasma-optical emission spectroscopy (ICP-OES) and ion chromatography (IC), for a total of four measurements per element per glass. Glass composition standards were also intermittently prepared and analyzed to assess the performance of the ICP-OES and IC instruments over the course of these analyses. Specifically, several samples of the Analytical Reference Glass-1 (ARG-1) (Smith 1993) and several samples of the low-activity reference material were included as part of the SRNL analytical plan. Table 2.3 lists the preparation and measurement methods used for each of the reported glass analytes.

A detailed analysis of the chemical composition measurements is published elsewhere (Hsieh 2022). A short summary of these analyses is included in Section 3.1.

Table 2.3. Preparation and Measurement Methods Used in Measuring Concentrations of the Analytes in the High-Aluminum Waste Glasses

Analyte	Preparation Method	Measurement Method
Al	LM	ICP-OES
B	PF	ICP-OES
Ca	LM	ICP-OES
Cr	LM	ICP-OES
F	KH	IC
Fe	LM	ICP-OES
K	LM	ICP-OES
Li	PF	ICP-OES
Mn	LM	ICP-OES
Na	LM	ICP-OES
P	LM	ICP-OES
Si	PF	ICP-OES
S	LM	ICP-OES
Zn	LM	ICP-OES
Zr	PF	ICP-OES

2.3 Glass Density

The room temperature density of each glass was measured according to the PNNL procedure *Density Using a Gas Pycnometer* (EWG-OP-0045)[1] using a MicroMeritics AccuPyc II 1340 gas pycnometer (MicroMeritics, Norcross, GA) with approximately 1.0 to 1.5 g of glass pieces. The glass was weighed and then loaded into a vial and placed within the instrument. The instrument then determined the volume by the difference in amount of helium gas needed to fill the vial with and without the glass present. After five runs for each glass, the average glass densities were calculated. The pycnometer calibration was checked before and after measurements for that day using a National Institute of Standards and Technology (NIST) traceable standard tungsten carbide ball. These results are discussed in Section 3.2.

2.4 Canister Centerline Cooling

A portion (~150 g) of each test glass was subjected to the simulated CCC temperature profile shown in Table 2.4 and Figure 2.1. This profile is the temperature schedule of CCC treatment for Hanford HLW glasses planned for use at the WTP [(2)] and modified by PNNL to include a 30 min soak at the final glass melt temperature (MT) listed in Table 2.1 before the cooling began. Pieces of quenched glass, < 3 cm in diameter, were placed in a Pt-alloy crucible and covered with a Pt-alloy lid. The glass samples were placed in a furnace preheated to the glass melting temperature. After 30 min at the melting temperature, the furnace temperature was quickly decreased to 1050 °C and the cooling profile started. It progressed down to about 400 °C based on seven cooling segments shown in Table 2.4.

[1] Russell RL. 2017. *Density Using a Gas Pycnometer*. EWG-OP-0045, Rev. 0.0.
[2] Petkus LL. 2003. "Canister Centerline Cooling Data, Revision 1," to C.A. Musick, CCN: 074851, October 29, 2003, River Protection Project, Hanford Tank Waste Treatment and Immobilization Plant, Richland, Washington.

Table 2.4. CCC Heat Treatment Schedule

Segment	Start Time (min)	Start Temp (°C)	Rate (°C/min)	End Time (min)	End Temp (°C)
1	0	MT	0.0	30	MT
2	30	1150	-12.5	38	1050
3	38	1050	-1.5556	83	980
4	83	980	-0.8065	145	930
5	145	930	-0.5914	238	875
6	238	875	-0.3876	367	825
7	367	825	-0.2525	565	775
8	565	775	-0.2778	745	725
9	745	725	-0.3040	1814	400

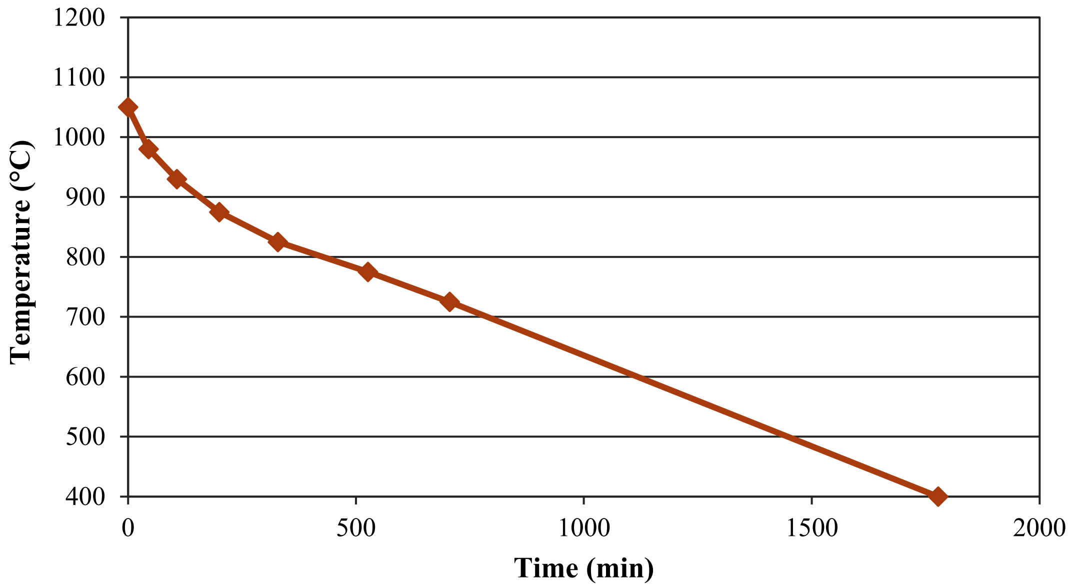

Figure 2.1. Plot of Temperature Schedule during CCC Treatment of Hanford High-Aluminum Glasses

The amounts and types of crystalline phases that formed during CCC treatment were analyzed by XRD according to Section 12.4.4 of the standard ASTM International procedure *Standard Test Method for Determining Liquidus Temperature of Immobilized Waste Glasses and Simulated Waste Glasses* (ASTM C1720). Powdered glass samples were prepared using roughly 5 wt% CeO_2 (51% crystallinity) as an internal standard phase with between 1 and 2 g of powdered glass. Glass and CeO_2 were milled together for 1 min in a 10 cm^3 tungsten carbide disc mill. The powdered glass samples were loaded into XRD sample holders and scanned at a 0.015° 2θ step size, 1.5 s dwell time, from 5° to 75° 2θ scan range. XRD spectra were analyzed with TOPAS 4.2 software (Bruker AXS Inc., Madison, Wisconsin) for phase identification and Rietveld refinement to semi-quantify the amounts of crystal phases on some samples with high crystalline content. These results are discussed in Section 3.3.

2.5 Viscosity

The viscosities of the first 15 quenched glasses were measured as a function of temperature using a fully automated Anton Parr FRS 1600 Furnace Rheometer System, according to the PNNL procedure *High-*

Temperature Viscosity Measurement Using Anton Paar FRS1600 (EWG-OP-0046, Rev. 0.0).[1] About 25 to 30 mL, or ~70 g, of crushed glass was placed into a Pt-alloy cylindrical cup. It was then heated to ~1150 °C and maintained until thermal equilibrium was reached. A Pt-alloy spindle was then lowered into the cup of molten glass. An initial torque reading (at a constant spindle speed) was taken at ~1150 °C with subsequent measurements at target temperatures of 1050 °C, 950 °C, 1150 °C, 1250 °C, and then 1150 °C at thermal equilibrium. The soak time was 30 min at each temperature.

The viscosities of the final 10 quenched glasses were measured as a function of temperature using the viscosity dependance to the shear stress and shear rate:

$$\eta = \frac{\tau}{\gamma} \tag{2.1}$$

A rotating spindle digital viscometer capable of measuring viscosities from 1 to 100 Pa·s (Brookfield Digital Model LVTD) was staged above a high-temperature Deltech furnace (Deltech Model DT-31-RS, Denver, Colorado) equipped with a Pt/Rh spindle to fit through a hole in the top of the furnace. A 50-mL glass sample was measured by weight using the measured glass density, added into a Pt/Rh alloy crucible of 100 mL with approximate dimensions of 5 cm diameter × 6 cm height. The crucible was placed into the furnace set at 1150 °C and the glass was left to melt for about 20 min before the spindle was lowered into the molten glass in the center of the crucible with the lower end of the rod at 1 cm above the bottom of the crucible. The furnace was programmed to follow a set ramp schedule at the following temperatures: 1150, 1050, 950, 1150, 1200 °C, and back to 1150 °C. The soak time was 30 min at each temperature before measurement. At each target temperature, the maximum and minimum spindle torque values were recorded three times each at 3-min intervals. The average of the three measurements was used for data analysis.

Prior to quenched glass viscosity measurements with both systems, the test instrumentation was calibrated using a standard glass (Defense Waste Processing Facility Startup Frit) as discussed in the literature (Crum et al. 2012). The temperature profile followed with both instruments allowed for the potential impacts of crystallization (at lower temperatures) and volatility (at high temperatures) to be assessed (via reproducibility) at the repeated T_M = 1150 °C.

These results are discussed in Section 3.4.

2.6 Electrical Conductivity

The EC (σ in S/m) as a function of temperature was calculated from the resistance (R' in Ω) and cell constant (K in m^{-1}) by:

$$\sigma = K/R_s \tag{2.2}$$

where R_s is the solution resistance obtained for the KCl calibration solutions and K is the cell constant and is linked to the geometry of the system.

A Biologic VSP-3E potentiostat connected to a two-blade Pt/Rh probe staged above a high-temperature Sentrotech furnace (Sentrotech Model ST-1200-7812, Strongsville, Ohio) was used to measure the molten glass impedance. Data was recorded at 1200, 1150, 1050, and 950 °C after roughly 30-min soaks at each temperature, allowing the program to collect impedance data at an applied voltage of 100 mV and

[1] McCarthy, BM. 2017. *High-Temperature Viscosity Measurement Using Anton Paar FRS1600*. EWG-OP-0046, Rev. 0.0.

frequencies of 0.5 Hz – 5x10^5 Hz, measuring 25 data points per decade, and repeating the scan three times for a total of four measurements per glass per temperature.

Approximately 18 g of quenched glass was added to an alumina crucible with the two-blade Pt/Rh probes attached perpendicular to one another 20 mm apart, and the assembly was loaded into the furnace at room temperature. The furnace was then slowly (~10 °C/min) ramped to 900 °C to prevent thermal shock to the crucibles and was successively fast ramped to 1200 °C to complete glass melting. The furnace was then held (~30 min) at 1200 °C to homogenize the glass before taking the first measurement. Each change in temperature was performed at a slow rate (~10 °C/min) and the glass was allowed to equilibrate at each temperature for ~ 30 min before the corresponding measurement was taken.

Solution resistance (R_s) was calculated by fitting the impedance spectra (i.e., Nyquist plots). A cell constant was determined using 0.1 M and 1.0 M KCl solutions measured at the same volume in the same alumina crucible and Pt/Rh probe apparatus. The conductivity was then calculated from Eq. (2.2).

These results are discussed in Section 3.5.

2.7 Equilibrium Crystal Fraction

Prior to measuring the CF, the furnace temperature accuracy was verified using ARG-1 glass (Smith 1993). Data measured and captured for the standard glass check was stored and maintained with the batch glass data.

The CF as a function of temperature was measured in Pt-alloy boats with tight fitting lids (to minimize volatility) according to the standard ASTM International procedure *Standard Test Method for Determining Liquidus Temperature of Immobilized Waste Glasses and Simulated Waste Glasses* (ASTM C1720). The samples were heat treated at 950 °C for 24 h and 850 °C for 48 h. At the end of the heat treatment, the samples were then cold water quenched to stop crystals forming on cooling.

The CF formed during heat treatment was analyzed by XRD as described in Section 2.4. These results are discussed in Section 3.6.

2.8 Product Consistency Test

PCT responses were measured in triplicate for quenched and CCC samples of each glass using Method A of the standard ASTM International procedure *Standard Test Methods for Determining Chemical Durability of Nuclear, Hazardous, and Mixed Waste Glasses and Multiphase Glass Ceramics: The Product Consistency Test (PCT)* (ASTM C1285). Also included in the PCT experimental test matrix and tested in triplicate were the ARM-1 glass (Mellinger and Daniel 1984) and blanks. Glass samples were ground, sieved to −100 +200 mesh, washed, and prepared according to the standard ASTM C1285 International procedure. The prepared glass was added to water in a 1.5 g to 15 mL ratio, resulting in a glass surface area-to-solution volume ratio of approximately 2000 m^{-1}. The vessels used were desensitized Type 304L stainless steel. The vessels were closed, sealed, and placed into an oven at 90 ± 2 °C for 7 days ± 3 h.

After 7 days at 90 °C, the vessels were removed from the oven and allowed to cool to room temperature. The final mass of the vessel and the solution pH were recorded on a data sheet. Each test solution was then filtered through a 0.45-µm-size filter and acidified with concentrated, high-purity HNO_3 to 1 vol% to assure that the cations present remained in solution. The resulting solutions were analyzed by ICP-OES at SRNL for Si, Na, B, and Li. Samples of a multi-element, standard solution were also analyzed as a check on the accuracy of the ICP-OES. Normalized releases (g/L) were calculated based on both target and measured compositions using the average of the logarithms of the leachate concentrations. Results from the PCT work are published elsewhere (Hsieh 2023b), and a short summary of these results is included in Section 3.7.

2.9 Toxicity Characteristic Leaching Procedure

The TCLP analyses were conducted at Southwest Research Institute on both quenched and CCC samples of all the high-aluminum matrix glasses. Glass samples in crushed form were extracted using U.S. Environmental Protection Agency (EPA) procedure SW-846 Method 1311 (EPA 1992a). Analyses of the extracted metals was done following EPA SW-846 Method 3010A (EPA 1992b) using ICP-OES. These results are discussed in Section 3.8.

2.10 Sulfur Solubility

Sulfur solubility was measured on the quenched glass samples. The procedure was developed by PNNL and can be found in Jin et al. (2019). There are three primary phases of testing with each glass: (1) saturation with sodium sulfate, (2) deionized water wash, and (3) analysis.

Saturation of the glass with sodium sulfate was performed by taking 50 g of each glass, grinding it, and then sieving through a #120 sieve (125 µm). Then, 3.82 g of Na_2SO_4 per 50 g of glass was added to the sieved powdered glass to maintain 4 mass% SO_3 added to the glass/salt system, and the combination was mixed for homogeneity. The mixture of baseline glass and Na_2SO_4 was melted at 1150 °C for 1 h in a Pt-alloy crucible with a tight-fitting lid. After melting, the mixture was poured onto a stainless-steel plate and quenched. The mixture was again mixed by crushing and sieving through a #120 sieve (125 µm) and placed back into the Pt-alloy crucible to melt at 1150 °C for 1 h the second time. After the second melting, the mixture was quenched by pouring onto a stainless-steel plate, mixed by crushing and sieving through a #120 sieve (125 µm), and melted under the same conditions for the third time. The glass, after three times re-melting and re-mixing, was crushed and sieved through the #120 sieve (125 µm).

From the sieved glass fraction, 2.0 g of sulfur saturated melt (SSM) glass and 20 g of deionized water were transferred into a centrifuge tube equipped with a 0.45-µm nylon filter. The centrifuge tube was closed and shaken by hand for ~2 min to ensure that the glass was completely exposed to the solution. After shaking, the centrifuge tubes were centrifuged at 3175 rpm for 5 min in a centrifuge instrument (Sorvall Legend Mach 1.6 model, Thermo Electron Corporation). The centrifuge filter with the washed glass powder was removed, and the rinse solution was decanted and stored for potential future use. The filter with glass powder was returned to the centrifuge tube and the washing procedure was repeated. After the second washing, the filter with glass powder was dried overnight in an 80 °C oven. To ensure there was enough sample for analysis, a fresh 2 g of the same glass was obtained, and the procedure described above was repeated and the resulting solutions combined.

The washed and filtered glasses were then analyzed by ICP-OES and IC at SRNL. Also, a representative sample was taken from each of the wash solutions generated from the preparation of the SSM samples. The sample was diluted according to expected concentrations of the species of interest in each of the solutions, and each sample was analyzed in triplicate by ICP-OES. Blanks and standards were used intermittently to assess the performance of each of the instruments and procedures.

The results are discussed in Section 3.9.

3.0 Results and Discussion

This section describes the results for the chemical composition, density, CCC, viscosity, EC, CF, PCT, TCLP, and sulfate solubility for the high-aluminum waste glasses studied.

3.1 Chemical Analysis of Glass Composition

Appendix B presents the targeted and average measured component concentrations (wt%) in the quenched glasses along with the percent differences. The composition analyses of the glass samples were performed as described in Section 2.2.

All the measured sums of oxides for the study glasses fell within the interval of 96.2 to 100 wt%, indicating acceptable recovery of the glass components within ± 5 wt%.

The following was observed in the samples:

- Cr_2O_3 relative differences were greater than 10% for HAlG-02-Q, HAlG-09-Q, HAlG-10-Q, HalG-12-Q, and HAlG-16-Q. These glasses had Cr_2O_3 and/or a Cr containing spinel phase formed.
- Li_2O relative difference was 12% for HAlG-02-Q.
- P_2O_5 relative differences were greater than 10% for HAlG-02-Q, HAlG-03-Q, HAlG-06-Q, HalG-07-1-Q, HAlG-08-Q, HAlG-10-Q, HAlG-18-Q, HAlG-20-Q, HAlG-21-Q, HAlG-22-Q, HAlG-23-Q, HAlG-24-Q, and HAlG-25-Q.
- ZrO_2 relative difference was 15% for HAlG-21-Q.

All relative differences ≥10 relative percent were for components with concentrations < 2 wt% in glass except for P_2O_5, which ranged from 1 to 4.5 wt%. The measured concentrations of P_2O_5 were below the targeted values, likely because of volatility during melting.

Based on the observations above, along with the overall analysis results presented in Appendix B, it was determined that the glasses had been batched correctly, and the target values were used in the resulting calculations. More details can be found in Hsieh (2022).

3.2 Density

The glass density measurements were obtained using the methods discussed in Section 2.3. These 24 density values have a minimum of 2.35 g/cm^3 and a maximum of 2.69 g/cm^3 with a median of 2.57 g/cm^3 and are presented in Table 3.1.

Table 3.1. Measured Densities of High-Aluminum Waste Glasses

Glass ID	Measured Density (g/cm^3)	Glass ID	Measured Density (g/cm^3)
HAlG-01	2.59	HAlG-14	2.59
HAlG-02	2.51	HAlG-15	2.38
HAlG-03	2.51	HAlG-16	2.63
HAlG-04	2.60	HAlG-17	2.53
HAlG-05	2.58	HAlG-18	2.57
HAlG-06	2.43	HAlG-19	2.59
HAlG-07-1	2.61	HAlG-20	2.48
HAlG-08	2.55	HAlG-21	2.67
HAlG-09	2.56	HAlG-22	2.35
HAlG-11	2.63	HAlG-23	2.49
HAlG-12	2.52	HAlG-24	2.58
HAlG-13	2.69	HAlG-25	2.57

3.3 Crystal Identification in Canister Centerline Cooling Glasses

The slow cooling of the molten glass in the canister centerline might impact glass durability by changing the residual glass composition (Kim et al. 1995; Kroll et al. 2019). Not all crystals affect durability in the same way, so identifying the crystal content after CCC is an important step toward understanding crystallization impacts on glass durability. Moreover, property-prediction models were formulated using quenched data; therefore, differences in glass durability responses after CCC via PCT and TCLP were also measured and compared.

This section presents and discusses the crystallinity of the CCC glasses obtained using the methods discussed in Section 2.4. The effects of CCC on PCT and TCLP are reported in Sections 3.7 and 3.8, respectively.

All of the glasses had at least some crystals present after CCC was performed. The XRD scans of the CCC glass samples identified primarily nepheline with spinel, eskolaite, and a couple minor zirconium containing phases. The crystal types and wt% crystallinity results are summarized in Table 3.2. Fourteen glasses had crystal content greater than 30 wt%, with several crystal types containing primarily nepheline with spinel and eskolaite. Eleven glasses had Zr containing phases (baddeleyite, parakeldyshite, and vlasovite). Nepheline was the predominant phase in these glasses because of the high aluminum content, and as the glass temperature slowly dropped below the nepheline liquidus temperature (T_L), it precipitated out of the glass. Nepheline precipitation reduces the durability of the glass by removing about 3 moles of network-forming oxides for every mole of nepheline. See Appendix D for photos of CCC-treated glasses and Appendix E for XRD spectra obtained from them.

Table 3.2. Weight Percent Crystallinity and Identification of Crystals by XRD in CCC-Treated Glasses

Glass ID	Starting CCC Temp (°C)	Wt% Crystallinity	Crystal Phase Identification
HAlG-01	1250	16.87	$KNaAlSiO_4$ (nepheline)
HAlG-02	1250	22.51	$KNaAlSiO_4$ (nepheline)
		1.66	Cr_2O_3
		1.64	Fe_2O_3
HAlG-03	1250	1.82	Mg_2SiO_4
		1.04	$KNaAlSiO_4$ (nepheline)
HAlG-04	1200	37.62	$KNaAlSiO_4$ (nepheline)
		0.81	Cr_2O_3
HAlG-05	1150	4.63	$NiCr_2O_4$ (spinel)
		3.92	$KNaAlSiO_4$ (nepheline)
		2.08	$KAlSiO_4$
HAlG-06	1150	23.03	$KNaAlSiO_4$ (nepheline)
		0.96	$NiCr_2O_4$ (spinel)
HAlG-07-1	1200	32.44	$KNaAlSiO_4$ (nepheline)
		4.79	$NiCr_2O_4$ (spinel)
HAlG-08	1150	23.19	$K_{0.25}Na_6Al_{6.24}Si_{9.76}O_{32}$ (nepheline)
		0.49	$NiCr_2O_4$ (spinel)
		4.67	Fe_2O_3
HAlG-09	1400	1.57	$KAlSiO_4$
		1.47	$KNaAlSiO_4$ (nepheline)
		0.92	$NiCr_2O_4$ (spinel)
HAlG-11	1350	29.10	Nepheline
		6.96	$Na_{1.15}(Al_{1.15}Si_{0.85}O_4)$ (nepheline)
		5.94	$Na_2Al_2(B_2O_7)$
		3.28	$KAlSiO_4$
		3.29	Na_2AlSiO_4 (nepheline)
		1.00	$NiCr_2O_4$ (spinel)
HAlG-12	1150	32.70	$K_{0.25}Na_6Al_{6.24}Si_{9.76}O_{32}$ (nepheline)
		1.18	Cr_2O_3
		3.35	$Na_2Al_2(B_2O_7)$
		2.14	$KAlSiO_4$
HAlG-13	1400	30.58	Nepheline
		3.97	$Na_2Al_2(B_2O_7)$
		3.29	$KAlSiO_4$
		5.15	Mg_2SiO_4
		2.88	$NiCr_2O_4$ (spinel)
		2.36	Na_2AlSiO_4 (nepheline)
		2.82	$Na_{1.15}(Al_{1.15}Si_{0.85}O_4)$ (nepheline)
HAlG-14	1150	28.80	Nepheline
		6.10	$NiCr_2O_4$ (spinel)
		1.47	$KAlSiO_4$
HAlG-15	1150	34.89	Nepheline
		1.75	$KAlSiO_4$
		3.64	$NiCr_2O_4$ (spinel)
HAlG-16	1400	35.11	Nepheline
		1.84	$KAlSiO_4$
		0.74	$NiCr_2O_4$ (spinel)
		2.29	$Na_2Al_2(B_2O_7)$

Glass ID	Starting CCC Temp (°C)	Wt% Crystallinity	Crystal Phase Identification
HAlG-17	1200	4.00	$K_{0.25}Na_6Al_{6.24}Si_{9.76}O_{32}$ (nepheline)
		0.91	$KAlSiO_4$
HAlG-18	1350	24.47	Nepheline
		6.37	$Na_2Al_2(B_2O_7)$
		2.96	$KAlSiO_4$
HAlG-19	1350	31.98	Nepheline
		3.27	$KAlSiO_4$
		2.59	$Na_2Al_2(B_2O_7)$
HAlG-20	1150	1.50	$KAlSiO_4$
		1.84	$Na_2Al_2(B_2O_7)$
		0.79	Cr_2O_3
		0.58	$Na_2ZrSi_2O_7$
		0.18	$Na_2ZrSi_4O_{11}$
HAlG-21	1150	31.60	Nepheline
		0.64	$Na_2ZrSi_2O_7$
		3.68	$Na_2Al_2(B_2O_7)$
		0.20	$Na_2ZrSi_4O_{11}$
HAlG-22	1150	35.10	Nepheline
		1.38	$NiCr_2O_4$ (spinel)
HAlG-23	1150	4.23	$NiCr_2O_4$ (spinel)
		0.56	Cr_2O_3
		3.13	Nepheline
		0.99	$Na_2ZrSi_2O_7$
		0.92	$KAlSiO_4$
		0.07	$Na_2ZrSi_4O_{11}$
HAlG-24	1150	3.20	$NiCr_2O_4$ (spinel)
		0.86	$KAlSiO_4$
HAlG-25	1150	19.60	Nepheline
		4.20	Fe_2O_3
		4.00	$KAlSiO_4$
		0.43	$NiCr_2O_4$ (spinel)

3.4 Viscosity

This section presents and discusses the viscosity results obtained using the methods discussed in Section 2.4. The results of the viscosity measurements are listed in Appendix F and summarized in Table 3.3.

At the melting temperature of 1150 °C, the acceptable viscosity range of HLW glass melts is 2 to 8 Pa·s to avoid processing issues (Vienna et al. 2009). The current glass formulations and optimal performance are centered closer to 5 Pa·s and therefore a narrower viscosity range of 4 to 6 Pa·s is the recommended range of estimated loading of HLW in glass (Vienna et al. 2016). Nine of the glasses in this study were outside the ranges of 2 to 8 Pa·s at 1150 °C viscosity, with one glass below it and the rest above it. Eighteen of the glasses were outside the optimal performance range of 4 to 6 Pa·s.

The Arrhenius model was used to fit the viscosity-temperature data for each waste glass:

$$\ln(\eta) = A + \frac{B}{T_K} \quad (3.1)$$

where *A* and *B* are independent of temperature (T_K), which is in Kelvin [T(°C) + 273.15]. Table 3.4 presents the values for the A and B coefficients for each glass. Table 3.4 summarizes the viscosity results at 1150 °C (η_{1150}) calculated using the Arrhenius equation [Eq. (3.1)]for each glass.

Table 3.3. Measured ln *η* (Pa-s) Values versus Target Temperature (in the sequence of measurement) for the High-Aluminum Waste Glasses Tested

Target *T*, °C	1150	1050	950	1150	1200	1150
Glass ID	ln *η* (Pa-s)	ln *η* (Pa-s)	ln *η* (Pa-s)	ln *η* (Pa-s)	ln *η* (Pa-s)	ln *η* (Pa-s)
HAlG-01	2.307	3.481	5.001	2.304	1.824	2.320
HAlG-02	1.706	2.652	3.881	1.667	1.319	1.721
HAlG-03	2.250	3.323	4.754	2.227	1.788	2.222
HAlG-04	2.511	3.598	4.934	2.502	1.992	2.474
HAlG-05	1.634	2.778	4.153	1.531	1.050	1.542
HAlG-06	2.415	3.462	4.799	2.385	1.939	2.395
HAlG-07-1	2.066	3.347	4.792	2.032	1.426	1.978
HAlG-08	2.018	3.246	4.716	1.979	1.473	1.955
HAlG-09	0.573	1.453	2.406	0.530	0.047	0.486
HAlG-11	1.491	2.586	3.819	1.529	1.070	1.543
HAlG-12	1.402	2.322	3.411	1.427	1.031	1.469
HAlG-13	1.338	2.341	3.525	1.340	0.889	1.307
HAlG-14	0.813	1.590	2.503	0.822	0.340	0.734
HAlG-15	2.323	3.144	NM	NM	NM	NM
HAlG-16	2.359	3.337	4.391	2.340	1.554	2.336
HAlG-17	2.247	3.015	3.982	2.164	1.479	2.158
HAlG-18	1.544	2.405	3.472	1.520	0.784	1.518
HAlG-19	1.584	2.540	3.610	1.563	0.827	1.570
HAlG-20	1.886	2.708	3.565	2.025	1.395	1.890
HAlG-21	1.429	2.442	3.525	1.503	0.665	1.395
HAlG-22	3.169	4.254	6.228	3.210	2.438	3.137
HAlG-23	1.987	2.645	3.500	1.953	1.271	1.888
HAlG-24	2.246	3.208	4.515	2.266	1.470	2.201
HAlG-25	2.551	4.384	5.593	2.894	1.595	2.402

Table 3.4. Fitted Coefficients of Arrhenius Model for Viscosity of High-Aluminum Waste Glasses Tested

	Arrhenius Coefficients				
Glass ID	A (ln Pa-s)	B (ln Pa-s*K)	η_{1150} (Pa-s)	η_{1100} (Pa-s)	η_{1200} (Pa-s)
HAlG-01	-13.8375	22995	10.20	18.37	5.89
HAlG-02	-11.3631	18606	5.54	8.92	3.55
HAlG-03	-12.8535	21487	9.45	16.38	5.66
HAlG-04	-12.3750	21160	12.12	20.83	7.32
HAlG-05	-14.2065	22460	4.84	8.60	2.83
HAlG-06	-12.1075	20650	11.07	18.78	6.76
HAlG-07-1	-15.0278	24267	7.58	14.11	4.25
HAlG-08	-14.5657	23573	7.39	13.51	4.21
HAlG-09	-11.2894	16796	1.67	2.57	1.12
HAlG-11	-12.4647	19913	4.61	7.68	2.87
HAlG-12	-10.6064	17133	4.19	6.50	2.79
HAlG-13	-12.0563	19054	3.80	6.18	2.41
HAlG-14	-9.9644	15272	2.16	3.19	1.50
HAlG-15	NA	NA	NA	NA	NA
HAlG-16	-11.7435	19736	8.38	13.89	5.23
HAlG-17	-10.1511	17274	7.30	11.36	4.84
HAlG-18	-11.7214	18552	3.73	5.99	2.39
HAlG-19	-12.2659	19397	3.92	6.43	2.47
HAlG-20	-8.9300	15249	5.97	8.81	4.15
HAlG-21	-12.7788	19930	3.41	5.68	2.12
HAlG-22	-15.5297	26294	19.07	37.38	10.19
HAlG-23	-8.9556	15233	5.75	8.49	4.00
HAlG-24	-12.8016	21087	7.52	12.89	4.55
HAlG-25	-17.9535	28916	10.66	22.35	5.35

NA = not applicable because not enough data points were obtained

3.5 Electrical Conductivity

This section presents and discusses the EC results obtained using the methods discussed in Section 2.6. Table 3.5 lists the EC versus temperature data for each of the glasses and Appendix G shows the plots for the EC versus temperature data obtained from the EC experiments.

The Arrhenius equation [Eq. (3.2)] was used to fit ε-temperature data for each waste glass:

$$\ln(\varepsilon) = A + \frac{B}{T_K} \tag{3.2}$$

where *A* and *B* are temperature independent and composition dependent coefficients, and temperature (T_K) is in Kelvin [T(°C) + 273.15]. Table 3.6 presents the values for the A and B coefficients obtained by fitting the equation to the ε-temperature data for each glass along with the calculated ε at 1150 °C (ε_{1150}) using Eq. (3.2) fit to each glass measured data.

Table 3.5. Measured Electrical Conductivity (S/m) Values versus Temperatures for the High-Aluminum Glasses

Target *T*, °C	950	1050	1150	1200	1250
Glass ID	Electrical Conductivity (S/m)				
HAlG-01	22.1	31.3	40.4	38.8	NM
HAlG-02	27.0	38.1	49.5	55.7	NM
HAlG-03	23.9	37.2	51.4	59.9	NM
HAlG-04	24.6	36.5	48.8	55.3	NM
HAlG-05	25.8	38.6	52.3	60.4	NM
HAlG-06	29.6	44.2	58.8	67.0	NM
HAlG-07-1	19.1	27.7	37.2	42.5	NM
HAlG-08	27.5	39.3	51.1	57.3	NM
HAlG-09	34.2	50.9	67.3	75.9	NM
HAlG-11	41.6	62.9	80.4	89.5	NM
HAlG-12	19.2	27.8	37.1	42.3	NM
HAlG-13	8.1	14.2	21.9	26.8	NM
HAlG-14	27.4	39.2	51.1	57.5	NM
HAlG-15	20.2	28.4	35.9	NM	41.9
HAlG-16	28.9	40.7	51.6	NM	61.9
HAlG-17	22.4	33.1	42.5	NM	52.5
HAlG-18	37.9	51.6	63.4	NM	72.3
HAlG-19	103.6	119.3	NM	NM	NM
HAlG-20	18.3	28.5	37.8	NM	46.5
HAlG-21	31.6	44.3	56.5	NM	67.5
HAlG-22	13.9	21.4	29.5	NM	37.2
HAlG-23	24.5	36.7	48.0	NM	57.7
HAlG-24	19.4	30.1	41.3	NM	53.1
HAlG-25	19.5	28.2	38.1	NM	47.1

NM = not measured

Table 3.6. Fitted Coefficients of the Arrhenius Model for Electrical Conductivity for the High-Aluminum Glasses

	Arrhenius Coefficients		
Glass ID	A, ln[S/m]	B, ln[S/m]-K	ε_{1150} (S/m)
HAlG-01	6.6790	-4337	40.4
HAlG-02	7.5527	-5195	49.5
HAlG-03	8.5732	-6590	51.4
HAlG-04	7.9858	-5834	48.8
HAlG-05	8.2472	-6101	52.3
HAlG-06	8.1882	-5854	58.8
HAlG-07-1	7.6500	-5740	37.2
HAlG-08	7.6515	-5293	51.1
HAlG-09	8.2358	-5733	67.3
HAlG-11	8.2454	-5492	80.4
HAlG-12	7.6079	-5683	37.1
HAlG-13	9.1033	-8556	21.9
HAlG-14	7.6821	-5335	51.1
HAlG-15	6.7489	-4545	35.0
HAlG-16	7.2442	-4718	50.9
HAlG-17	7.4227	-5241	42.1
HAlG-18	6.9509	-4021	61.9
HAlG-19	NA	NA	NA
HAlG-20	7.6800	-5794	36.9
HAlG-21	7.3390	-4728	55.5
HAlG-22	7.6705	-6133	28.8
HAlG-23	7.5303	-5243	46.8
HAlG-24	8.0981	-6250	40.7
HAlG-25	7.4800	-5495	37.3

NA = not applicable

3.6 Crystal Fraction

The long idling of the leftover glass in the melter at low temperatures may promote crystal formation, impacting glass durability by sequestering glass forming chemicals and/or glass processability by settling in the melter and clogging the pour sprout (Vienna et al. 2001). Therefore, the study of crystalline phases and quantities in isothermal heat-treatments is part of the regular investigation of HLW glasses.

This section presents and discusses the CF results obtained using the methods discussed in Section 2.7. See Appendix H for photos of CF heat-treated glasses at 950 °C and Appendix I for XRD spectra obtained from them.

Only two glasses had insufficient crystals to perform XRD analysis when treated at 950 °C for 24 h; however, they formed crystals (primarily nepheline) when treated at 850 °C for 48 h. The glasses contained spinel or nepheline, or both, except for HAlG-20, which only had Cr_2O_3. Several glasses also contained Cr_2O_3 and/or baddeleyite. The total crystallinity ranged from 0 to 20 wt% at 950 °C and from

0.9 to 32 wt% at 850 °C. Six of these glasses had spinel >2 wt% at 950 °C. These results are summarized in Table 3.7.

Table 3.7. Weight Percent Crystallinity and Identification of Crystals by XRD in Heat-Treated High-Aluminum Waste Glasses

Glass ID	Temp (°C)	Wt% Crystallinity	Crystal Phase Identification
HAlG-01	950	0	None
	850	20.16	Nepheline
		0.77	$KAlSiO_4$
		0.61	ZrO_2
HAlG-02	950	0.59	Cr_2O_3
		0.99	$NiCr_2O_4$ (spinel)
		1.06	$KAlSiO_4$
	850	5.57	$KNaAlSiO_4$ (nepheline)
		0.64	Cr_2O_3
		1.41	$KAlSiO_4$
		1.42	$NiCr_2O_4$ (spinel)
HAlG-03	950	1.00	$KAlSiO_4$
		0.67	Mg_2SiO_4
	850	1.08	$KAlSiO_4$
		1.07	Mg_2SiO_4
HAlG-04	950	9.20	$KNaAlSiO_4$ (nepheline)
		2.29	$NiCr_2O_4$ (spinel)
		6.24	$KAlSiO_4$
		0.74	$Na_7Al_6Si_6O_{24}S_3$
	850	20.90	$KNaAlSiO_4$ (nepheline)
		2.13	$NiCr_2O_4$ (spinel)
		1.87	$KAlSiO_4$
HAlG-05	950	0.19	Cr_2O_3
		2.62	$NiCr_2O_4$ (spinel)
		1.08	ZrO_2
		1.32	$KAlSiO_4$
	850	0.41	Cr_2O_3
		3.15	$NiCr_2O_4$ (spinel)
		1.11	ZrO_2
		1.71	$KAlSiO_4$
HAlG-06	950	0.61	Cr_2O_3
		0.81	$NiCr_2O_4$ (spinel)
	850	8.49	$KNaAlSiO_4$ (nepheline)
		2.49	$NiCr_2O_4$ (spinel)
		0.48	Cr_2O_3
		3.35	$KAlSiO_4$
HAlG-07-1	950	13.43	$KNaAlSiO_4$ (nepheline)
		2.01	$NiCr_2O_4$ (spinel)
		0.48	ZrO_2
		1.73	$KAlSiO_4$
	850		
		24.35	$KNaAlSiO_4$ (nepheline)
		2.66	$NiCr_2O_4$ (spinel)
		0.44	ZrO_2
		0.25	$KAlSiO_4$

Glass ID	Temp (°C)	Wt% Crystallinity	Crystal Phase Identification
HAlG-08	950	0.41	Cr_2O_3
		1.91	$NiCr_2O_4$ (spinel)
		2.43	$KAlSiO_4$
	850	6.71	$KNaAlSiO_4$ (nepheline)
		0.99	$NiCr_2O_4$ (spinel)
		0.86	$KAlSiO_4$
HAlG-09	950	1.07	$NiCr_2O_4$ (spinel)
		1.40	$KAlSiO_4$
		1.80	ZrO_2
	850	1.67	$NiCr_2O_4$ (spinel)
		1.54	$KAlSiO_4$
		2.67	ZrO_2
HAlG-11	950	7.82	$KNaAlSiO_4$ (nepheline)
		8.11	$Na_7Al_6Si_6O_{24}S_3$
		0.88	$NiCr_2O_4$ (spinel)
		2.83	ZrO_2
	850	19.15	$KNaAlSiO_4$ (nepheline)
		6.54	$Na_7Al_6Si_6O_{24}S_3$
		2.14	$KAlSiO_4$
		1.08	$NiCr_2O_4$ (spinel)
		2.95	ZrO_2
HAlG-12	950	0.84	$NiCr_2O_4$ (spinel)
		1.95	$KAlSiO_4$
		1.65	ZrO_2
	850	10.28	$KNaAlSiO_4$ (nepheline)
		1.11	$Na_7Al_6Si_6O_{24}S_3$
		1.00	$KAlSiO_4$
		0.80	$NiCr_2O_4$ (spinel)
		1.63	ZrO_2
HAlG-13	950	8.29	$KNaAlSiO_4$ (nepheline)
		0.46	$KAlSiO_4$
		3.29	$NiCr_2O_4$ (spinel)
		2.38	ZrO_2
	850	21.45	$KNaAlSiO_4$ (nepheline)
		0.99	Sodium aluminum silicon oxide
		1.73	$KAlSiO_4$
		3.28	$NiCr_2O_4$ (spinel)
		2.51	ZrO_2
		0.42	Mg_2SiO_4
HAlG-14	950	2.76	$NiCr_2O_4$ (spinel)
	850	5.15	$KNaAlSiO_4$ (nepheline)
		2.03	$Na_7Al_6Si_6O_{24}S_3$
		0.54	$KAlSiO_4$
		3.62	$NiCr_2O_4$ (spinel)
HAlG-15	950	1.34	$NiCr_2O_4$ (spinel)
		12.47	$KNaAlSiO_4$ (nepheline)
	850	0.91	$Na_7Al_6Si_6O_{24}S_3$
		0.14	$KAlSiO_4$
		1.48	$NiCr_2O_4$ (spinel)

Glass ID	Temp (°C)	Wt% Crystallinity	Crystal Phase Identification
HAlG-16	950	11.26	$KNaAlSiO_4$ (nepheline)
		0.91	$KAlSiO_4$
		1.49	$NiCr_2O_4$ (spinel)
		1.52	ZrO_2
	850	20.43	$KNaAlSiO_4$ (nepheline)
		1.40	$KAlSiO_4$
		1.39	$NiCr_2O_4$ (spinel)
		1.85	ZrO_2
HAlG-17	950	0	None
	850	5.60	$KNaAlSiO_4$ (nepheline)
		1.17	$KAlSiO_4$
HAlG-18	950	1.35	ZrO_2
		16.08	Nepheline
	850	1.50	ZrO_2
		1.43	$Na_7Al_6Si_6O_{24}S_3$
HAlG-19	950	0.76	$Na_7Al_6Si_6O_{24}S_3$
		0.89	ZrO_2
		1.09	$NiCr_2O_4$ (spinel)
		16.97	$KNaAlSiO_4$ (nepheline)
	850	1.09	ZrO_2
		2.22	$NiCr_2O_4$ (spinel)
HAlG-20	950	0.84	Cr_2O_3
	850	0.87	Cr_2O_3
HAlG-21	950	2.42	$NiCr_2O_4$ (spinel)
	850	19.23	$KNaAlSiO_4$ (nepheline)
		3.16	$NiCr_2O_4$ (spinel)
		0.30	Na_2ZrSi_2O
HAlG-22	950	1.19	$KAlSiO_4$
		1.80	$NiCr_2O_4$ (spinel)
	850	2.03	$KNaAlSiO_4$ (nepheline)
		1.08	$KAlSiO_4$
		2.20	$NiCr_2O_4$ (spinel)
HAlG-23	950	0.40	$NiCr_2O_4$ (spinel)
	850	0.63	$NiCr_2O_4$ (spinel)
		0.26	Na_2ZrSi_2O
HAlG-24	950	0.25	ZrO_2
		1.80	$NiCr_2O_4$ (spinel)
	850	0.51	ZrO_2
		2.34	$NiCr_2O_4$ (spinel)
HAlG-25	950	0.51	$NiCr_2O_4$ (spinel)
		2.75	Cr_2O_3
		8.90	$KNaAlSiO_4$ (nepheline)
	850	0.94	$NiCr_2O_4$ (spinel)
		3.51	Cr_2O_3

3.7 Product Consistency Test

This section presents and discusses the PCT results obtained using the methods discussed in Section 2.8. The PCT results are published elsewhere (Hsieh 2023b) and are summarized here in Table 3.8. The PCT results were normalized to the target glass compositions.

A review of the PCT data resulted in the following observations:

- The CCC heat treatment had a large impact on most of the PCT results. Several CCC glasses had a notably higher normalized release for all analytes than the quenched version and were higher than the environmental assessment benchmark (see Table 3.9) for all analytes.
- All of the CCC glasses that failed the PCT had nepheline present in amounts >20 wt% crystallinity except for two, which only had 3.9% (HAlG-05) and 16.9% (HAlG-01).

Table 3.8. PCT Normalized Concentration Release Results for High-Aluminum Glasses

Glass ID	Type	B (g/L)	Na (g/L)	Li (g/L)	Si (g/L)
HAlG-01	Quenched	0.477	0.680	<2.17	0.269
	CCC	46.3	15.5	32.7	0.133
HAlG-02	Quenched	7.14	4.77	5.59	0.221
	CCC	79.5	39.9	23.8	0.121
HAlG-03	Quenched	1.50	1.01	<1.16	0.283
	CCC	4.53	2.14	2.43	0.179
HAlG-04	Quenched	0.609	0.791	<2.82	0.370
	CCC	93.1	35.1	67.4	0.344
HAlG-05	Quenched	6.86	5.03	5.39	0.184
	CCC	26.7	15.9	12.8	0.169
HAlG-06	Quenched	NM	NM	NM	NM
	CCC	NM	NM	NM	NM
HAlG-07-1	Quenched	2.66	2.21	<6.15	0.232
	CCC	79.9	35.2	<6.15	<0.043
HAlG-08	Quenched	3.28	2.20	2.35	0.320
	CCC	87.2	35.1	8.99	0.093
HAlG-09	Quenched	6.39	4.21	5.39	0.248
	CCC	10.2	5.50	7.35	0.219
HAlG-11	Quenched	79.4	37.7	25.2	0.319
	CCC	24.8	6.52	18.2	0.181
HAlG-12	Quenched	2.77	1.94	1.72	0.230
	CCC	89.7	36.7	79.6	0.110
HAlG-13	Quenched	1.17	1.59	0.944	0.436
	CCC	37.9	8.75	42.5	0.713
HAlG-14	Quenched	7.43	5.67	5.58	0.699
	CCC	39.7	17.7	26.3	0.727
HAlG-15	Quenched	0.422	0.687	0.459	0.386
	CCC	98.7	14.9	43.5	0.767
HAlG-16	Quenched	3.10	1.88	1.87	0.309

Glass ID	Type	B (g/L)	Na (g/L)	Li (g/L)	Si (g/L)
	CCC	91.4	28.1	42.6	0.144
HAlG-17	Quenched	0.671	0.678	0.448	0.284
	CCC	12.5	4.55	9.08	0.175
HAlG-18	Quenched	83.8	50.7	17.1	0.365
	CCC	55.4	32.0	22.4	0.160
HAlG-19	Quenched	2.21	2.66	1.25	0.565
	CCC	31.8	10.2	20.0	0.265
HAlG-20	Quenched	5.49	2.80	4.01	0.234
	CCC	4.80	2.66	3.82	0.236
HAlG-21	Quenched	74.1	27.1	27.5	0.101
	CCC	82.6	27.1	31.4	0.445
HAlG-22	Quenched	0.320	0.495	0.374	0.269
	CCC	89.1	17.1	52.7	0.243
HAlG-23	Quenched	1.81	1.04	1.44	0.321
	CCC	1.21	0.847	1.82	0.370
HAlG-24	Quenched	0.398	0.463	0.501	0.222
	CCC	0.358	0.393	0.413	0.216
HAlG-25	Quenched	3.15	2.17	2.31	0.317
	CCC	86.2	35.1	9.36	0.104

NM = not measured   Red font indicates above the PCT release limit.

Table 3.9. WTP PCT Normalized Release Limits to HLW Glass (g/L)

Constraint Description	Value	Source
PCT normalized B release	$rPCT_B$ <16.70 (g/L) $\ln(rPCT_B)$, g/L <2.82	DOE 2000
PCT normalized Li release	$rPCT_{Li}$ <9.57 (g/L) $\ln(rPCT_{Li,})$, g/L <2.26	DOE 2000
PCT normalized Na release	$rPCT_{Na}$ <13.35 (g/L) $\ln(rPCT_{Na})$, g/L <2.59	DOE 2000

Figure 3.1 compares the PCT normalized releases of B with the normalized releases of Na and Li for the quenched glass samples. This shows that the B and the Na and Li release rates are similar for the quenched glasses. Figure 3.2 compares the PCT normalized releases of B with the normalized release of Na and Li for the CCC glass samples. This shows that the PCT normalized releases of B are typically higher than those of Na. This may be due to the Na crystallizing out of the glass composition into the nepheline phase.

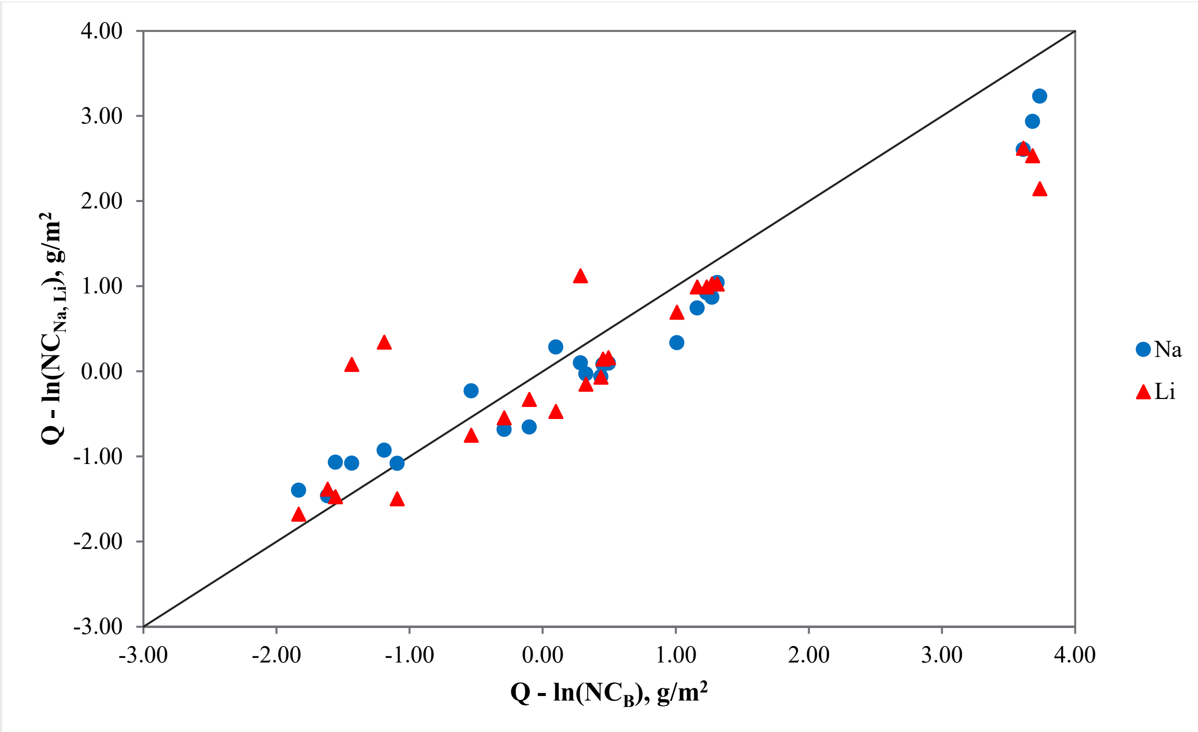

Figure 3.1. Comparison of PCT Normalized Release Rates of B with Na and Li for Quenched Samples of High-Aluminum Glasses

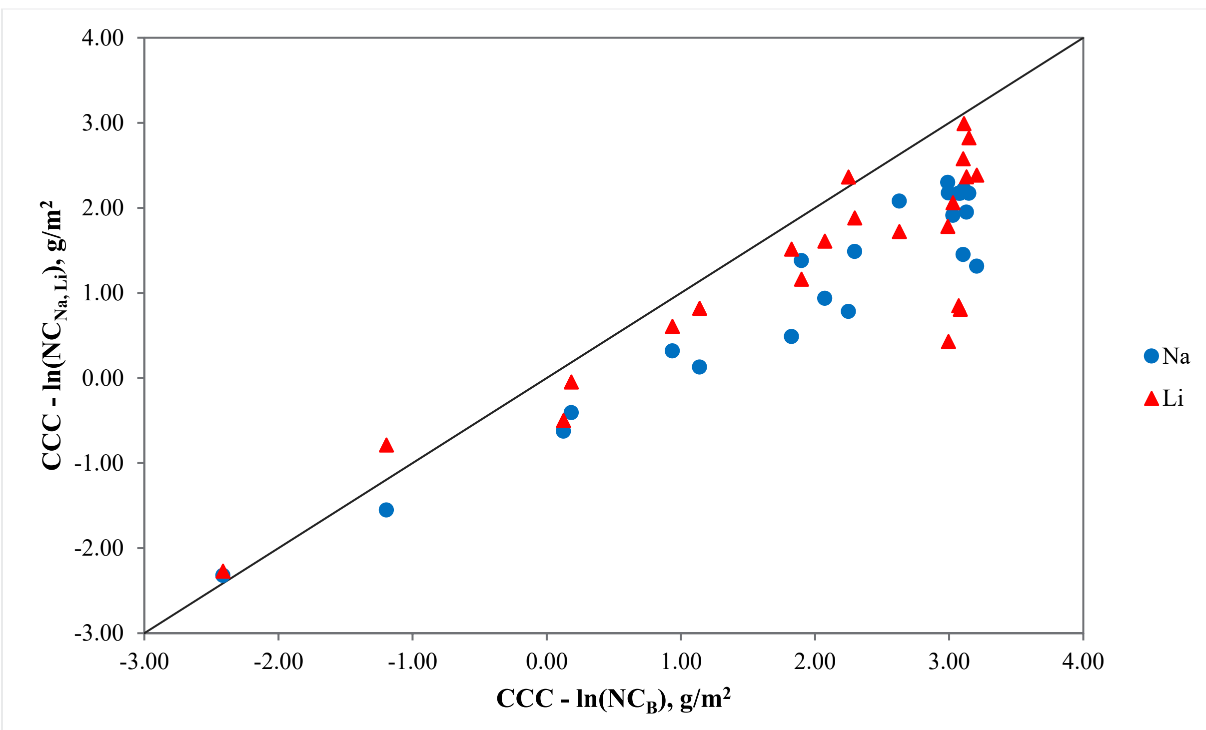

Figure 3.2. Comparison of PCT Normalized Release Rates of B with Na and Li for CCC Samples of High-Aluminum Glasses

Figure 3.3 compares the normalized releases of the quenched and CCC glasses. When significant crystals containing Al and Si (>10 wt%) are present in the glass, CCC-treated samples can have notably higher release rates than quenched samples. This tends to be because the crystals (primarily nepheline) remove the glass formers (Si and Al) from the bulk glass structure and composition, making it less durable.

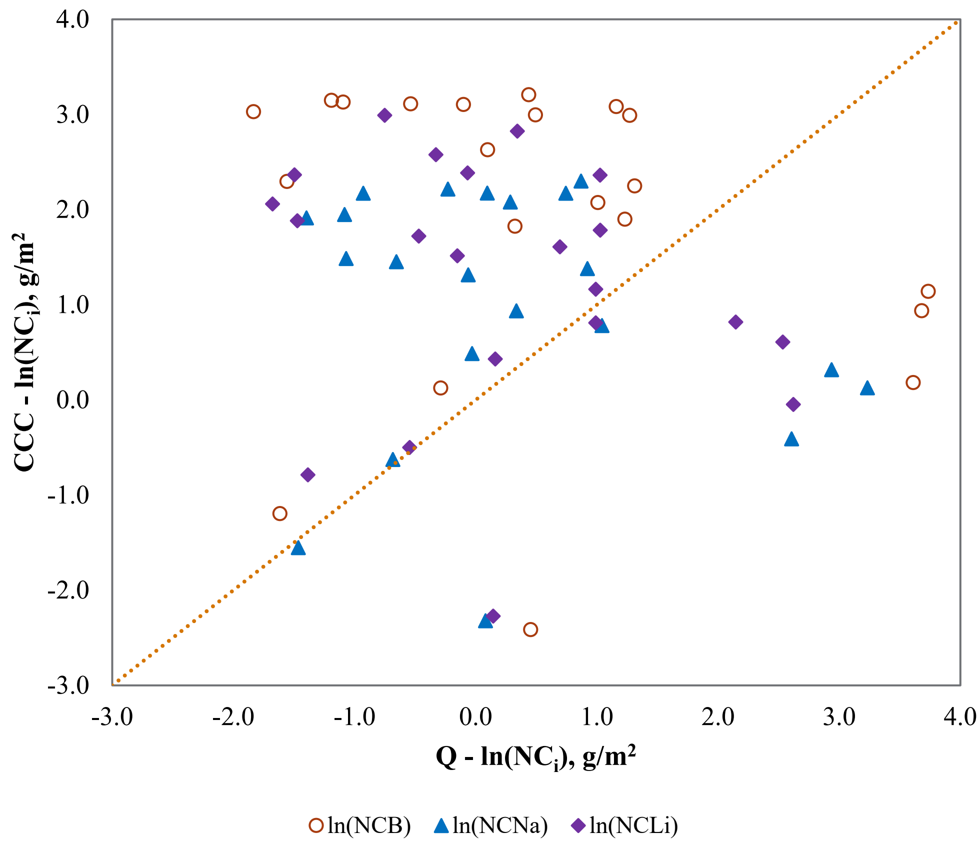

Figure 3.3. Comparison of the Normalized Release Rates of the Quenched and CCC High-Aluminum Glasses

3.8 Toxic Characterization Leach Profile

This section presents and discusses the TCLP results obtained using the methods discussed in Section 2.9. The TCLP results for Q and CCC glasses are listed in Table 3.10 and Table 3.11, respectively. The WTP delisting limits, toxicity, and Universal Treatment Standards (UTS) limits as set by Resource Conservation and Recovery Act (RCRA) are listed in Table 3.12.

All of the quenched glasses passed the Hanford delisting limit. Twelve CCC glasses failed to pass the Hanford delisting limit for Cd of 0.48 mg/L and eight CCC glasses failed to pass the Hanford delisting limit for Cr of 4.95 mg/L. All of the glasses that failed had >25 wt% nepheline present after CCC. The other CCC glasses passed the Hanford delisting limit for all measured elements.

Table 3.10. TCLP Results from the Quenched High-Aluminum Glasses

Sample ID	As (mg/L)	Ba (mg/L)	Cd (mg/L)	Cr (mg/L)	Pb (mg/L)	Hg (mg/L)	Se (mg/L)	Ag (mg/L)	B (mg/L)
HAlG-01	<0.050	<0.100	0.0471	<0.010	<0.015	<0.0001	<0.050	<0.020	1.21
HAlG-02	<0.050	<0.100	[0.0153]	0.0726	<0.015	<0.0001	<0.050	<0.020	3.69
HAlG-03	<0.050	<0.100	[0.0130]	[0.0145]	<0.015	<0.0001	<0.050	<0.020	1.83
HAlG-04	<0.050	<0.100	0.0813	0.0909	<0.015	<0.0001	<0.050	<0.020	2.61
HAlG-05	<0.050	<0.100	0.0404	0.0274	<0.015	<0.0001	<0.050	<0.020	4.04
HAlG-06	<0.050	<0.100	<0.010	0.0210	<0.015	<0.0001	<0.050	<0.020	2.05
HAlG-07-1	<0.050	<0.100	0.0992	[0.0192]	<0.015	<0.0001	<0.050	<0.020	3.69
HAlG-08	<0.050	<0.100	<0.010	[0.0194]	<0.015	<0.0001	<0.050	<0.020	2.66
HAlG-09	<0.050	<0.100	<0.010	0.0877	<0.015	<0.0001	<0.050	<0.020	2.61
HAlG-11	<0.050	<0.100	0.0670	1.93	<0.015	<0.0001	<0.050	<0.020	6.53
HAlG-12	<0.050	<0.100	0.0896	0.331	<0.015	<0.0001	<0.050	<0.020	6.19
HAlG-13	<0.050	<0.100	0.0854	0.0420	<0.015	<0.0001	<0.050	<0.020	2.62
HAlG-14	<0.050	<0.100	[0.0167]	0.298	<0.015	<0.0001	<0.050	<0.020	6.72
HAlG-15	<0.050	<0.100	0.0202	0.346	<0.015	<0.0001	<0.050	<0.020	1.29
HAlG-16	<0.050	<0.100	[0.0130]	0.147	<0.015	<0.0001	<0.050	<0.020	1.38
HAlG-17	<0.050	<0.100	0.0297	0.0242	<0.015	<0.0001	<0.050	<0.020	2.48
HAlG-18	<0.050	<0.100	0.0248	0.138	<0.015	<0.0001	<0.050	<0.020	1.73
HAlG-19	<0.050	<0.100	[0.0199]	0.291	<0.015	<0.0001	<0.050	<0.020	2.34
HAlG-20	<0.050	<0.100	[0.0129]	[0.0162]	<0.015	<0.0001	<0.050	<0.020	2.33
HAlG-21	<0.050	<0.100	0.261	0.634	<0.015	<0.0001	<0.050	<0.020	62.1
HAlG-22	<0.050	<0.100	0.0459	0.0380	<0.015	<0.0001	<0.050	<0.020	1.48
HAlG-23	<0.050	<0.100	0.028	0.034	<0.015	<0.0001	<0.050	<0.020	2.44
HAlG-24	<0.050	<0.100	0.0478	0.0212	0.151	<0.0001	<0.050	<0.020	2.85
HAlG-25	<0.050	<0.100	<0.010	[0.0101]	<0.015	<0.0001	<0.050	<0.020	1.21

[ ] = greater than limit of detection but less than the limit of quantitation

Table 3.11. TCLP Results from the CCC High-Aluminum Glasses

Sample ID	As (mg/L)	Ba (mg/L)	Cd (mg/L)	Cr (mg/L)	Pb (mg/L)	Hg (mg/L)	Se (mg/L)	Ag (mg/L)	B (mg/L)
HAlG-01	<0.050	<0.100	1.21	<0.0100	<0.015	<0.0001	<0.050	<0.020	38.4
HAlG-02	<0.050	<0.100	0.263	0.996	<0.015	<0.0001	<0.050	<0.020	94.3
HAlG-03	<0.050	<0.100	0.0252	<0.0100	<0.015	<0.0001	<0.050	<0.020	2.44
HAlG-04	<0.050	<0.100	4.12	5.20	<0.015	<0.0001	<0.050	<0.020	243
HAlG-05	<0.050	<0.100	0.370	<0.0100	<0.015	<0.0001	<0.050	<0.020	40.5
HAlG-06	<0.050	<0.100	0.126	0.179	<0.015	<0.0001	<0.050	<0.020	26.3
HAlG-07-1	<0.050	<0.100	2.40	[0.0172]	<0.015	<0.0001	<0.050	<0.020	190
HAlG-08	<0.050	<0.100	0.204	<0.0100	<0.015	<0.0001	<0.050	<0.020	122
HAlG-09	<0.050	<0.100	0.158	1.57	<0.015	<0.0001	<0.050	<0.020	58.5
HAlG-11	<0.050	<0.100	1.33	144	<0.015	<0.0001	<0.050	<0.020	618
HAlG-12	<0.050	<0.100	2.74	9.22	<0.015	<0.0001	<0.050	<0.020	418
HAlG-13	<0.050	<0.100	0.503	11.9	<0.015	<0.0001	<0.050	<0.020	935
HAlG-14	<0.050	<0.100	0.827	37.7	<0.015	<0.0001	<0.050	<0.020	893
HAlG-15	<0.050	<0.100	0.862	15.5	<0.015	<0.0001	<0.050	<0.020	171
HAlG-16	<0.050	<0.100	0.256	26.4	<0.015	<0.0001	<0.050	<0.020	291
HAlG-17	<0.050	<0.100	0.447	0.384	<0.015	<0.0001	<0.050	<0.020	41.1
HAlG-18	<0.050	<0.100	3.11	78.3	<0.015	<0.0001	<0.050	<0.020	428
HAlG-19	<0.050	<0.100	1.51	39.2	<0.015	<0.0001	<0.050	<0.020	411
HAlG-20	<0.050	<0.100	0.0249	<0.0100	<0.015	<0.0001	<0.050	<0.020	4.37
HAlG-21	<0.050	<0.100	6.61	4.21	<0.015	<0.0001	<0.050	<0.020	567
HAlG-22	<0.050	<0.100	4.01	2.85	<0.015	<0.0001	<0.050	<0.020	179
HAlG-23	0.104	<0.100	0.0371	<0.0100	<0.015	<0.0001	<0.050	<0.020	3.40
HAlG-24	<0.050	<0.100	0.0912	<0.0100	0.284	<0.0001	<0.050	[0.210]	5.75
HAlG-25	<0.050	<0.100	0.212	<0.0100	<0.015	<0.0001	<0.050	<0.020	148

[ ] = greater than limit of detection but less than the limit of quantitation

Table 3.12. Waste Treatment and Immobilization Plant Delisting Limits, and Resource Conservation and Recovery Act Toxicity and UTS Limits for TCLP (40 CFR 268)

Element	Ag	As	Ba	Cd	Cr	Hg	Pb	Se
WTP Delisting Limit (mg/L)	3.07	0.616	100	0.48	4.95	0.2	5	1
RCRA Toxicity Limit (mg/L)	5	5	100	1	5	0.2	5	1
RCRA UTS Limit (mg/L)	0.14	5	21	0.11	0.6	0.025	0.75	5.7

Figure 3.4 and Figure 3.5 plot the toxicity leaching behaviors of Cr and Cd, respectively, in the normalized form with respect to the normalized B release. Both chromium and cadmium generally showed lower leaching behavior than that of B in both quenched and CCC glasses; however, the leaching of B, Cd, and Cr all tended to increase after CCC treatment. This indicates that the CCC causes the glass to become less durable due to large amounts of nepheline precipitating as the glass cools and affects the glass TCLP behavior negatively for the B, Cd, and Cr leaching.

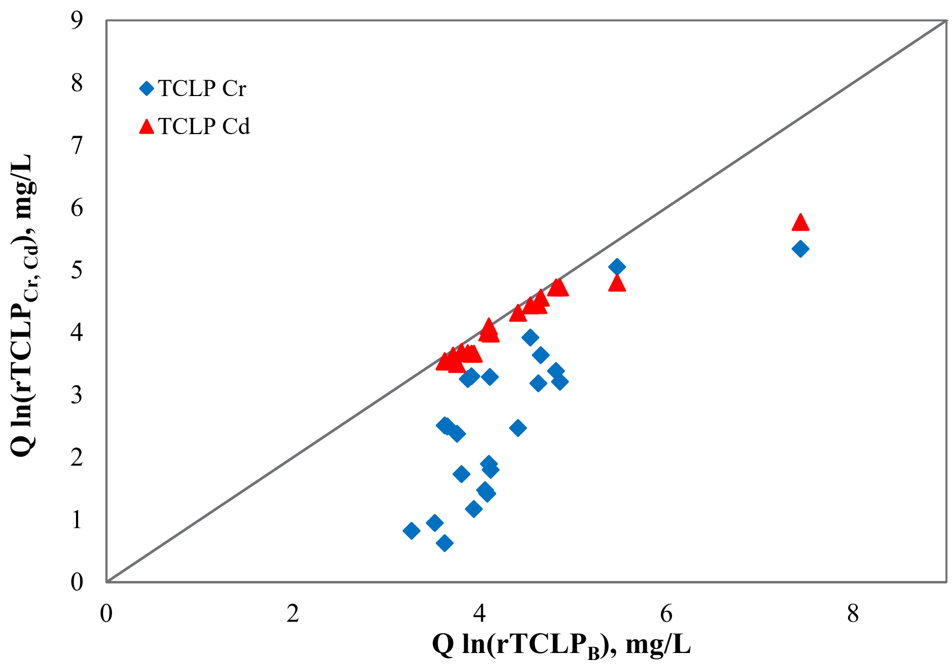

Figure 3.4. TCLP Normalized Releases (mg/L) of Cr and Cd Compared to Normalized B Releases (mg/L) for Quenched Samples of HLW Glasses in the High-Aluminum Study

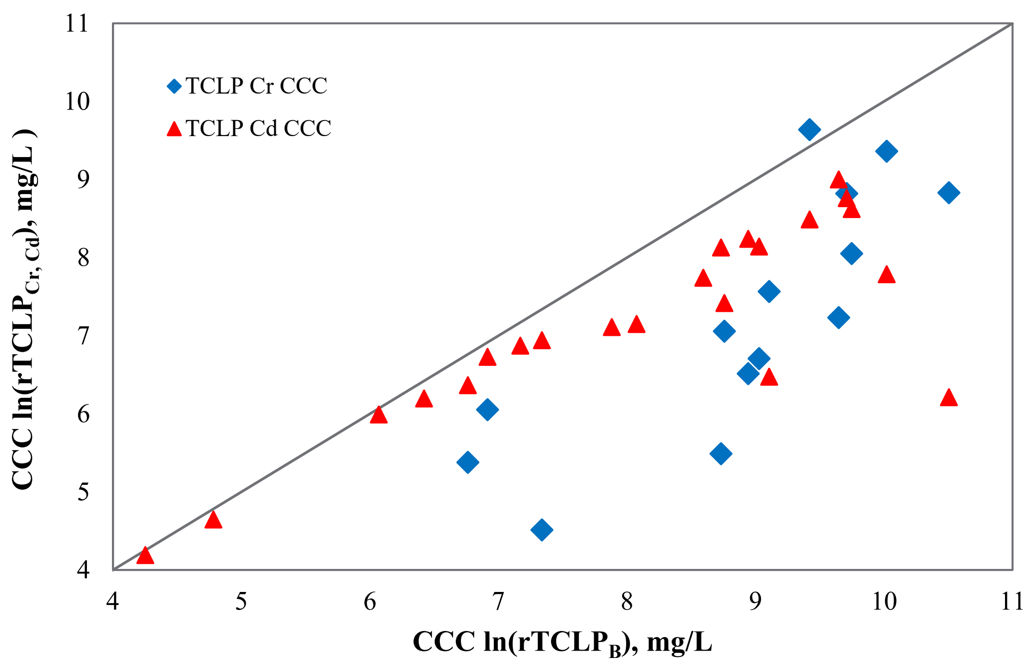

Figure 3.5. TCLP Normalized Releases (mg/L) of Cr and Cd Compared to Normalized B Releases (mg/L) for CCC Samples of HLW Glasses in the High-Aluminum Study

The glasses were divided into three groups depending on the quantity of crystals present, and the TCLP normalized release (rTCLP) of quenched versus CCC samples were plotted. Figure 3.6, Figure 3.7, and Figure 3.8 report the rTCLP$_B$, rTCLP$_{Cr}$, and rTCLP$_{Cd}$ results, respectively. It can be seen from these plots that the amount of crystallinity in the glasses has a large effect on the amount of leaching and failing the

TCLP. With the primary crystal formed in these glasses being nepheline, this is not unexpected as nepheline is known to reduce the durability of the glass.

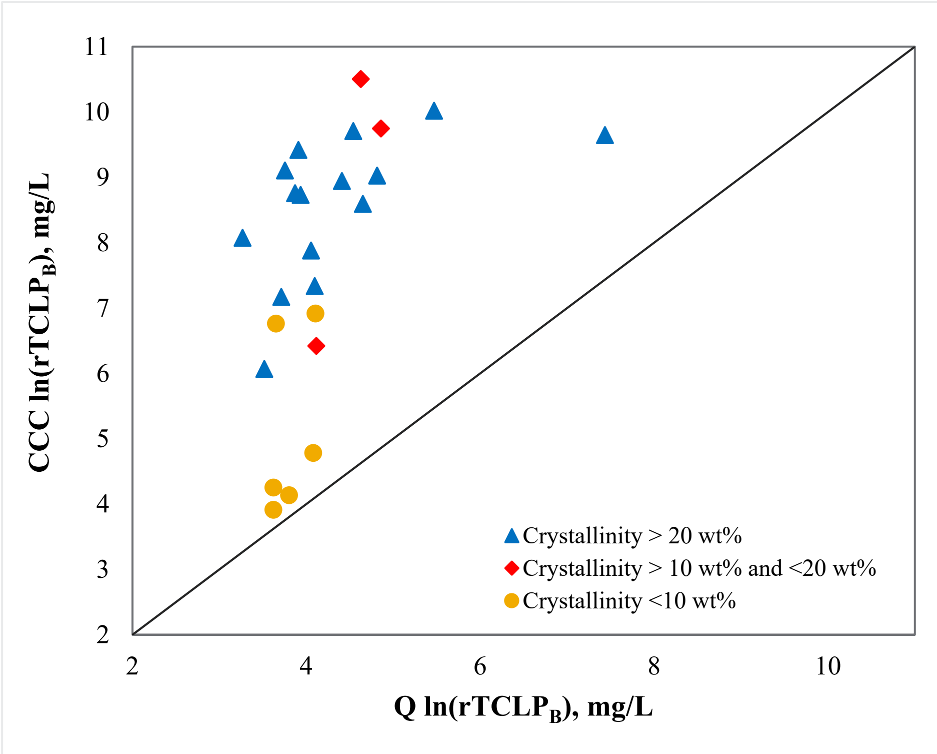

Figure 3.6. Q Versus CCC $rTCLP_B$ Natural Logarithmic Scale of High-Aluminum HLW Glasses

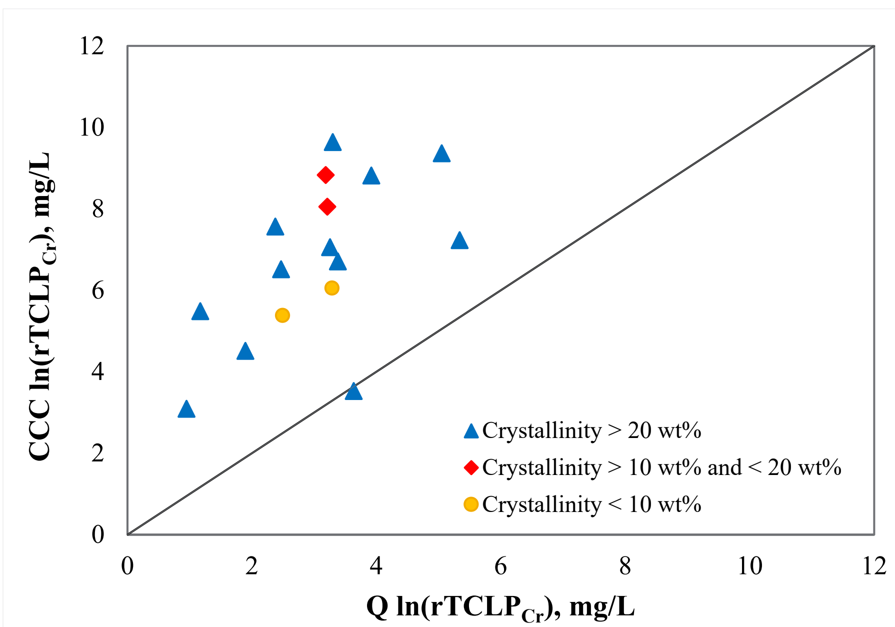

Figure 3.7. Q Versus CCC $rTCLP_{Cr}$ Natural Logarithmic Scale of High-Aluminum HLW Glasses

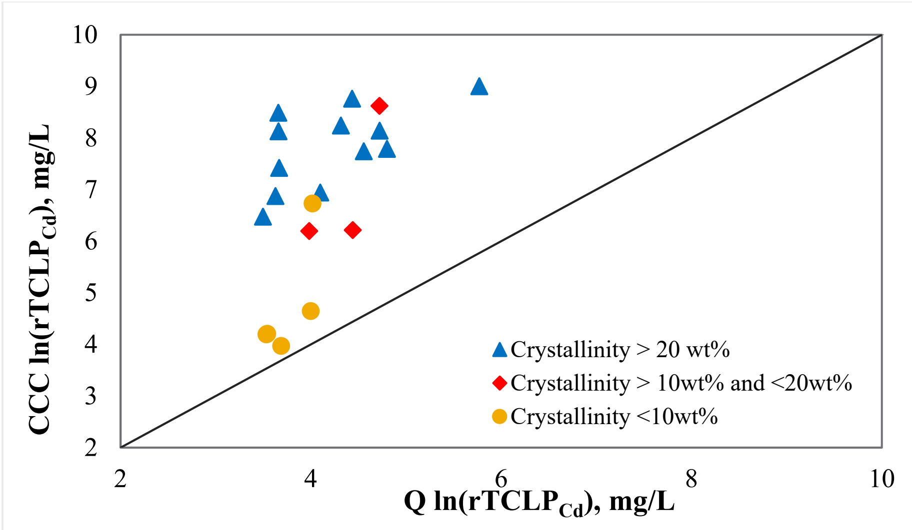

Figure 3.8. Q Versus CCC $rTCLP_{Cd}$ Natural Logarithmic Scale of High-Aluminum HLW Glasses

3.9 Sulfur Solubility Results

Sulfur solubility (i.e., the SSM SO_3 concentrations) of each glass was determined experimentally by measuring SO_3 retention after SSM as discussed in Section 2.10. These results are shown in Table 3.13. The SO_3 concentrations in the baseline glasses were all below 0.45 wt% (including 10 glasses below the detection limit of 0.125 wt%). After SSM, there was a significant increase of SO_3 mass fraction, which is considered the experimentally determined SO_3 solubility of the glass. The SO_3 solubility (i.e., the SSM SO_3 concentration) was between 0.6 and 1.3 wt%, with a majority just under 1 wt%.

All measurements for each oxide in each glass were averaged to determine a representative chemical composition for the SSM version of each glass. A sum of oxides was also computed for each glass based on the averaged, measured values. These values are presented in Appendix J. Comparisons of the overall analyzed glass compositions after normalization of the baseline and sulfur-saturated glass samples showed that after the sulfur-saturation, other major glass components only have negligible changes except for F, which has high volatilization during multiple times of melting and/or extraction into the salt. The K_2O also decreases, possibly due to being washed out in the salt phase.

All measurements for each analyte in each wash solution were averaged to determine a representative chemical composition for each solution; these are reported by Hsieh (2023a)and are presented in Appendix J.

Table 3.13. Target and Saturated Concentrations of SO_3 in High-Aluminum Glasses

	SO_3 wt%		
Sample ID	Target Baseline	Measured Baseline	Sulfate-Saturated
HAlG-01	0.49	0.40	0.83
HAlG-02	0.10	<0.13	0.97
HAlG-03	0.15	<0.13	0.81
HAlG-04	0.42	0.39	0.66
HAlG-05	0.29	0.24	0.80
HAlG-06	0.12	<0.13	0.80
HAlG-07-1	0.41	0.38	0.61
HAlG-08	0.07	<0.13	0.85
HAlG-09	0.11	<0.13	1.23
HAlG-11	0.22	0.17	0.56
HAlG-12	0.31	0.26	0.76
HAlG-13	0.39	0.32	0.96
HAlG-14	0.06	<0.13	0.98
HAlG-15	0.20	0.17	0.93
HAlG-16	0.15	<0.13	0.71
HAlG-17	0.21	0.21	0.89
HAlG-18	0.25	0.23	0.91
HAlG-19	0.09	<0.13	0.87
HAlG-20	0.15	<0.13	1.16
HAlG-21	0.32	0.30	0.93
HAlG-22	0.46	0.41	0.99
HAlG-23	0.27	0.26	1.29
HAlG-24	0.30	0.28	1.09
HAlG-25	0.07	<0.13	0.85

4.0 Conclusion

A glass matrix containing high Al_2O_3 with a total of 25 glasses was designed as described in this report, expanding the DFHLW glass compositional ranges. This matrix was designed by a space-filling method, using component concentration boundaries obtained by expanding the existing database and results from the EWG formulations. This 25-glass matrix met the success criteria for dispersion ratio and range of coverage. The designed glass compositions were made and tested, including composition crystallinity in CCC and isothermal heat-treated samples, density, viscosity, EC, chemical durability, and sulfate solubility. However, one glass (HAlG-10) could not be melted and therefore was not tested.

One objective of the study was to generate data on both sides of current property constraints. Table 4.1 summarizes the HAlG glasses passing or failing the property constraints. Only two glasses met all the property constraints. Twenty-one quenched glasses met the PCT durability constraint; however, 17 glasses failed this constraint after undergoing the CCC treatment. Additionally, eight glasses did not meet the viscosity constraints, one failed the EC constraints, and six exceeded the allowable $T_{2\%}$ for spinel crystal formation. All but two glasses formed nepheline, causing them to fail. All glasses satisfied the SO_3 solubility limit.

These glasses were intentionally designed with high aluminum concentrations (20 to 29 wt%) and a high likelihood of nepheline formation during CCC, which is known to negatively affect glass durability. Some glasses were expected to either fail or approach property constraints to fill data gaps in poorly understood regions of the compositional space due to lack of data.

The resulting dataset provides valuable information to improve model accuracy and reduce prediction uncertainty near property limit boundaries. These insights will ultimately support the development of more robust glass formulation strategies, enabling higher waste loading, reducing operational risks, and expanding the processing envelope.

Table 4.1. Summary of the 24 HAlG Glasses Passing or Failing Property Constraints. Property constraints were taken from Vienna et al. (2024).

Glass ID	w_{SO3}	η_{1150}	ε_{1150}	PCT Q	PCT CCC	TCLP Q	TCLP CCC	Meas NP F/P	Spinel $T_{2\%}$
Constraints	SO_3 in Glass < w_{SO3}	20 to 80 Poise	10 to 70 S/m	<6.44 g/m^2	<6.44 g/m^2	Cr <5 mg/L	Cr <5 mg/L	Measured Nepheline Formation	F if Spinel vol% >2% at 950 °C
HAlG-01	P	F	P	P	F	P	P	F	P
HAlG-02	P	P	P	P	F	P	P	F	P
HAlG-03	P	F	P	P	P	P	P	F	P
HAlG-04	P	F	P	P	F	P	F	F	F
HAlG-05	P	P	P	P	F	P	P	F	F
HAlG-06	P	F	P	P	P	P	P	F	P
HAlG-07-1	P	P	P	P	F	P	P	F	F
HAlG-08	P	P	P	P	F	P	P	F	P
HAlG-09	P	P	P	P	P	P	P	F	P
HAlG-11	P	P	F	F	F	P	F	F	P
HAlG-12	P	P	P	P	F	P	F	F	P
HAlG-13	P	P	P	P	F	P	F	F	F
HAlG-14	P	P	P	P	F	P	F	F	F
HAlG-15	P	F	P	P	F	P	F	F	P
HAlG-16	P	F	P	P	F	P	F	F	P
HAlG-17	P	P	P	P	P	P	P	F	P
HAlG-18	P	P	P	F	F	P	F	F	P
HAlG-19	P	P	P	P	F	P	F	F	P
HAlG-20	P	P	P	P	P	P	P	P	P
HA1G-21	P	P	P	F	F	P	P	F	F
HAlG-22	P	F	P	P	F	P	P	F	P
HAlG-23	P	P	P	P	P	P	P	F	P
HAlG-24	P	P	P	P	P	P	P	P	P
HAlG-25	P	F	P	P	F	P	P	F	P

5.0 References

10 CFR 830 Subpart A, *Quality Assurance Requirements.* Code of Federal Regulations, as amended.

40 CFR 268, *Land Disposal Restrictions*. Code of Federal Regulations, as amended.

ASTM C1285, *Standard Test Methods for Determining Chemical Durability of Nuclear, Hazardous, and Mixed Waste Glasses and Multiphase Glass Ceramics: The Product Consistency Test (PCT)*. ASTM International, West Conshohocken, PA.

ASTM C1720, *Standard Test Method for Determining Liquidus Temperature of Immobilized Waste Glasses and Simulated Waste Glasses*. ASTM International, West Conshohocken, PA.

Bergmann, LM, JK Bernards, GA Hersi, KT Pak, AN Praga, AJ Schubick, UE Zaher, and SN Tilanus. 2022. *High-Level Waste Analysis of Alternatives Model Results Report.* RPP-RPT-61957, Rev. 3, Washington River Protection Solutions, Richland, WA.

Crum, JV, TB Edwards, RL Russell, PJ Workman, MJ Schweiger, RF Schumacher, DE Smith, DK Peeler, and JD Vienna. 2012. "DWPF Startup Frit Viscosity Measurement Round Robin Results." *Journal of the American Ceramic Society*, 95(7):2196-2205.

DOE. 1996. *Waste Acceptance Product Specifications for Vitrified High-Level Waste Forms (WAPS)*. DOE/EM-0093, U.S. Department of Energy, Office of Environmental Management, Washington, D.C.

DOE. 2000. *Design, Construction, and Commissioning of the Hanford Tank Waste Treatment and Immobilization Plant*. Contract DE-AC27-01RV14136, as amended, U.S. Department of Energy, Office of River Protection, Richland, WA.

DOE. 2012. Memorandum, "Enhanced WTP Glass Composition Envelope Development," to C Swan. Inter-Entity Work Order M0ORV00020, October 18, 2012, U.S. Department of Energy, Office of River Protection, Richland, WA.

DOE Order 414.1D, *Quality Assurance*. U.S. Department of Energy, Washington, D.C.

EPA. 1992a. *Toxicity Characteristic Leaching Procedure.* SW-846 Method 1311, Rev. 0. U. S. Environmental Protection Agency, Washington, D.C.

EPA. 1992b. *Acid Digestion of Aqueous Samples and Extracts for Total Metals for Analysis by FLAA or ICP Spectroscopy*. SW-846 Method 3010A, Rev. 1. U. S. Environmental Protection Agency, Washington, D.C.

Goel, A, JS McCloy, R Pokorny, and AA Kruger. 2019. "Challenges with vitrification of Hanford High-Level Waste (HLW) to borosilicate glass—An overview." *Journal of Crystalline Solids: X*, 4:100033.

Hsieh, M. 2022. *Composition Measurements of the HLW HAlG Glasses*. SRNL-STI-2022-00297, Rev. 0, Savannah River National Laboratory, Aiken, SC.

Hsieh, M. 2023a. *Characterization of the Sulfur-Saturated Melt Versions of the HLW HAlG Glasses*. SRNL-STI-2022-00562, Rev. 0, Savannah River National Laboratory, Aiken, SC.

Hsieh, M. 2023b. *Product Consistency Test Results for the HLW HAlG Glasses*. SRNL-STI-2022-00659, Rev. 0, Savannah River National Laboratory, Aiken, SC.

Jin T, DS Kim, LP Darnell, BL Weese, NL Canfield, M Bliss, MJ Schweiger, JD Vienna, and AA Kruger. 2019. "A Crucible Salt Saturation Method for Determining Sulfur Solubility in Glass Melt." *International Journal of Applied Glass Science* 10:92-102.

Kim, DS, DK Peeler, and PR Hrma. 1995. "Effect of Crystallization on the Chemical Durability of Simulated Nuclear Waste Glasses." In *Ceramic Transactions* 61, V Jain, R Palmer (Eds), Environmental Issues and Waste Management Technologies, American Ceramic Society, Westerville, OH, 177–185.

Kroll, JO, ZJ Nelson, CH Skidmore, DR Dixon, and JD Vienna. 2019. "Formulation of High-Al_2O_3 Waste Glasses from Projected Hanford Waste Compositions and Assessment of Current Glass Property Models," *Journal of Non-Crystalline Solids* 517, 17-25.

Lu X, I Sargin, and JD Vienna. 2021. "Predicting nepheline precipitation in waste glasses using ternary submixture model and machine learning." *Journal of American Ceramic Society* 104:5636-5647.

Mellinger, GB and JL Daniel. 1984. *Approved Reference and Testing Materials for Use in Nuclear Waste Management Research and Development Programs*. PNL-4955-2, Pacific Northwest Laboratory, Richland, WA.

NQA-1-2012, *Quality Assurance Requirements for Nuclear Facility Application.* American Society of Mechanical Engineers, New York, NY.

Parsons. 2023. *Waste Treatment and Immobilization Plant High Level Waste Treatment Analysis of Alternatives*. DE-NA0002895, Parsons Corporation, Boston, MA.

Piepel GF, SK Cooley, A Heredia-Langner, SM Landmesser, WK Kot, H Gan, and IL Pegg. 2008. *IHLW PCT, VHT, Viscosity, and Electrical Conductivity Model Development*. VSL-07R1240-4, Rev. 0, Vitreous State Laboratory, The Catholic University of America, Washington, D.C.

Smith, GL. 1993. *Characterization of Analytical Reference Glass-1 (ARG-1)*. PNL-8992, Pacific Northwest Laboratory, Richland, WA.

Vienna, JD, P Hrma, JV Crum, and M Mika. 2001. "Liquidus temperature-composition model for multi-component glasses in the Fe, Cr, Ni, and Mn spinel primary phase field." *Journal of Non-Crystalline Solids* 292(1-3):1-24.

Vienna, JD, A Fluegal, DS Kim, and P Hrma. 2009. *Glass Property Data and Models for Estimating High-Level Waste Glass Volume*. PNNL-18501, Pacific Northwest National Laboratory, Richland, WA.

Vienna, JD, DC Skorski, D Kim, and J Matyas, 2013. *Glass Property Models and Constraints for Estimating Glass to be Produced at Hanford by Implementing Current Advanced Glass Formulation Efforts.* PNNL-22631, Rev. 1, ORP-58289, Pacific Northwest National Laboratory, Richland, WA.

Vienna, JD, GF Piepel, DS Kim, JV Crum, CE Lonergan, BA Stanfill, BJ Riley, SK Cooley, and T Jin. 2016. *2016 Update of Hanford Glass Property Models and Constraints for Use in Estimating the Glass Mass to be Produced at Hanford by Implementing Current Enhanced Glass Formulation Efforts*. PNNL-25835, Pacific Northwest National Laboratory, Richland, WA.

Vienna, JD, JO Kroll, PR Hrma, JB Lang, and JV Crum. 2017. "Submixture model to predict nepheline precipitation in waste glasses." *International Journal of Applied Glass Science* 8(2):143-157.

Vienna, JD, X Lu, P Ferkl, LL Gunnell, A Heredia-Langner, NA Lumetta, T Jin, and JT Reiser. 2024. *Glass Property-Composition Models Update for use in Direct Feed High-Level Waste Flowsheet Development,* PNNL-35884, Pacific Northwest National Laboratory, Richland, WA.

Appendix A – Morphology/Color of Each Quenched Glass

The photos in this appendix show each glass after the final melting in a Pt-alloy crucible at the specified melt temperature.

Figure A.1. Photo of Glass HAlG-01 Morphology of Third Melt at 1250 °C for 1 h

Figure A.2. Photo of Glass HAlG-02 Morphology of Third Melt at 1250 °C for 1 h

Figure A.3. Photo of Glass HAlG-03 Morphology of Fourth Melt at 1250 °C for 1 h

Figure A.4. Photo of Glass HAlG-04 Morphology of Second Melt at 1200 °C for 1 h

Figure A.5. Photo of Glass HAlG-05 Morphology of Second Melt at 1150 °C for 1 h

Figure A.6. Photo of Glass HAlG-06 Morphology of Second Melt at 1150 °C for 1 h

Figure A.7. Photo of Glass HAlG-07-1 Morphology of Fourth Melt at 1200 °C for 1 h

Figure A.8. Photo of Glass HAlG-08 Morphology of Second Melt at 1150 °C for 1 h

Figure A.9. Photo of Glass HAlG-09 Morphology of Fourth Melt at 1400 °C for 1 h

Figure A.10. Photo of Glass HAlG-10 Morphology of Second Melt at 1300 °C for 1 h

Figure A.11. Photo of Glass HAlG-11 Morphology of Third Melt at 1350 °C for 1 h

Figure A.12. Photo of Glass HAlG-12 Morphology of Fourth Melt at 1150 °C for 2 h

Figure A.13. Photo of Glass HAlG-13 Morphology of Second Melt at 1400 °C for 1 h

Figure A.14. Photo of Glass HAlG-14 Morphology of Second Melt Stirred at 1150 °C for 1 h

Figure A.15. Photo of Glass HAlG-15 Morphology of Second Melt at 1150 °C for 1 h

Figure A.16. Photo of Glass HAlG-16 Morphology of Second Melt Stirred at 1400 °C for 1 h

Figure A.17. Photo of Glass HAlG-17 Morphology of Third Melt at 1200 °C for 1 h

Figure A.18. Photo of Glass HAlG-18 Morphology of Third Melt at 1250 °C for 1 h

Figure A.19. Photo of Glass HAlG-19 Morphology of Second Melt Stirred at 1300 °C for 1 h

Figure A.20. Photo of Glass HAlG-20 Morphology of Second Melt at 1150 °C for 1 h

Figure A.21. Photo of Glass HALG-21 Morphology of Second Melt at 1150 °C for 1 h

Figure A.22. Photo of Glass HAlG-22 Morphology of Third Melt at 1150 °C for 1 h

Figure A.23. Photo of Glass HAlG-23 Morphology of Second Melt at 1150 °C for 1 h

Figure A.24. Photo of Glass HAlG-24 Morphology of Second Melt Stirred at 1150 °C for 1 h

Figure A.25. Photo of Glass HAlG-25 Morphology of Second Melt Stirred at 1150 °C for 1 h

Appendix B – XRD of Quenched Glasses

This appendix shows the X-ray diffraction (XRD) plots of the high-aluminum glasses after melting and quenching. These glasses were found to range from being amorphous to developing crystals of primarily spinel and chromium oxide with some nepheline, as shown in the following plots. The percentage of crystal content reported in the XRD scans is presented before any adjustments were made from spiking with 5 wt% of high-purity cerium oxide. The data is corrected not only for the amount of cerium oxide introduced into the samples, but also to account for the fact that the cerium oxide used was only 51% crystalline.

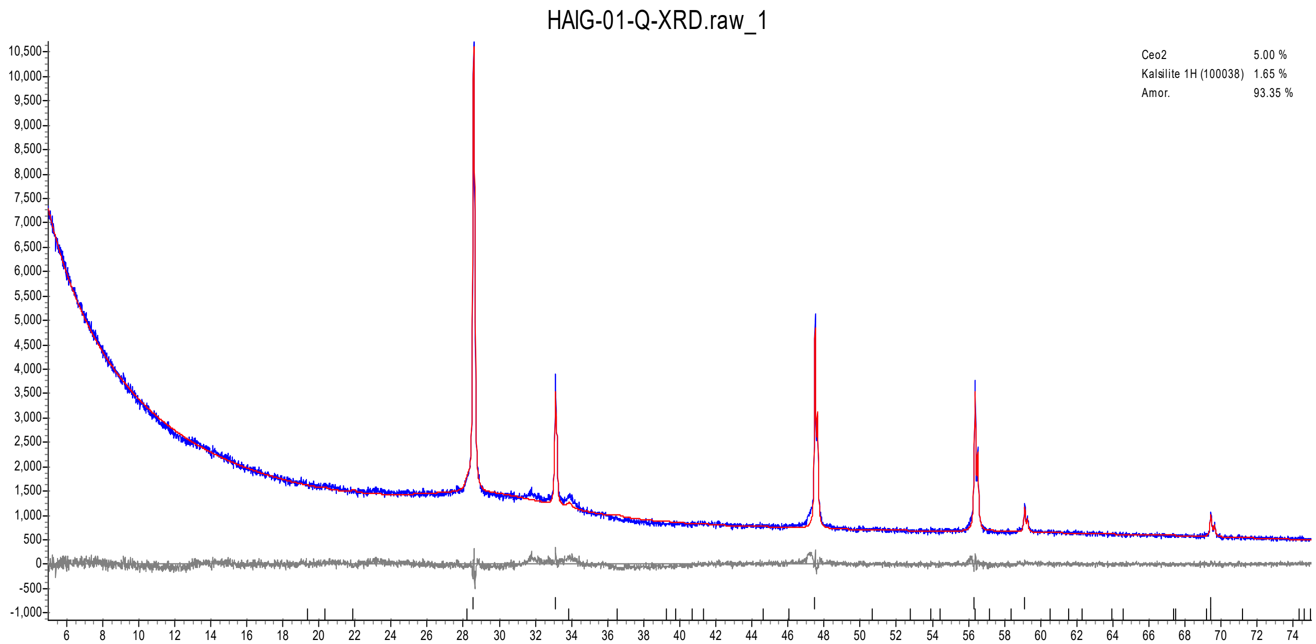

Phase Name	Wt% of Spiked	Wt% in Spiked Sample	Wt% in Original Sample
CeO_2	2.564	2.564	0.000
$KAlSiO_4$	0.000	1.077	1.134

Figure B.1. XRD Spectrum of Quenched Glass HAlG-01

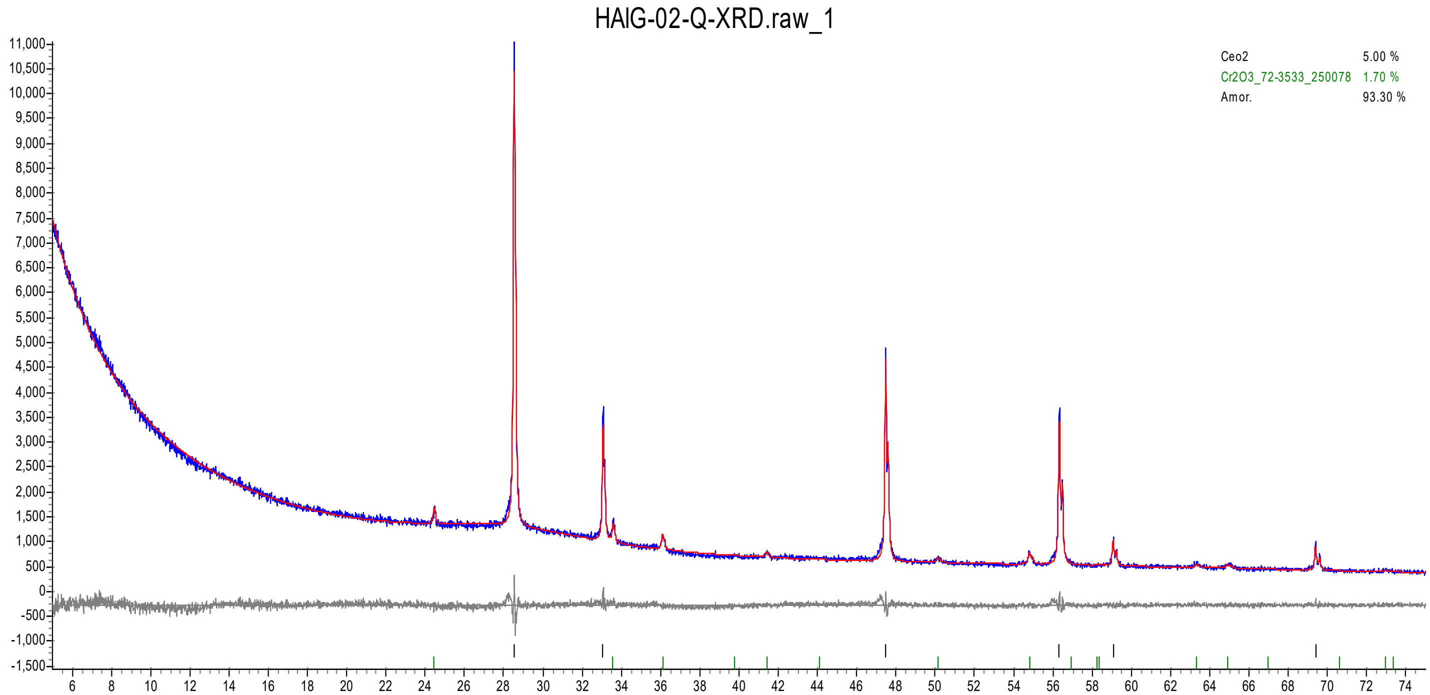

Phase Name	Wt% of Spiked	Wt% in Spiked Sample	Wt% in Original Sample
CeO_2	2.565	2.565	0.000
Cr_2O_3	0.000	0.910	0.958

Figure B.2. XRD Spectrum of Quenched Glass HAlG-02

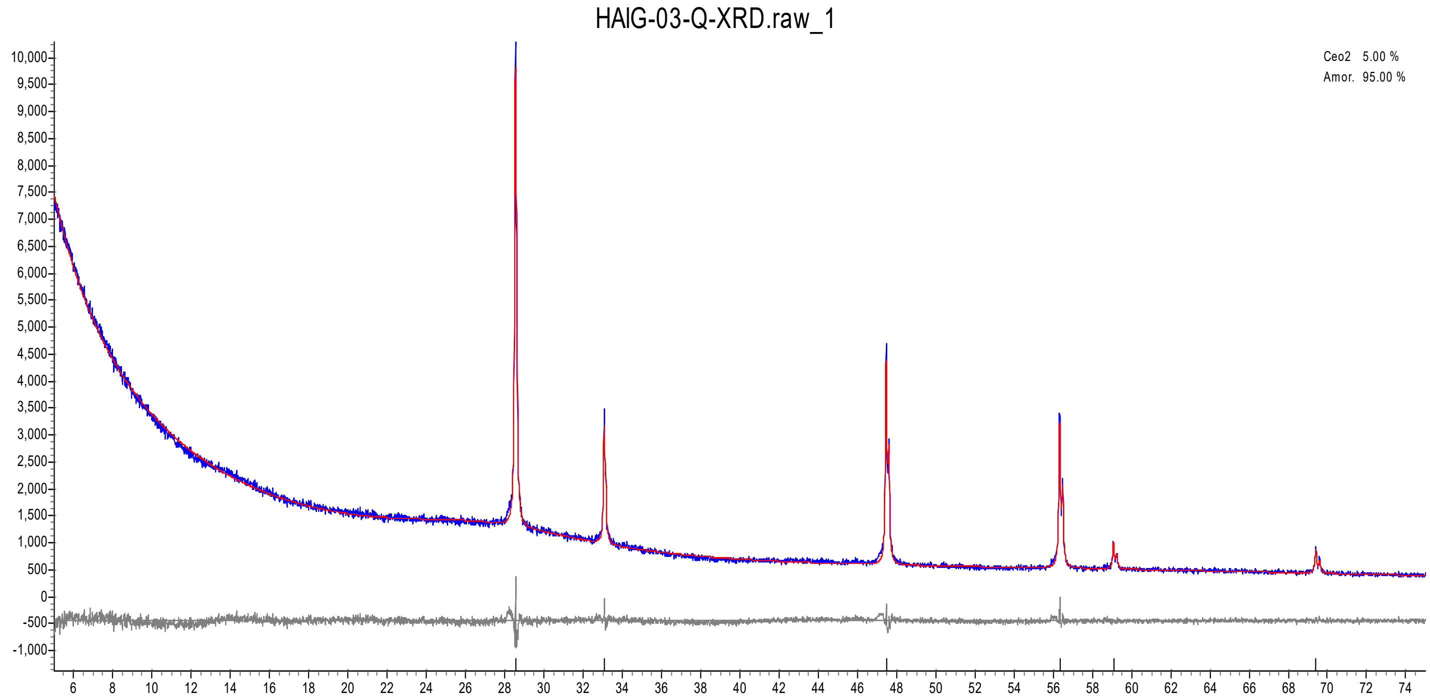

Figure B.3. XRD Spectrum of Quenched Glass HAlG-03

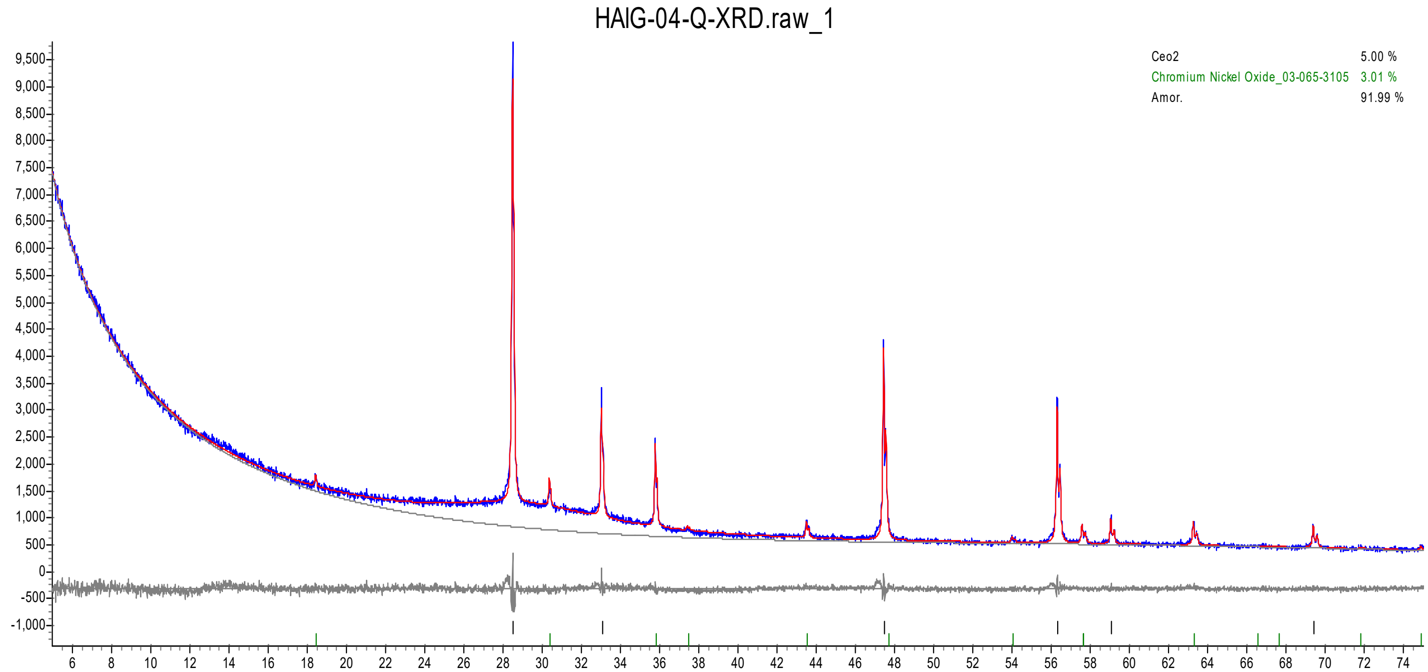

Phase Name	Wt% of Spiked	Wt% in Spiked Sample	Wt% in Original Sample
CeO_2	2.564	2.564	0.000
$NiCr_2O_4$ (Spinel)	0.000	1.642	1.729

Figure B.4. XRD Spectrum of Quenched Glass HAlG-04

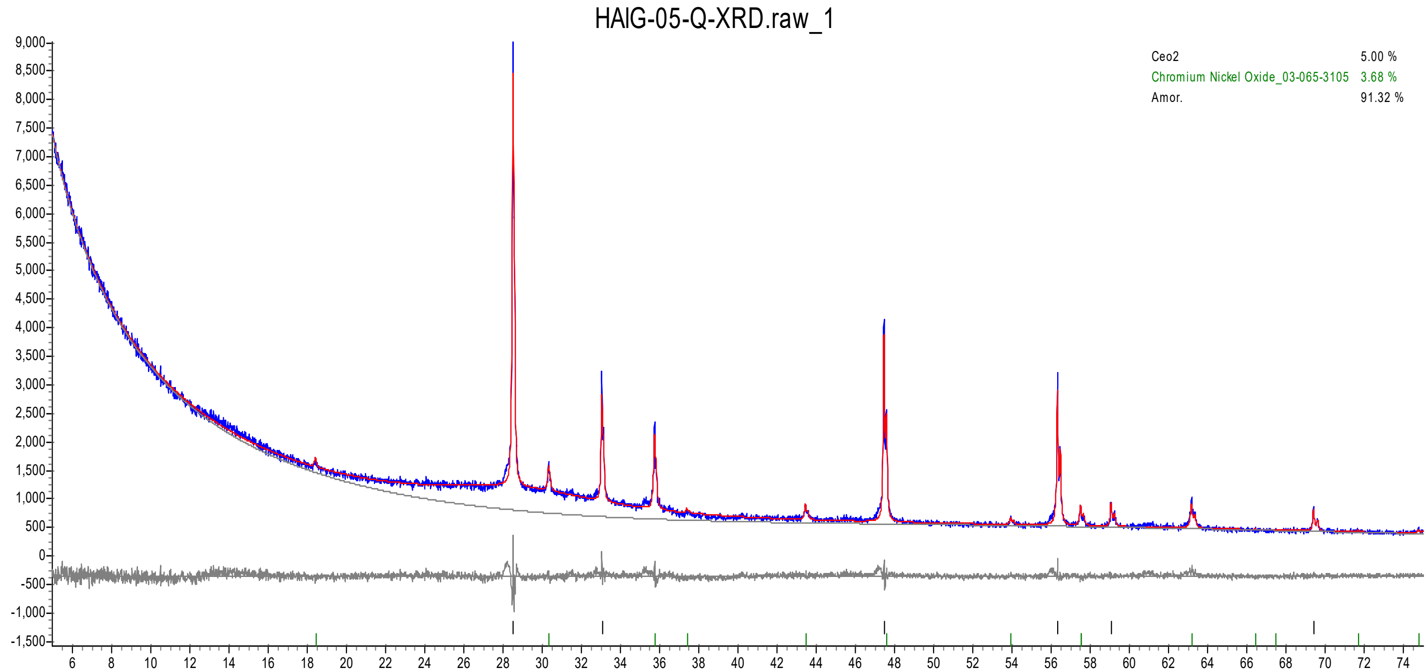

Phase Name	Wt% of Spiked	Wt% in Spiked Sample	Wt% in Original Sample
CeO_2	2.565	2.565	0.000
$NiCr_2O_4$ (Spinel)	0.000	1.992	2.097

Figure B.5. XRD Spectrum of Quenched Glass HAlG-05

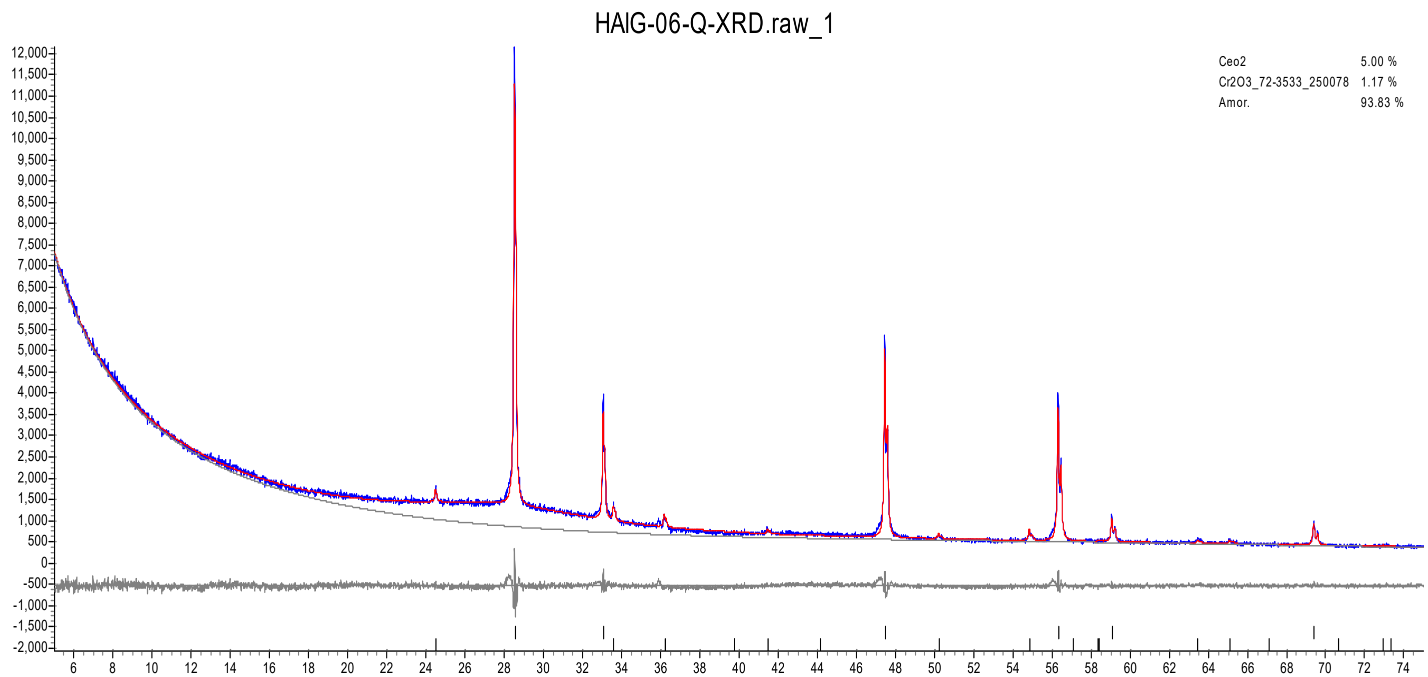

Phase Name	Wt% of Spiked	Wt% in Spiked Sample	Wt% in Original Sample
CeO_2	2.563	2.563	0.000
Cr_2O_3	0.000	0.647	0.681

Figure B.6. XRD Spectrum of Quenched Glass HAlG-06

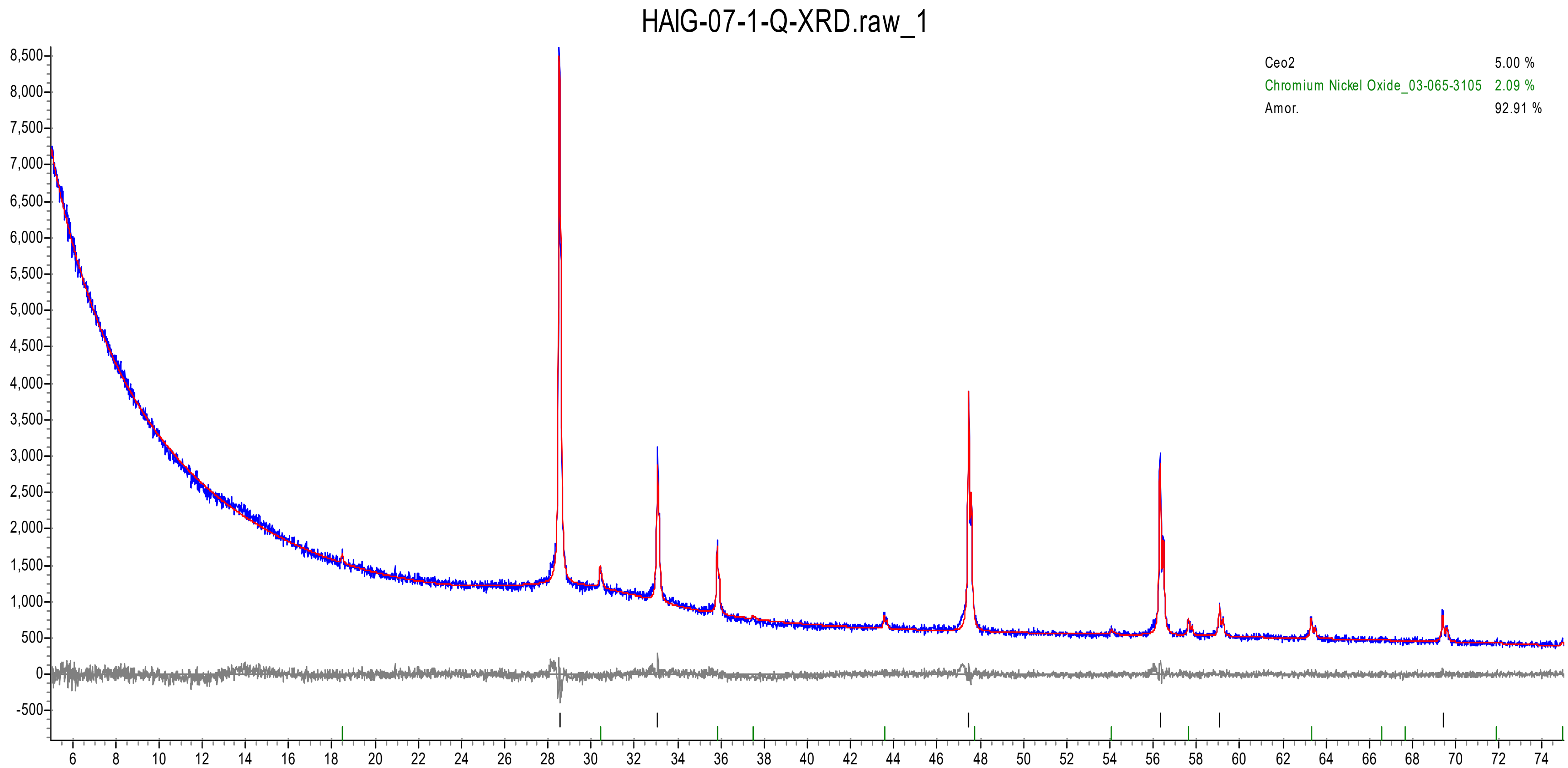

Phase Name	Wt% of Spiked	Wt% in Spiked Sample	Wt% in Original Sample
CeO_2	2.562	2.562	0.000
$NiCr_2O_4$ (Spinel)	0.000	1.147	1.207

Figure B.7. XRD Spectrum of Quenched Glass HAlG-07-1

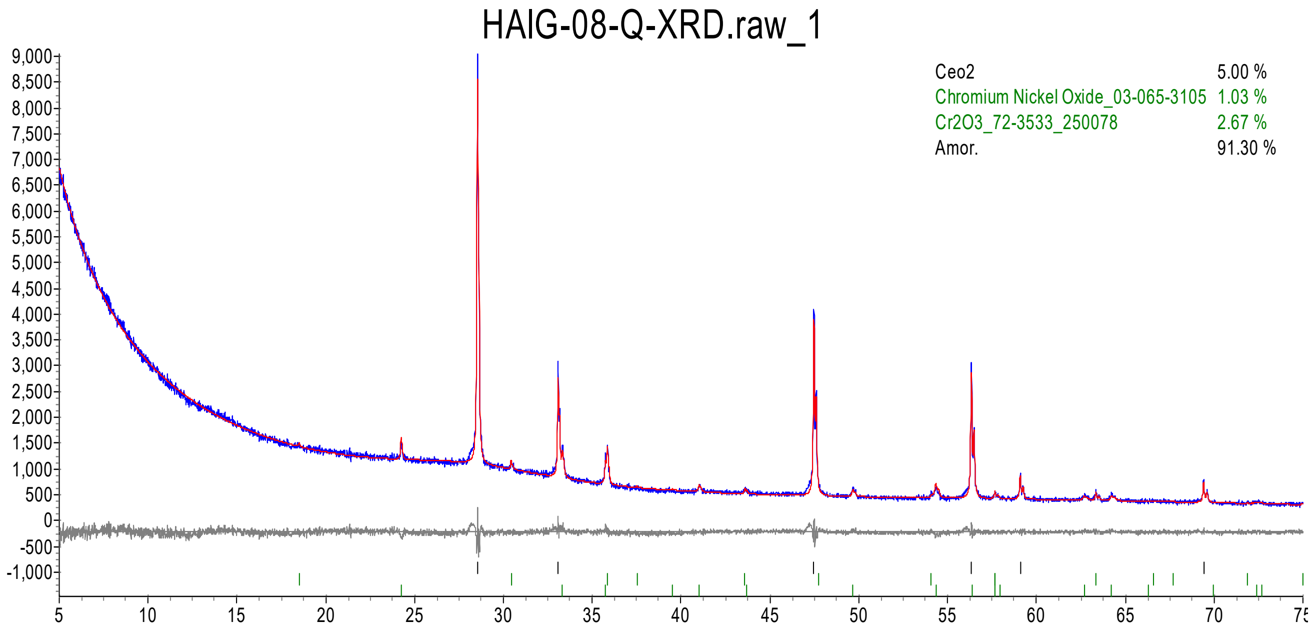

Phase Name	Wt% of Spiked	Wt% in Spiked Sample	Wt% in Original Sample
CeO_2	2.563	2.563	0.000
$NiCr_2O_4$ (Spinel)	0.000	0.585	0.615
$Cr_{0.75}Fe_{1.25}O_3$	0.000	1.531	1.612

Figure B.8. XRD Spectrum of Quenched Glass HAlG-08

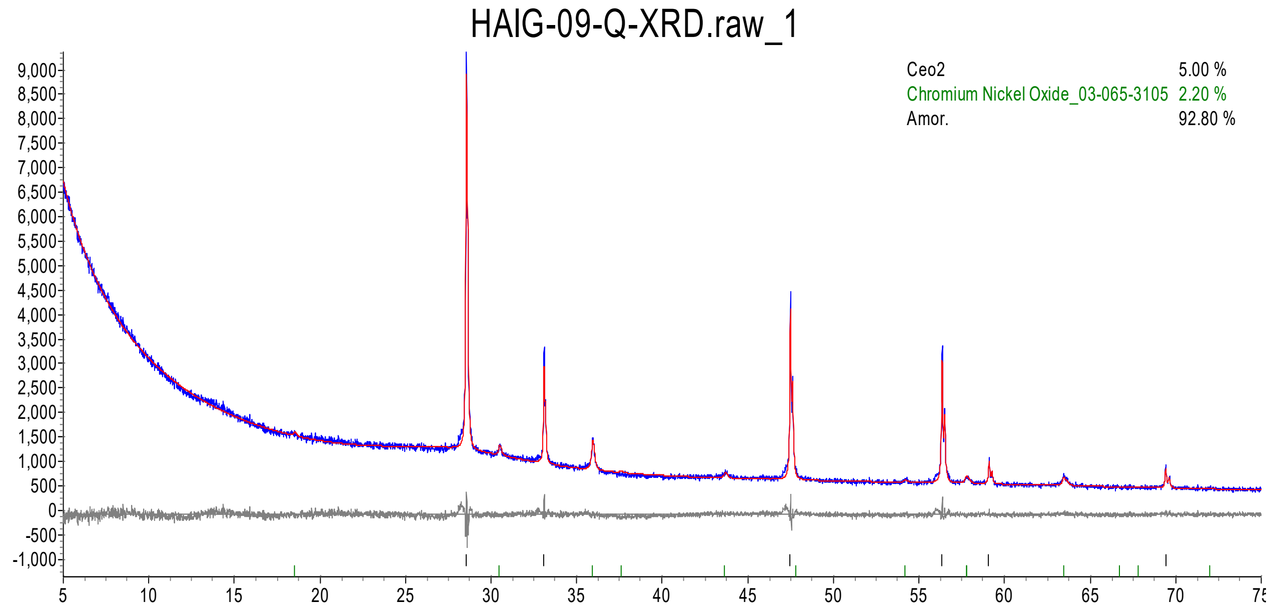

Phase Name	Wt% of Spiked	Wt% in Spiked Sample	Wt% in Original Sample
CeO_2	2.565	2.565	0.000
$NiCr_2O_4$ (Spinel)	0.000	1.287	1.354

Figure B.9. XRD Spectrum of Quenched Glass HAlG-09

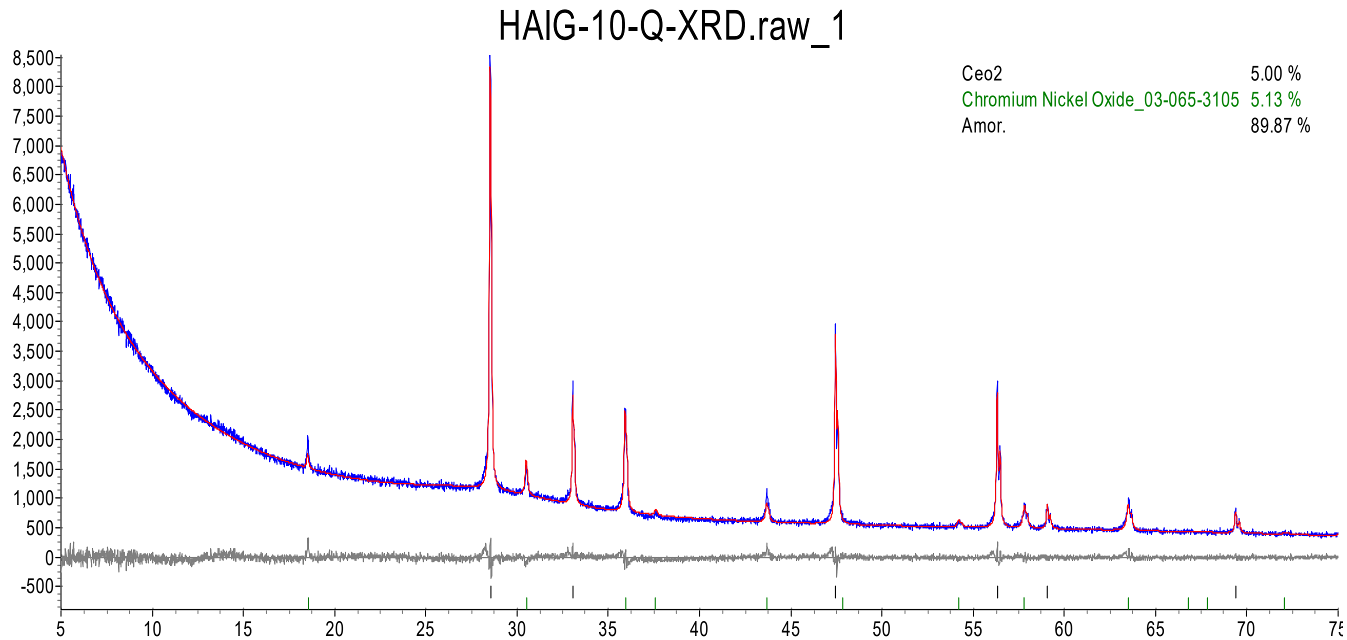

Phase Name	Wt% of Spiked	Wt% in Spiked Sample	Wt% in Original Sample
CeO_2	2.564	2.564	0.000
$NiCr_2O_4$ (Spinel)	0.000	2.841	2.991

Figure B.10. XRD Spectrum of Quenched Glass HAlG-10

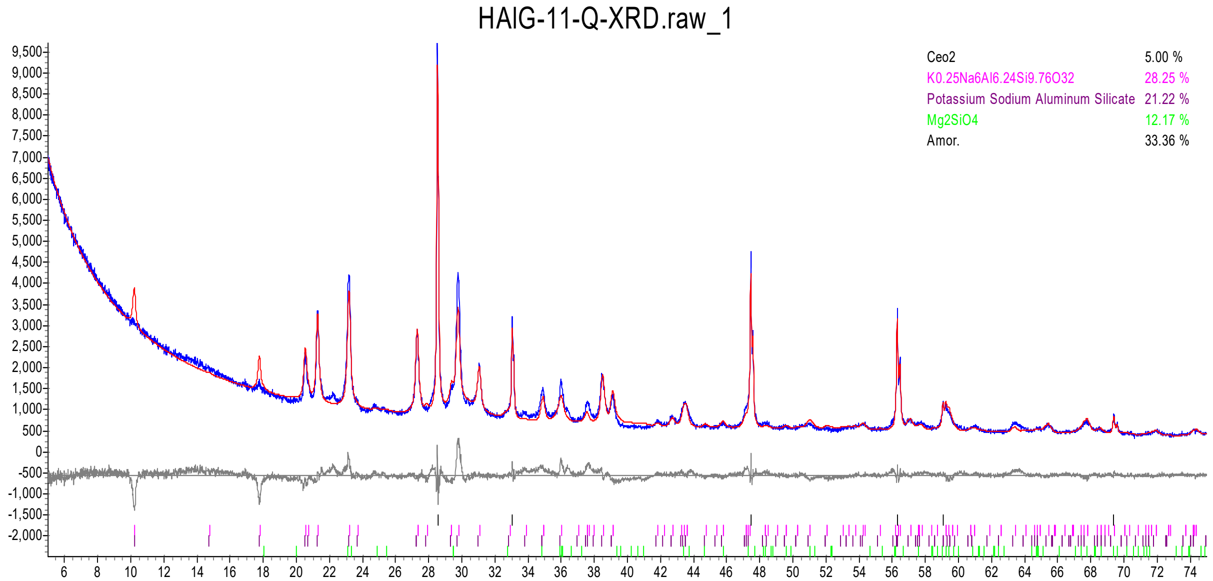

Phase Name	Wt% of Spiked	Wt% in Spiked Sample	Wt% in Original Sample
CeO_2	2.564	2.564	0.000
KNaAlSiO (Nepheline)	0.000	30.412	32.013
Mg_2SiO_4	0.000	3.546	3.733

Figure B.11. XRD Spectrum of Quenched Glass HAlG-11

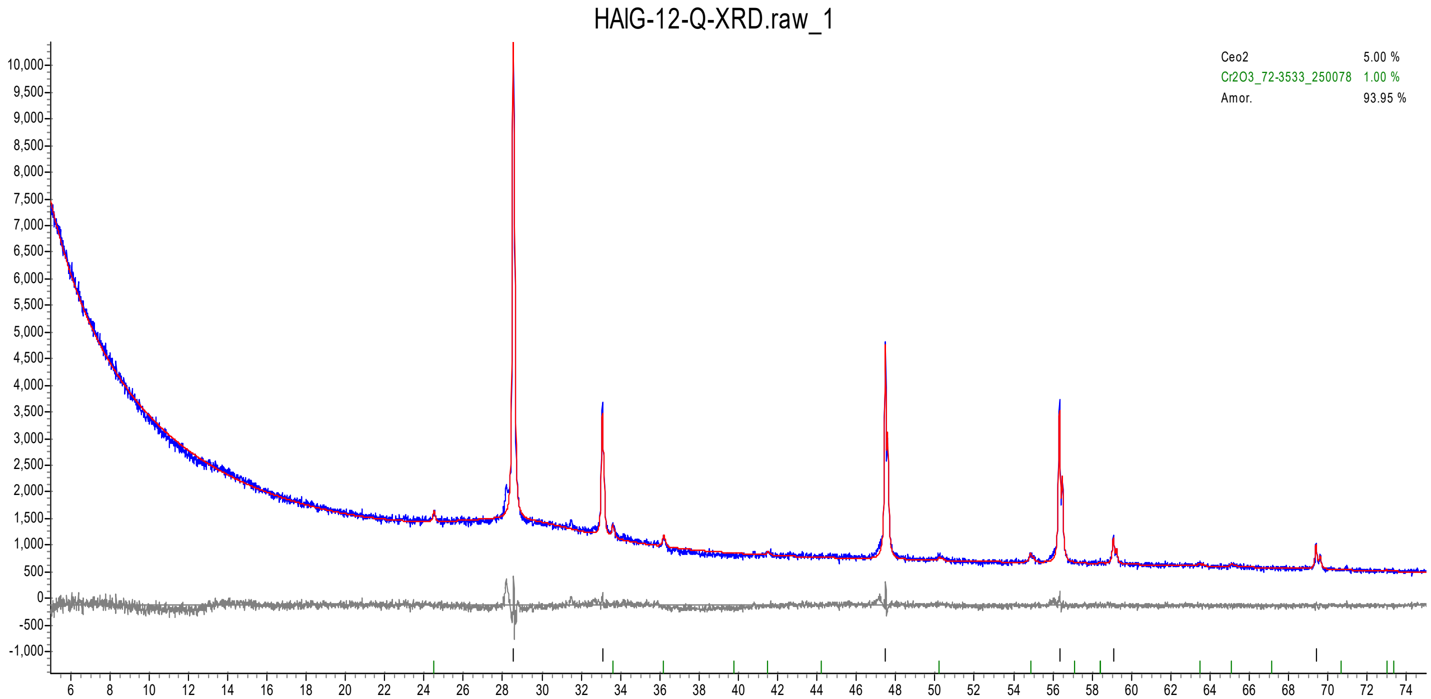

Phase Name	Wt% of Spiked	Wt% in Spiked Sample	Wt% in Original Sample
CeO_2	2.564	2.564	0.000
Cr_2O_3	0.000	0.531	0.559

Figure B.12. XRD Spectrum of Quenched Glass HAlG-12

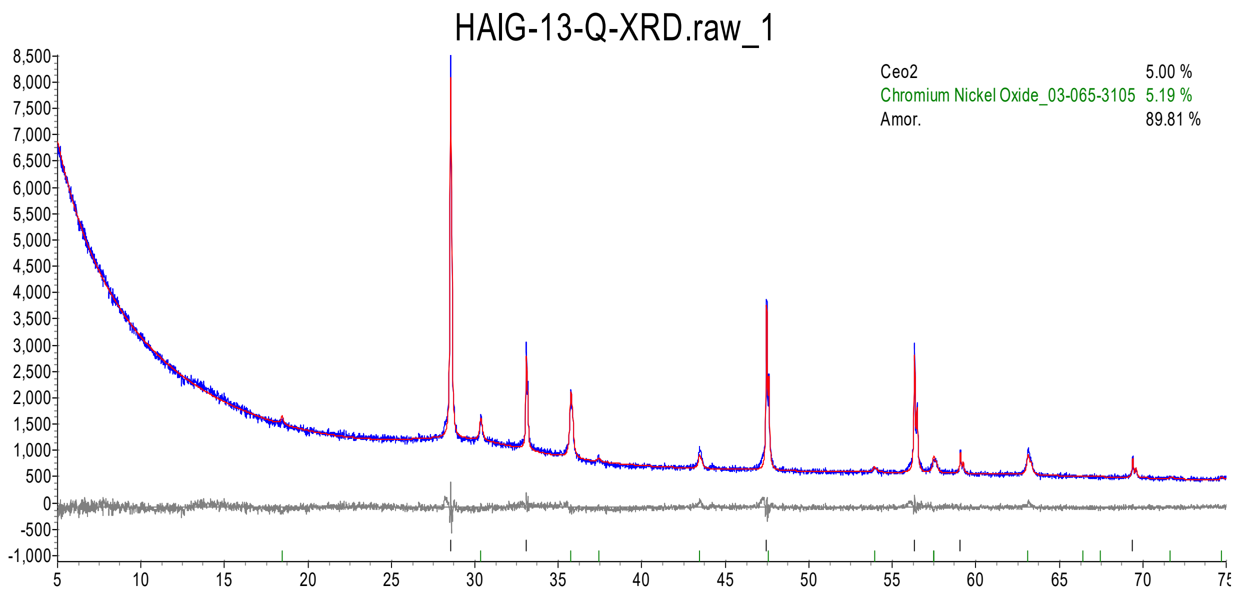

Phase Name	Wt% of Spiked	Wt% in Spiked Sample	Wt% in Original Sample
CeO_2	2.563	2.563	0.000
$NiCr_2O_4$ (Spinel)	0.000	2.833	2.982

Figure B.13. XRD Spectrum of Quenched Glass HAlG-13

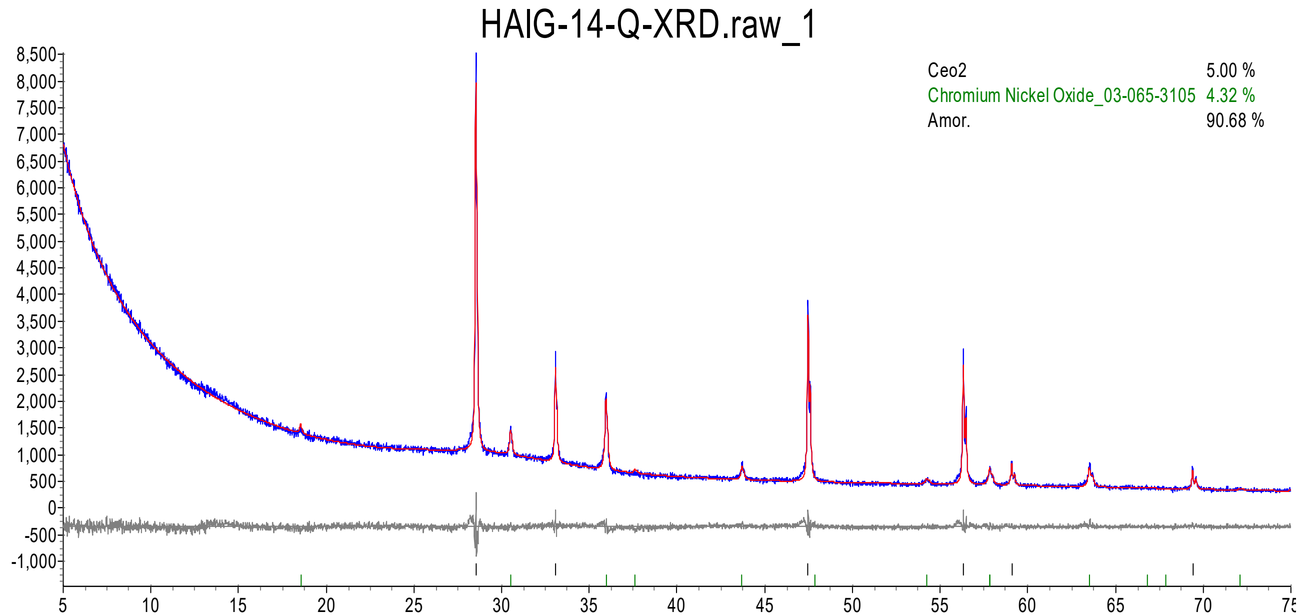

Phase Name	Wt% of Spiked	Wt% in Spiked Sample	Wt% in Original Sample
CeO_2	2.566	2.566	0.000
$NiCr_2O_4$ (Spinel)	0.000	2.359	2.483

Figure B.14. XRD Spectrum of Quenched Glass HAlG-14

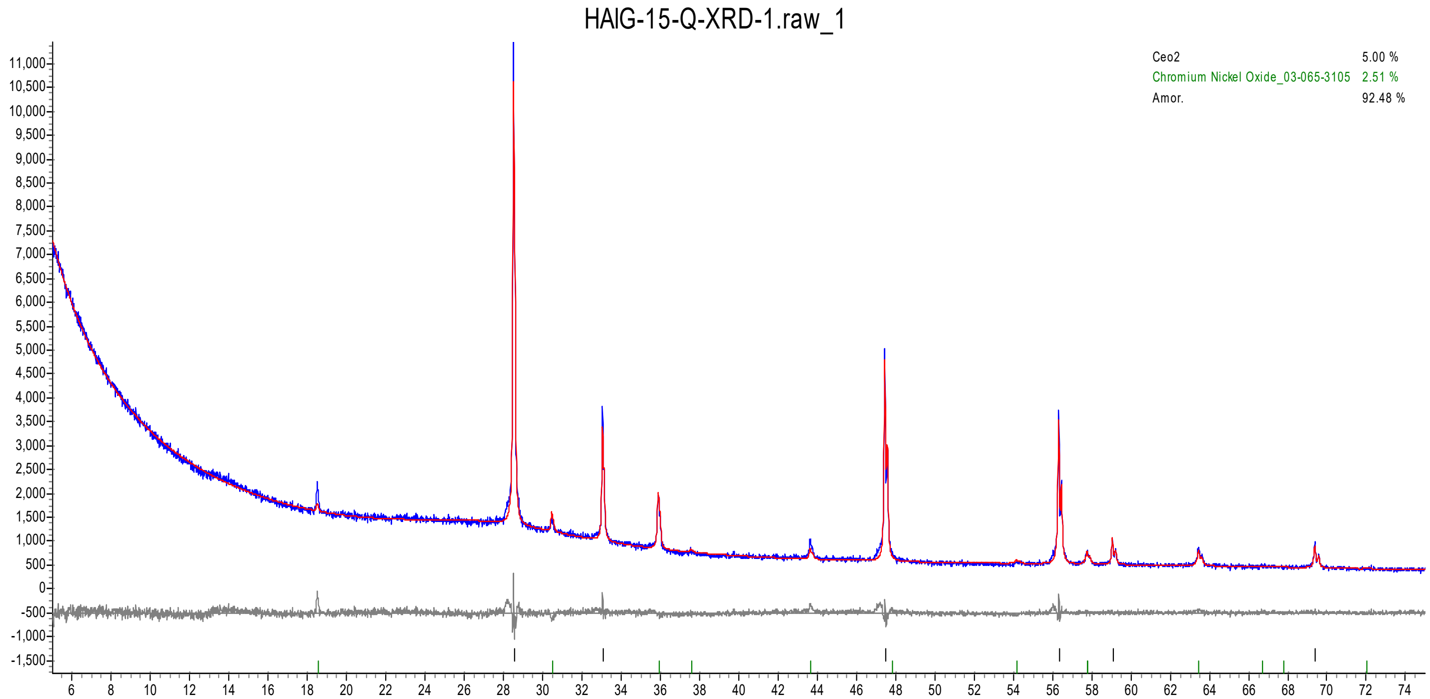

Phase Name	Wt% of Spiked	Wt% in Spiked Sample	Wt% in Original Sample
CeO_2	2.565	2.565	0.000
$NiCr_2O_4$ (Spinel)	0.000	1.403	1.477

Figure B.15. XRD Spectrum of Quenched Glass HAlG-15

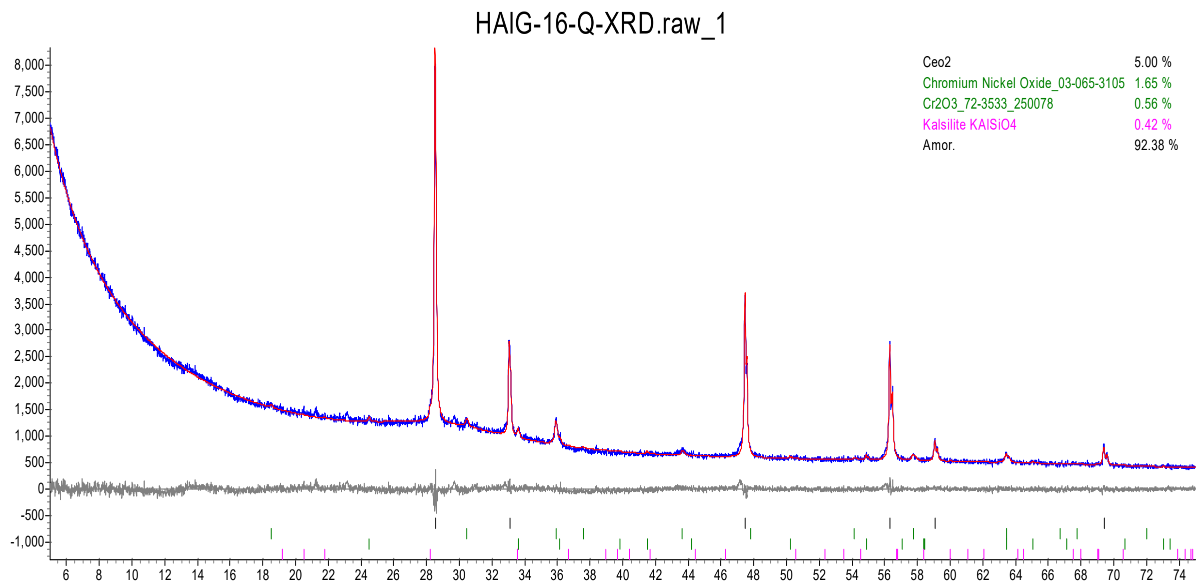

Phase Name	Wt% of Spiked	Wt% in Spiked Sample	Wt% in Original Sample
CeO_2	2.564	2.564	0.000
$NiCr_2O_4$ (Spinel)	0.000	0.940	0.990
Cr_2O_3	0.000	0.271	0.286
$KAlSiO_4$	0.000	0.258	0.272

Figure B.16. XRD Spectrum of Quenched Glass HAlG-16

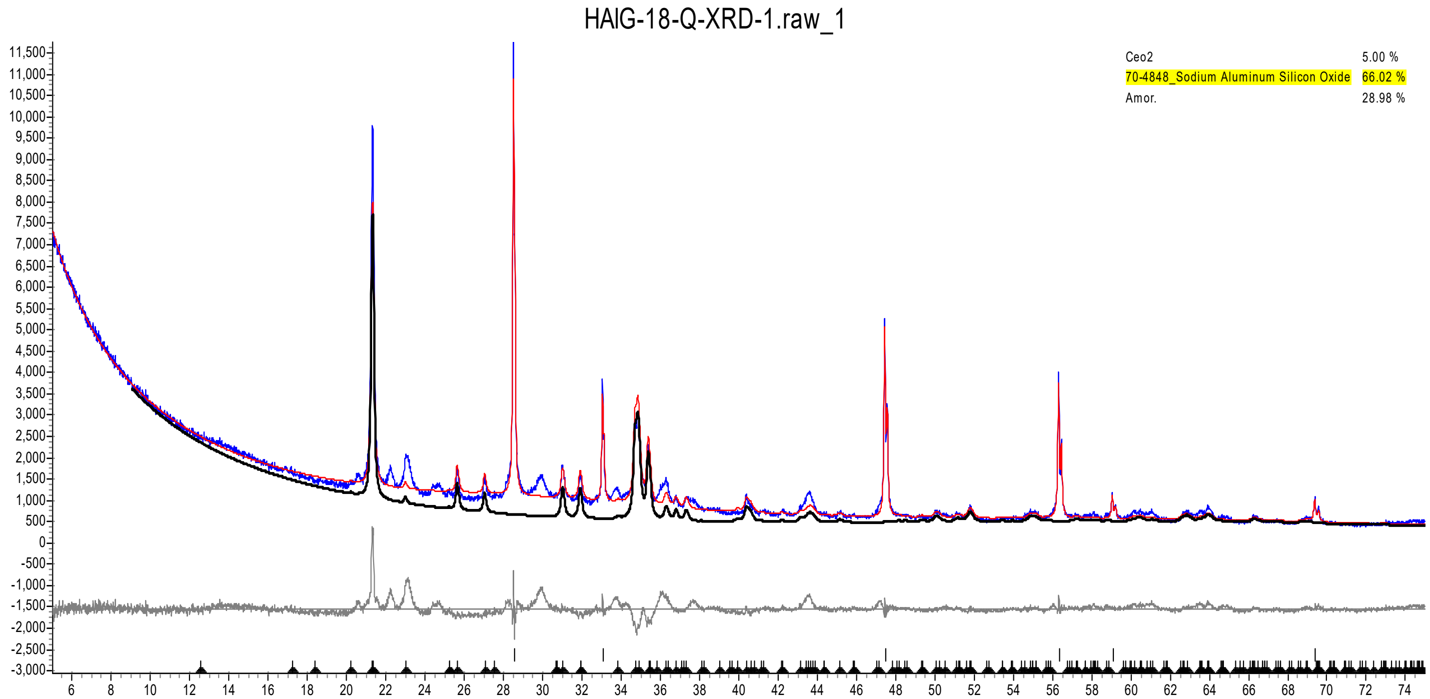

Phase Name	Wt% of Spiked	Wt% in Spiked Sample	Wt% in Original Sample
CeO_2	2.564	2.564	0.000
$NaAlSiO_4$	0.000	35.409	37.274

Figure B.17. XRD Spectrum of Quenched Glass HAlG-18

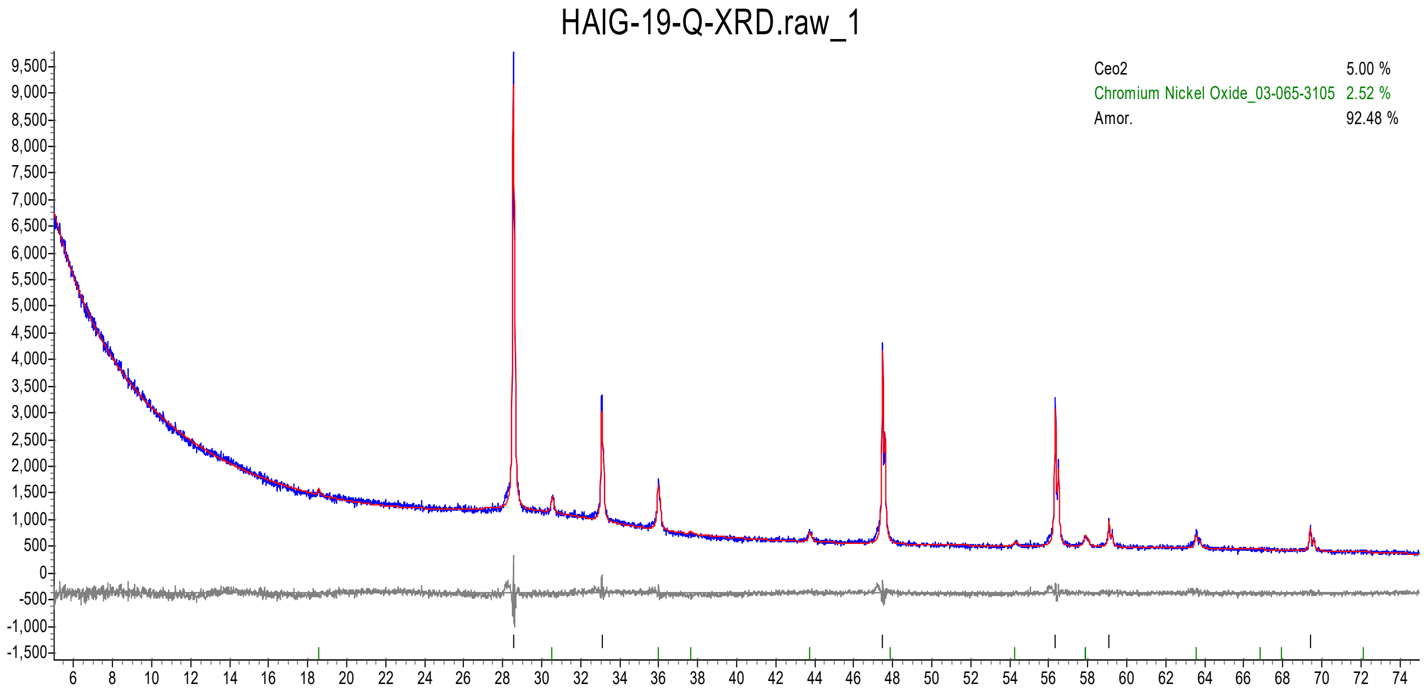

Phase Name	Wt% of Spiked	Wt% in Spiked Sample	Wt% in Original Sample
CeO_2	2.564	2.564	0.000
$NiCr_2O_4$ (Spinel)	0.000	1.374	1.446

Figure B.18. XRD Spectrum of Quenched Glass HAlG-19

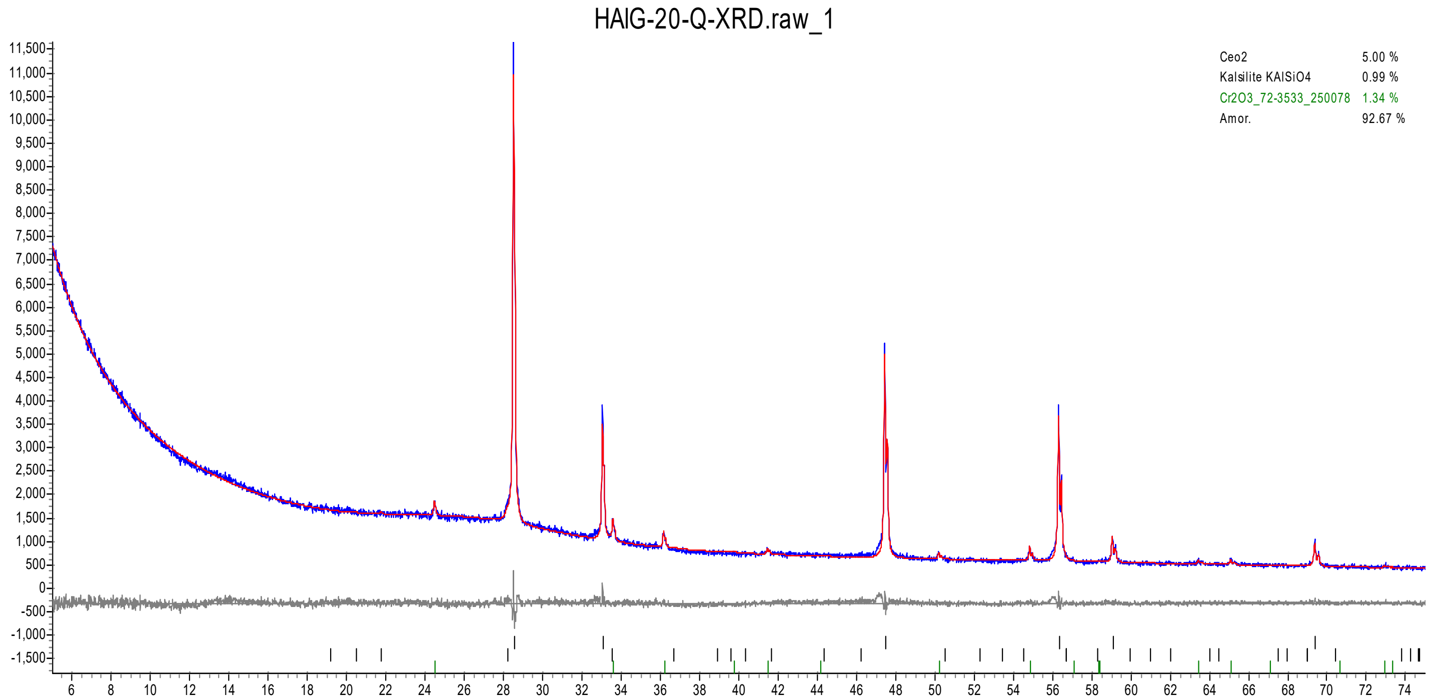

Phase Name	Wt% of Spiked	Wt% in Spiked Sample	Wt% in Original Sample
CeO_2	2.563	2.563	0.000
$KAlSiO_4$	0.000	0.895	0.942
Cr_2O_3	0.000	0.798	0.840

Figure B.19. XRD Spectrum of Quenched Glass HAlG-20

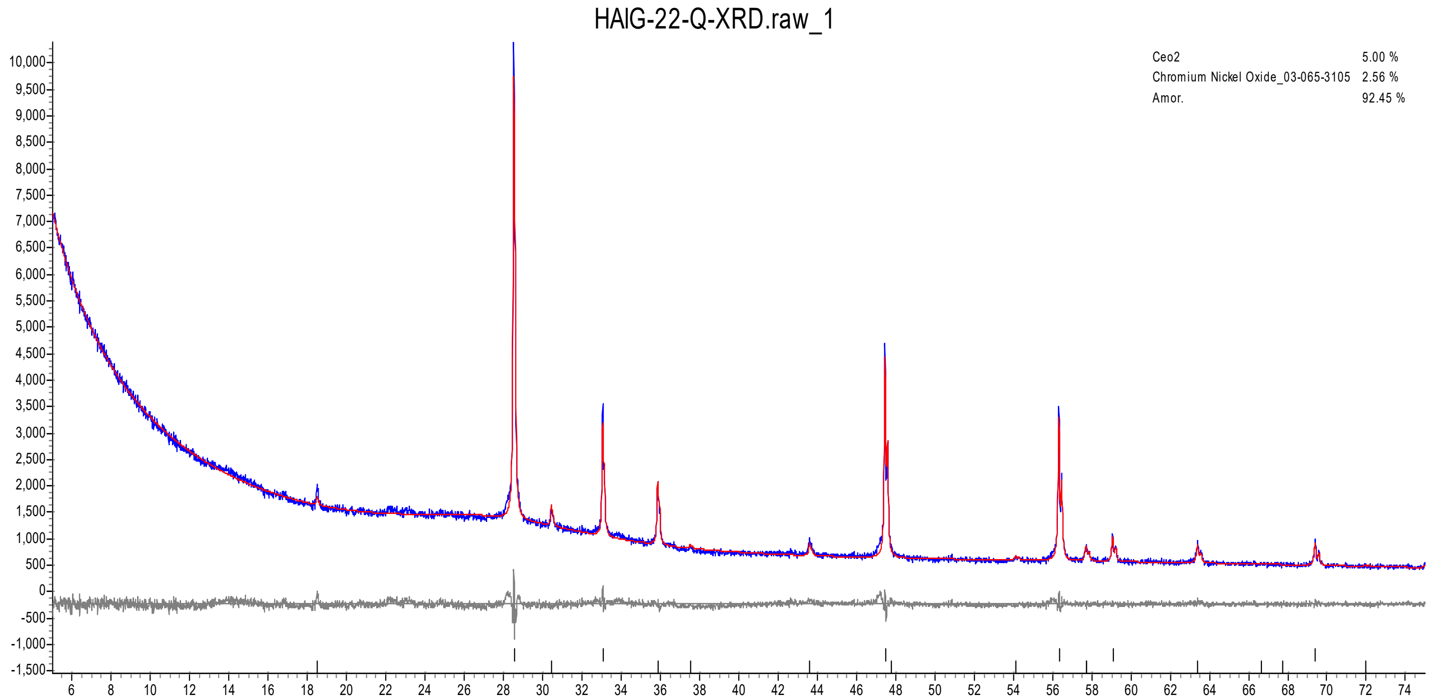

Phase Name	Wt% of Spiked	Wt% in Spiked Sample	Wt% in Original Sample
CeO_2	2.562	2.562	0.000
$NiCr_2O_4$ (Spinel)	0.000	1.425	1.499

Figure B.20. XRD Spectrum of Quenched Glass HAlG-22

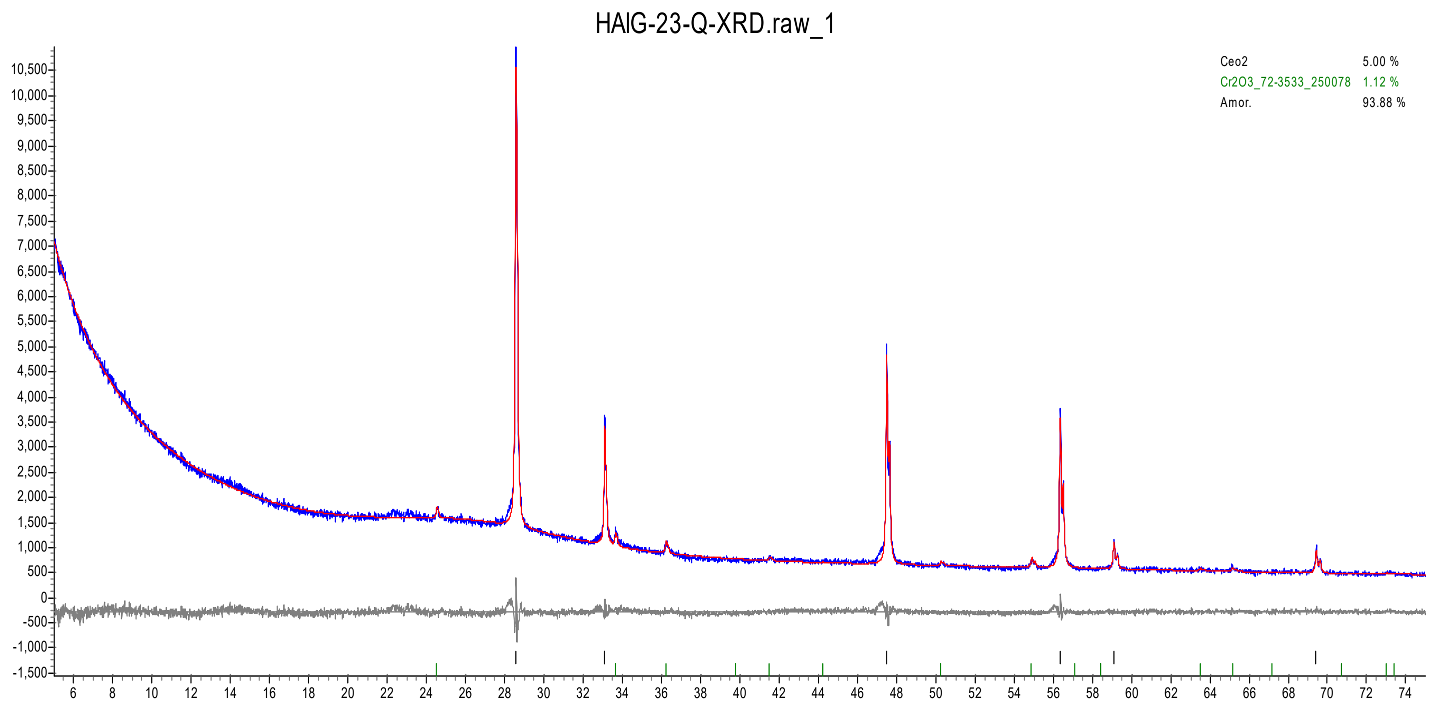

Phase Name	Wt% of Spiked	Wt% in Spiked Sample	Wt% in Original Sample
CeO_2	2.565	2.565	0.000
Cr_2O_3	0.000	0.650	0.684

Figure B.21. XRD Spectrum of Quenched Glass HAlG-23

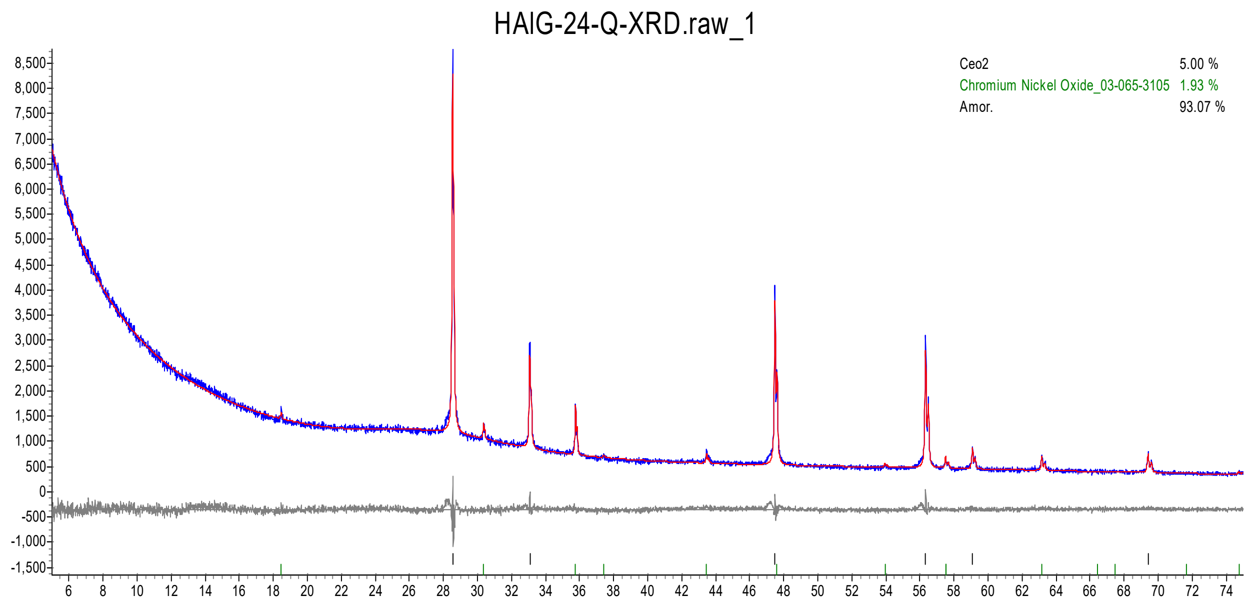

Phase Name	Wt% of Spiked	Wt% in Spiked Sample	Wt% in Original Sample
CeO_2	2.565	2.565	0.000
$NiCr_2O_4$ (Spinel)	0.000	1.081	1.138

Figure B.22. XRD Spectrum of Quenched Glass HAlG-24

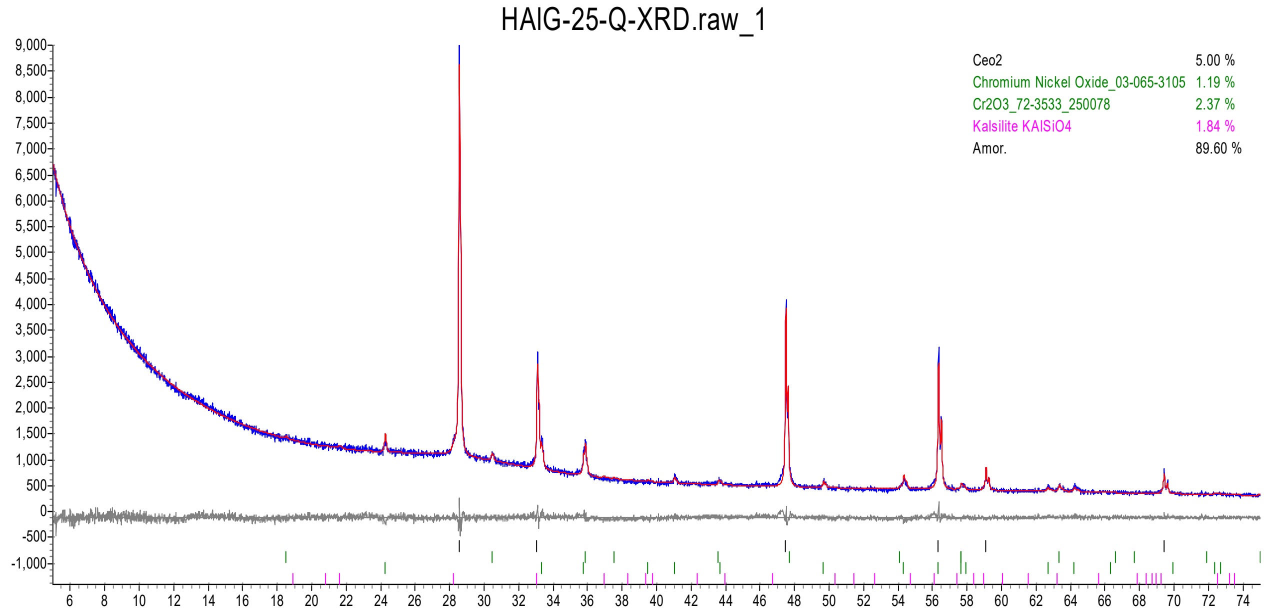

Phase Name	Wt% of Spiked	Wt% in Spiked Sample	Wt% in Original Sample
CeO_2	2.564	2.564	0.000
$NiCr_2O_4$ (Spinel)	0.000	0.707	0.744
$Cr_{0.75}Fe_{1.25}O_3$	0.000	1.431	1.506
$KAlSiO_4$	0.000	1.069	1.125

Figure B.23. XRD Spectrum of Quenched Glass HAlG-25

Appendix C – Analyzed High-Aluminum Glass Compositions

The data in this appendix compares the targeted glass compositions with the analyzed glass compositions and their percent differences. There appeared to be overall agreement in all samples, and the targeted compositions are adequate for use in future work to develop property-composition models.

Table C.1. Comparison of Targeted and Analyzed High-Aluminum Glass Compositions

Glass ID	HAlG-01			HAlG-02			HAlG-03			HAlG-04		
Component	Targeted (wt%)	Analyzed (wt%)	% Diff	Targeted (wt%)	Analyzed (wt%)	% Diff	Targeted (wt%)	Analyzed (wt%)	% Diff	Targeted (wt%)	Analyzed (wt%)	% Diff
Ag_2O	0	NM	NA	0	NM	NA	0	NM	NA	0	NM	NA
Al_2O_3	20.24	20.20	-0.17	23.89	23.30	-2.48	20.11	19.60	-2.52	20.67	20.30	-1.80
B_2O_3	9.50	9.18	-3.41	19.74	19.20	-2.73	15.72	15.10	-3.94	10.21	9.97	-2.33
Bi_2O_3	0.714	0.679	-4.90	0.143	0.137	-4.20	0.213	0.204	-4.23	0.621	0.606	-2.42
CaO	1.43	1.47	2.87	0.286	0.317	10.84	0.426	0.446	4.69	1.24	1.21	-2.58
CdO	0.143	0.128	-10.49	0.029	<0.0286	NA	0.043	0.038	-10.70	0.124	0.115	-7.26
Cr_2O_3	0.019	<0.0365	NA	1.60	1.12	-29.82	0.172	0.174	1.16	1.13	1.08	-4.00
F	0.820	0.737	-10.12	0.164	0.120	-26.83	0.244	0.184	-24.59	0.713	0.707	-0.84
Fe_2O_3	1.36	1.29	-5.15	4.78	4.62	-3.27	5.69	5.41	-4.89	6.89	6.75	-2.07
K_2O	2.10	1.99	-5.19	0.420	0.441	5.00	0.625	0.623	-0.32	1.82	1.82	-0.22
Li_2O	0.495	0.545	10.10	1.07	1.20	12.25	0.930	0.857	-7.85	0.382	0.524	37.17
MgO	0.714	0.700	-1.96	0.143	0.147	2.80	0.213	0.208	-2.35	0.621	0.620	-0.16
MnO	0.087	0.086	-0.92	0.017	0.025	45.88	0.026	0.035	33.08	0.076	0.085	11.84
Na_2O	19.99	19.10	-4.44	19.22	19.30	0.44	16.75	16.00	-4.46	19.52	19.40	-0.62
NiO	1.14	1.08	-5.51	0.229	0.213	-6.99	0.341	0.324	-4.99	0.993	0.934	-5.94
P_2O_5	4.21	3.87	-8.10	3.71	3.28	-11.54	3.37	2.81	-16.59	0.371	0.356	-4.04
PbO	0	NM	NA	0	NM	NA	0	NM	NA	0	NM	NA
RuO_2	0	NM	NA	0	NM	NA	0	NM	NA	0	NM	NA
SiO_2	31.47	31.90	1.37	22.27	22.40	0.58	32.77	33.00	0.70	33.00	33.10	0.29
SO_3	0.486	0.400	-17.70	0.097	<0.125	NA	0.145	<0.129	NA	0.422	0.390	-7.58
SrO	0.147	0.114	-22.45	0.029	<0.0286	NA	0.044	<0.0591	NA	0.128	0.102	-20.31
TiO_2	0.286	0.286	0.00	0.057	<0.0848	NA	0.085	0.105	23.53	0.248	0.287	15.73
ZnO	0.241	0.241	0.00	0.048	<0.0622	NA	0.072	0.073	1.53	0.210	0.221	5.24
ZrO_2	4.41	4.27	-3.20	2.07	1.94	-6.28	2.02	1.85	-8.42	0.604	0.591	-2.15
Total	100.00	98.30	-1.70	100.00	98.10	-1.90	100.00	97.20	-2.80	100.00	99.20	-0.80

Table C.1. (cont.)

Glass ID	HAlG-05			HAlG-06			HAlG-07-1			HAlG-08		
Component	Targeted (wt%)	Analyzed (wt%)	% Diff	Targeted (wt%)	Analyzed (wt%)	% Diff	Targeted (wt%)	Analyzed (wt%)	% Diff	Targeted (wt%)	Analyzed (wt%)	% Diff
Ag_2O	0	NM	NA	0	NM	NA	0	NM	NA	0	NM	NA
Al_2O_3	20.04	19.90	-0.72	27.86	27.30	-2.01	23.73	23.60	-0.56	24.33	23.90	-1.75
B_2O_3	21.20	20.50	-3.28	19.58	18.80	-3.96	11.33	11.00	-2.87	14.82	14.50	-2.15
Bi_2O_3	0.428	0.399	-6.78	0.182	0.178	-2.20	0.597	0.586	-1.84	0.096	<0.111	NA
CaO	0.856	0.822	-3.97	0.365	0.402	10.14	1.19	1.16	-2.77	0.192	0.219	14.06
CdO	0.086	0.078	-9.53	0.036	0.033	-8.06	0.119	0.111	-6.72	0.019	<0.0286	NA
Cr_2O_3	0.662	0.635	-4.08	1.19	1.15	-3.28	0.074	0.079	6.62	0.649	0.774	19.26
F	0.491	0.397	-19.14	0.209	0.163	-22.01	0.685	0.567	-17.23	0.110	0.087	-21.00
Fe_2O_3	11.09	10.40	-6.20	1.47	1.46	-0.48	9.08	8.84	-2.68	10.65	10.40	-2.37
K_2O	1.26	1.21	-3.74	0.536	0.560	4.48	1.75	1.74	-0.74	0.283	0.302	6.71
Li_2O	0.452	0.449	-0.66	0.322	0.346	7.45	0.175	<0.219	NA	1.80	1.81	0.78
MgO	0.428	0.414	-3.27	0.182	0.187	2.75	0.597	0.599	0.34	0.096	0.109	13.54
MnO	0.052	0.067	27.88	0.022	0.024	9.55	0.073	0.087	19.04	0.012	0.030	152.50
Na_2O	15.72	14.80	-5.85	19.66	19.60	-0.33	19.84	19.70	-0.71	17.48	17.70	1.24
NiO	0.685	0.630	-8.03	0.292	0.283	-3.08	0.954	0.865	-9.33	0.154	0.210	36.36
P_2O_5	0.780	0.831	6.54	2.32	1.97	-15.16	2.10	1.86	-11.22	4.36	3.84	-11.87
PbO	0	NM	NA	0	NM	NA	0	NM	NA	0	NM	NA
RuO_2	0	NM	NA	0	NM	NA	0	NM	NA	0	NM	NA
SiO_2	22.02	22.00	-0.11	25.23	25.10	-0.53	24.84	25.00	0.66	24.76	24.70	-0.23
SO_3	0.291	0.240	-17.53	0.124	<0.125	NA	0.406	0.378	-6.90	0.065	<0.125	NA
SrO	0.088	0.067	-24.32	0.038	<0.0591	NA	0.123	0.098	-20.41	0.020	<0.0591	NA
TiO_2	0.171	0.201	17.54	0.073	0.125	71.23	0.239	0.268	12.13	0.038	0.088	132.11
ZnO	0.145	0.142	-2.07	0.062	0.093	49.84	0.202	0.209	3.47	0.033	<0.0622	NA
ZrO_2	3.06	2.87	-6.18	0.247	0.228	-7.69	1.90	1.82	-4.16	0.041	<0.135	NA
Total	100.00	97.00	-3.00	100.00	98.20	-1.80	100.00	98.80	-1.20	100.00	101.00	1.00

Table C.1. (cont.)

Glass ID	HAlG-09			HAlG-10			HAlG-11			HAlG-12		
Component	Targeted (wt%)	Analyzed (wt%)	% Diff	Targeted (wt%)	Analyzed (wt%)	% Diff	Targeted (wt%)	Analyzed (wt%)	% Diff	Targeted (wt%)	Analyzed (wt%)	% Diff
Ag_2O	0	NM	NA	0	NM	NA	0	NM	NA	0	NM	NA
Al_2O_3	21.12	20.70	-1.97	20.17	19.60	-2.82	24.52	24.20	-1.30	21.07	21.10	0.17
B_2O_3	21.79	21.20	-2.69	17.66	16.40	-7.13	8.84	8.41	-4.91	16.13	15.60	-3.31
Bi_2O_3	0.156	0.152	-2.56	0.120	0.115	-4.17	0.316	0.305	-3.48	0.455	0.433	-4.84
CaO	0.312	0.375	20.19	0.240	0.251	4.58	0.631	0.704	11.57	0.910	0.891	-2.09
CdO	0.031	<0.0286	NA	0.024	<0.0286	NA	0.063	0.054	-14.44	0.091	0.079	-13.19
Cr_2O_3	1.06	0.948	-10.40	1.88	2.64	40.43	1.81	1.77	-1.99	1.65	1.31	-20.36
F	0.179	0.132	-26.26	0.138	0.098	-28.77	0.362	0.288	-20.44	0.522	0.416	-20.31
Fe_2O_3	4.81	4.74	-1.43	7.49	7.53	0.57	1.73	1.72	-0.46	0.170	0.196	15.29
K_2O	0.459	0.469	2.18	0.352	0.342	-2.84	0.927	0.916	-1.19	1.34	1.34	0.22
Li_2O	5.62	5.61	-0.20	4.94	4.83	-2.13	4.59	4.44	-3.25	0.713	0.755	5.89
MgO	0.156	0.175	12.18	0.120	0.131	9.17	0.316	0.321	1.58	0.455	0.471	3.52
MnO	0.019	0.027	43.16	0.015	0.029	92.67	0.039	0.041	5.64	0.056	0.053	-4.64
Na_2O	13.62	13.60	-0.11	15.44	14.50	-6.09	19.94	19.70	-1.19	19.36	19.30	-0.33
NiO	0.250	0.240	-4.00	0.192	0.234	21.88	0.505	0.498	-1.39	0.728	0.661	-9.20
P_2O_5	1.36	1.33	-1.92	4.08	3.65	-10.60	3.70	3.40	-8.01	1.06	1.11	4.52
PbO	0	NM	NA	0	NM	NA	0	NM	NA	0	NM	NA
RuO_2	0	NM	NA	0	NM	NA	0	NM	NA	0	NM	NA
SiO_2	23.22	23.30	0.33	22.65	22.10	-2.41	25.78	25.90	0.47	28.59	28.90	1.08
SO_3	0.106	<0.125	NA	0.082	<0.125	NA	0.215	0.165	-23.26	0.309	0.260	-15.86
SrO	0.032	<0.0591	NA	0.025	<0.0591	NA	0.065	<0.0591	NA	0.094	0.075	-20.64
TiO_2	0.062	0.124	100.00	0.048	<0.0834	NA	0.126	0.173	37.30	0.182	0.224	23.08
ZnO	0.053	<0.0695	NA	0.041	<0.0622	NA	0.107	0.120	12.15	0.154	0.149	-3.25
ZrO_2	5.60	5.34	-4.66	4.31	4.04	-6.20	5.43	4.93	-9.21	5.96	5.70	-4.36
Total	100.00	98.70	-1.30	100.00	96.80	-3.20	100.00	98.10	-1.90	100.00	99.10	-0.90

Table C.1. (cont.)

Glass ID	HAlG-13			HAlG-14			HAlG-15			HAlG-16		
Component	Targeted (wt%)	Analyzed (wt%)	% Diff	Targeted (wt%)	Analyzed (wt%)	% Diff	Targeted (wt%)	Analyzed (wt%)	% Diff	Targeted (wt%)	Analyzed (wt%)	% Diff
Ag_2O	0	NM	NA	0	NM	NA	0	NM	NA	0	NM	NA
Al_2O_3	20.42	20.40	-0.08	22.89	22.40	-2.14	22.43	22.10	-1.45	21.59	21.40	-0.88
B_2O_3	8.24	7.87	-4.51	16.77	16.10	-3.98	8.65	8.47	-2.02	10.39	9.77	-5.94
Bi_2O_3	0.574	0.533	-7.14	0.087	<0.111	NA	0.297	0.294	-1.01	0.223	0.203	-8.97
CaO	1.15	1.09	-5.05	0.173	0.183	5.78	0.595	0.629	5.71	0.445	0.456	2.47
CdO	0.115	0.099	-14.17	0.017	<0.0286	NA	0.059	0.054	-8.31	0.045	0.033	-26.44
Cr_2O_3	0.254	0.338	33.07	1.76	1.86	5.98	1.95	1.85	-5.13	2.00	1.59	-20.30
F	0.659	0.580	-11.99	0.100	0.082	-18.20	0.341	0.315	-7.62	0.256	0.199	-22.27
Fe_2O_3	8.61	8.26	-4.04	9.98	9.46	-5.19	1.29	1.26	-2.02	4.21	4.11	-2.28
K_2O	1.69	1.55	-8.12	0.255	0.252	-1.18	0.874	0.900	2.97	0.654	0.665	1.68
Li_2O	4.81	4.88	1.50	5.34	5.50	3.09	5.93	6.01	1.42	2.54	2.42	-4.84
MgO	0.574	0.571	-0.52	0.087	0.088	1.15	0.297	0.302	1.68	0.223	0.203	-8.97
MnO	0.070	0.080	14.57	0.011	0.027	145.45	0.036	0.037	3.89	0.027	0.031	16.30
Na_2O	16.85	15.90	-5.62	18.63	17.50	-6.05	14.89	14.60	-1.93	19.04	18.90	-0.75
NiO	0.919	0.899	-2.18	0.139	0.204	46.76	0.476	0.464	-2.52	0.356	0.308	-13.48
P_2O_5	0.644	0.728	13.04	0.795	0.769	-3.27	0.176	<0.29	NA	2.21	2.16	-2.17
PbO	0	NM	NA	0	NM	NA	0	NM	NA	0	NM	NA
RuO_2	0	NM	NA	0	NM	NA	0	NM	NA	0	NM	NA
SiO_2	28.13	28.20	0.25	22.23	22.20	-0.13	40.15	40.30	0.38	30.50	30.60	0.32
SO_3	0.390	0.319	-18.21	0.059	<0.125	NA	0.202	0.174	-13.86	0.151	<0.125	NA
SrO	0.118	0.092	-22.20	0.018	<0.0591	NA	0.061	<0.0591	NA	0.046	<0.0591	NA
TiO_2	0.230	0.262	13.91	0.035	<0.0834	NA	0.119	0.166	39.50	0.089	0.129	44.94
ZnO	0.194	0.191	-1.55	0.029	<0.0622	NA	0.101	0.109	7.92	0.075	0.075	0.53
ZrO_2	5.37	5.29	-1.49	0.614	0.635	3.42	1.10	1.04	-5.11	4.93	4.64	-5.96
Total	100.00	98.20	-1.80	100.00	97.80	-2.20	100.00	99.40	-0.60	100.00	98.10	-1.90

Table C.1. (cont.)

Glass ID	HAlG-17			HAlG-18			HAlG-19			HAlG-20		
Component	Targeted (wt%)	Analyzed (wt%)	% Diff	Targeted (wt%)	Analyzed (wt%)	% Diff	Targeted (wt%)	Analyzed (wt%)	% Diff	Targeted (wt%)	Analyzed (wt%)	% Diff
Ag_2O	0	NM	NA	0	NM	NA	0	NM	NA	0	NM	NA
Al_2O_3	20.62	20.40	-1.05	28.57	28.50	-0.24	27.63	27.40	-0.85	20.92	21.20	1.35
B_2O_3	13.13	12.80	-2.52	11.16	10.90	-2.32	8.02	7.92	-1.28	20.02	19.40	-3.07
Bi_2O_3	0.305	0.288	-5.57	0.366	0.346	-5.46	0.136	0.131	-3.68	0.217	0.210	-3.23
CaO	0.610	0.620	1.64	0.732	0.725	-0.96	0.271	0.283	4.43	0.434	0.456	5.07
CdO	0.061	0.054	-10.82	0.073	0.064	-13.01	0.027	0.024	-11.85	0.043	0.040	-7.44
Cr_2O_3	0.132	0.425	221.97	0.745	0.700	-6.04	0.846	0.797	-5.79	1.27	1.36	7.26
F	0.350	0.302	-13.71	0.420	0.353	-15.95	0.156	0.129	-17.31	0.249	0.204	-17.07
Fe_2O_3	0.763	0.748	-1.97	0.518	0.499	-3.67	6.14	5.97	-2.71	0.735	0.711	-3.27
K_2O	0.896	0.916	2.23	1.08	1.06	-1.40	0.398	0.394	-1.01	0.638	0.664	4.08
Li_2O	2.63	2.74	4.14	5.87	5.66	-3.51	5.50	5.60	1.80	3.53	3.41	-3.37
MgO	0.305	0.320	4.92	0.366	0.358	-2.19	0.136	0.139	2.21	0.217	0.218	0.46
MnO	0.037	0.038	3.24	0.045	0.043	-3.56	0.017	0.027	55.88	0.026	0.028	5.77
Na_2O	17.52	17.50	-0.11	18.73	17.80	-4.97	19.79	19.70	-0.43	14.14	14.30	1.12
NiO	0.488	0.575	17.83	0.586	0.548	-6.48	0.217	0.204	-5.99	0.347	0.400	15.27
P_2O_5	1.05	0.977	-6.60	3.97	3.28	-17.44	1.69	1.56	-7.64	4.48	3.91	-12.66
PbO	0	NM	NA	0	NM	NA	0	NM	NA	0	NM	NA
RuO_2	0	NM	NA	0	NM	NA	0	NM	NA	0	NM	NA
SiO_2	36.48	36.70	0.59	22.87	23.10	1.02	26.12	26.30	0.69	29.26	29.30	0.12
SO_3	0.207	0.161	-22.22	0.249	0.234	-6.02	0.092	<0.125	NA	0.148	<0.129	NA
SrO	0.063	<0.0591	NA	0.075	<0.0591	NA	0.028	0.023	-17.86	0.045	<0.0591	NA
TiO_2	0.122	0.171	40.16	0.146	0.173	18.49	0.054	0.106	96.30	0.087	0.095	9.43
ZnO	0.103	0.104	0.97	0.124	0.122	-1.61	0.046	<0.0622	NA	0.073	0.082	12.88
ZrO_2	4.13	3.96	-4.14	3.31	3.02	-8.87	2.69	2.55	-5.10	3.13	2.82	-9.85
Total	100.00	99.80	-0.20	100.00	97.50	-2.50	100.00	99.50	-0.50	100.00	98.90	-1.10

Table C.1. (cont.)

Glass ID	HAlG-21			HAlG-22			HAlG-23			HAlG-24		
Component	Targeted (wt%)	Analyzed (wt%)	% Diff	Targeted (wt%)	Analyzed (wt%)	% Diff	Targeted (wt%)	Analyzed (wt%)	% Diff	Targeted (wt%)	Analyzed (wt%)	% Diff
Ag_2O	0	NM	NA	0	NM	NA	0	NM	NA	0.020	NM	NA
Al_2O_3	22.74	21.90	-3.71	20.65	20.20	-2.20	20.90	20.60	-1.43	22.00	21.50	-2.27
B_2O_3	11.78	11.40	-3.21	9.29	8.96	-3.57	17.49	16.90	-3.40	15.50	15.10	-2.58
Bi_2O_3	0.466	0.430	-7.73	0.675	0.640	-5.19	0.401	0.380	-5.24	1.00	0.981	-1.90
CaO	0.932	0.873	-6.33	1.35	1.48	9.63	0.803	0.793	-1.25	3.50	3.47	-0.86
CdO	0.093	0.083	-11.18	0.135	0.121	-10.37	0.080	0.071	-11.38	0.100	0.089	-11.50
Cr_2O_3	0.445	0.427	-4.04	1.72	1.74	1.05	0.881	0.822	-6.70	0.750	0.701	-6.53
F	0.535	0.462	-13.64	0.775	0.722	-6.84	0.461	0.415	-9.98	0.300	0.253	-15.67
Fe_2O_3	8.15	7.74	-5.05	1.18	1.11	-5.53	0.192	0.204	6.25	5.50	5.29	-3.82
K_2O	1.37	1.33	-2.92	1.98	1.98	-0.15	1.18	1.23	4.33	0.700	0.683	-2.43
Li_2O	4.64	4.71	1.49	4.32	4.40	1.92	5.73	5.52	-3.58	3.00	3.11	3.67
MgO	0.466	0.438	-6.01	0.675	0.683	1.19	0.401	0.404	0.75	0.500	0.498	-0.40
MnO	0.057	0.065	14.74	0.082	0.081	-0.98	0.049	0.048	-3.06	1.00	0.931	-6.90
Na_2O	15.86	15.30	-3.55	13.16	13.30	1.03	11.08	11.30	2.02	11.50	11.50	0.00
NiO	0.746	0.690	-7.51	1.08	1.01	-6.48	0.642	0.592	-7.79	0.400	0.368	-8.00
P_2O_5	4.30	3.47	-19.25	2.58	2.19	-15.15	3.42	2.99	-12.68	1.00	0.718	-28.20
PbO	0	NM	NA	0	NM	NA	0	NM	NA	0.300	NM	NA
RuO_2	0	NM	NA	0	NM	NA	0	NM	NA	0.005	NM	NA
SiO_2	25.48	25.20	-1.09	37.12	37.30	0.50	33.54	33.50	-0.13	31.50	31.50	0.00
SO_3	0.317	0.295	-6.94	0.459	0.406	-11.55	0.273	0.255	-6.59	0.300	0.275	-8.33
SrO	0.096	0.072	-25.10	0.139	0.108	-22.30	0.083	0.065	-22.17	0.120	0.099	-17.58
TiO_2	0.186	0.193	3.76	0.270	0.286	5.93	0.161	0.173	7.45	0.00	<0.0834	NA
ZnO	0.158	0.155	-1.90	0.228	0.228	0.00	0.136	0.136	0.00	0.00	<0.0622	NA
ZrO_2	1.18	1.00	-15.25	2.13	2.04	-4.14	2.10	1.90	-9.48	1.00	0.945	-5.50
Total	100.00	96.20	-3.80	100.00	99.00	-1.00	100.00	98.20	-1.80	100.00	98.20	-1.80

Table C.1. (cont.)

Glass ID	HAlG-25		
Component	Targeted (wt%)	Analyzed (wt%)	% Diff
Ag_2O	0	NM	NA
Al_2O_3	24.33	24.10	-0.93
B_2O_3	14.82	14.30	-3.50
Bi_2O_3	0.096	<0.111	NA
CaO	0.192	0.215	11.98
CdO	0.019	<0.0286	NA
Cr_2O_3	0.649	0.616	-5.08
F	0.110	0.086	-21.73
Fe_2O_3	10.65	10.50	-1.44
K_2O	0.283	0.308	8.83
Li_2O	1.80	1.88	4.68
MgO	0.096	0.102	6.25
MnO	0.012	0.031	159.17
Na_2O	17.48	17.70	1.24
NiO	0.154	0.144	-6.49
P_2O_5	4.36	3.86	-11.41
PbO	0	NM	NA
RuO_2	0	NM	NA
SiO_2	24.76	24.80	0.18
SO_3	0.065	<0.125	NA
SrO	0.020	<0.0591	NA
TiO_2	0.038	0.085	123.68
ZnO	0.033	<0.0622	NA
ZrO_2	0.041	<0.135	NA
Total	100.00	99.20	-0.80

Appendix D – Canister Centerline Cooling Glass Photographs

This appendix contains photos of glasses after canister centerline cooling (CCC) treated beginning at the glass melting temperature. Each showed different responses to the CCC treatment as indicated by these photos.

Figure D.1. Glass HAlG-1 after CCC

Figure D.2. Glass HAlG-02 after CCC

Figure D.3. Glass HAlG-03 after CCC

Figure D.4. Glass HAlG-04 after CCC

Figure D.5. Glass HAlG-05 after CCC

Figure D.6. Glass HAlG-06 after CCC

Figure D.7. Glass HAlG-07-1 after CCC

Figure D.8. Glass HAlG-08 after CCC

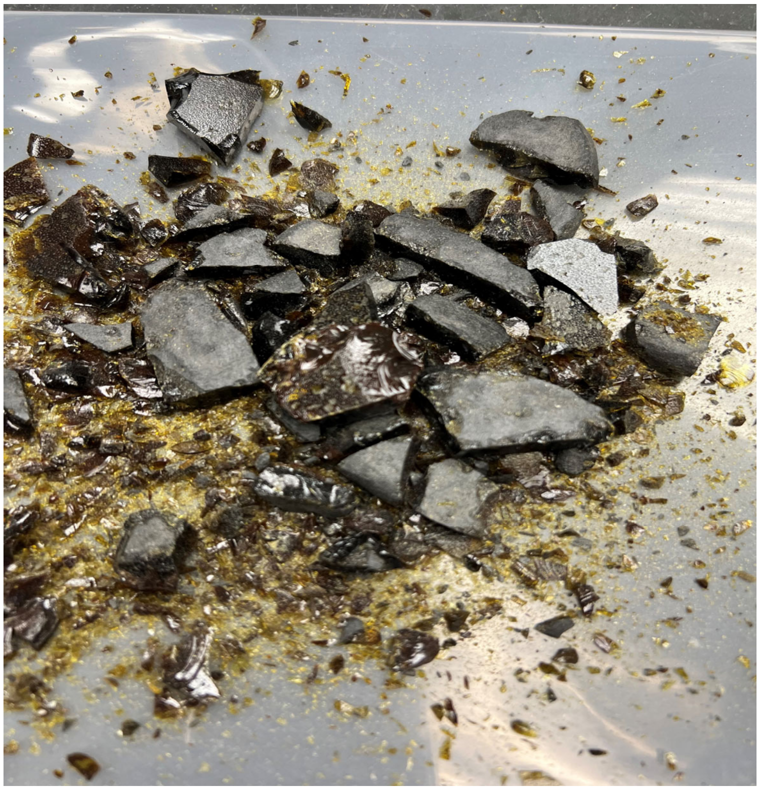

Figure D.9. Glass HAlG-09 after CCC

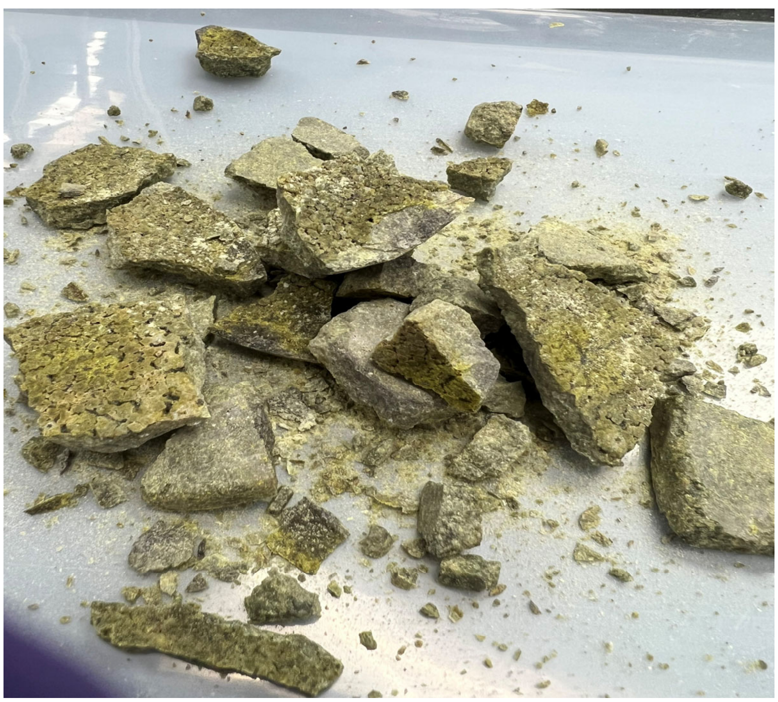

Figure D.10. Glass HAlG-11 CCC

Figure D.11. Glass HAlG-12 after CCC

Figure D.12. Glass HAlG-13 after CCC

Figure D.13. Glass HAlG-14 after CCC

Figure D.14. Glass HAlG-15 after CCC

Figure D.15. Glass HAlG-16 after CCC

Figure D.16. Glass HAlG-17 after CCC

Figure D.17. Glass HAlG-18 after CCC

Figure D.18. Glass HAlG-19 after CCC

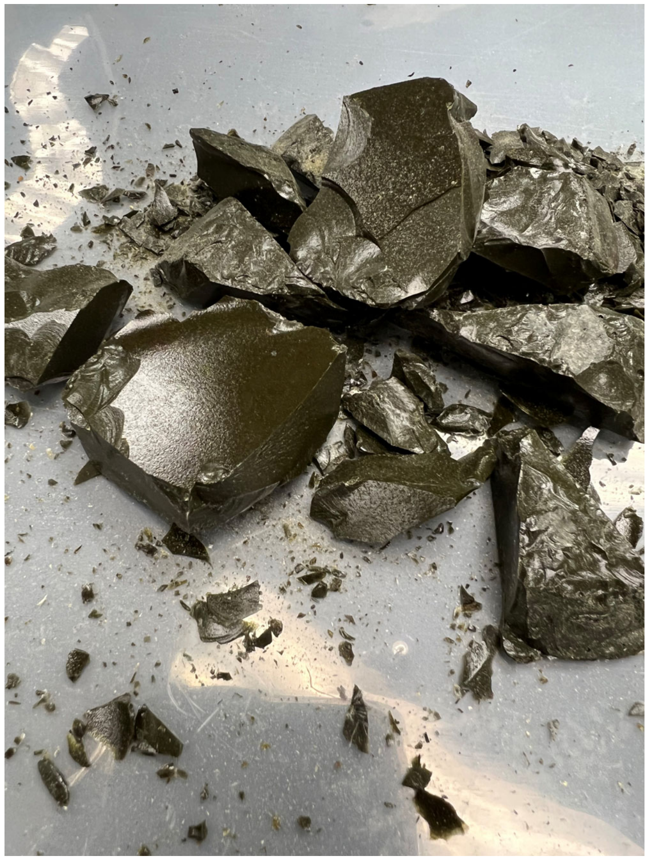

Figure D.19. Glass HAlG-20 after CCC

Figure D.20. Glass HAlG-21 after CCC

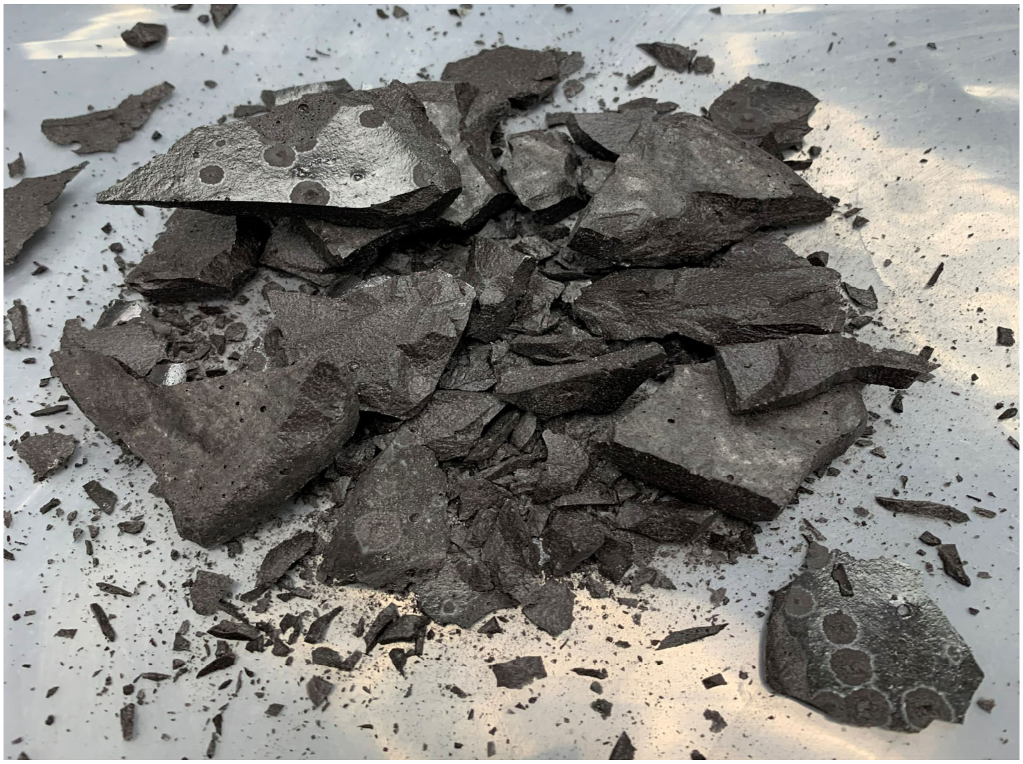

Figure D.21. Glass HAlG-22 after CCC

Figure D.22. Glass HAlG-23 after CCC

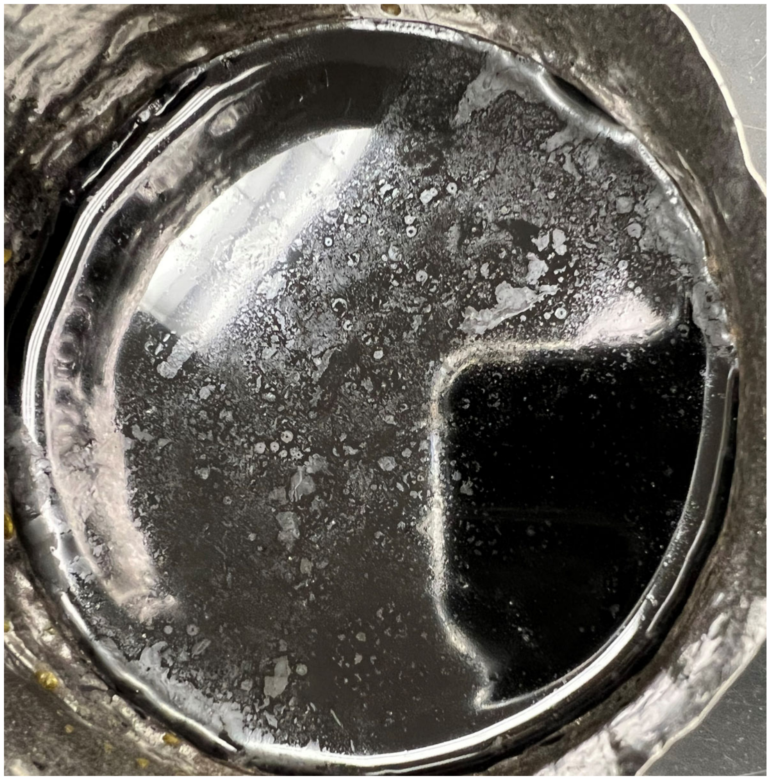

Figure D.23. Glass HAlG-24 after CCC

Figure D.24. Glass HAlG-25 after CCC

Appendix E – XRD of Canister Centerline Cooling Treated Glasses

This appendix shows the X-ray diffraction (XRD) plots of the high-aluminum glasses after canister centerline cooling (CCC) treatment. These glasses show primarily nepheline, spinel, and chromium oxide. There were no amorphous glasses after CCC treatment. The percentage of crystal content reported in the XRD scans is presented before any adjustments were made from spiking with 5 wt% of high-purity cerium oxide. The data is corrected not only for the amount of cerium oxide introduced into the samples, but also to account for the fact that the cerium oxide used was only 51% crystalline.

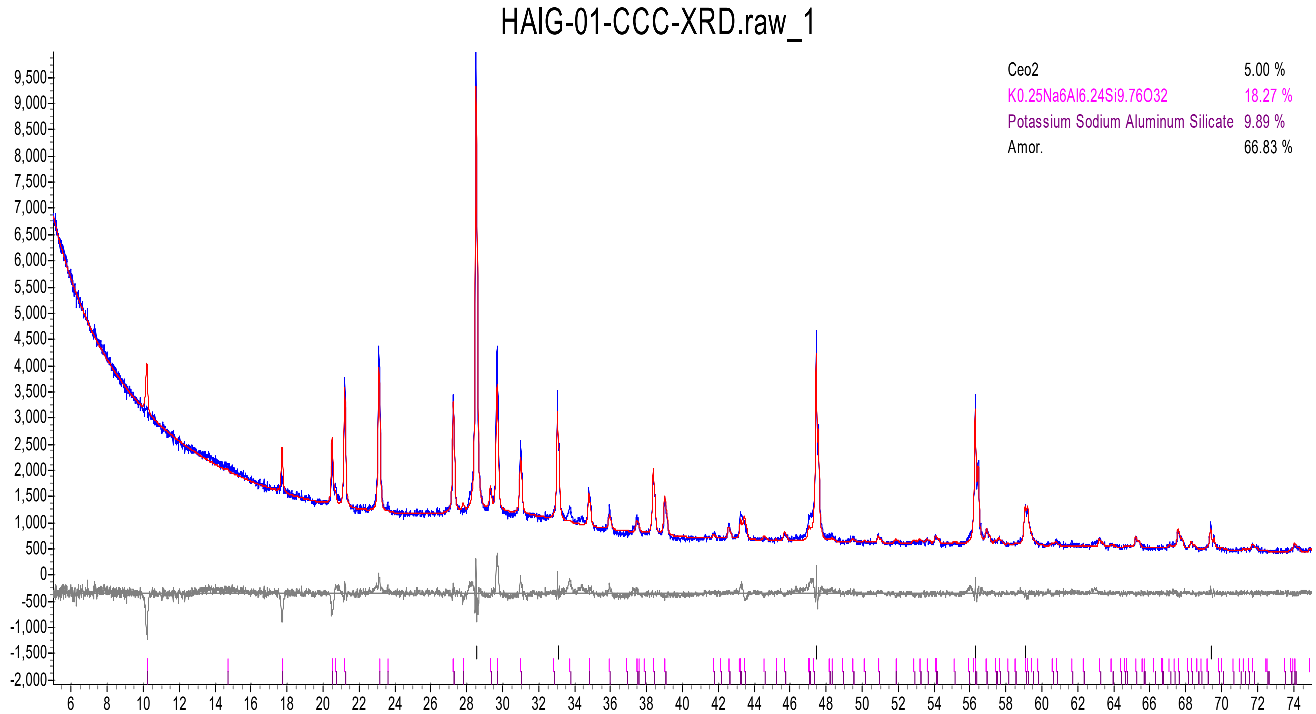

Phase Name	Wt% of Spiked	Wt% in Spiked Sample	Wt% in Original Sample
CeO_2	2.563	2.563	0.000
$KNaAlSiO_4$ (Nepheline)	0.000	16.029	16.873

Figure E.1. XRD Spectrum of CCC-Treated Glass HAlG-01

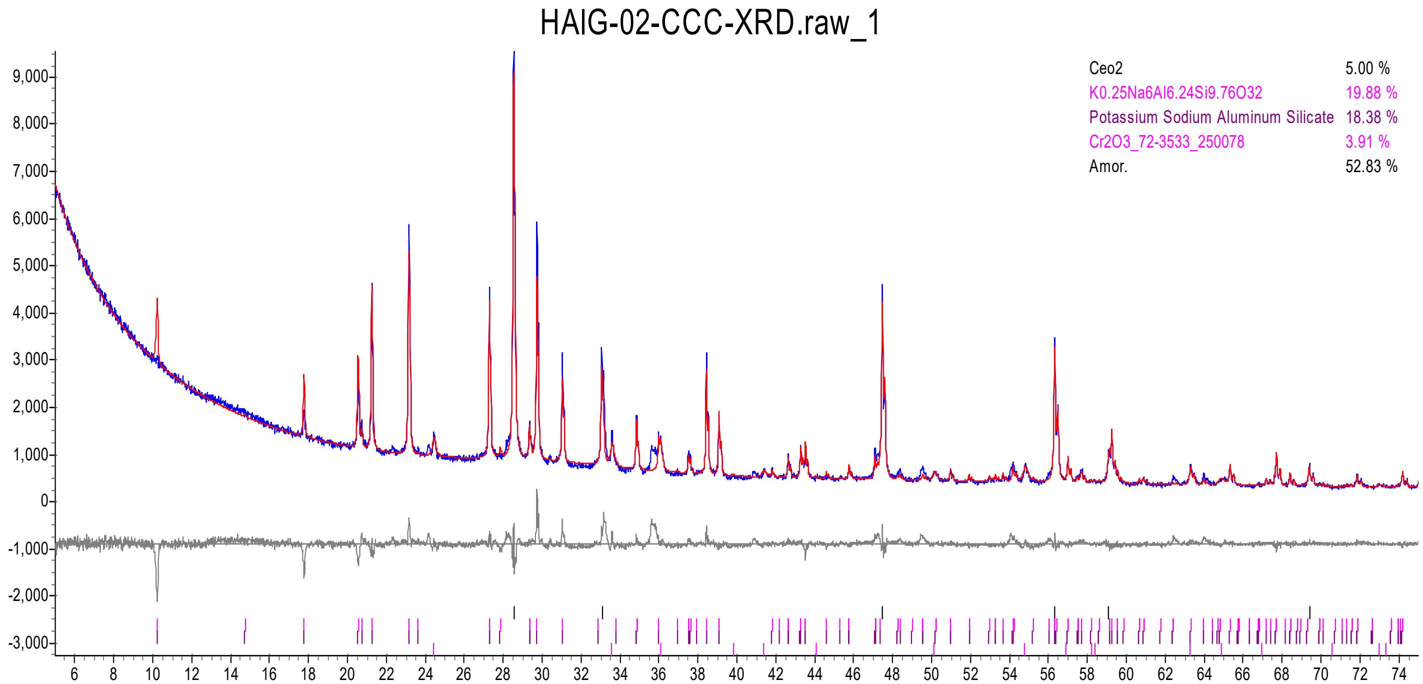

Phase Name	Wt% of Spiked	Wt% in Spiked Sample	Wt% in Original Sample
CeO_2	2.564	2.564	0.000
$KNaAlSiO_4$ (Nepheline)	0.000	21.385	22.511
Cr_2O_3	0.000	1.576	1.659
Fe_2O_3	0.000	1.553	1.635

Figure E.2. XRD Spectrum of CCC-Treated Glass HAlG-02

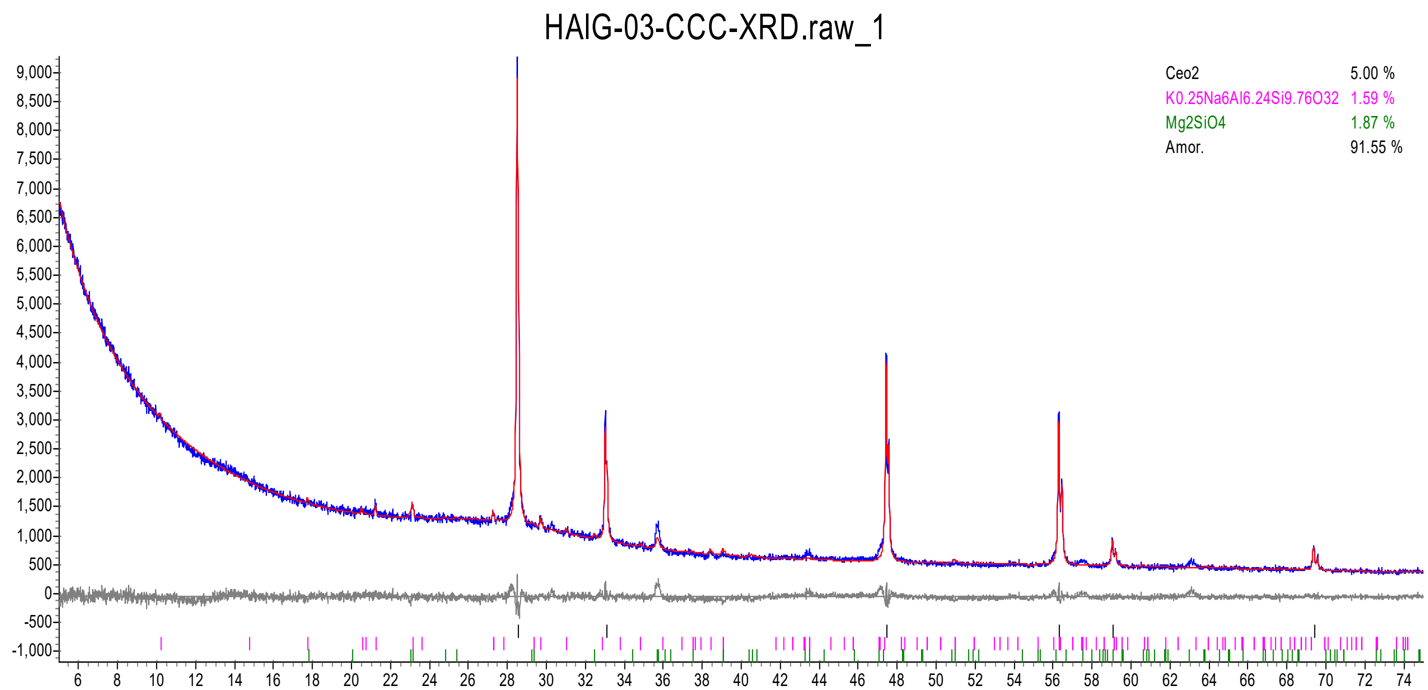

Phase Name	Wt% of Spiked	Wt% in Spiked Sample	Wt% in Original Sample
CeO_2	2.562	2.562	0.000
$KNaAlSiO_4$ (Nepheline)	0.000	0.991	1.043
Mg_2SiO_4	0.000	1.724	1.815

Figure E.3. XRD Spectrum of CCC-Treated Glass HAlG-03

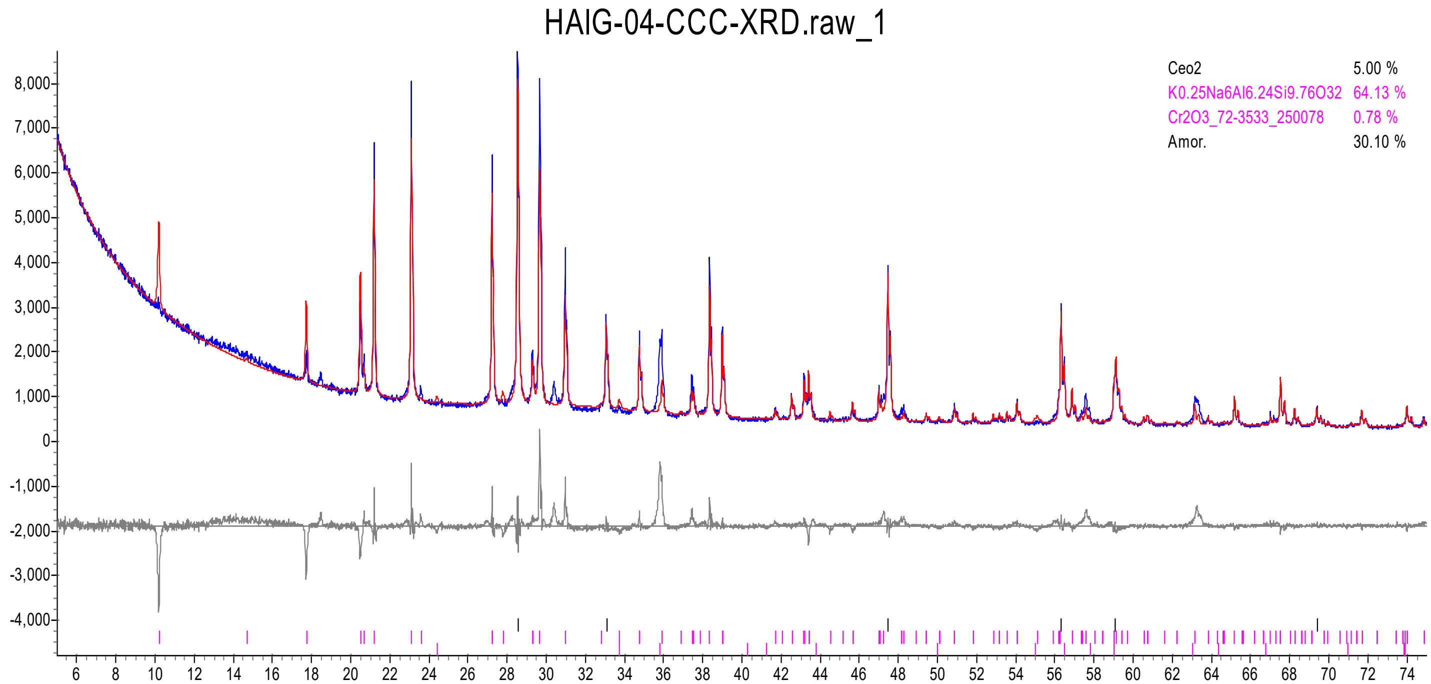

Phase Name	Wt% of Spiked	Wt% in Spiked Sample	Wt% in Original Sample
CeO_2	2.564	2.564	0.000
$KNaAlSiO_4$ (Nepheline)	0.000	35.741	37.623
Cr_2O_3	0.000	0.768	0.809

Figure E.4. XRD Spectrum of CCC-Treated Glass HAlG-04

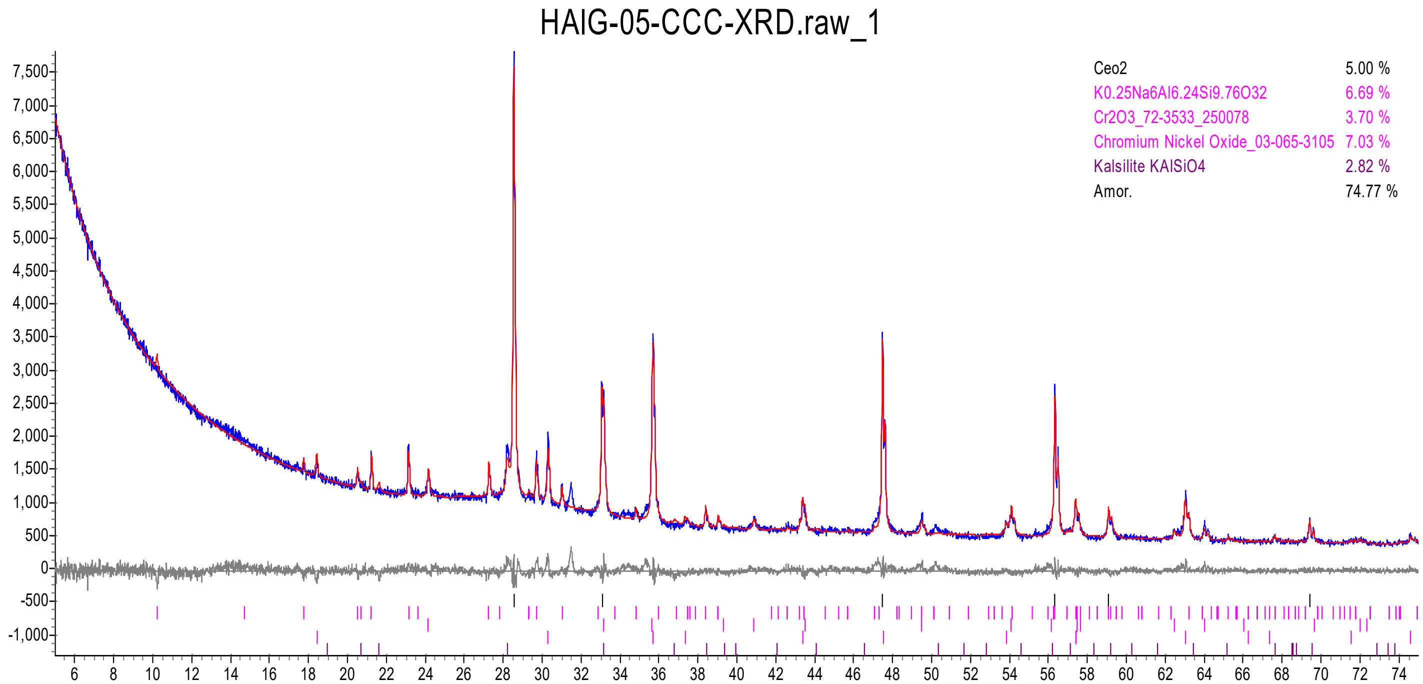

Phase Name	Wt% of Spiked	Wt% in Spiked Sample	Wt% in Original Sample
CeO_2	2.565	2.565	0.000
$KNaAlSiO_4$ (Nepheline)	0.000	3.722	3.918
$KAlSiO_4$	0.000	1.977	2.081
$NiCr_2O_4$ (Spinel)	0.000	4.394	4.625

Figure E.5. XRD Spectrum of CCC-Treated Glass HAlG-05

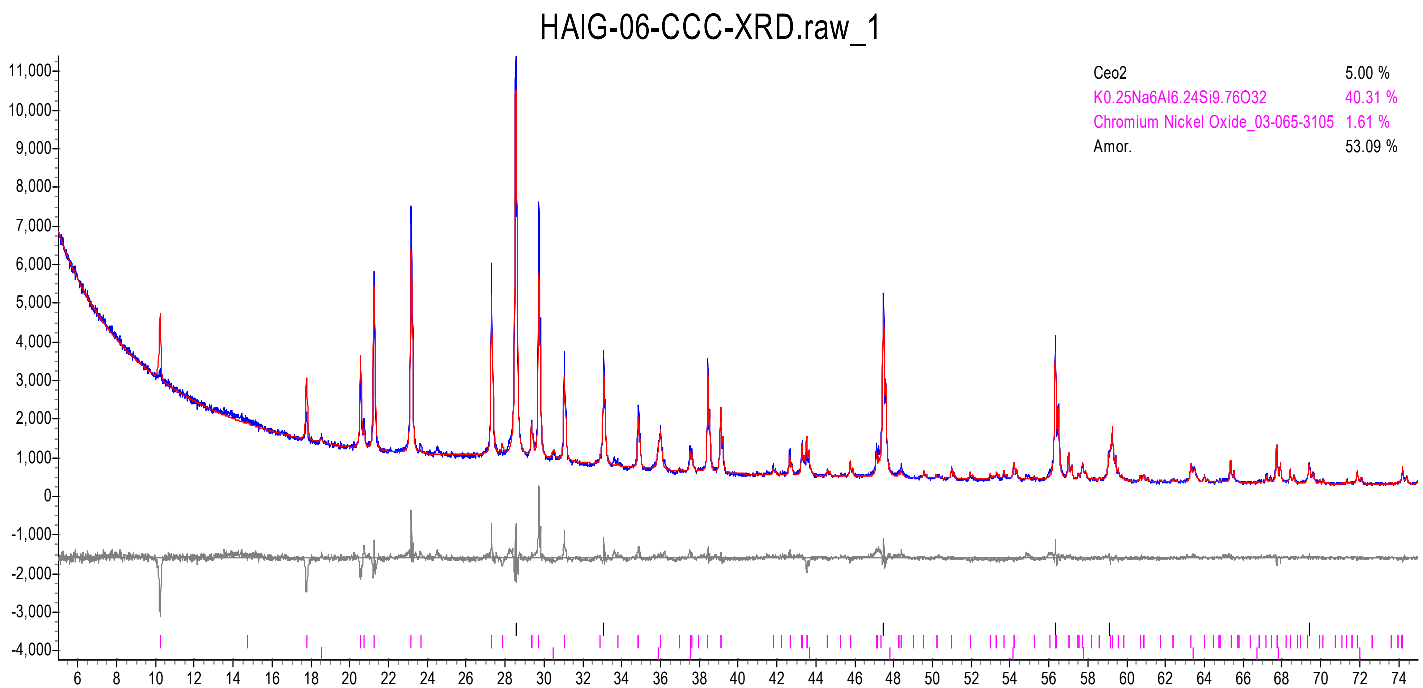

Phase Name	Wt% of Spiked	Wt% in Spiked Sample	Wt% in Original Sample
CeO_2	2.563	2.563	0.000
$KNaAlSiO_4$ (Nepheline)	0.000	21.882	23.034
$NiCr_2O_4$ (Spinel)	0.000	0.907	0.955

Figure E.6. XRD Spectrum of CCC-Treated Glass HAlG-06

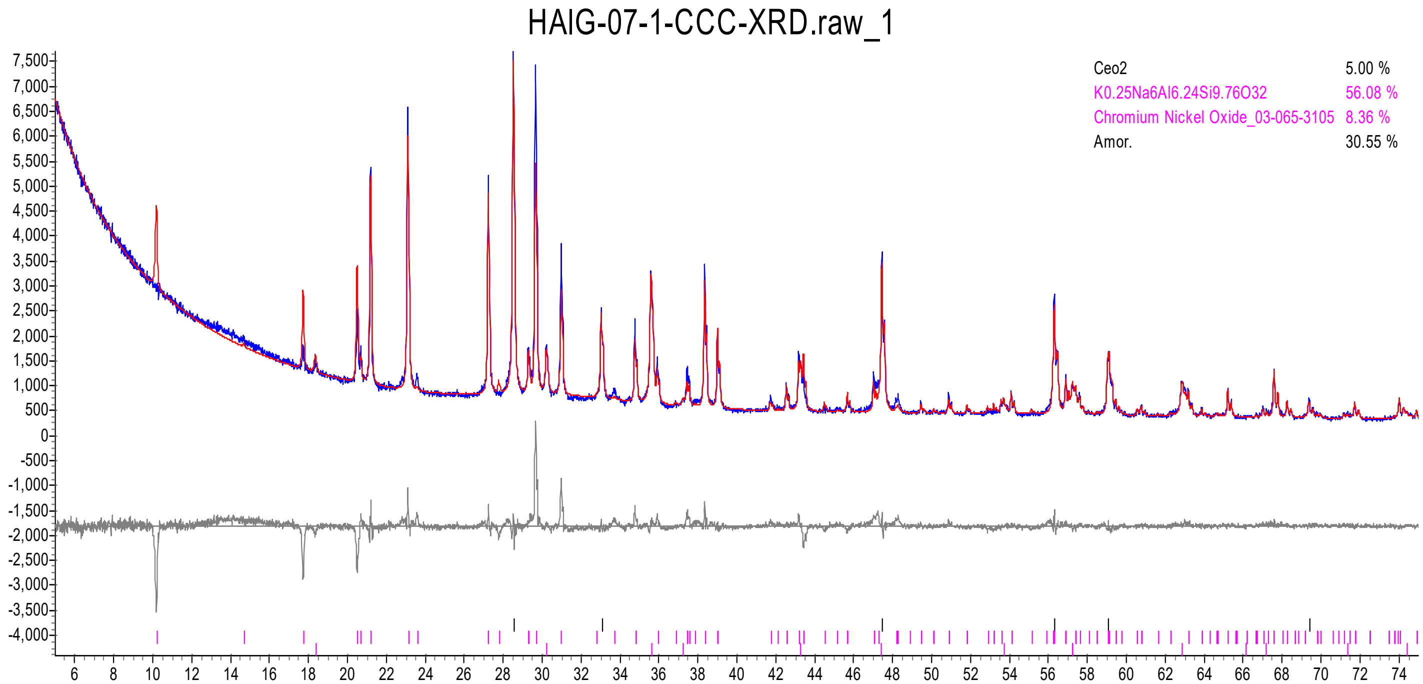

Phase Name	Wt% of Spiked	Wt% in Spiked Sample	Wt% in Original Sample
CeO_2	2.565	2.565	0.000
$KNaAlSiO_4$ (Nepheline)	0.000	30.813	32.436
$NiCr_2O_4$ (Spinel)	0.000	4.546	4.786

Figure E.7. XRD Spectrum of CCC-Treated Glass HAlG-07-1

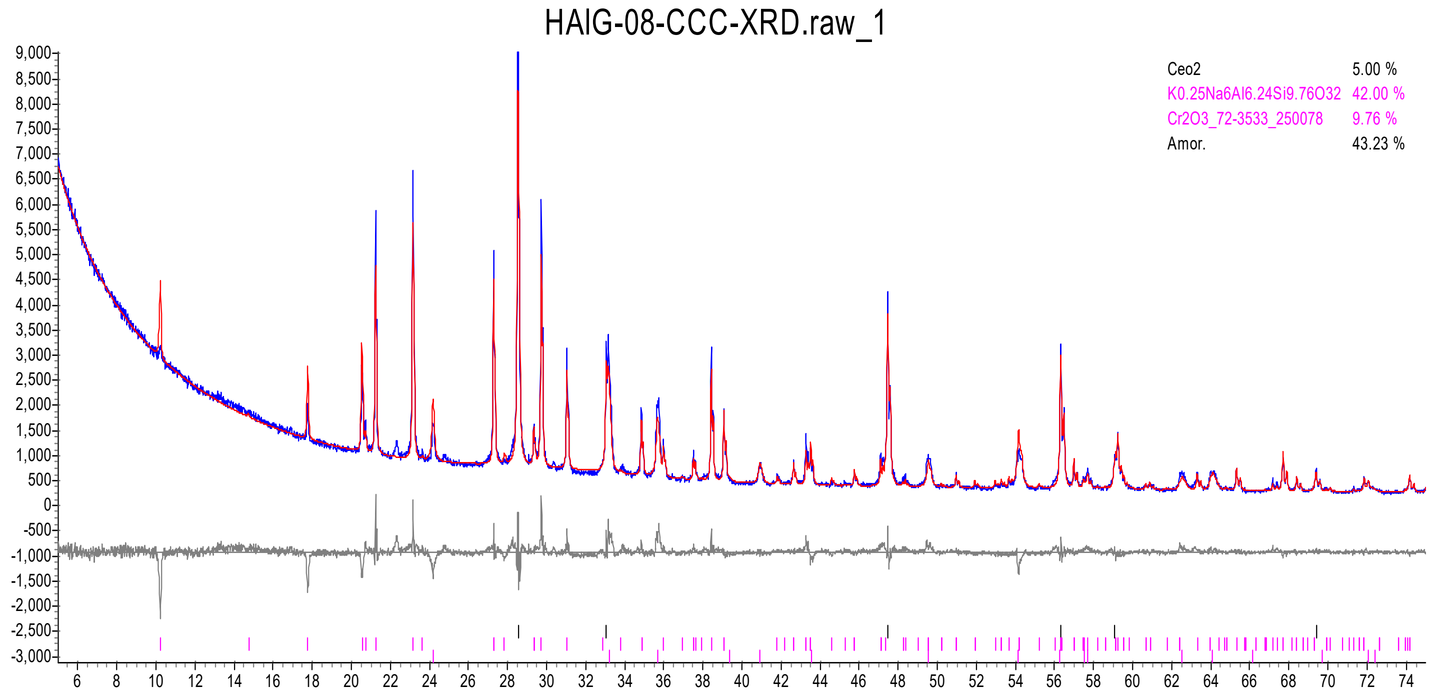

Phase Name	Wt% of Spiked	Wt% in Spiked Sample	Wt% in Original Sample
CeO_2	2.564	2.564	0.000
$K_{0.25}Na_6Al_{6.24}Si_{9.76}O_{32}$ (Nepheline)	0.000	23.194	24.415
$NiCr_2O_4$ (Spinel)	0.000	0.488	0.513
Fe_2O_3	0.000	4.673	4.919

Figure E.8. XRD Spectrum of CCC-Treated Glass HAlG-08

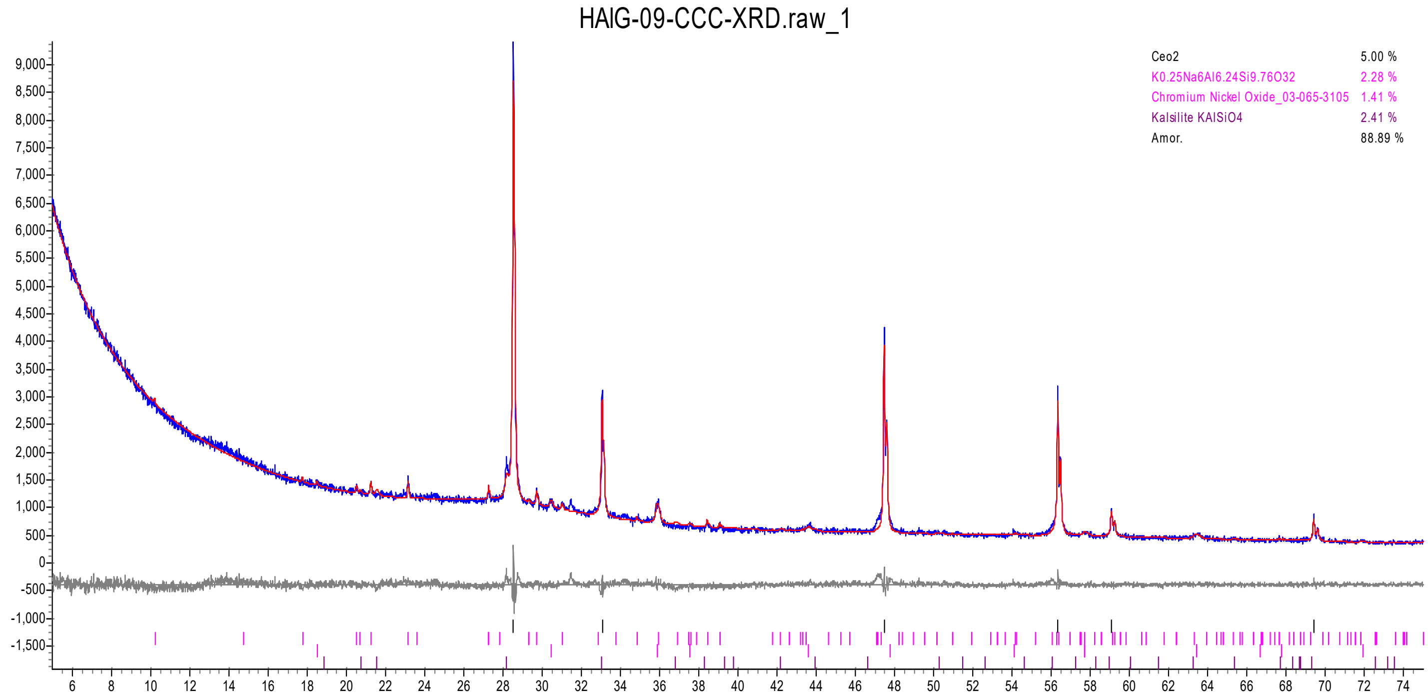

Phase Name	Wt% of Spiked	Wt% in Spiked Sample	Wt% in Original Sample
CeO_2	2.565	2.565	0.000
$KAlSiO_4$	0.000	1.495	1.574
$K_{0.25}Na_6Al_{6.24}Si_{9.76}O_{32}$ (Nepheline)	0.000	1.400	1.474
$NiCr_2O_4$ (Spinel)	0.000	0.870	0.916

Figure E.9. XRD Spectrum of CCC-Treated Glass HFG1-09

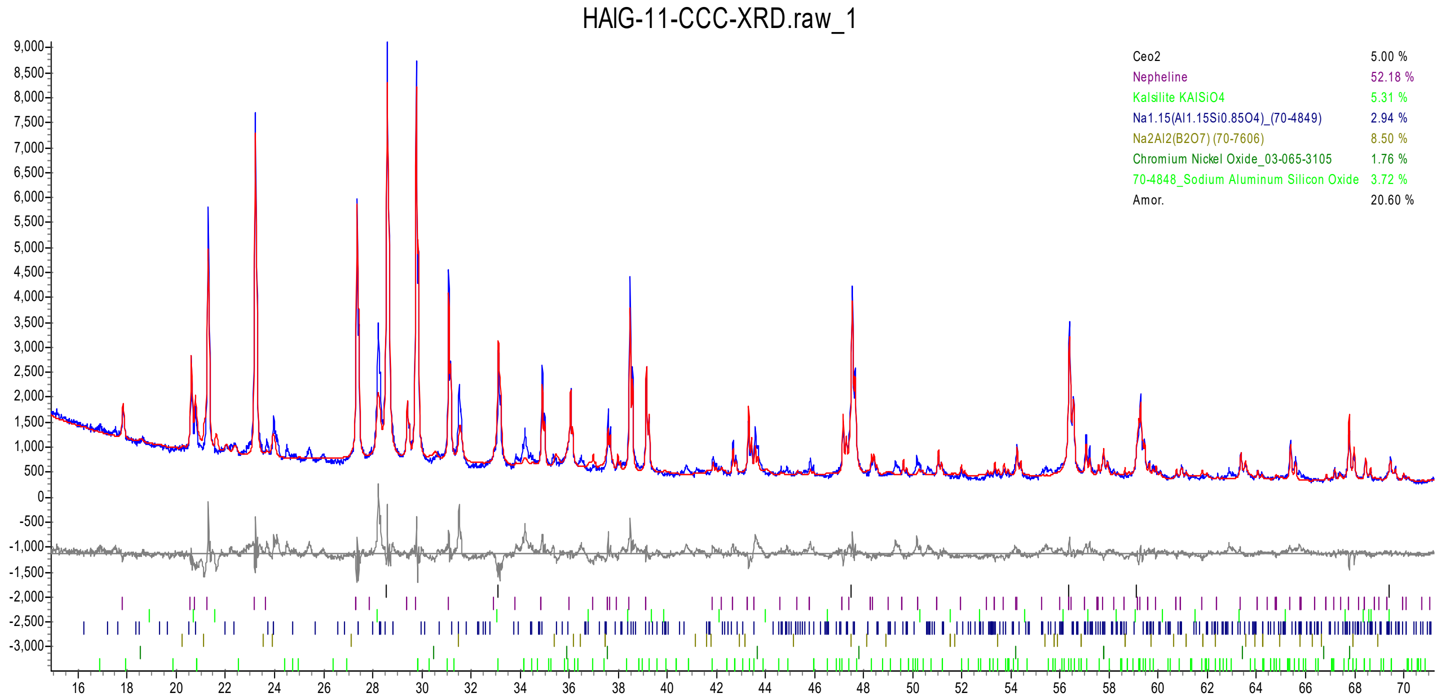

Phase Name	Wt% of Spiked	Wt% in Spiked Sample	Wt% in Original Sample
CeO_2	2.564	2.564	0.000
Nepheline	0.000	37.383	39.350
$Na_2Al_2(B_2O_7)$	0.000	5.644	5.941
$KAlSiO_4$	0.000	3.113	3.276
$NiCr_2O_4$ (Spinel)	0.000	0.948	0.998

Figure E.10. XRD Spectrum of CCC-Treated Glass HAlG-11

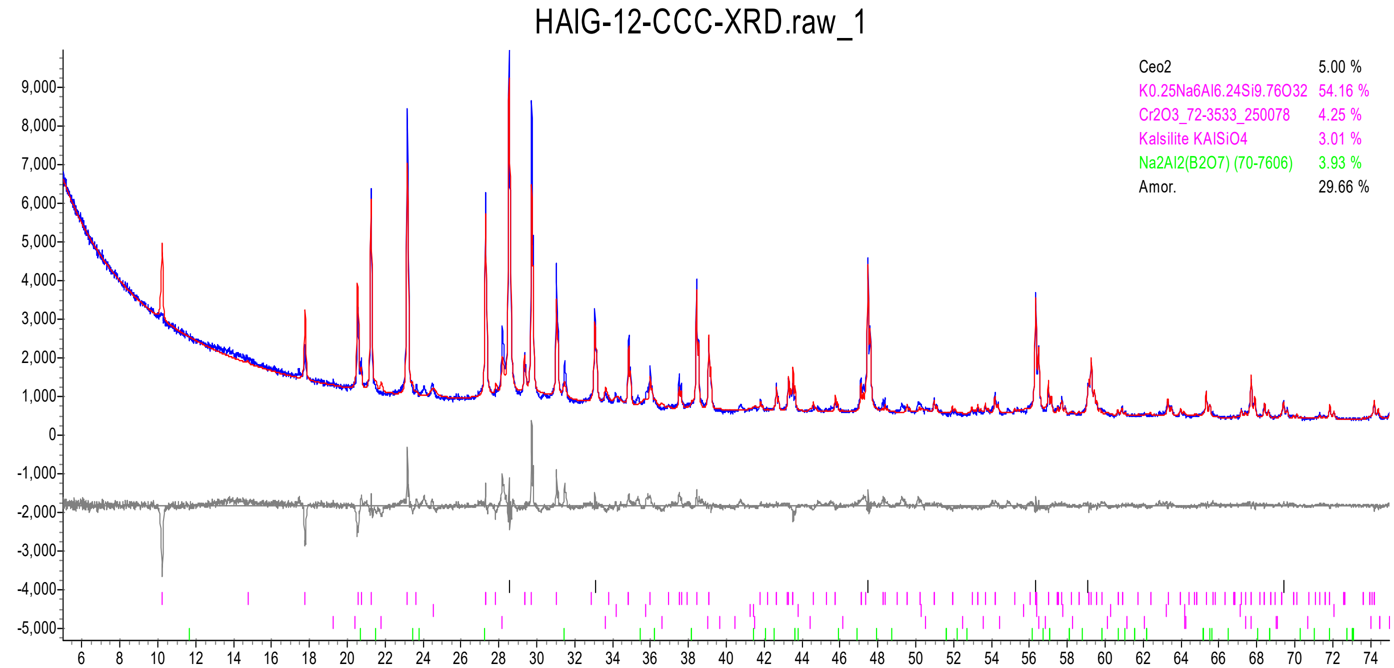

Phase Name	Wt% of Spiked	Wt% in Spiked Sample	Wt% in Original Sample
CeO_2	2.562	2.562	0.000
$K_{0.25}Na_6Al_{6.24}Si_{9.76}O_{32}$ (Nepheline)	0.000	31.061	32.695
Cr_2O_3	0.000	1.125	1.184
$KAlSiO_4$	0.000	2.030	2.136
$Na_2Al_2(B_2O_7)$	0.000	3.179	3.346

Figure E.11. XRD Spectrum of CCC-Treated Glass HAlG-12

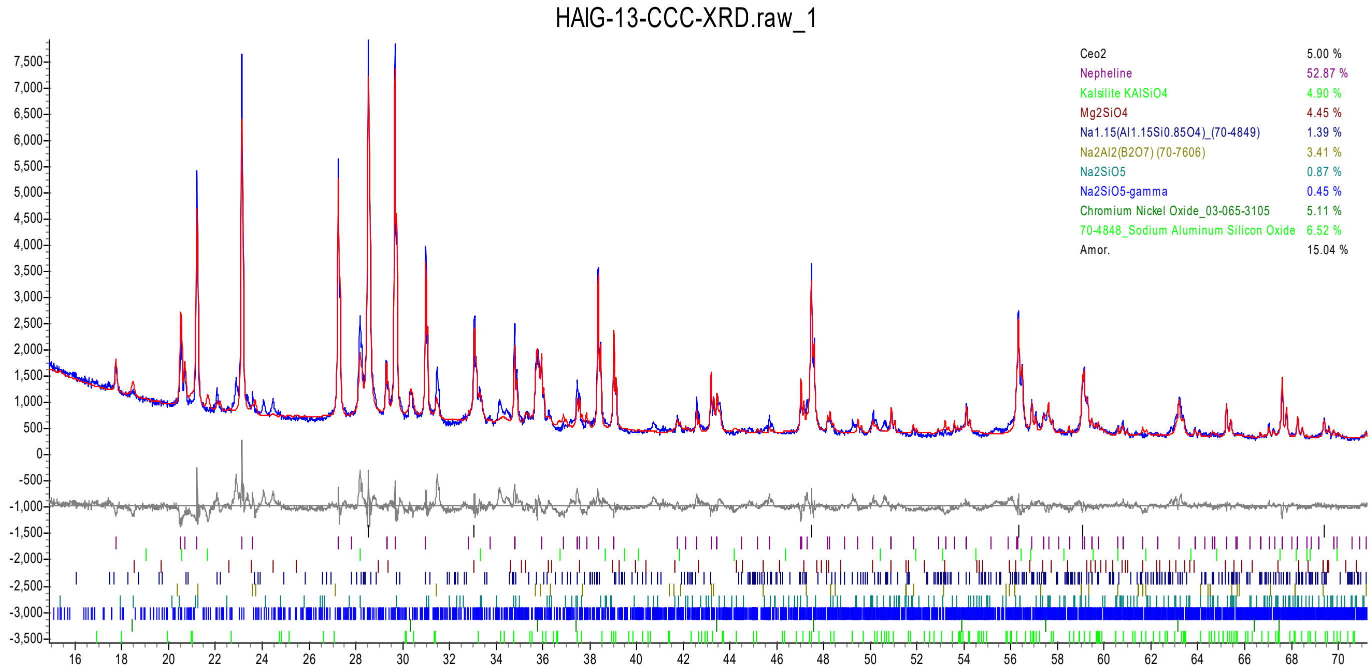

Phase Name	Wt% of Spiked	Wt% in Spiked Sample	Wt% in Original Sample
CeO_2	2.565	2.565	0.000
Nepheline	0.000	31.735	33.406
$NiCr_2O_4$ (Spinel)	0.000	2.736	2.880
Mg_2SiO_4	0.000	4.889	5.147
$KAlSiO_4$	0.000	3.121	3.285
$Na_2Al_2SiO_6$	0.000	2.240	2.358
$Na_2Al_2(B_2O_7)$	0.000	1.944	2.046

Figure E.12. XRD Spectrum of CCC-Treated Glass HAlG-13

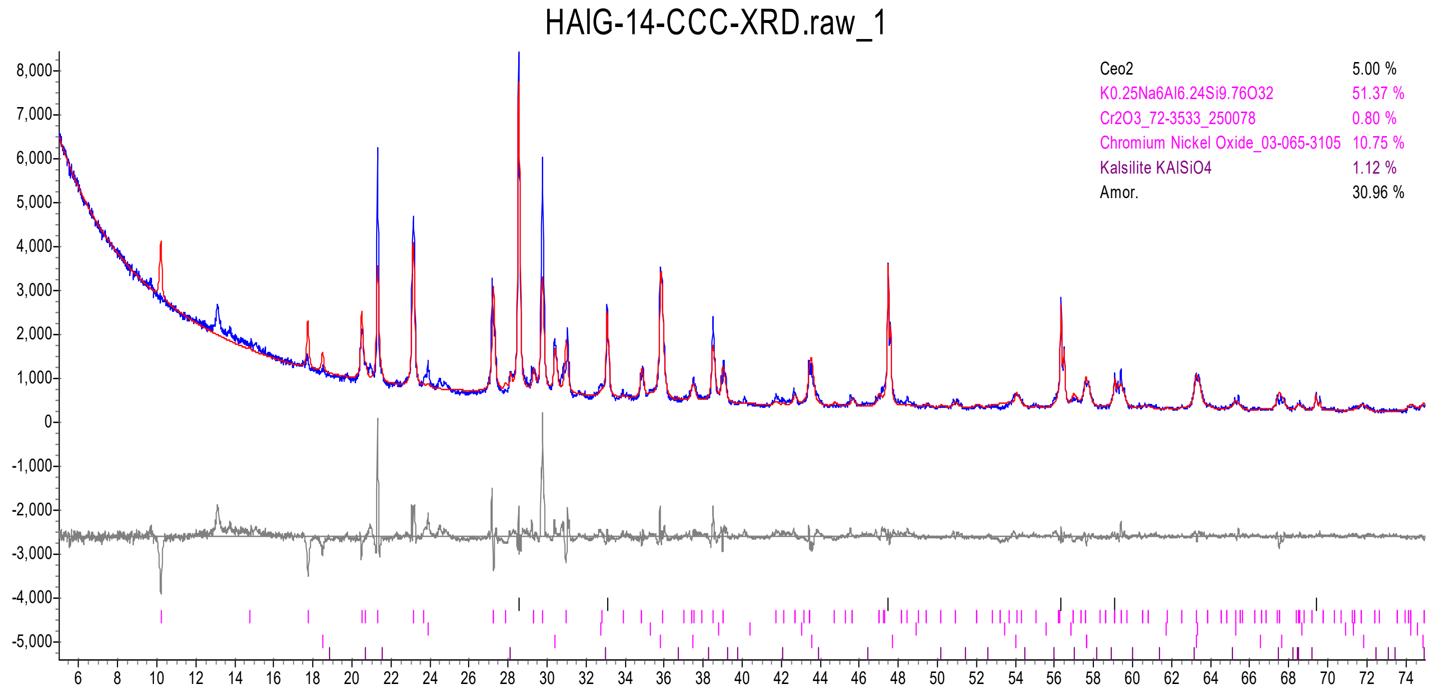

Phase Name	Wt% of Spiked	Wt% in Spiked Sample	Wt% in Original Sample
CeO_2	2.563	2.563	0.000
Nepheline	0.000	27.356	28.795
$KAlSiO_4$	0.000	1.400	1.474
$NiCr_2O_4$ (Spinel)	0.000	5.791	6.096

Figure E.13. XRD Spectrum of CCC-Treated Glass HAlG-14

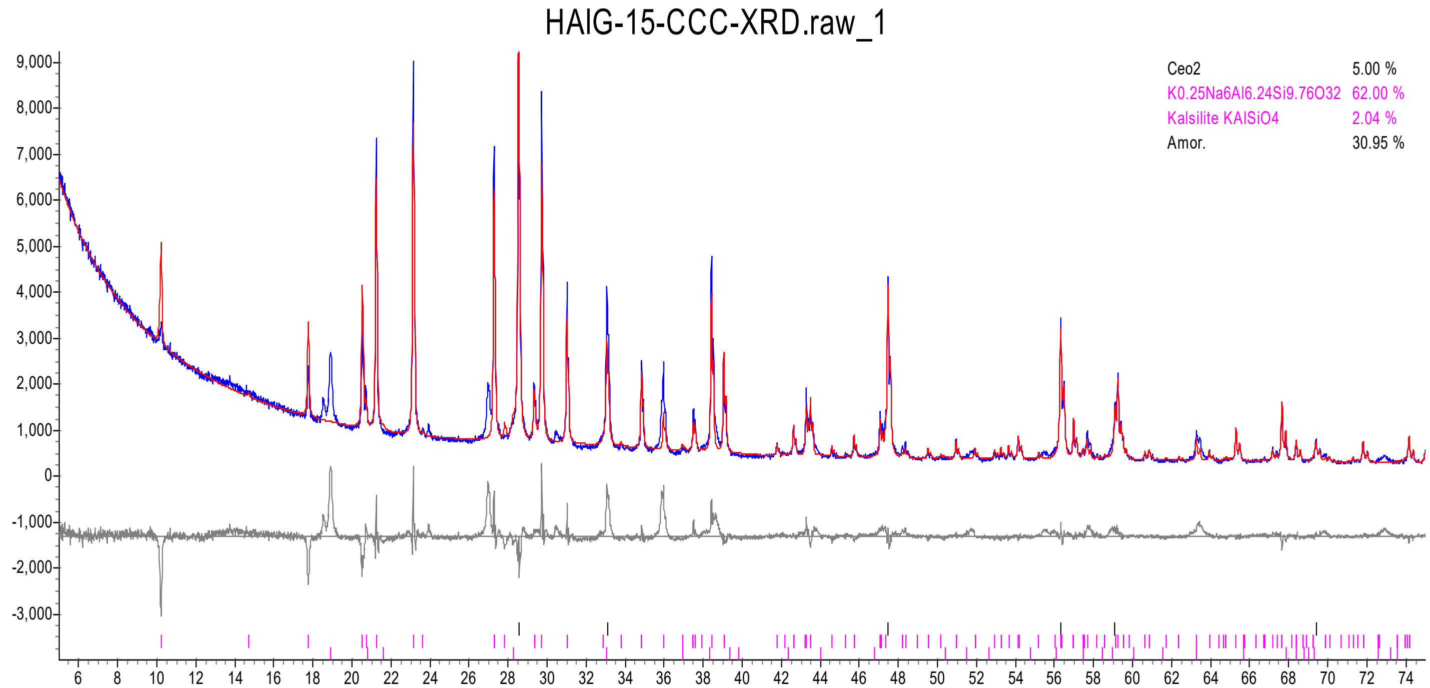

Phase Name	Wt% of Spiked	Wt% in Spiked Sample	Wt% in Original Sample
CeO_2	2.564	2.564	0.000
Nepheline	0.000	33.143	34.888
$KAlSiO_4$	0.000	3.455	3.637
$NiCr_2O_4$ (Spinel)	0.000	1.666	1.753

Figure E.14. XRD Spectrum of CCC-Treated Glass HAlG-15

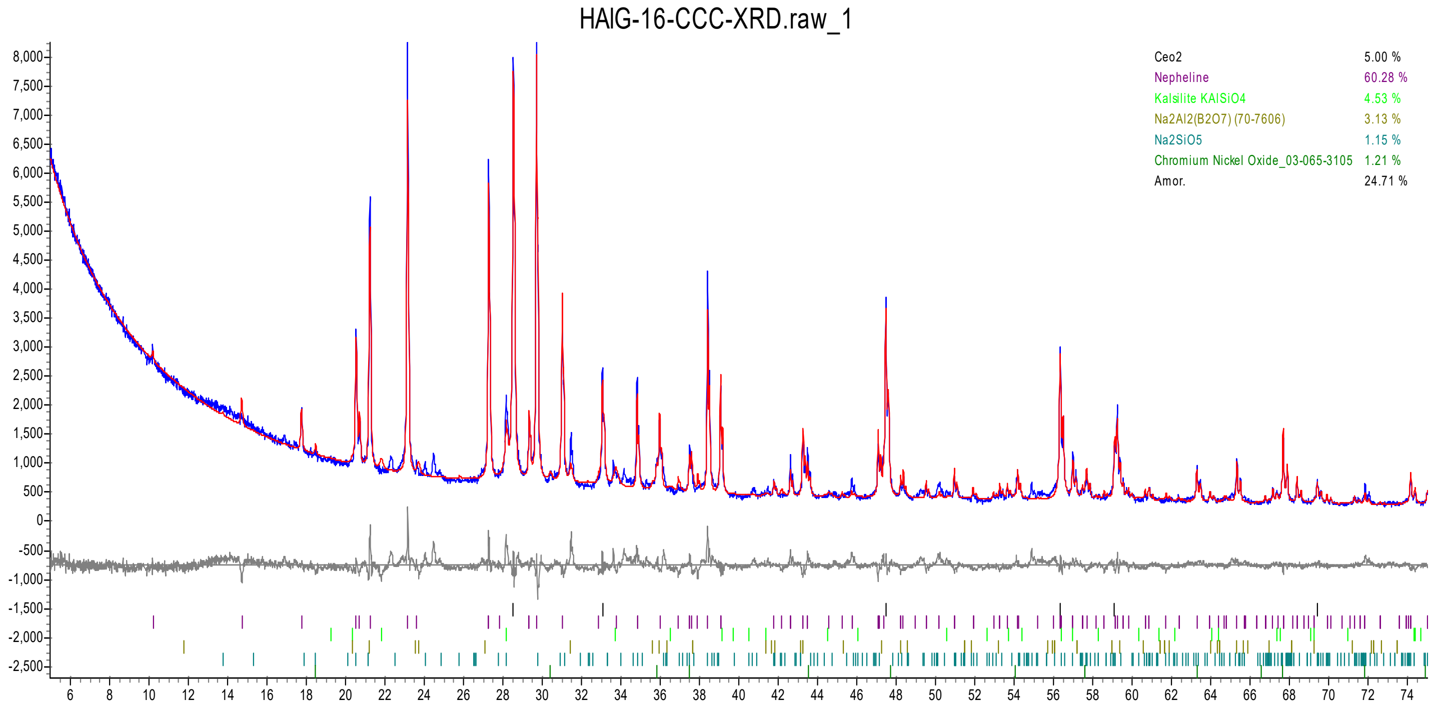

Phase Name	Wt% of Spiked	Wt% in Spiked Sample	Wt% in Original Sample
CeO_2	2.563	2.563	0.000
Nepheline	0.000	33.353	35.108
$Na_2Al_2(B_2O_7)$	0.000	2.176	2.290
$KAlSiO_4$	0.000	1.752	1.844
$NiCr_2O_4$ (Spinel)	0.000	0.698	0.735

Figure E.15. XRD Spectrum of CCC-Treated Glass HAlG-16

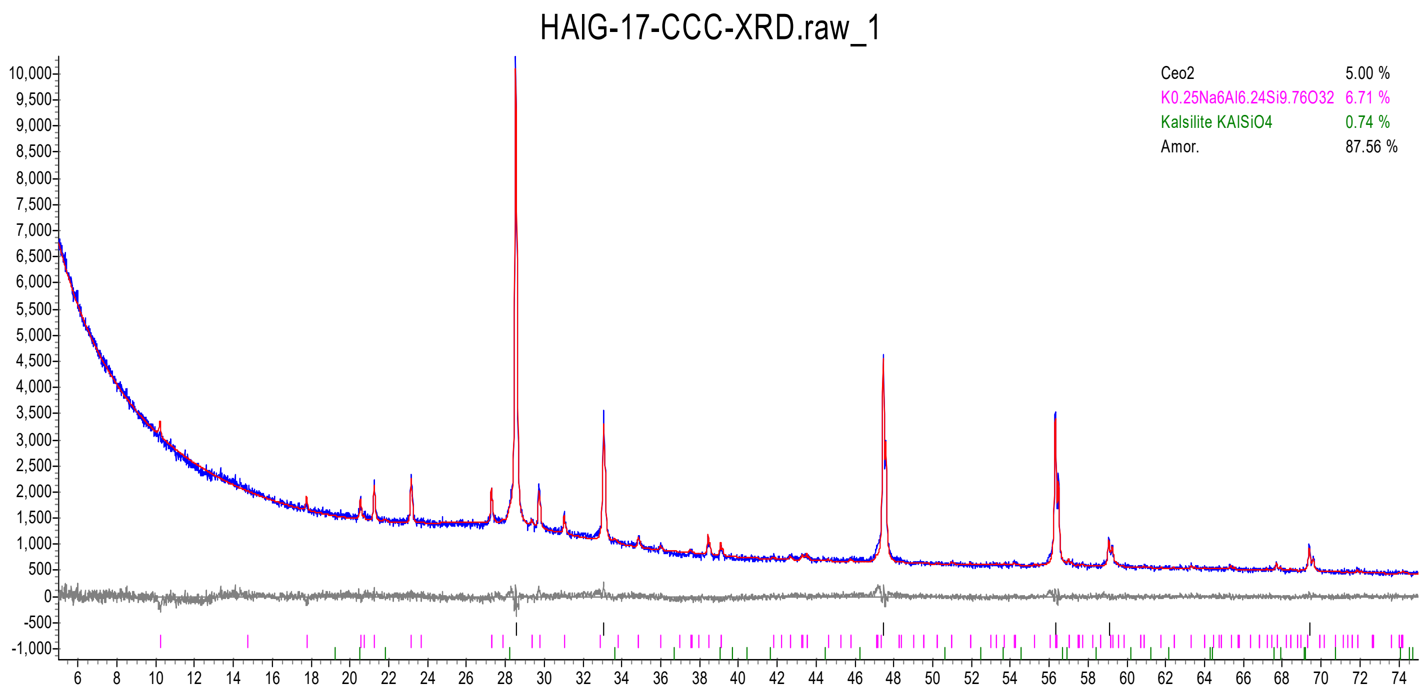

Phase Name	Wt% of Spiked	Wt% in Spiked Sample	Wt% in Original Sample
CeO_2	2.563	2.563	0.000
Nepheline	0.000	3.796	3.996
$KAlSiO_4$	0.000	0.860	0.906

Figure E.16. XRD Spectrum of CCC-Treated Glass HAlG-17

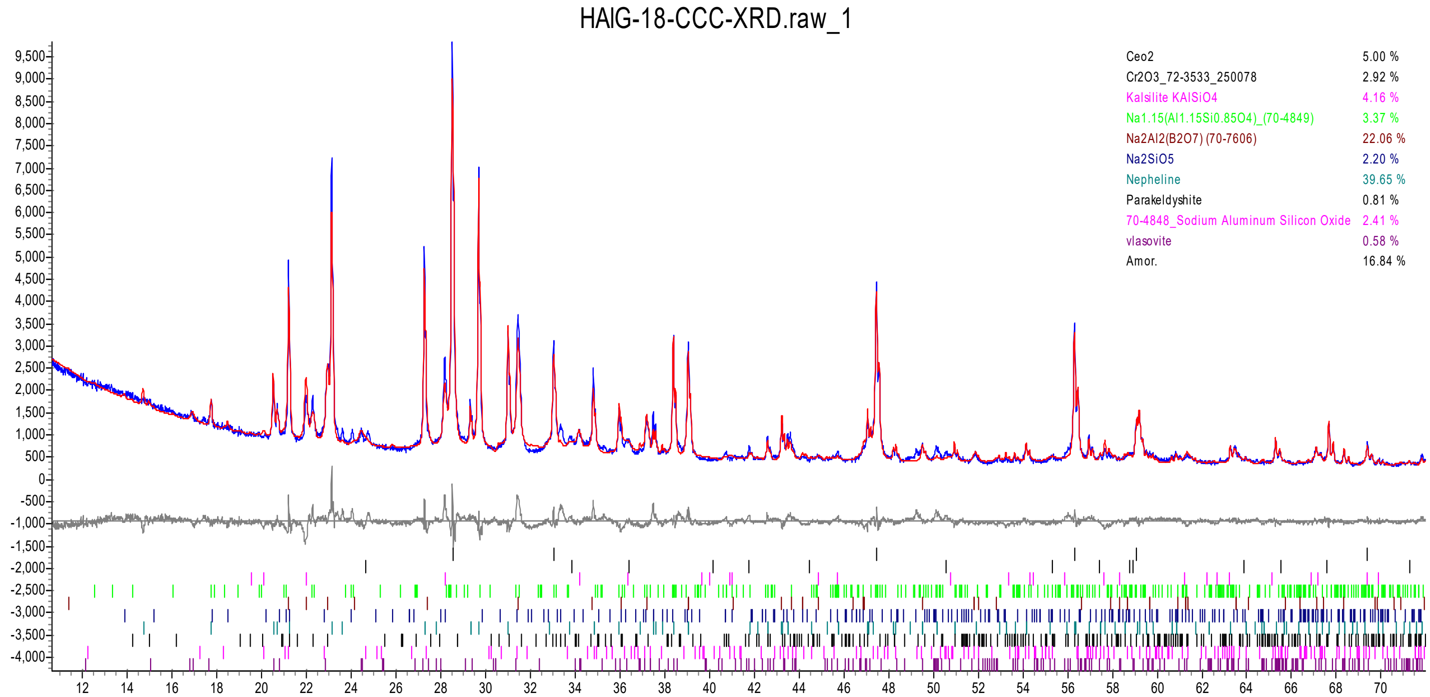

Phase Name	Wt% of Spiked	Wt% in Spiked Sample	Wt% in Original Sample
CeO_2	2.562	2.562	0.000
Nepheline	0.000	23.246	24.468
$Na_2Al_2(B_2O_7)$	0.000	6.054	6.372
$KAlSiO_4$	0.000	2.809	2.957

Figure E.17. XRD Spectrum of CCC-Treated Glass HAlG-18

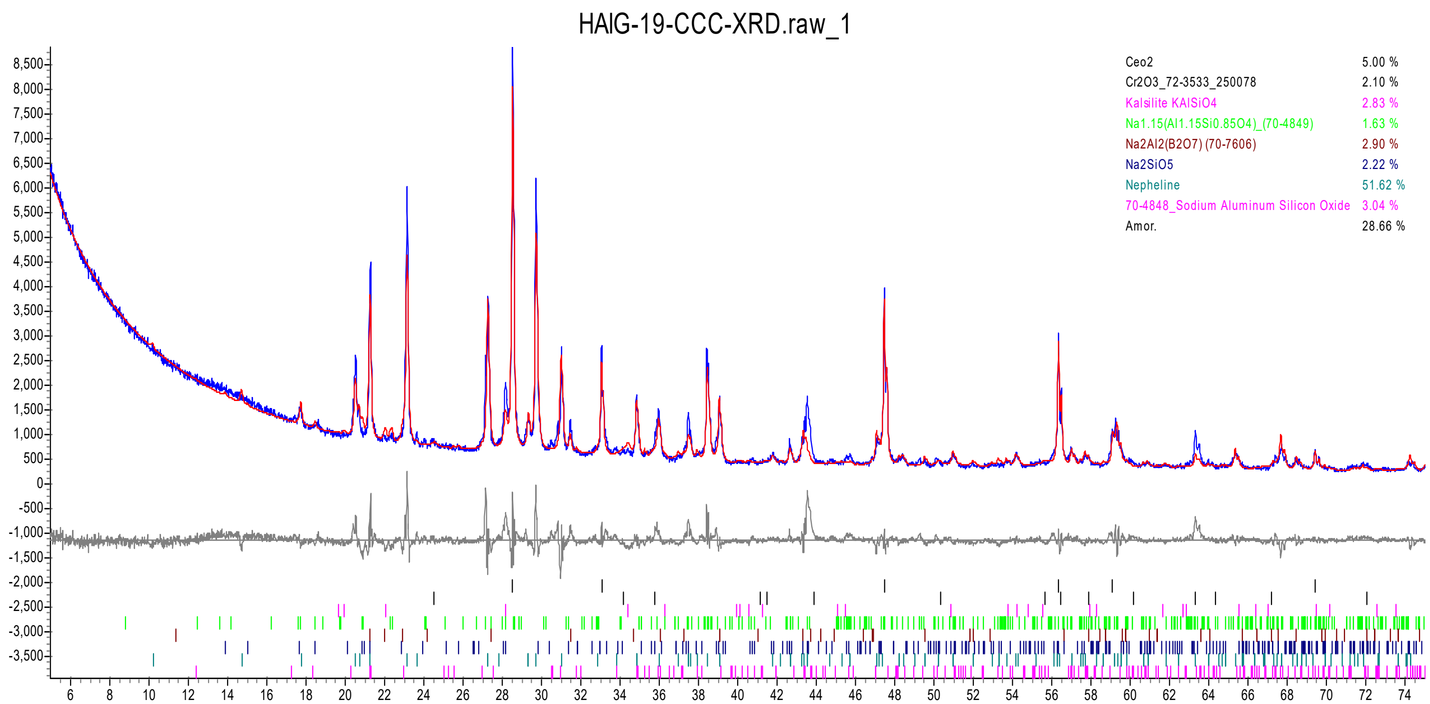

Phase Name	Wt% of Spiked	Wt% in Spiked Sample	Wt% in Original Sample
CeO_2	2.564	2.564	0.000
Nepheline	0.000	30.378	31.976
$Na_2Al_2(B_2O_7)$	0.000	2.462	2.591
$KAlSiO_4$	0.000	3.105	3.269

Figure E.18. XRD Spectrum of CCC-Treated Glass HAlG-19

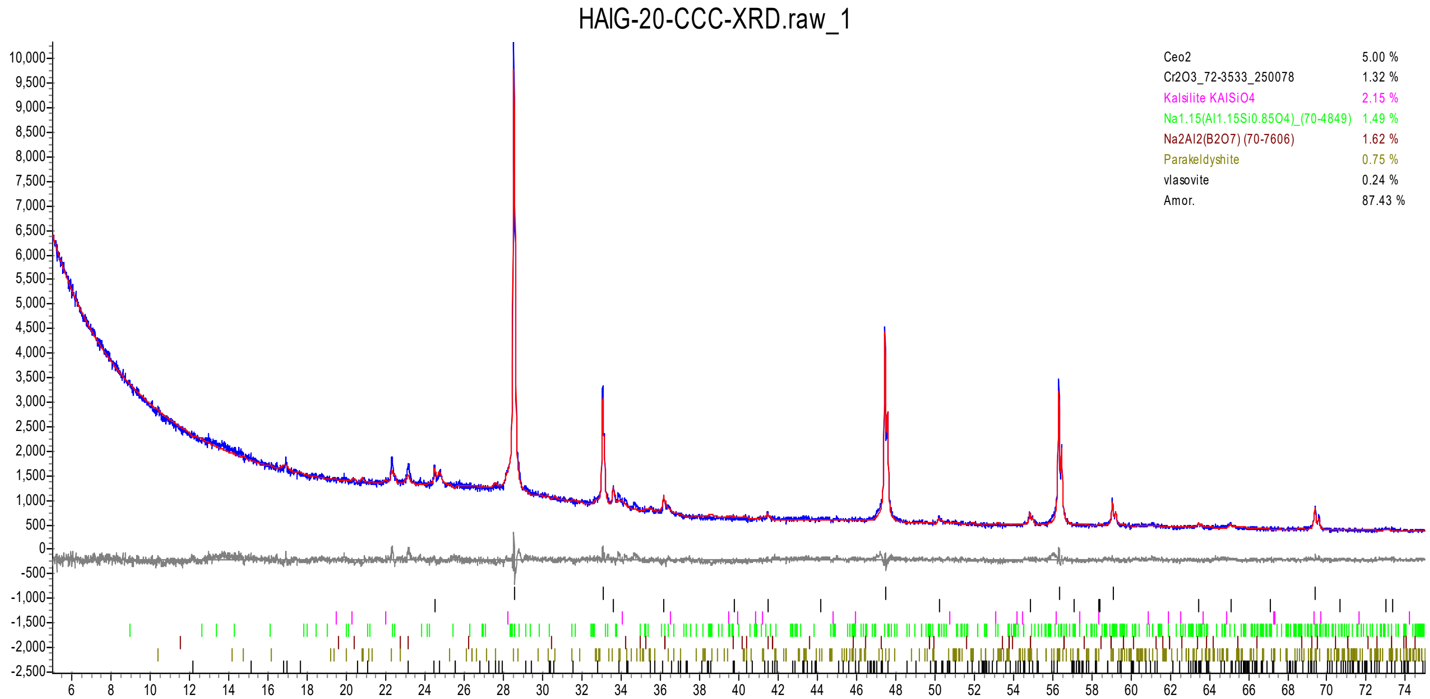

Phase Name	Wt% of Spiked	Wt% in Spiked Sample	Wt% in Original Sample
CeO_2	2.563	2.563	0.000
$KAlSiO_4$	0.000	1.426	1.501
$Na_2Al_2(B_2O_7)$	0.000	1.746	1.837
Cr_2O_3	0.000	0.750	0.789
Na_2ZrSi_2O	0.000	0.549	0.578
$Na_2ZrSi_4O_{11}$	0.000	0.172	0.181

Figure E.19. XRD Spectrum of CCC-Treated Glass HAlG-20

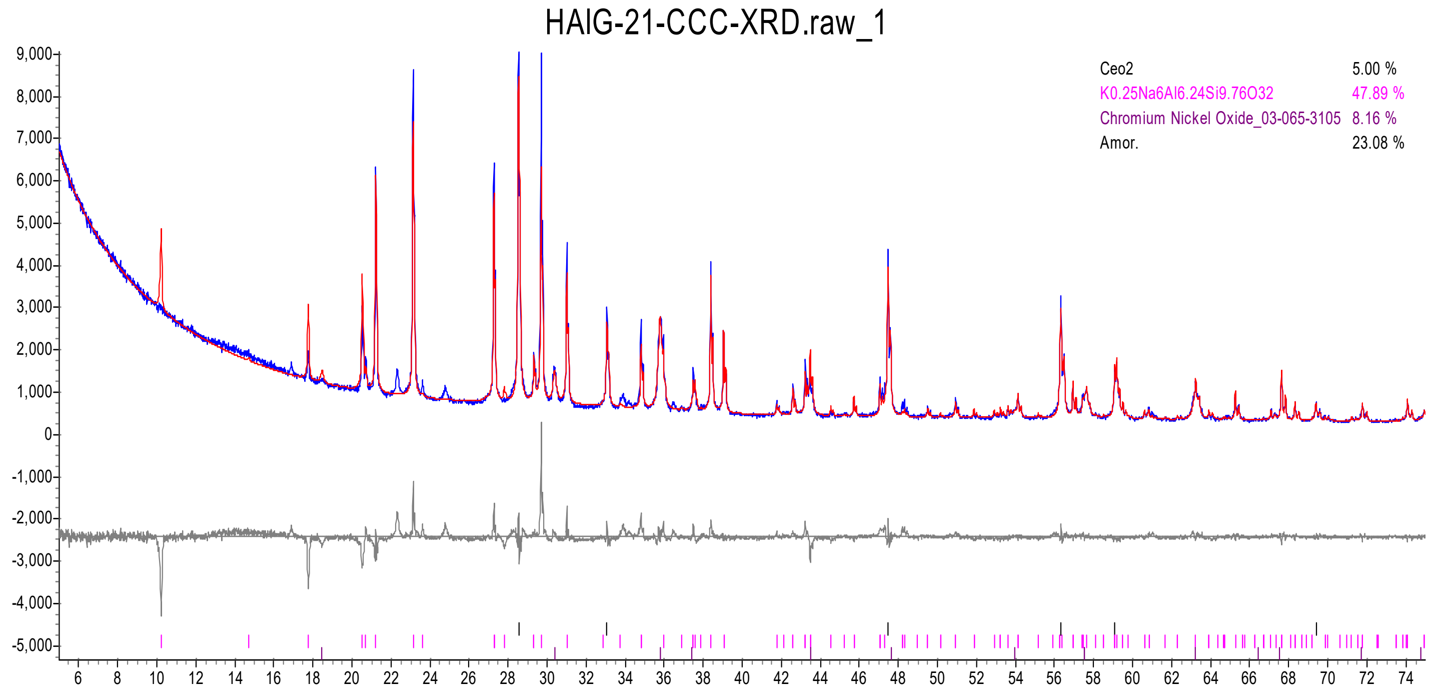

Phase Name	Wt% of Spiked	Wt% in Spiked Sample	Wt% in Original Sample
CeO_2	2.563	2.563	0.000
Nepheline	0.000	30.020	31.599
$Na_2Al_2(B_2O_7)$	0.000	3.495	3.678
Na_2ZrSi_2O	0.000	0.612	0.644
$Na_2ZrSi_4O_{11}$	0.000	0.191	0.201

Figure E.20. XRD Spectrum of CCC-Treated Glass HAlG-21

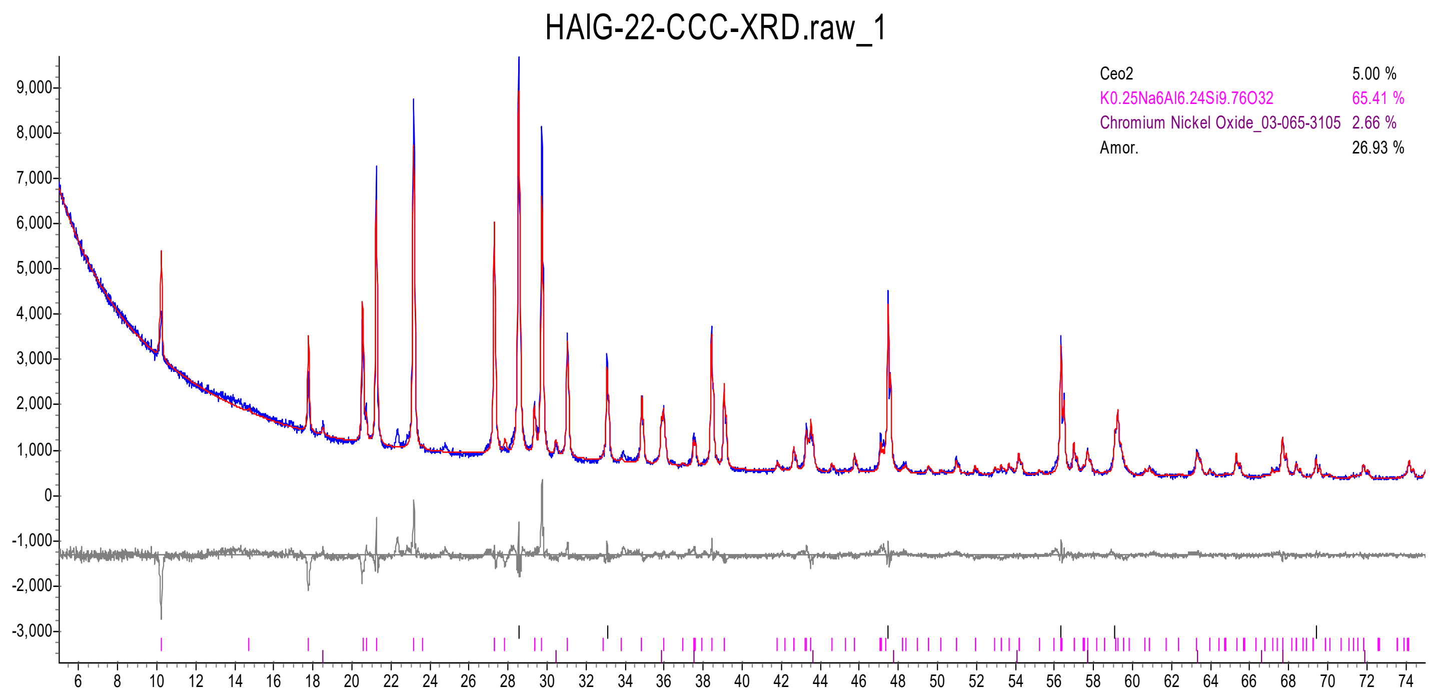

Phase Name	Wt% of Spiked	Wt% in Spiked Sample	Wt% in Original Sample
CeO_2	2.563	2.563	0.000
Nepheline	0.000	33.346	35.100
$NiCr_2O_4$ (Spinel)	0.000	1.313	1.382

Figure E.21. XRD Spectrum of CCC-Treated Glass HAlG-22

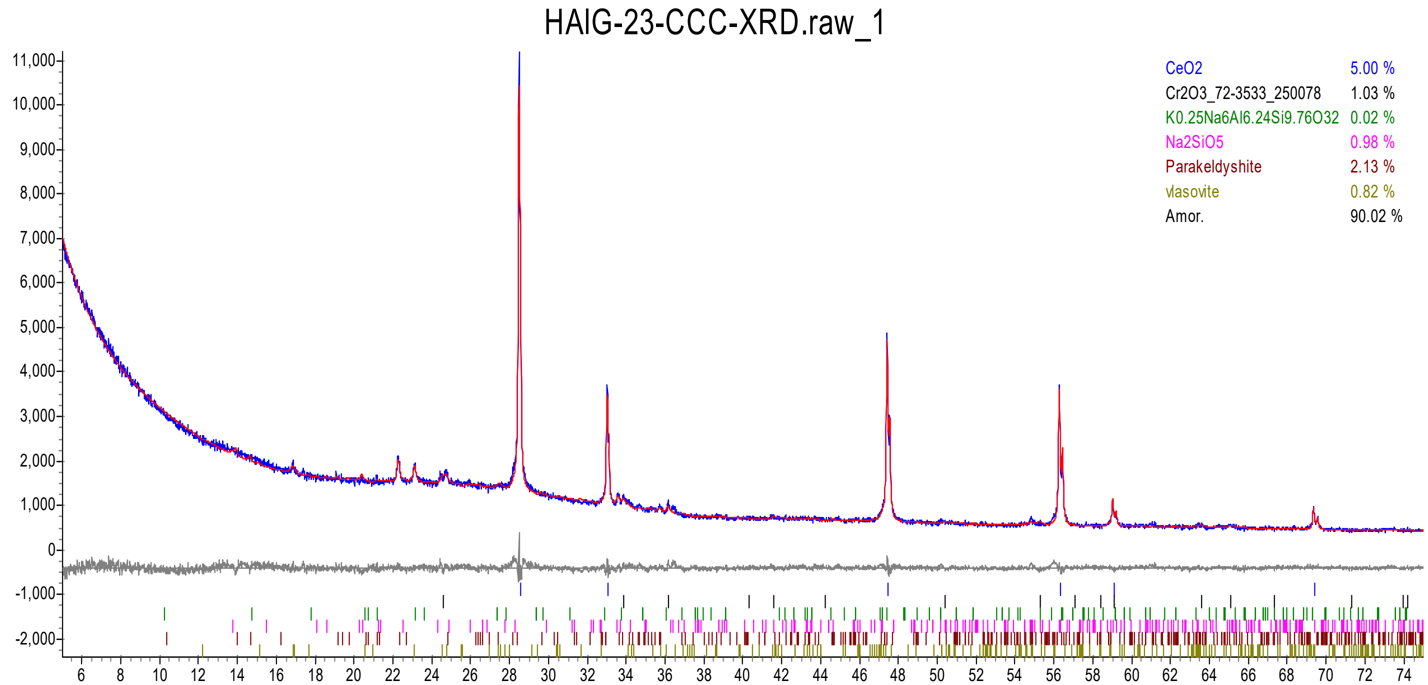

Phase Name	Wt% of Spiked	Wt% in Spiked Sample	Wt% in Original Sample
CeO_2	2.565	2.565	0.000
Nepheline	0.000	2.975	3.132
Cr_2O_3	0.000	0.528	0.556
$NiCr_2O_4$ (Spinel)	0.000	4.017	4.228
$KAlSiO_4$	0.000	0.875	0.921
Na_2ZrSi_2O	0.000	0.940	0.990
$Na_2ZrSi_4O_{11}$	0.000	0.069	0.072

Figure E.22. XRD Spectrum of CCC-Treated Glass HAlG-23

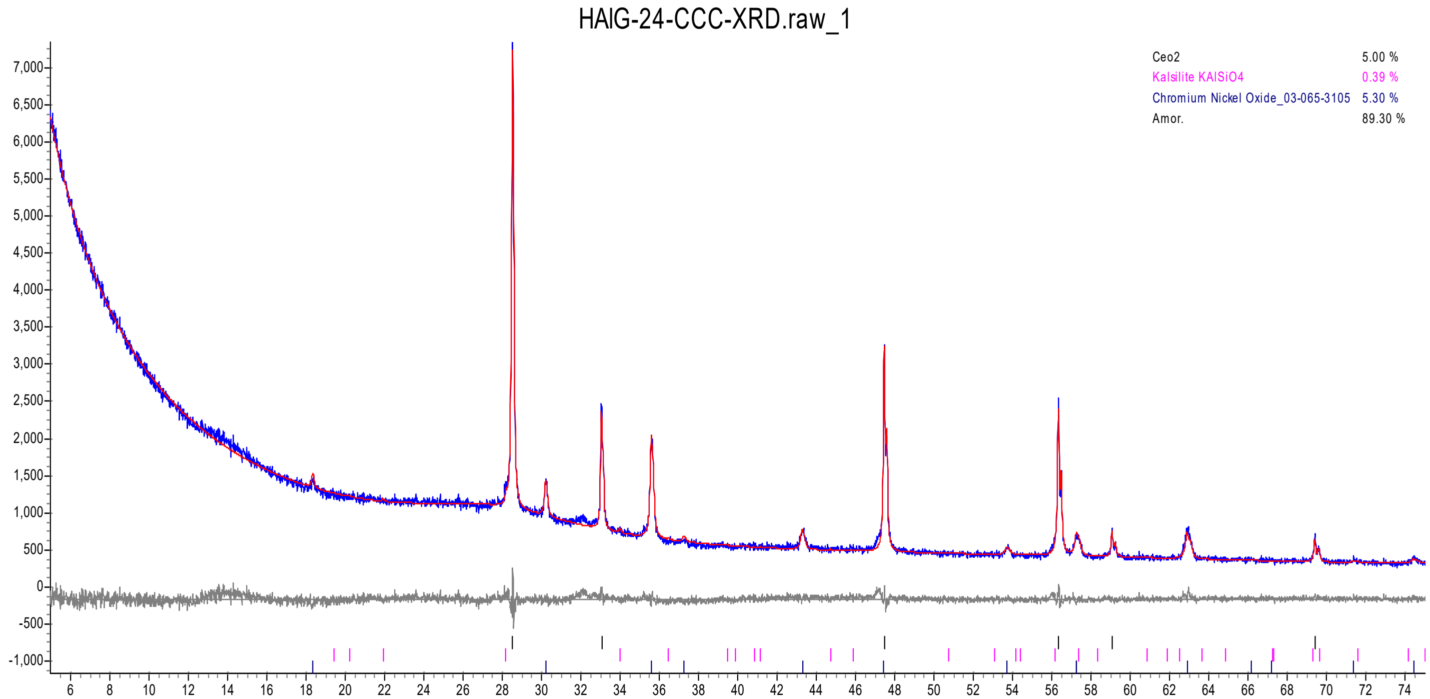

Phase Name	Wt% of Spiked	Wt% in Spiked Sample	Wt% in Original Sample
CeO_2	2.565	2.565	0.000
$NiCr_2O_4$ (Spinel)	0.000	3.036	3.196
$KAlSiO_4$	0.000	0.820	0.863

Figure E.23. XRD Spectrum of CCC-Treated Glass HAlG-24

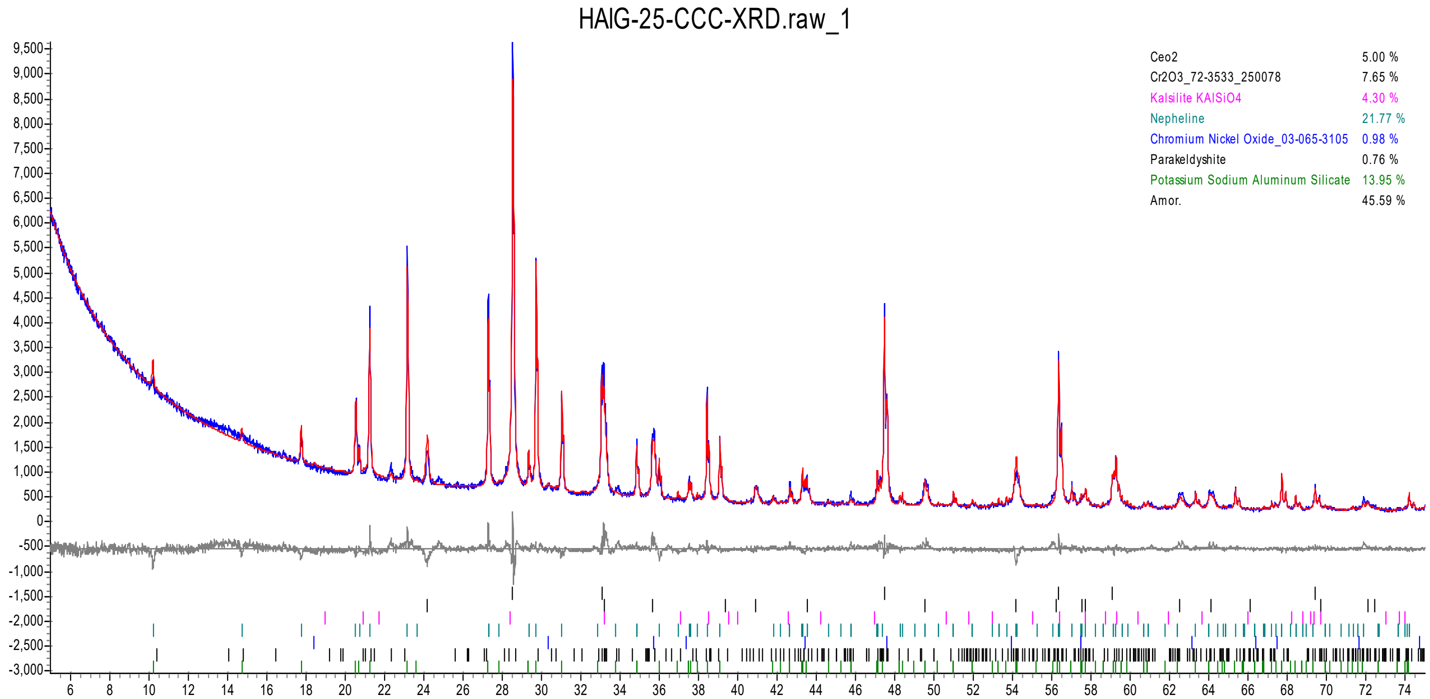

Phase Name	Wt% of Spiked	Wt% in Spiked Sample	Wt% in Original Sample
CeO_2	2.563	2.563	0.000
Nepheline	0.000	18.616	19.596
$NiCr_2O_4$ (Spinel)	0.000	0.410	0.432
$KAlSiO_4$	0.000	3.799	3.999
Fe_2O_3	0.000	3.991	4.201
Na_2ZrSi_2O	0.000	0.343	0.361

Figure E.24. XRD Spectrum of CCC-Treated Glass HAlG-25

Appendix F – Viscosity Data

This appendix presents the measured viscosity data for each of the glasses in this matrix. The plots shown in this appendix are fitted to the Arrhenius equation:

$$\ln(\eta) = A + \frac{B}{T_K} \tag{F.1}$$

where A and B are independent of temperature and temperature (T_K) is in K (T(°C) + 273.15).

The intent of the figures and Arrhenius equation fits presented in this appendix is mainly to assess trends in the data and provide observations about whether there may be sufficient curvature in the data to consider Vogel-Fulcher-Tamman (VFT) fits in the subsequent work that will decide between fitting the viscosity-temperature data to the Arrhenius or VFT equations. All the glasses in this matrix appear to have very good fits to the Arrhenius equation and do not show a need for fitting to the VFT model.

F.1 Glass HAIG1-1 Viscosity Data

Table F.1. Viscosity Data for Glass HAlG-01

Measured Temp., °C	Viscosity, Pa-s	1/T x10000, K^{-1}	ln η, Pa-s
1150	10.04	0.70267	2.3067
1050	32.49	0.75577	3.4808
950	148.57	0.81756	5.0011
1150	10.01	0.70267	2.3038
1200	6.20	0.67882	1.8240
1150	10.17	0.70267	2.3198

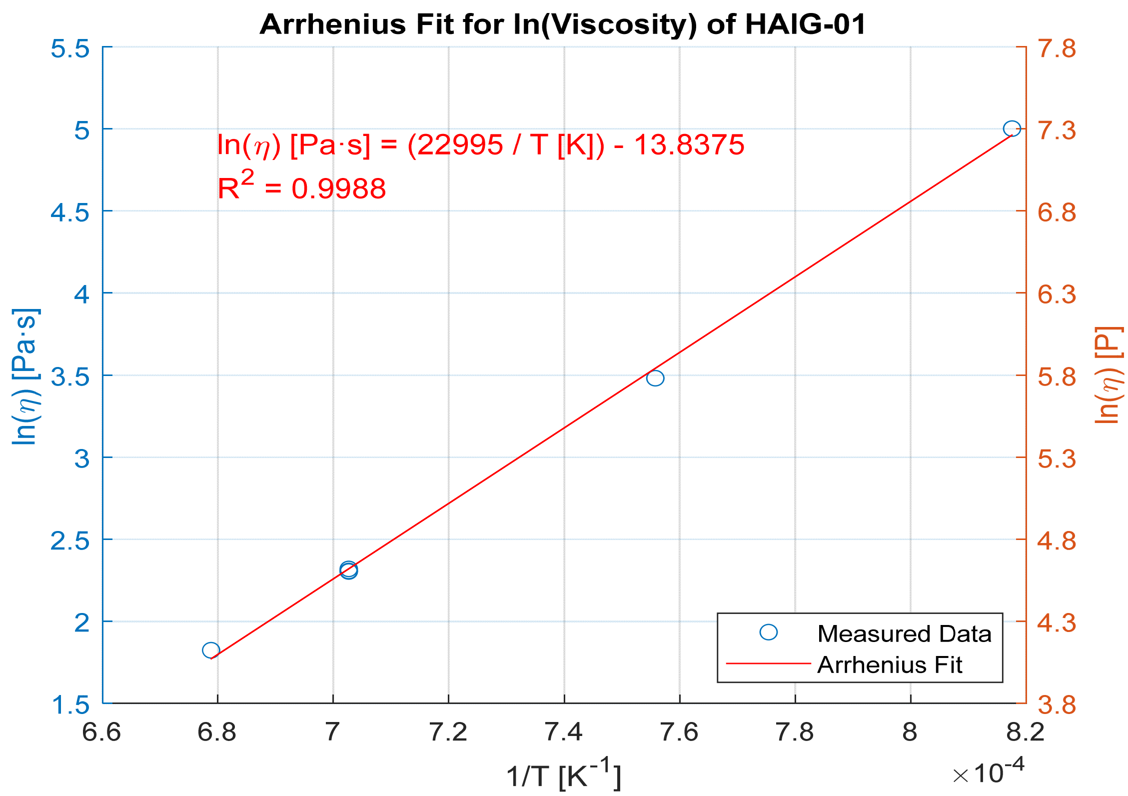

Figure F.1. Viscosity-Temperature Data and Arrhenius Equation Fit for Glass HAlG-01

F.2 Glass HAlG-02 Viscosity Data

Table F.2. Viscosity Data for Glass HAlG-02

Measured Temp., °C	Viscosity, Pa-s	1/T x10000, K^{-1}	ln η, Pa-s
1150	5.51	0.70267	1.7062
1050	14.19	0.75577	2.6522
950	48.46	0.81756	3.8808
1150	5.29	0.70267	1.6667
1200	3.74	0.67882	1.3194
1150	5.59	0.70267	1.7207

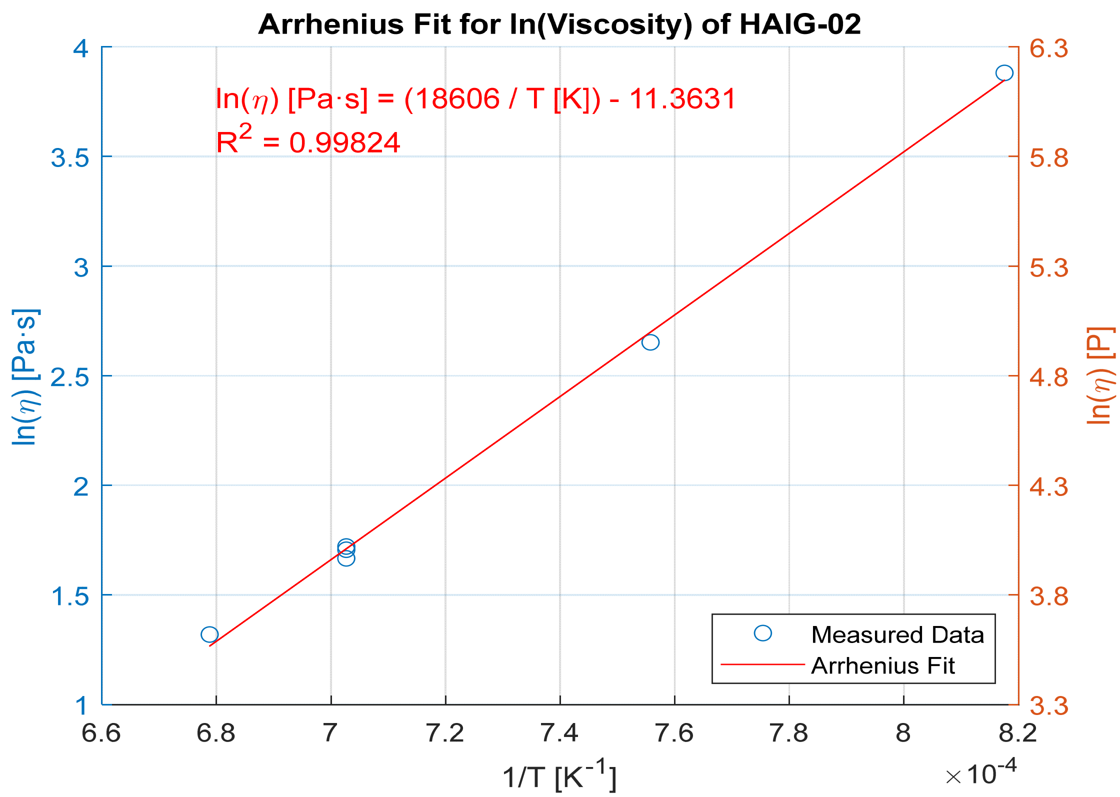

Figure F.2. Viscosity-Temperature Data and Arrhenius Equation Fit for Glass HAlG-02

F.3 Glass HAlG-03 Viscosity Data

Table F.3. Viscosity Data for Glass HAlG-03

Measured Temp., °C	Viscosity, Pa-s	1/T x10000, K^{-1}	ln η, Pa-s
1150	9.49	0.70267	2.2498
1050	27.74	0.75577	3.3230
950	115.99	0.81756	4.7535
1150	9.27	0.70267	2.2271
1200	5.98	0.67882	1.7878
1150	9.23	0.70267	2.2223

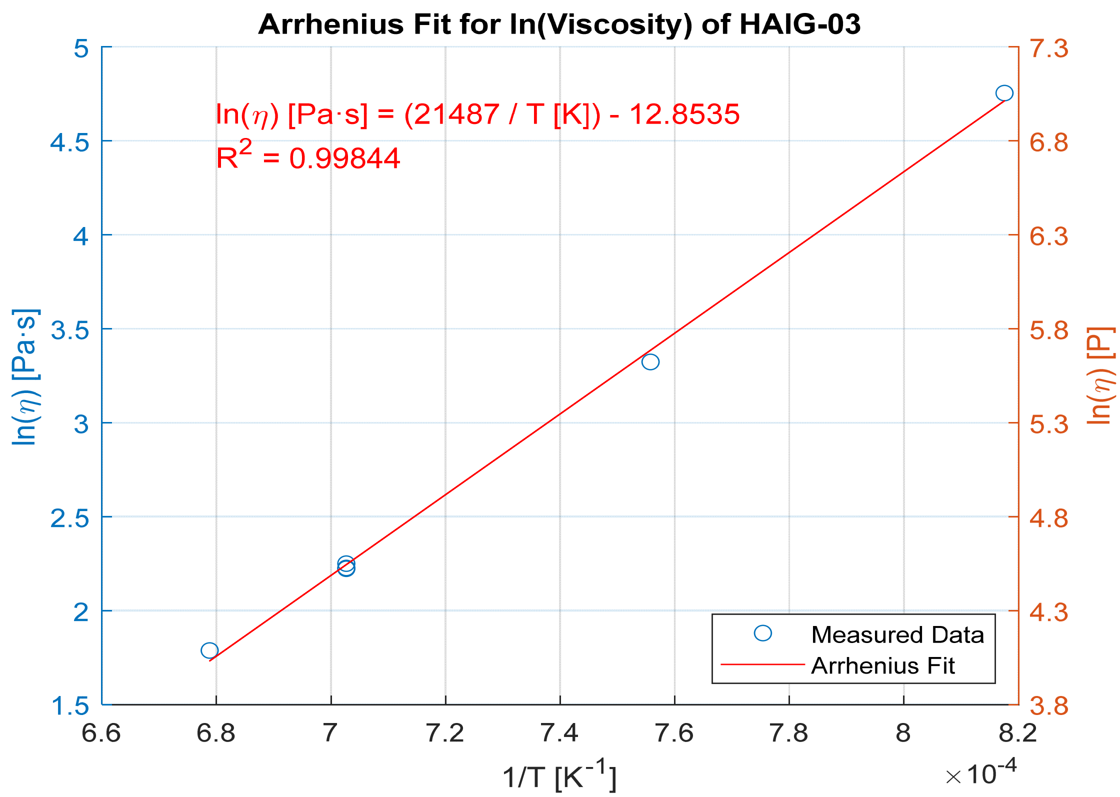

Figure F.3. Viscosity-Temperature Data and Arrhenius Equation Fit for Glass HAlG-03

F.4 Glass HAlG-04 Viscosity Data

Table F.4. Viscosity Data for Glass HAlG-04

Measured Temp., °C	Viscosity, Pa-s	1/T x10000, K-1	ln η, Pa-s
1150	12.32	0.70267	2.5112
1050	36.54	0.75577	3.5983
950	138.98	0.81756	4.9343
1150	12.21	0.70267	2.5018
1200	7.33	0.67882	1.9923
1150	11.87	0.70267	2.4741

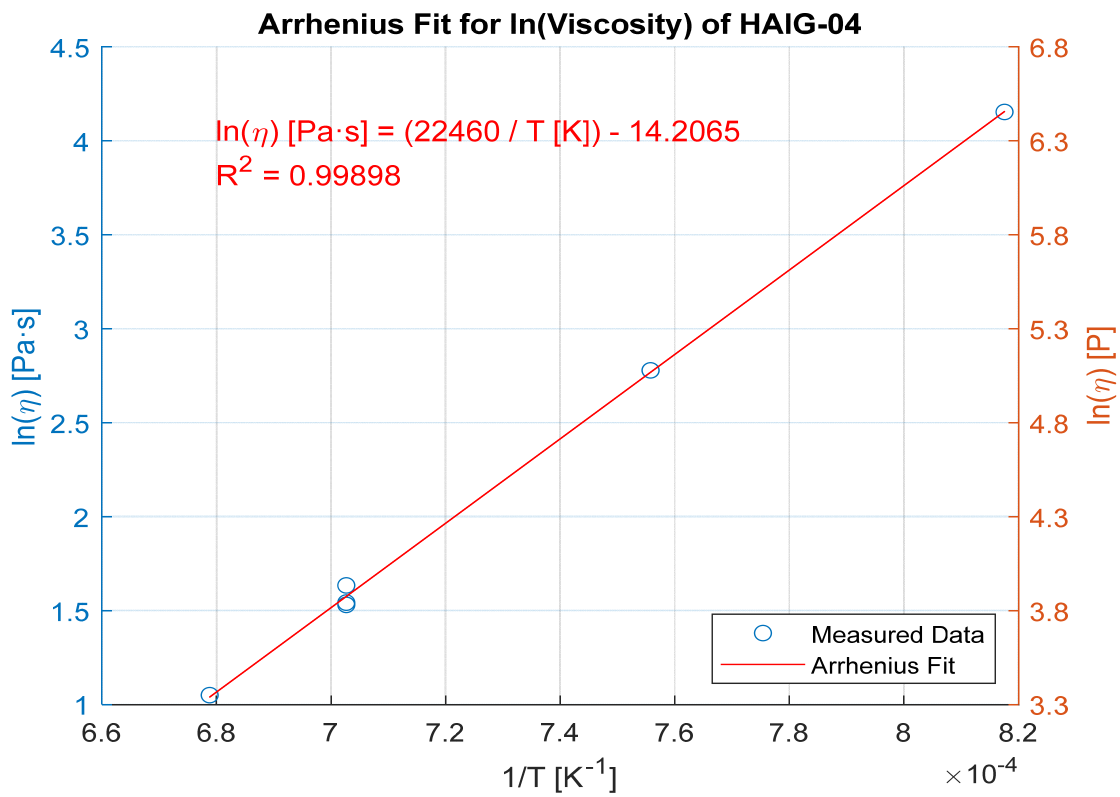

Figure F.4. Viscosity-Temperature Data and Arrhenius Equation Fit for Glass HAlG-04

F.5 Glass HAlG-05 Viscosity Data

Table F.5. Viscosity Data for Glass HAlG-05

Measured Temp., °C	Viscosity, Pa-s	1/T x10000, K^{-1}	ln η, Pa-s
1150	5.12	0.70267	1.6339
1050	16.09	0.75577	2.7783
950	63.63	0.81756	4.1531
1150	4.62	0.70267	1.5305
1200	2.86	0.67882	1.0503
1150	4.68	0.70267	1.5424

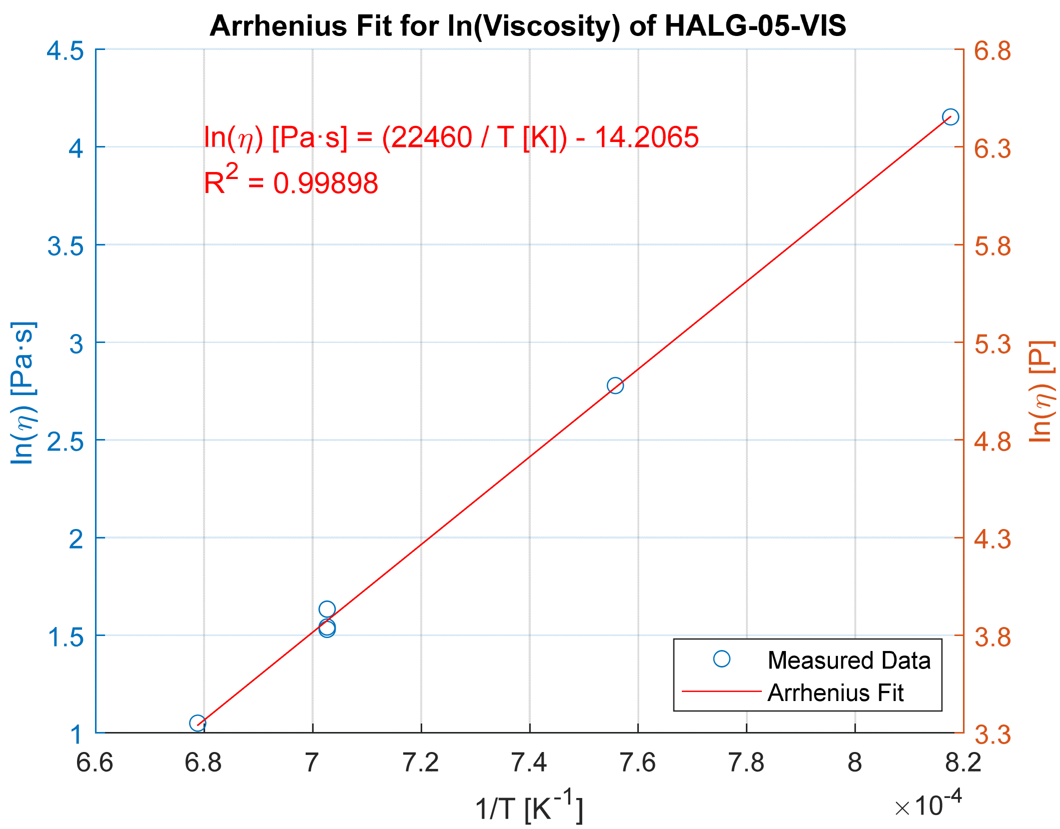

Figure F.5. Viscosity-Temperature Data and Arrhenius Equation Fit for Glass HAlG-05

F.6 Glass HAlG-06 Viscosity Data

Table F.6. Viscosity Data for Glass HAlG-06

Measured Temp., °C	Viscosity, Pa-s	1/T x10000, K^{-1}	ln η, Pa-s
1150	11.19	0.70267	2.4148
1050	31.88	0.75577	3.4619
950	121.36	0.81756	4.7988
1150	10.86	0.70267	2.3849
1200	6.95	0.67882	1.9387
1150	10.97	0.70267	2.3949

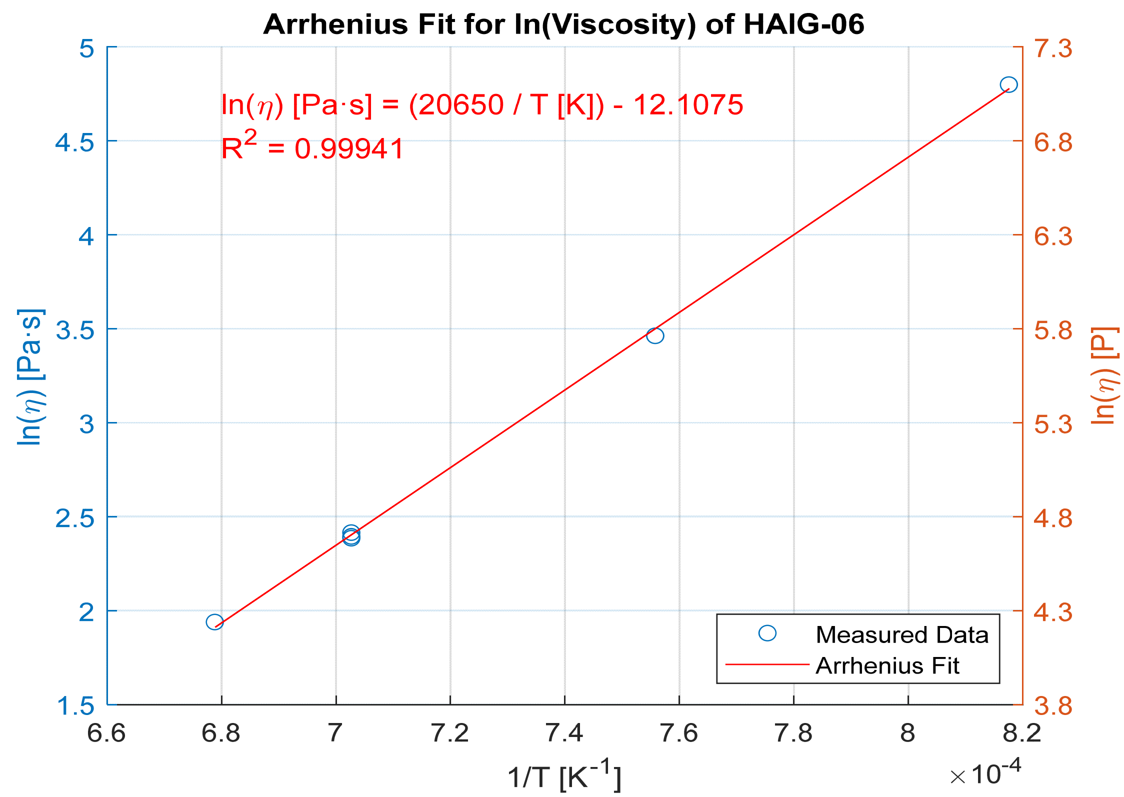

Figure F.6. Viscosity-Temperature Data and Arrhenius Equation Fit for Glass HAlG-06

F.7 Glass HAIG-07-1 Viscosity Data

Table F.7. Viscosity Data for Glass HAlG-07-1

Measured Temp., °C	Viscosity, Pa-s	1/T x10000, K^{-1}	ln η, Pa-s
1150	7.89	0.70267	2.0661
1050	28.41	0.75577	3.3468
950	120.54	0.81756	4.7920
1150	7.63	0.70267	2.0317
1200	4.16	0.67882	1.4258
1150	7.23	0.70267	1.9781

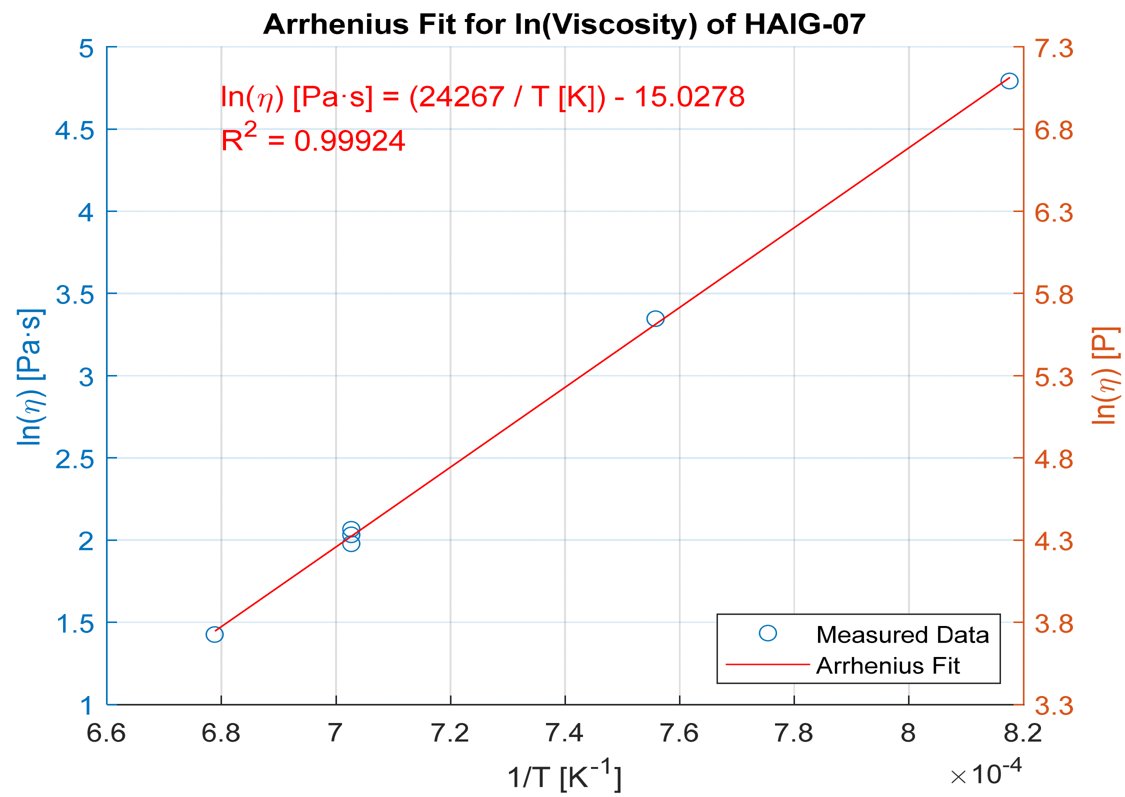

Figure F.7. Viscosity-Temperature Data and Arrhenius Equation Fit for Glass HAlG-07-1

F.8 Glass HAlG-08 Viscosity Data

Table F.8. Viscosity Data for Glass HAlG-08

Measured Temp., °C	Viscosity, Pa-s	1/T x10000, K^{-1}	ln η, Pa-s
1150	7.52	0.70267	2.0181
1050	25.70	0.75577	3.2463
950	111.71	0.81756	4.7159
1150	7.23	0.70267	1.9787
1200	4.36	0.67882	1.4732
1150	7.06	0.70267	1.9546

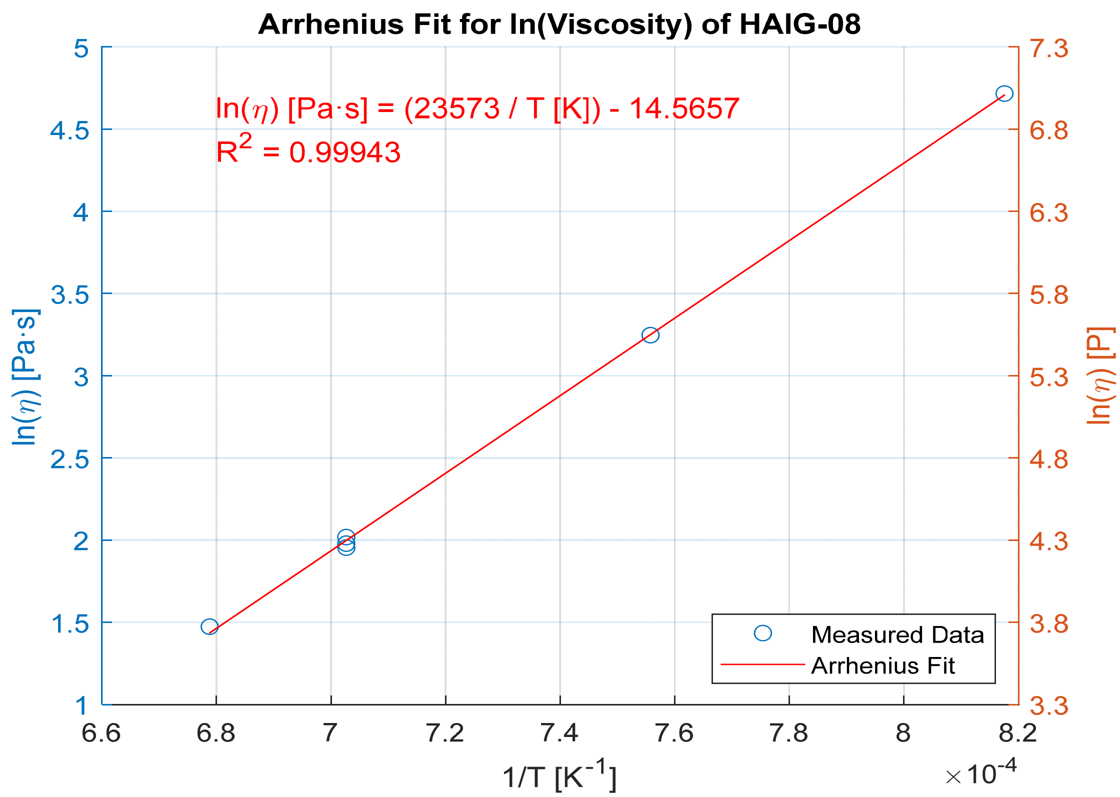

Figure F.8. Viscosity-Temperature Data and Arrhenius Equation Fit for Glass HAlG-08

F.9 Glass HAlG-09 Viscosity Data

Table F.9. Viscosity Data for Glass HAlG-09

Measured Temp., °C	Viscosity, Pa-s	1/T x10000, K^{-1}	ln η, Pa-s
1150	1.77	0.70267	0.5733
1050	4.28	0.75577	1.4530
950	11.09	0.81756	2.4062
1150	1.70	0.70267	0.5297
1200	1.05	0.67882	0.0473
1150	1.63	0.70267	0.4859

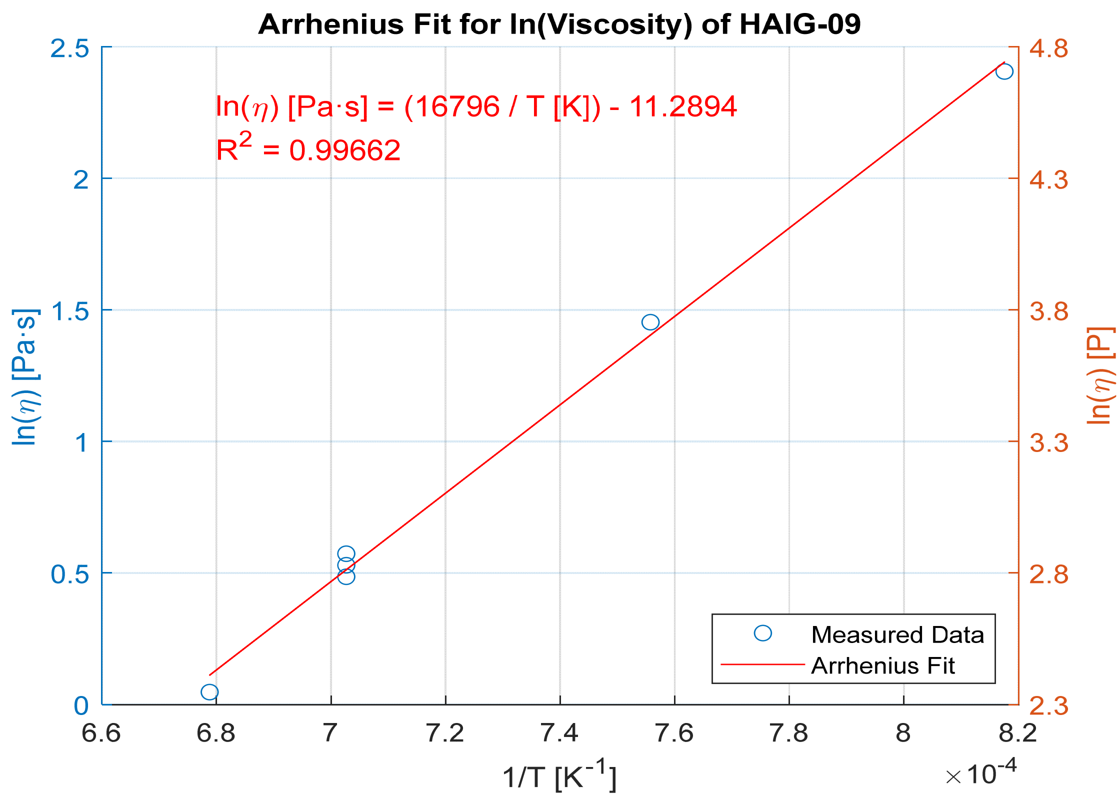

Figure F.9. Viscosity-Temperature Data and Arrhenius Equation Fit for Glass HAlG-09

F.10 Glass HAlG-11 Viscosity Data

Table F.10. Viscosity Data for Glass HAlG-11

Measured Temp., °C	Viscosity, Pa-s	1/T x10000, K^{-1}	ln η, Pa-s
1150	4.44	0.70267	1.4908
1050	13.28	0.75577	2.5860
950	45.55	0.81756	3.8189
1150	4.61	0.70267	1.5289
1200	2.91	0.67882	1.0696
1150	4.68	0.70267	1.5433

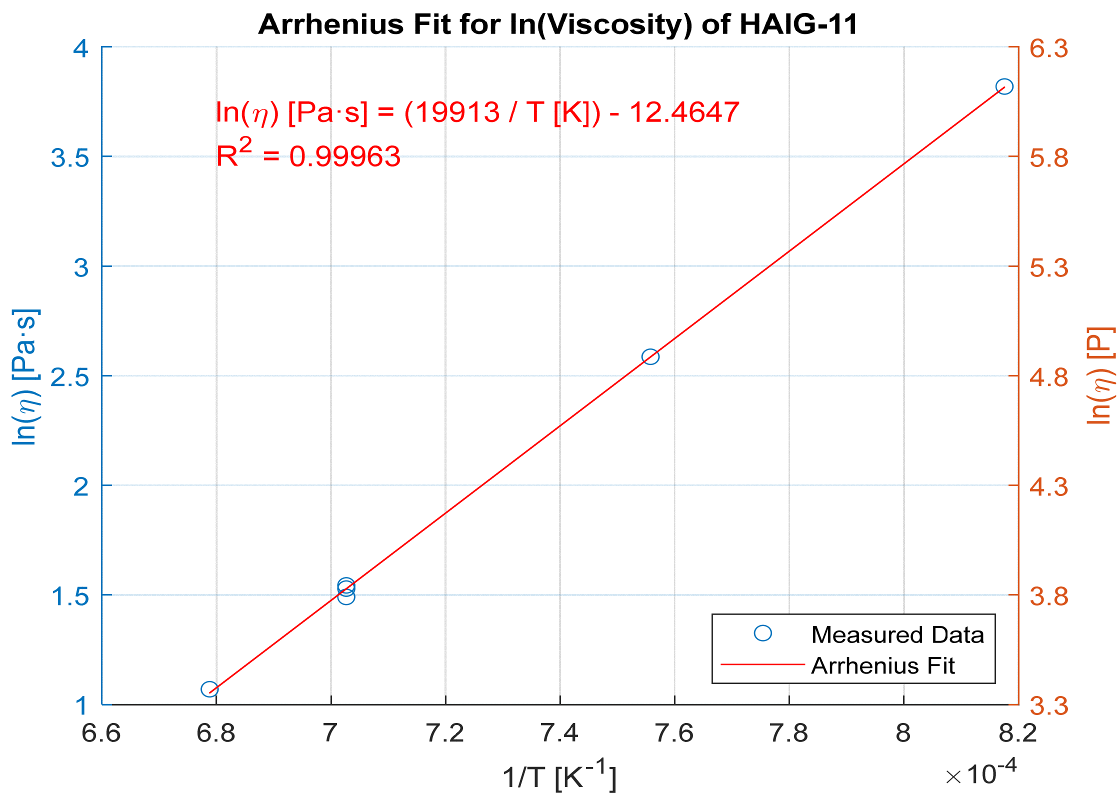

Figure F.10. Viscosity-Temperature Data and Arrhenius Equation Fit for Glass HAlG-11

F.11 Glass HAlG-12 Viscosity Data

Table F.11. Viscosity Data for Glass HAlG-12

Measured Temp., °C	Viscosity, Pa-s	1/T x10000, K^{-1}	ln η, Pa-s
1150	4.06	0.70267	1.4022
1050	10.20	0.75577	2.3224
950	30.30	0.81756	3.4111
1150	4.17	0.70267	1.4269
1200	2.80	0.67882	1.0309
1150	4.34	0.70267	1.4687

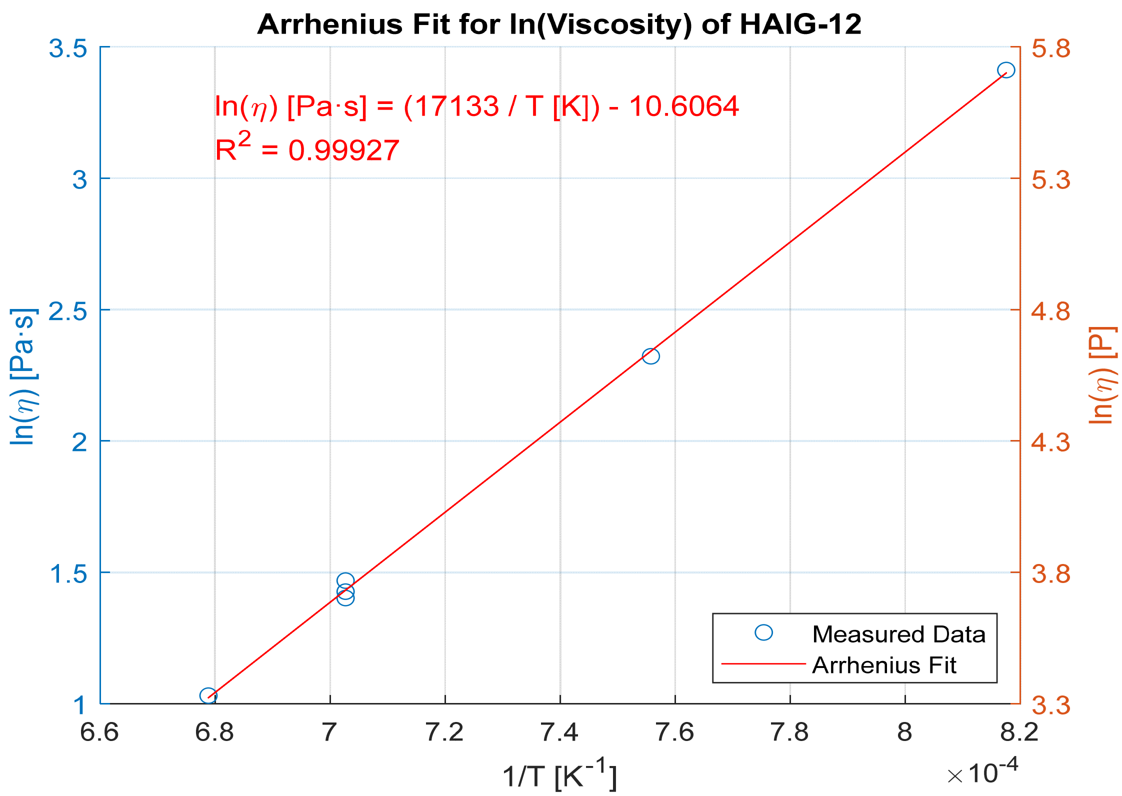

Figure F.11. Viscosity-Temperature Data and Arrhenius Equation Fit for Glass HAlG-12

F.12 Glass HAlG-13 Viscosity Data

Table F.12. Viscosity Data for Glass HAlG-13

Measured Temp., °C	Viscosity, Pa-s	1/T x10000, K^{-1}	ln η, Pa-s
1150	3.81	0.70267	1.3377
1050	10.39	0.75577	2.3409
950	33.97	0.81756	3.5254
1150	3.82	0.70267	1.3403
1200	2.43	0.67882	0.8890
1150	3.70	0.70267	1.3074

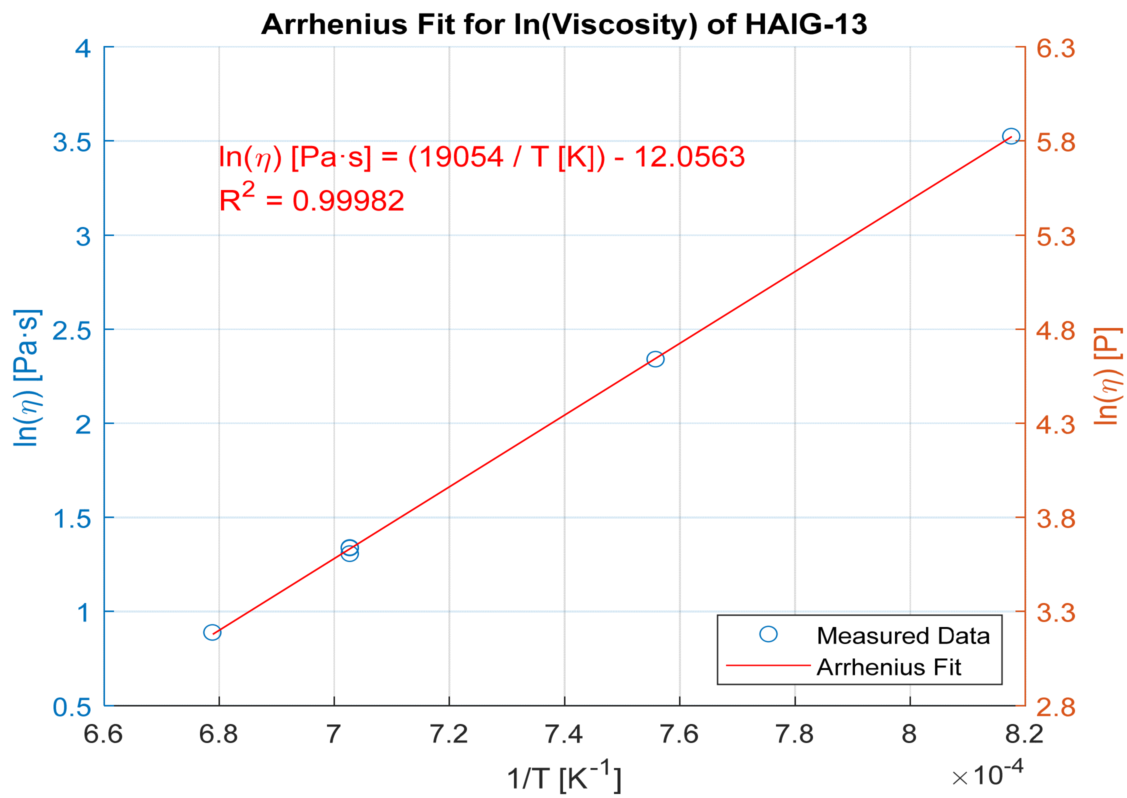

Figure F.12. Viscosity-Temperature Data and Arrhenius Equation Fit for Glass HAlG-13

F.13 Glass HAlG-14 Viscosity Data

Table F.13. Viscosity Data for Glass HAlG-14

Measured Temp., °C	Viscosity, Pa-s	1/T x10000, K^{-1}	ln η, Pa-s
1150	2.25	0.70267	0.8127
1050	4.90	0.75577	1.5895
950	12.22	0.81756	2.5030
1150	2.28	0.70267	0.8222
1200	1.41	0.67882	0.3400
1150	2.08	0.70267	0.7344

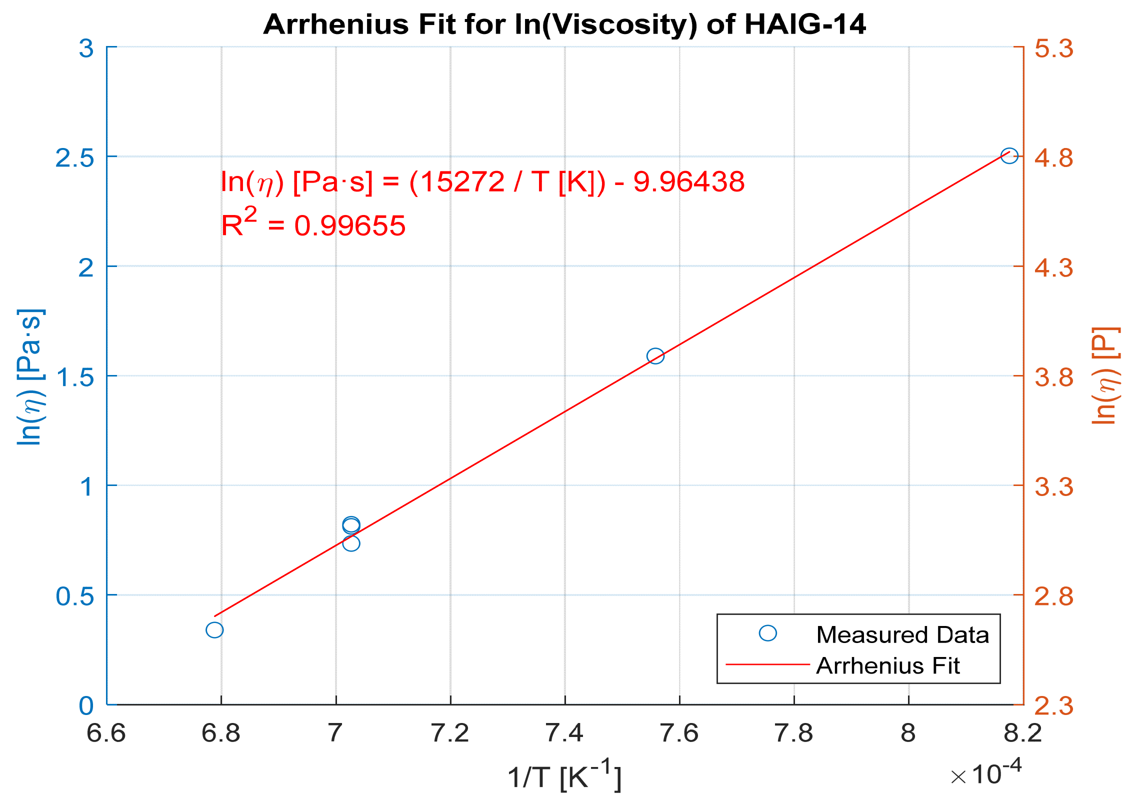

Figure F.13. Viscosity-Temperature Data and Arrhenius Equation Fit for Glass HAlG-14

F.14 Glass HAlG-15 Viscosity Data

Table F.14. Viscosity Data for Glass HAlG-15

Measured Temp., °C	Viscosity, Pa-s	1/T x10000, K^{-1}	ln η, Pa-s
1150	10.21	0.70267	2.3232
1050	23.19	0.75577	3.1437

F.15 Glass HAlG-16 Viscosity Data

Table F.15. Viscosity Data for Glass HAlG-16

Measured Temp., °C	Viscosity, Pa-s	1/T x10000, K^{-1}	ln η, Pa-s
1124	10.58	0.7160	1.0244
1034	28.14	0.7649	1.4493
953	80.71	0.8160	1.9069
1126	10.38	0.7150	1.0160
1217	4.73	0.6711	0.6749
1128	10.34	0.7138	1.0147

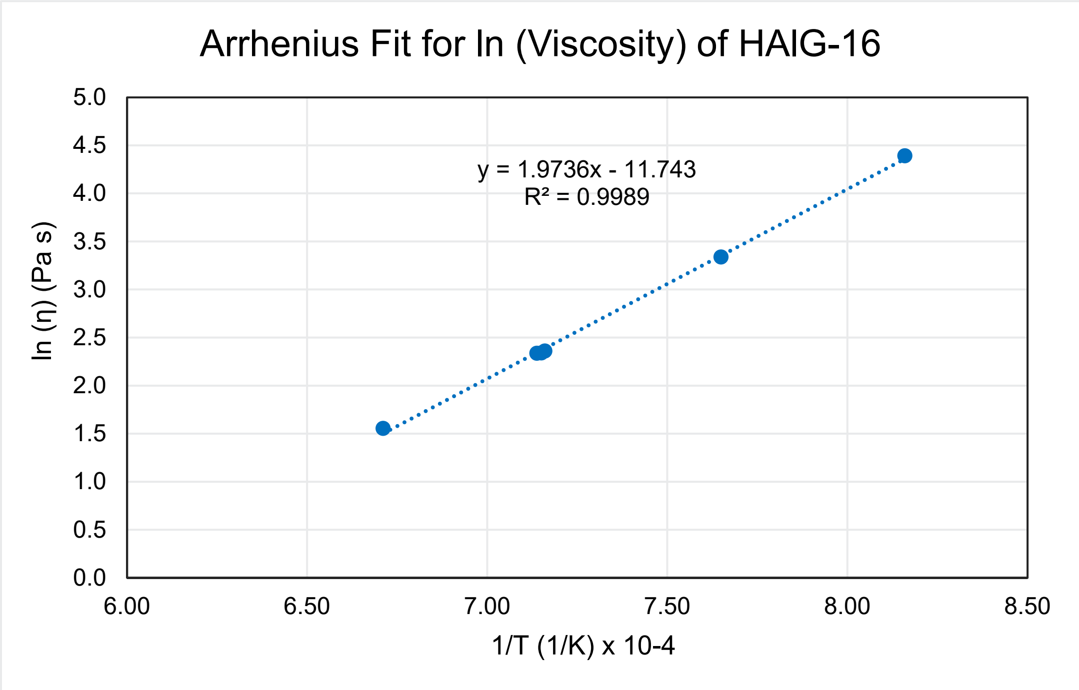

Figure F.14. Viscosity-Temperature Data and Arrhenius Equation Fit for Glass HAlG-16

F.16 Glass HAlG-17 Viscosity Data

Table F.16. Viscosity Data for Glass HAlG-17

Measured Temp., °C	Viscosity, Pa-s	1/T x10000, K^{-1}	ln η, Pa-s
1124	9.46	0.7160	2.2466
1034	20.39	0.7649	3.0148
953	53.64	0.8160	3.9822
1126	8.71	0.7150	2.1645
1217	4.39	0.6711	1.4785
1128	8.65	0.7138	2.1578

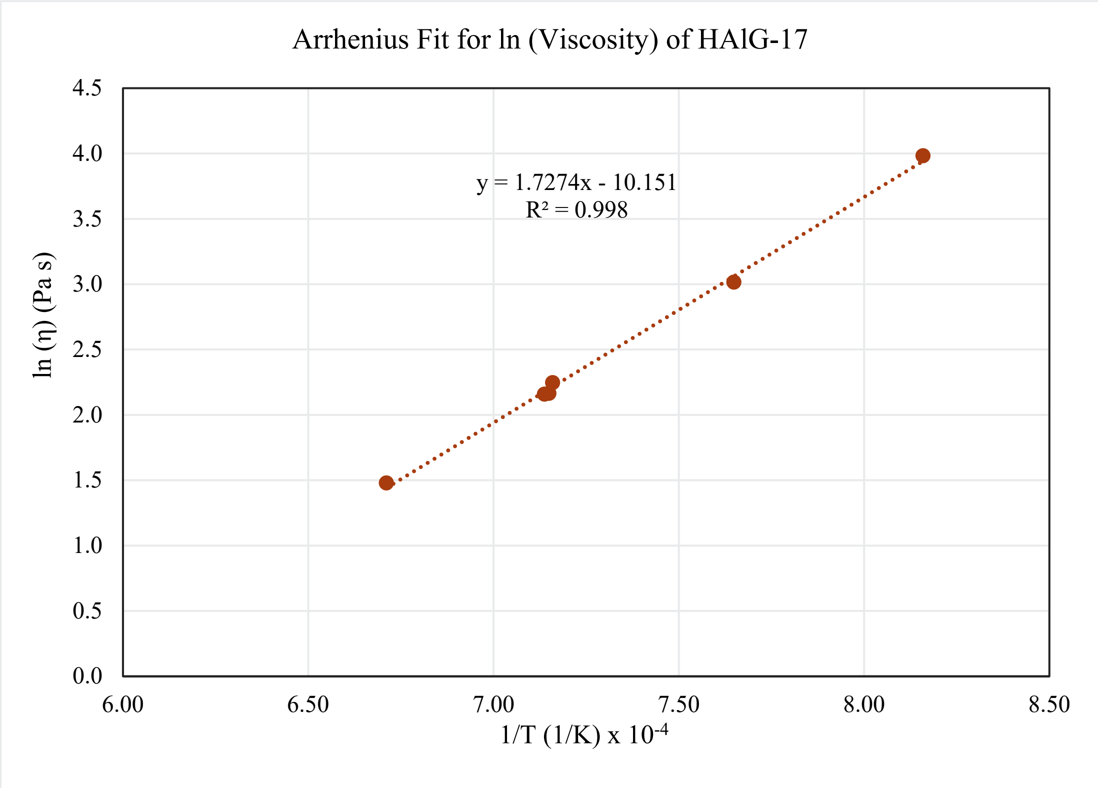

Figure F.15. Viscosity-Temperature Data and Arrhenius Equation Fit for Glass HAlG-17

F.17 Glass HAlG-18 Viscosity Data

Table F.17. Viscosity Data for Glass HAlG-18

Measured Temp., °C	Viscosity, Pa-s	1/T x10000, K^{-1}	ln η, Pa-s
1124	4.68	0.7160	1.5443
1034	11.08	0.7649	2.4052
953	32.20	0.8160	3.4721
1126	4.57	0.7150	1.5198
1217	2.19	0.6711	0.7844
1128	4.56	0.7138	1.5179

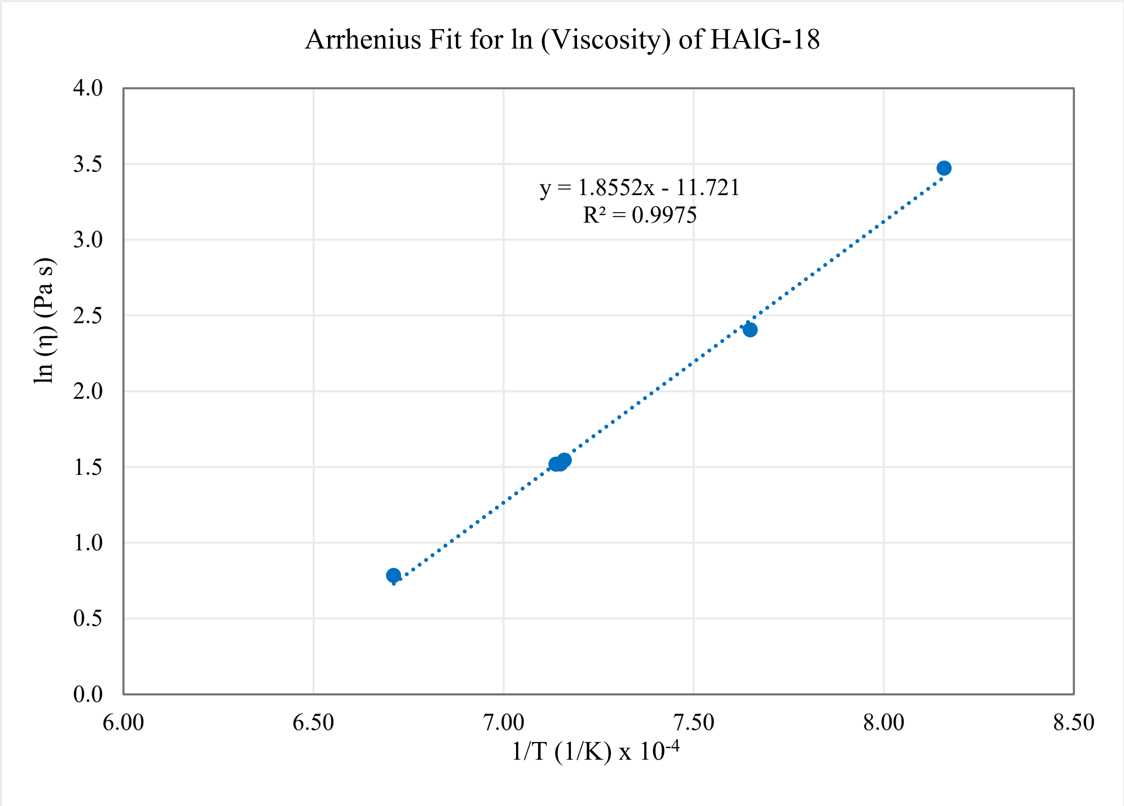

Figure F.16. Viscosity-Temperature Data and Arrhenius Equation Fit for Glass HAlG-18

F.18 Glass HAlG-19 Viscosity Data

Table F.18. Viscosity Data for Glass HAlG-19

Measured Temp., °C	Viscosity, Pa-s	1/T x10000, K^{-1}	ln η, Pa-s
1124	4.87	0.7160	1.5836
1034	12.67	0.7649	2.5395
953	36.97	0.8160	3.6102
1126	4.77	0.7150	1.5629
1217	2.29	0.6711	0.8273
1128	4.81	0.7138	1.5698

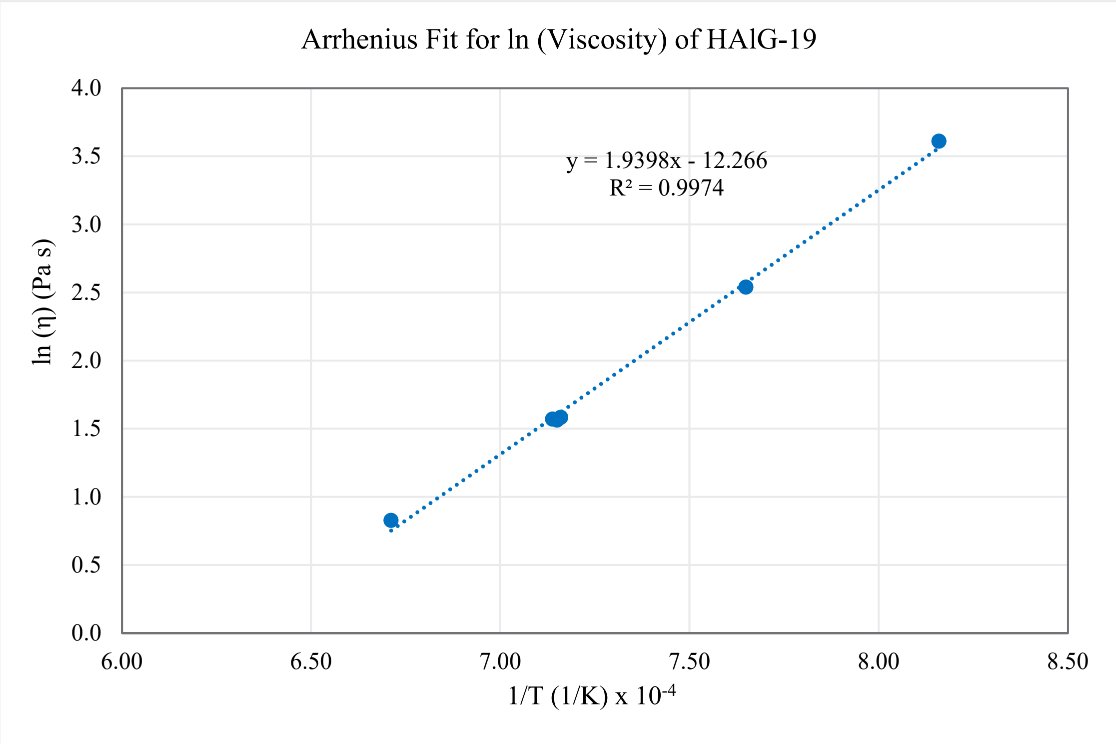

Figure F.17. Viscosity-Temperature Data and Arrhenius Equation Fit for Glass HAlG-19

F.19 Glass HAlG-20 Viscosity Data

Table F.19. Viscosity Data for Glass HAlG-20

Measured Temp., °C	Viscosity, Pa-s	1/T x10000, K^{-1}	ln η, Pa-s
1124	6.59	0.7160	1.886
1034	14.99	0.7649	2.708
953	35.35	0.8160	3.565
1126	7.58	0.7150	2.025
1217	4.03	0.6711	1.395
1128	6.62	0.7138	1.890

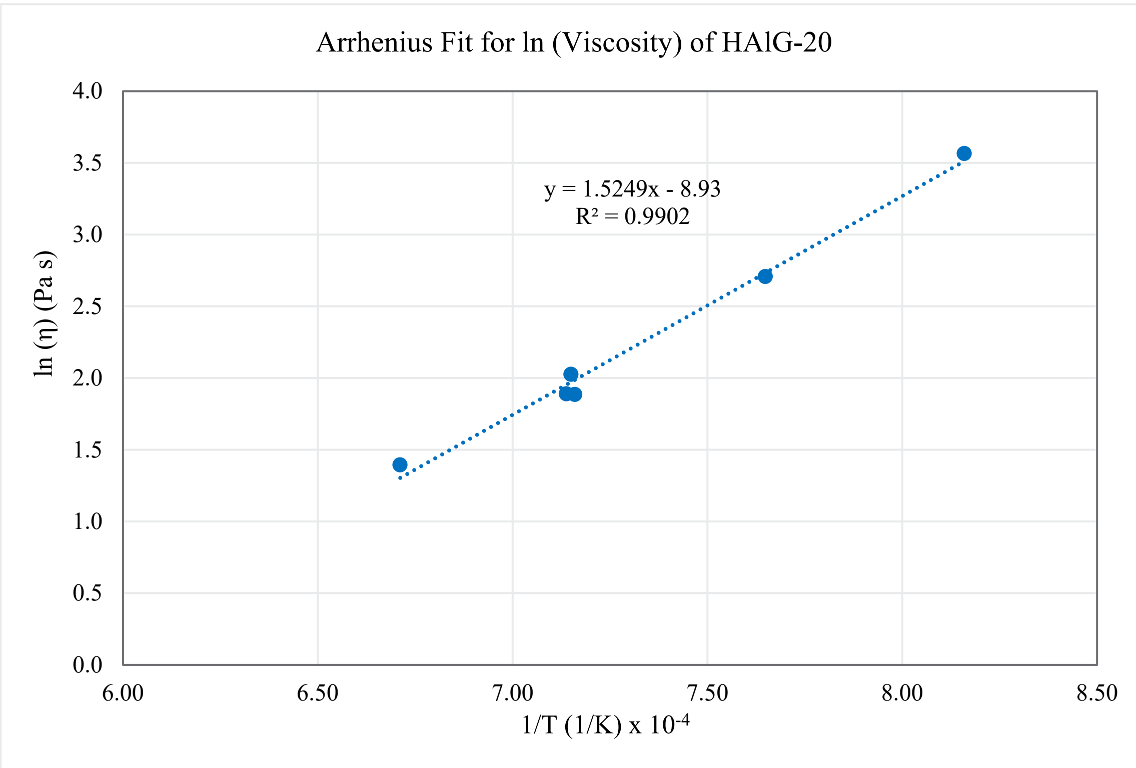

Figure F.18. Viscosity-Temperature Data and Arrhenius Equation Fit for Glass HAlG-20

F.20 Glass HAlG-21 Viscosity Data

Table F.20. Viscosity Data for Glass HAlG-21

Measured Temp., °C	Viscosity, Pa-s	1/T x10000, K^{-1}	ln η, Pa-s
1124	4.17	0.7160	1.4288
1034	11.50	0.7649	2.4420
953	33.94	0.8160	3.5247
1126	4.49	0.7150	1.5026
1217	1.94	0.6711	0.6649
1128	4.09	0.7138	1.3948

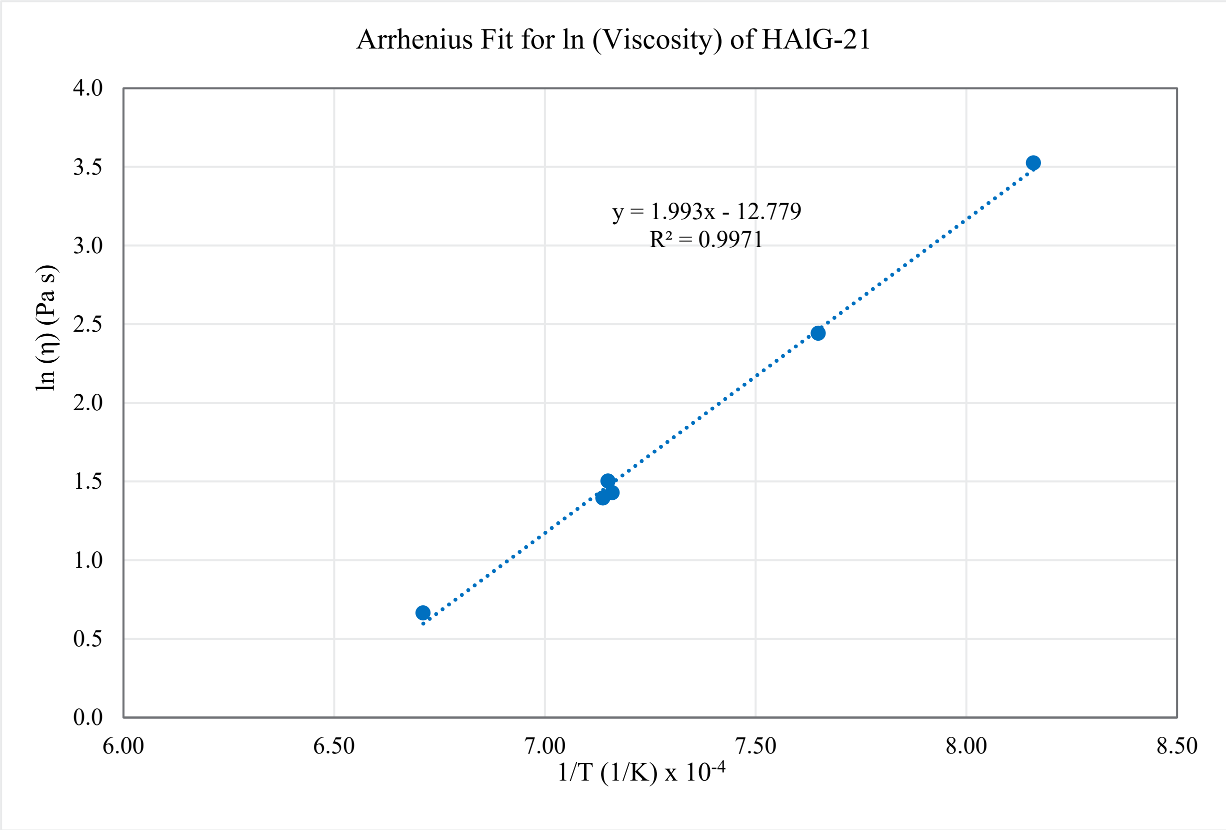

Figure F.19. Viscosity-Temperature Data and Arrhenius Equation Fit for Glass HAlG-21

F.21 Glass HAlG-22 Viscosity Data

Table F.21. Viscosity Data for Glass HAlG-22

Measured Temp., °C	Viscosity, Pa-s	1/T x10000, K^{-1}	ln η, Pa-s
1124	23.78	0.7160	3.1690
1034	70.37	0.7649	4.2537
953	506.66	0.8160	6.2278
1126	24.77	0.7150	3.2098
1217	11.45	0.6711	2.4383
1128	23.03	0.7138	3.1369

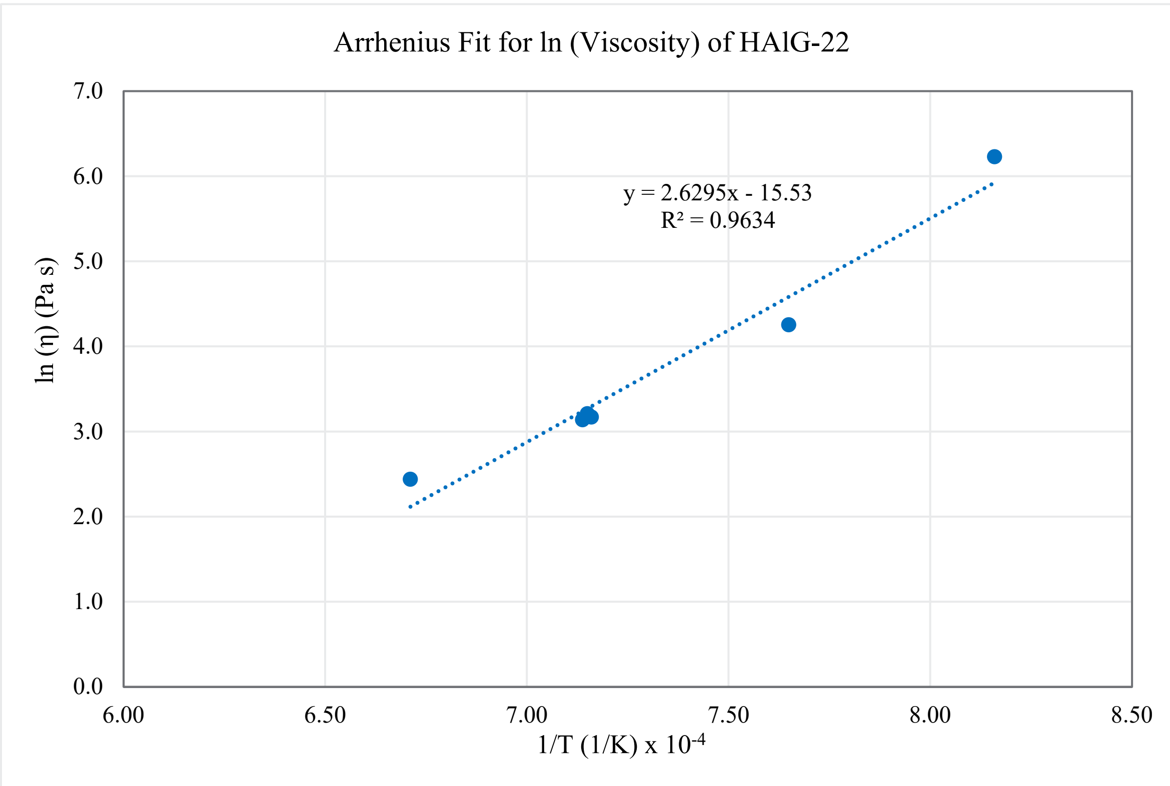

Figure F.20. Viscosity-Temperature Data and Arrhenius Equation Fit for Glass HAlG-22

F.22 Glass HAlG-23 Viscosity Data

Table F.22. Viscosity Data for Glass HAlG-23

Measured Temp., °C	Viscosity, Pa-s	1/T x10000, K^{-1}	ln η, Pa-s
1124	7.29	0.7160	1.9866
1034	14.08	0.7649	2.6450
953	33.12	0.8160	3.5001
1126	7.05	0.7150	1.9526
1217	3.57	0.6711	1.2715
1128	6.61	0.7138	1.8884

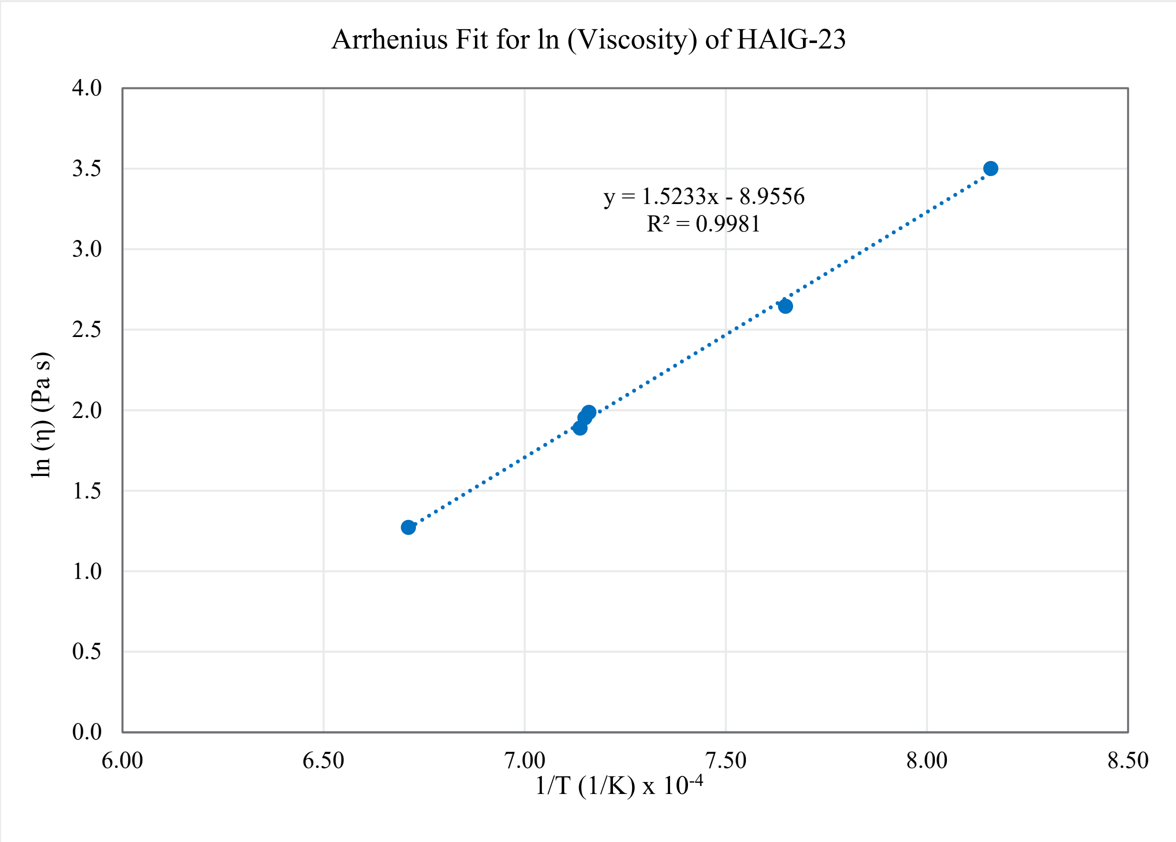

Figure F.21. Viscosity-Temperature Data and Arrhenius Equation Fit for Glass HAlG-23

F.23 Glass HAlG-24 Viscosity Data

Table F.23. Viscosity Data for Glass HAlG-24

Measured Temp., °C	Viscosity, Pa-s	1/T x10000, K^{-1}	ln η, Pa-s
1124	9.45	0.7160	2.2460
1034	24.73	0.7649	3.2082
953	91.41	0.8160	4.5153
1126	9.64	0.7150	2.2663
1217	4.35	0.6711	1.4699
1128	9.03	0.7138	2.2008

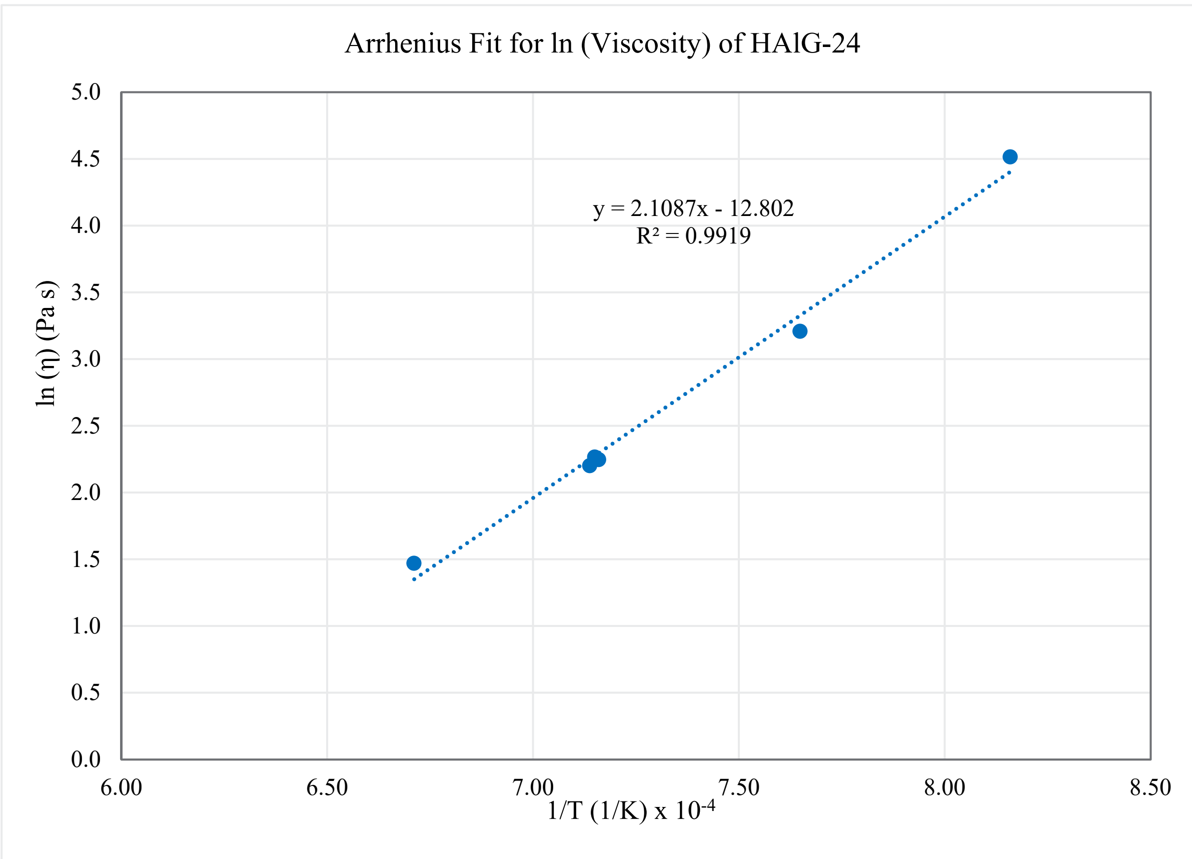

Figure F.22. Viscosity-Temperature Data and Arrhenius Equation Fit for Glass HAlG-24

F.24 Glass HAlG-25 Viscosity Data

Table F.24. Viscosity Data for Glass HAlG-25

Measured Temp., °C	Viscosity, Pa-s	1/T x10000, K^{-1}	ln η, Pa-s
1124	12.81	0.7160	2.5506
1034	80.16	0.7649	4.3840
953	268.48	0.8160	5.5928
1126	18.07	0.7150	2.8942
1217	4.93	0.6711	1.5954
1128	11.05	0.7138	2.4025

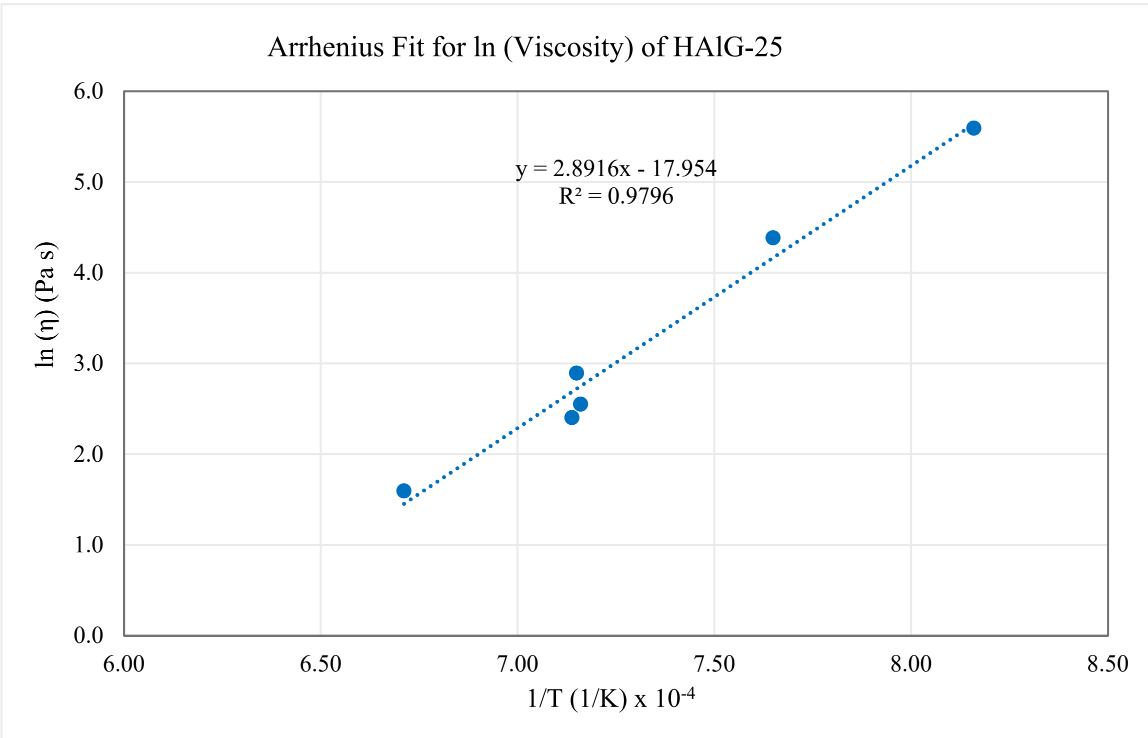

Figure F.23. Viscosity-Temperature Data and Arrhenius Equation Fit for Glass HAlG-25

Appendix G – Electrical Conductivity Data

This appendix presents the measured electrical conductivity data for each of the glasses in this matrix. The plots shown in this appendix are fitted to the Arrhenius equation:

$$\ln(\varepsilon) = A + \frac{B}{T_K} \quad \text{(G.1)}$$

where A and B are independent of temperature (T_K) is in K (T(°C) + 273.15).

G.1 Glass HAlG-01 Electrical Conductivity Data

Table G.1. Electrical Conductivity Data for Glass HAlG-01

Temperature, °C	Conductivity, S/m	1/T, K^{-1}	ln ε (S/m)
950	22.11	0.000818	3.0962
1050	31.34	0.000756	3.4449
1150	40.42	0.000703	3.6993
1200	38.79	0.000679	3.6581

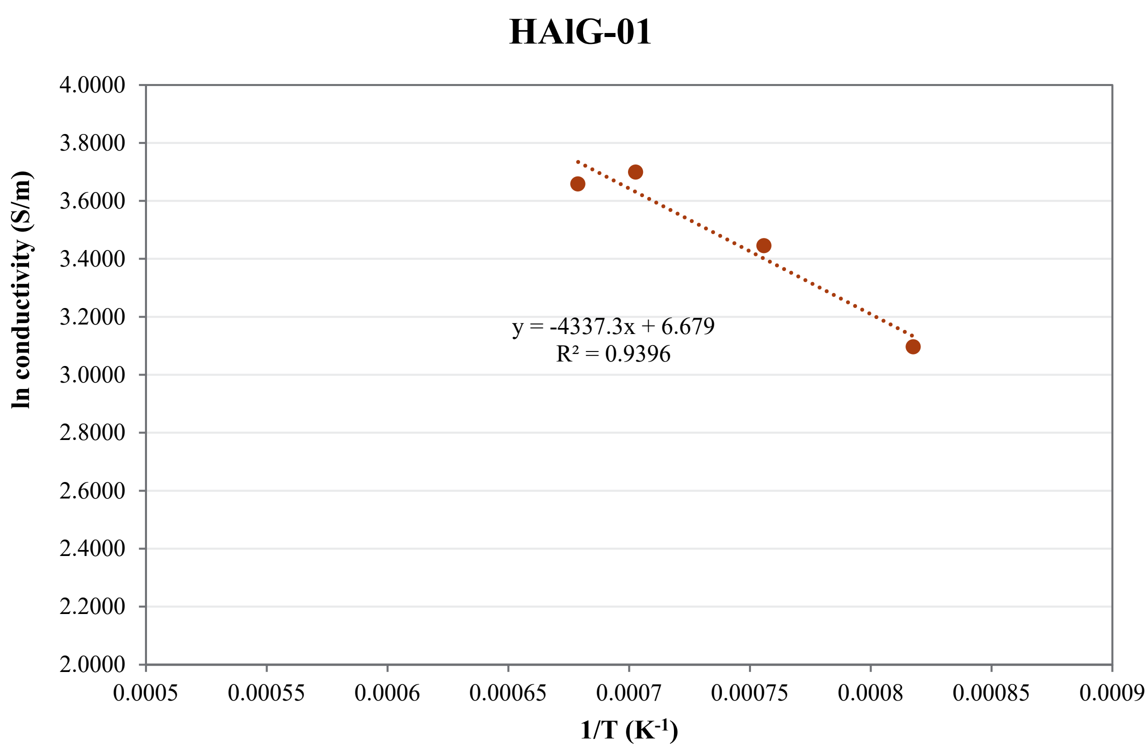

Figure G.1. Electrical Conductivity-Temperature Data and Arrhenius Equation Fit for Glass HAlG-01

G.2 Glass HAlG-02 Electrical Conductivity Data

Table G.2. Electrical Conductivity Data for Glass HAlG-02

Temperature, °C	Conductivity, S/m	1/T, K^{-1}	ln ε, S/m
950	27.03	0.000818	3.2971
1050	38.08	0.000756	3.6396
1150	49.47	0.000703	3.9014
1200	55.69	0.000679	4.0198

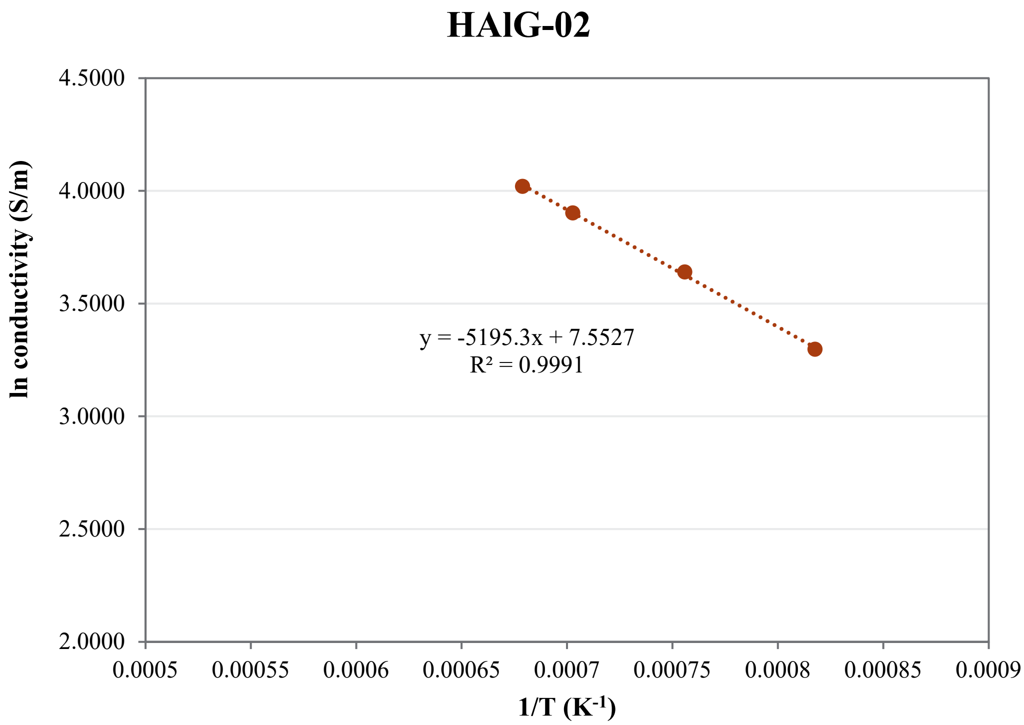

Figure G.2. Electrical Conductivity-Temperature Data and Arrhenius Equation Fit for Glass HAlG-02

G.3 Glass HAlG-03 Electrical Conductivity Data

Table G.3. Electrical Conductivity Data for Glass HAlG-03

Temperature, °C	Conductivity, S/m	1/T, K^{-1}	ln ε, S/m
950	23.88	0.000818	3.1731
1050	37.16	0.000756	3.6152
1150	51.37	0.000703	3.9391
1200	59.87	0.000679	4.0922

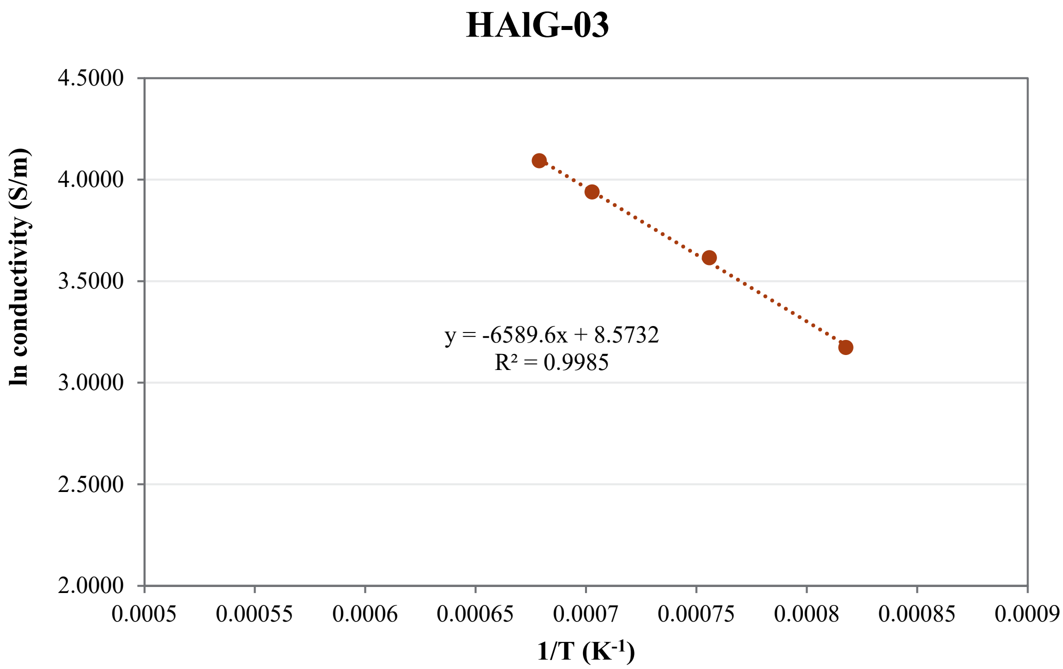

Figure G.3. Electrical Conductivity-Temperature Data, Arrhenius Equation Fit, and Polynomial Fit for Glass HAlG-03

G.4 Glass HAlG-04 Electrical Conductivity Data

Table G.4. Electrical Conductivity Data for Glass HAlG-04

Temperature, °C	Conductivity, S/m	1/T, K^{-1}	ln ε, S/m
950	24.59	0.000818	3.2023
1050	36.54	0.000756	3.5984
1150	48.83	0.000703	3.8883
1200	55.30	0.000679	4.0127

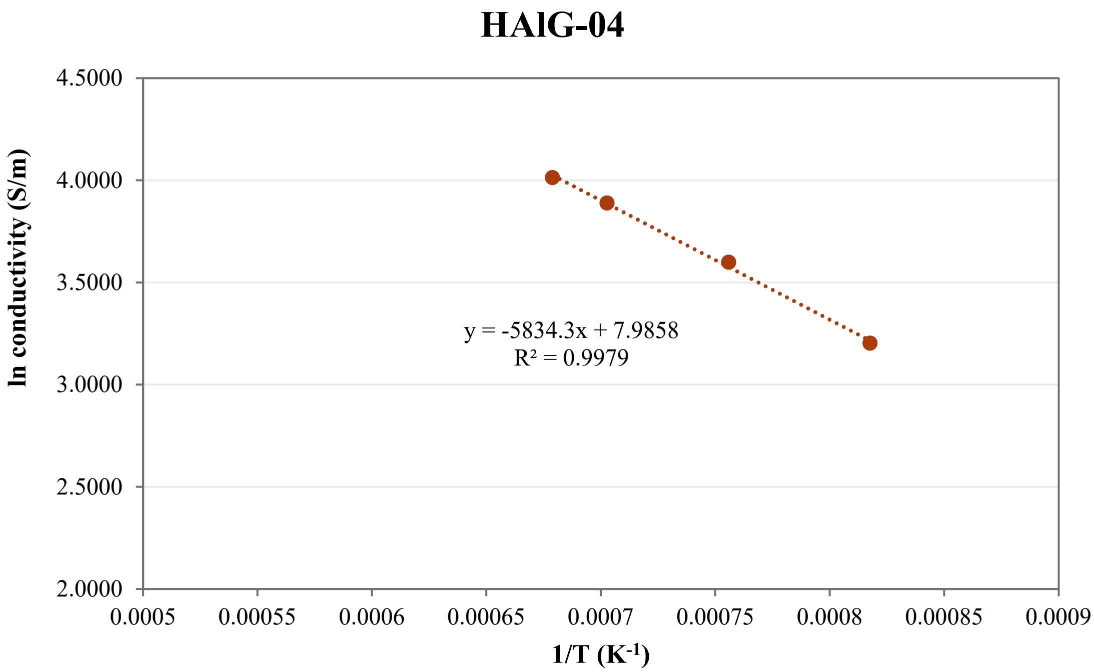

Figure G.4. Electrical Conductivity-Temperature Data, Arrhenius Equation Fit, and Polynomial Fit for Glass HAlG-04

G.5 Glass HAlG-05 Electrical Conductivity Data

Table G.5. Electrical Conductivity Data for Glass HAlG-05

Temperature, °C	Conductivity, S/m	1/T, K^{-1}	ln ε, S/m
950	25.80	0.000818	3.2505
1050	38.56	0.000756	3.6522
1150	52.26	0.000703	3.9562
1200	60.43	0.000679	4.1014

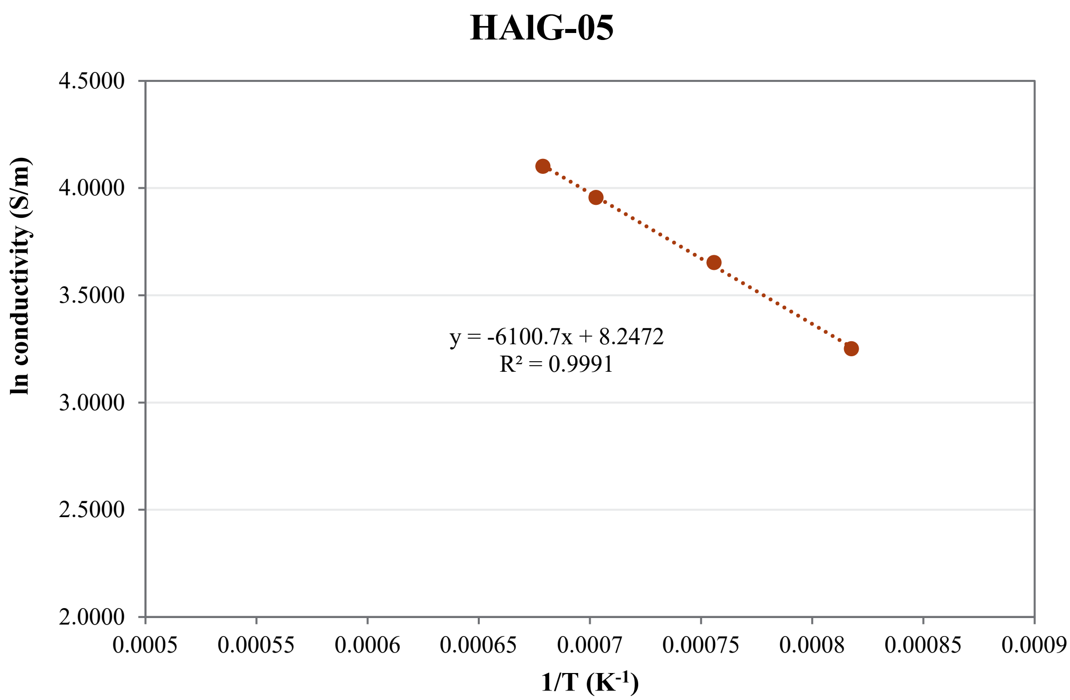

Figure G.5. Electrical Conductivity-Temperature Data, Arrhenius Equation Fit, and Polynomial Fit for Glass HAlG-05

G.6 Glass HAlG-06 Electrical Conductivity Data

Table G.6. Electrical Conductivity Data for Glass HAlG-06

Temperature, °C	Conductivity, S/m	1/T, K^{-1}	ln ε, S/m
950	29.63	0.000818	3.3889
1050	44.15	0.000756	3.7876
1150	58.76	0.000703	4.0734
1200	67.00	0.000679	4.2046

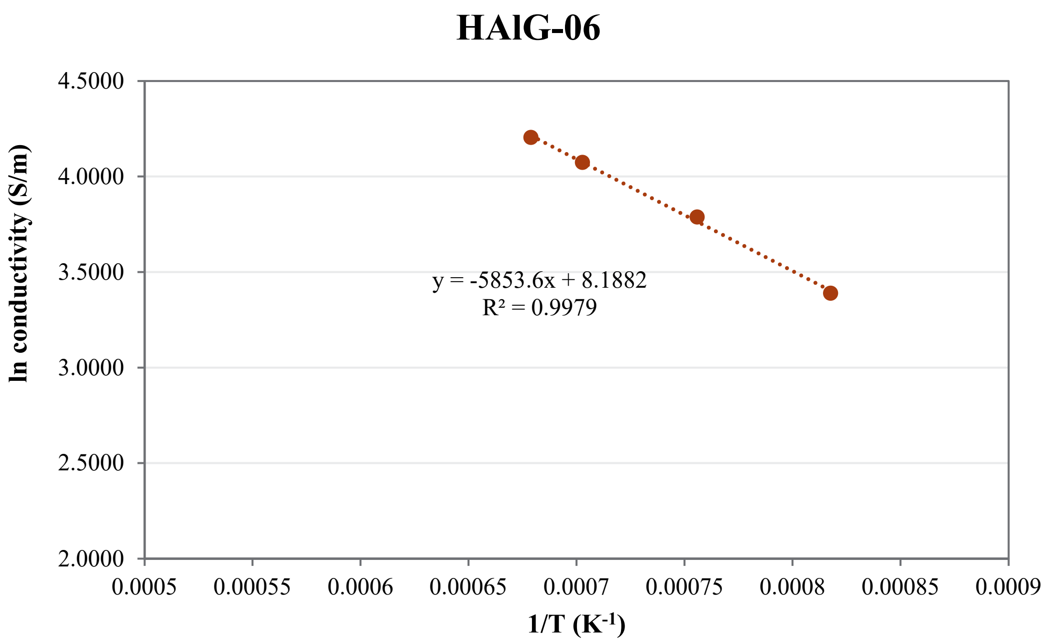

Figure G.6. Electrical Conductivity-Temperature Data, Arrhenius Equation Fit, and Polynomial Fit for Glass HAlG-06

G.7 Glass HAlG-07 Electrical Conductivity Data

Table G.7. Electrical Conductivity Data for Glass HAlG-07

Temperature, °C	Conductivity, S/m	1/T, K^{-1}	ln ε, S/m
950	19.13	0.000818	2.9513
1050	27.69	0.000756	3.3210
1150	37.21	0.000703	3.6167
1200	42.46	0.000679	3.7486

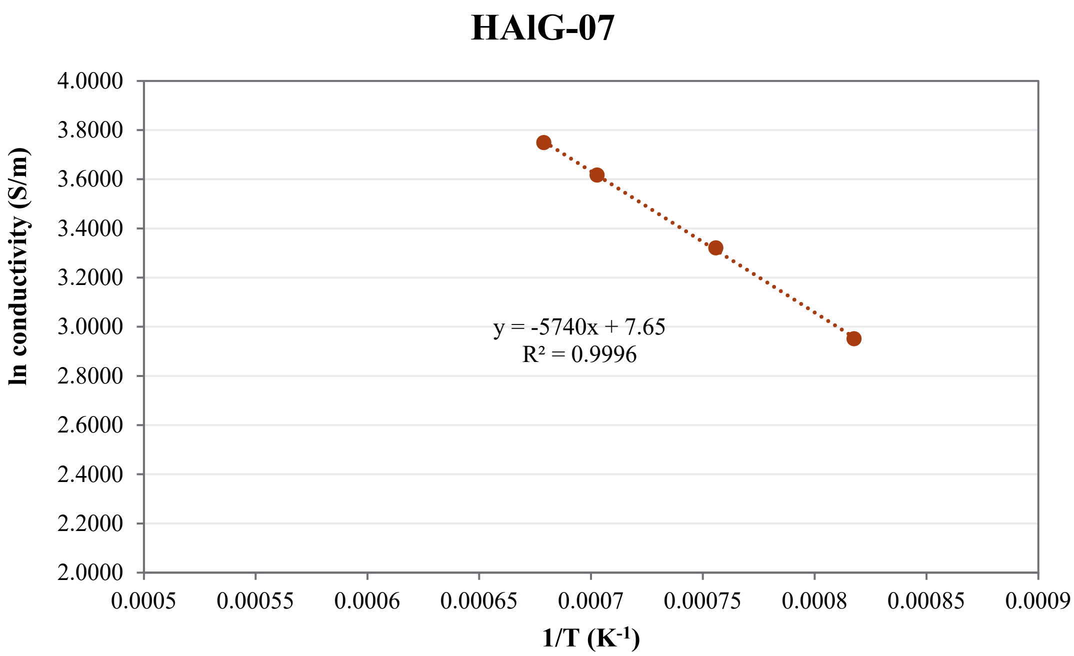

Figure G.7. Electrical Conductivity-Temperature Data and Arrhenius Equation Fit for Glass HAlG-07

G.8 Glass HAlG-08 Electrical Conductivity Data

Table G.8. Electrical Conductivity Data for Glass HAlG-08

Temperature, °C	Conductivity, S/m	1/T, K^{-1}	ln ε, S/m
950	27.48	0.000818	3.3133
1050	39.25	0.000756	3.6700
1150	51.07	0.000703	3.9332
1200	57.35	0.000679	4.0492

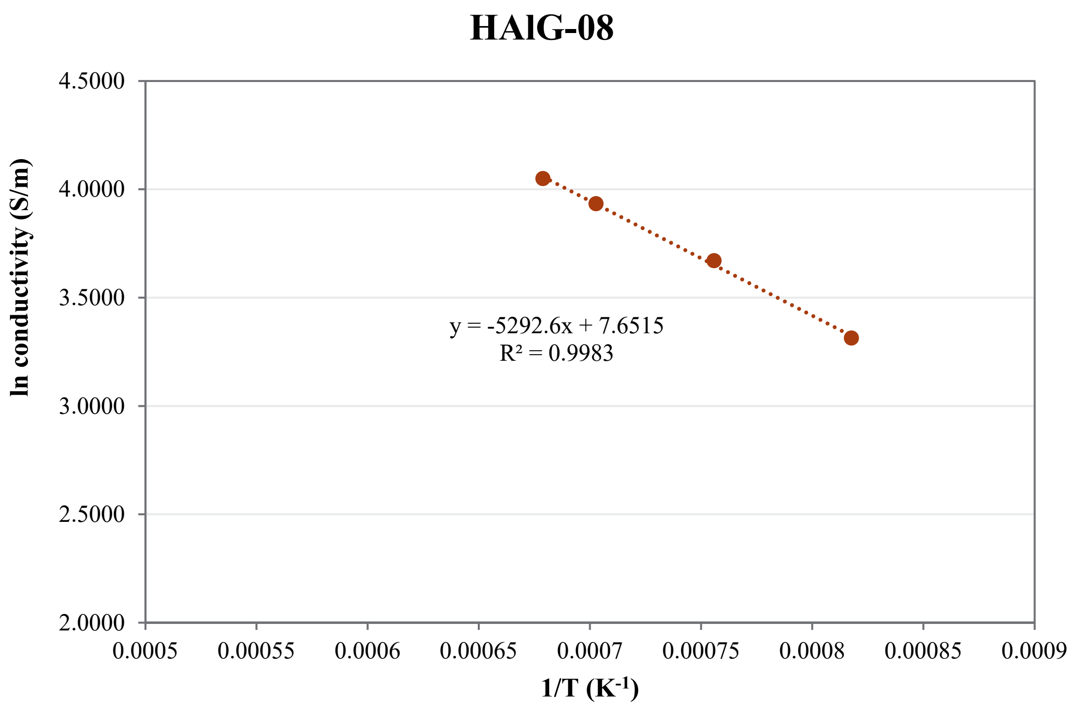

Figure G.8. Electrical Conductivity-Temperature Data and Arrhenius Equation Fit for Glass HAlG-08

G.9 Glass HAlG-09 Electrical Conductivity Data

Table G.9. Electrical Conductivity Data for Glass HAlG-09

Temperature, °C	Conductivity, S/m	1/T, K^{-1}	ln ε, S/m
950	34.21	0.000818	3.5325
1050	50.91	0.000756	3.9300
1150	67.34	0.000703	4.2097
1200	75.89	0.000679	4.3293

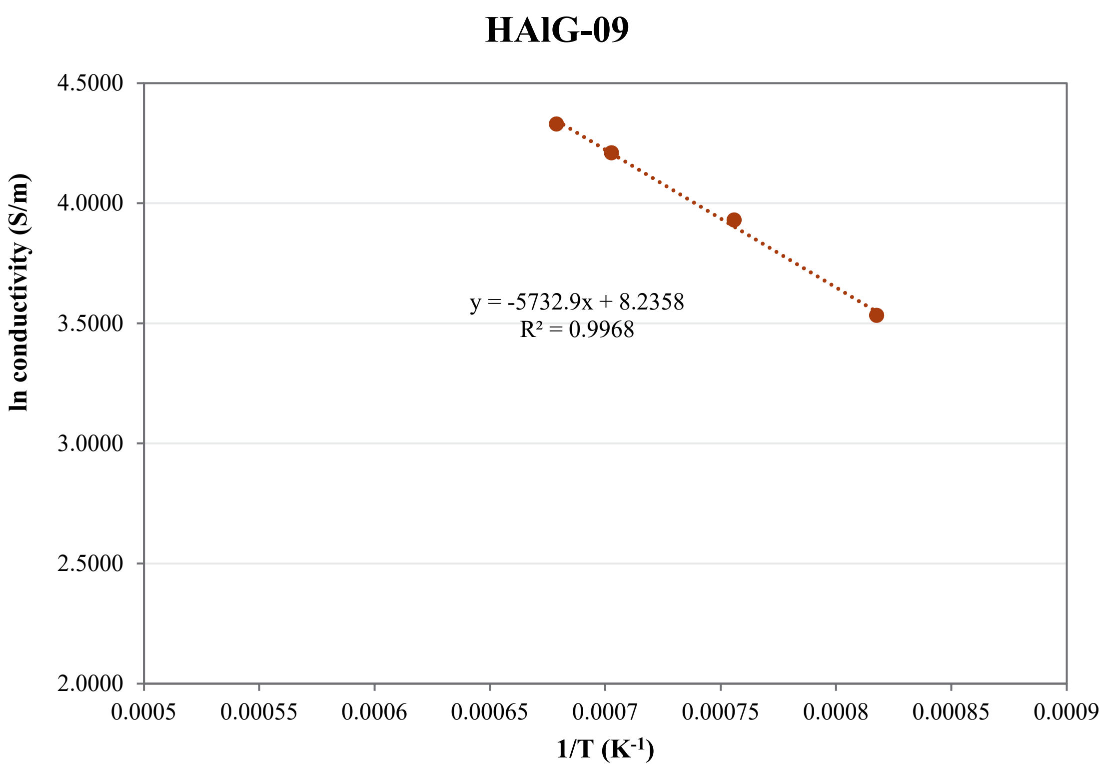

Figure G.9. Electrical Conductivity-Temperature Data and Arrhenius Equation Fit for Glass HAlG-09

G.10 Glass HAlG-11 Electrical Conductivity Data

Table G.10. Electrical Conductivity Data for Glass HAlG-11

Temperature, °C	Conductivity, S/m	1/T, K^{-1}	ln ε, S/m
950	41.59	0.000818	3.7279
1050	62.88	0.000756	4.1413
1150	80.45	0.000703	4.3876
1200	89.48	0.000679	4.4940

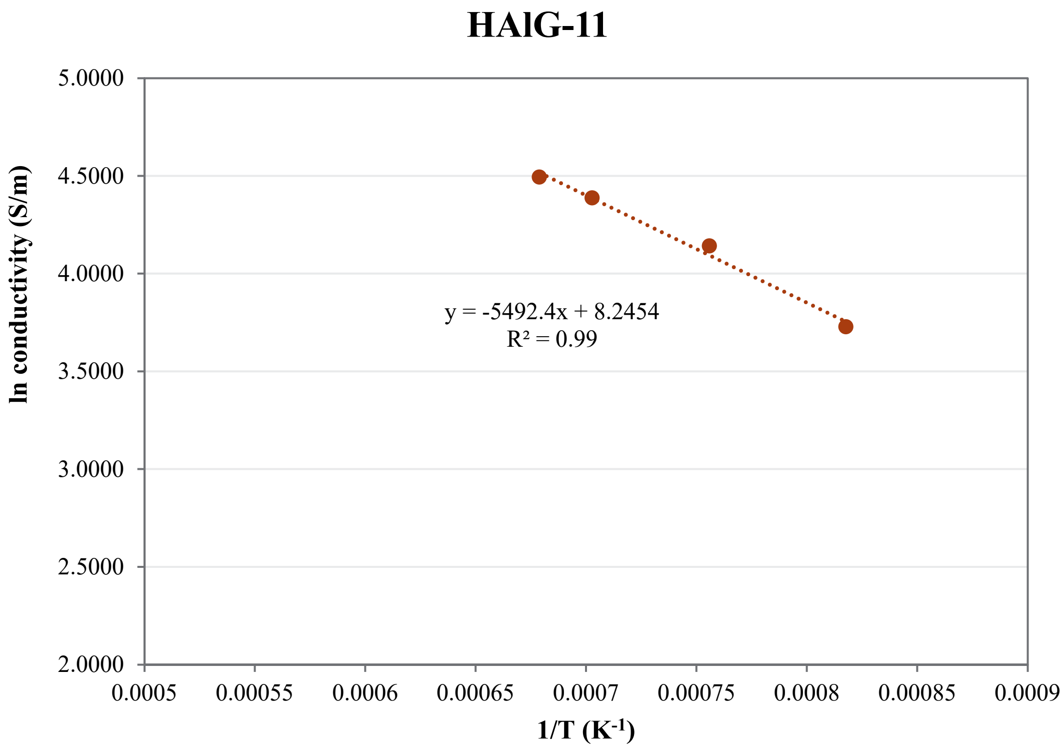

Figure G.10. Electrical Conductivity-Temperature Data, Arrhenius Equation Fit, and Polynomial Fit for Glass HAlG-11

G.11 Glass HAlG-12 Electrical Conductivity Data

Table G.11. Electrical Conductivity Data for Glass HAlG-12

Temperature, °C	Conductivity, S/m	1/T, K^{-1}	ln ε, S/m
950	19.18	0.000818	2.9539
1050	27.84	0.000756	3.3266
1150	37.06	0.000703	3.6124
1200	42.33	0.000679	3.7454

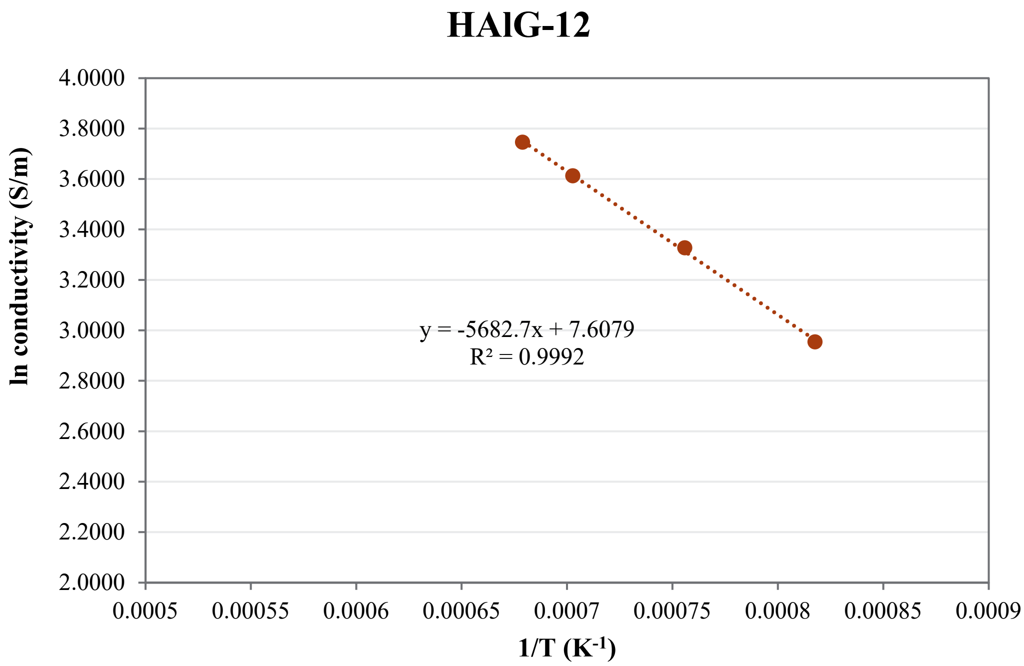

Figure G.11. Electrical Conductivity-Temperature Data and Arrhenius Equation Fit for Glass HAlG-12

G.12 Glass HAlG-13 Electrical Conductivity Data

Table G.12. Electrical Conductivity Data for Glass HAlG-13

Temperature, °C	Conductivity, S/m	1/T, K^{-1}	ln ε, S/m
950	8.14	0.000818	2.0970
1050	14.23	0.000756	2.6554
1150	21.92	0.000703	3.0875
1200	26.80	0.000679	3.2885

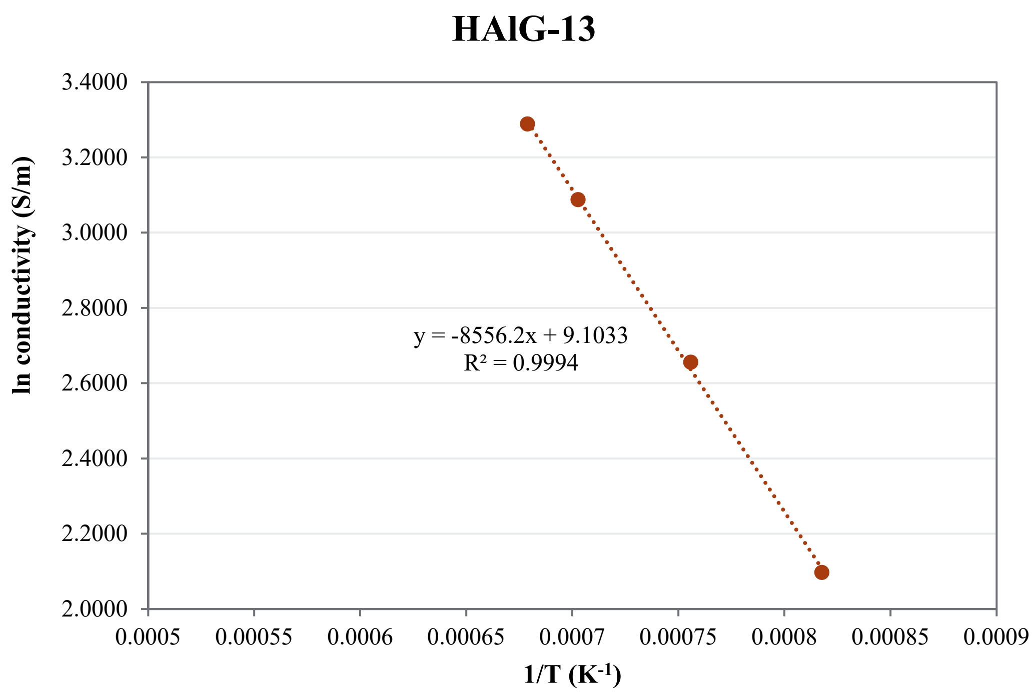

Figure G.12. Electrical Conductivity-Temperature Data and Arrhenius Equation Fit for Glass HAlG-13

G.13 Glass HAlG-14 Electrical Conductivity Data

Table G.13. Electrical Conductivity Data for Glass HAlG-14

Temperature, °C	Conductivity, S/m	1/T, K^{-1}	ln ε, S/m
950	27.37	0.000818	3.3095
1050	39.19	0.000756	3.6685
1150	51.10	0.000703	3.9339
1200	57.47	0.000679	4.0513

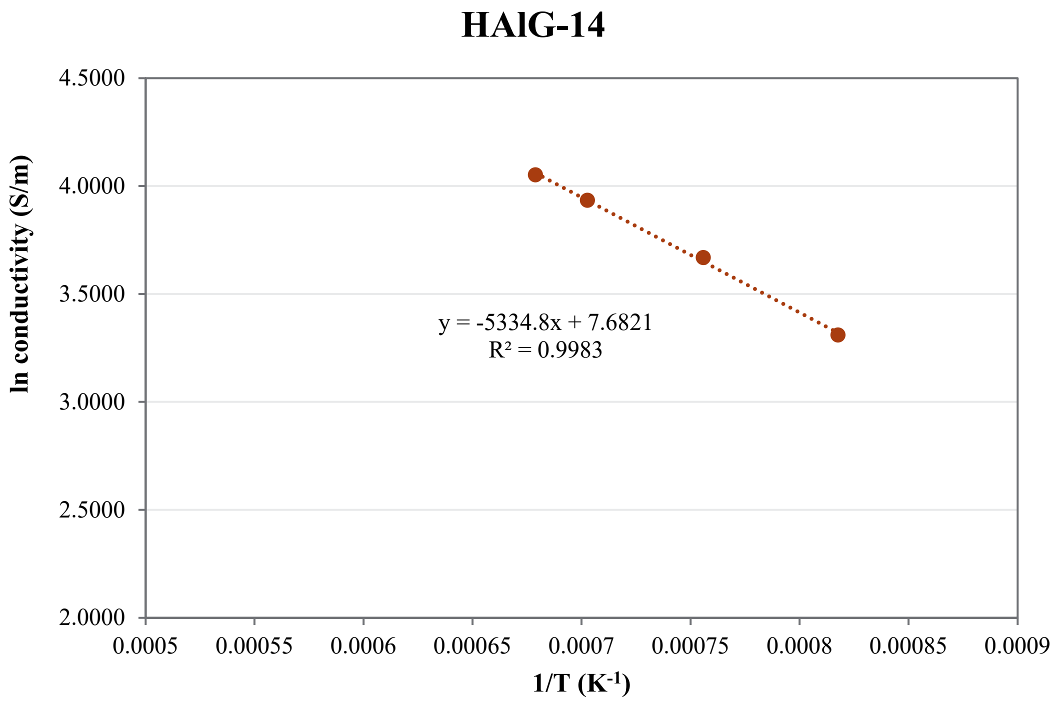

Figure G.13. Electrical Conductivity-Temperature Data and Arrhenius Equation Fit for Glass HAlG-14

G.14 Glass HAlG-15 Electrical Conductivity Data

Table G.14. Electrical Conductivity Data for Glass HAlG-15

Temperature, °C	Conductivity, S/m	1/T, K^{-1}	ln ε, S/m
950	20.2	0.000818	3.01
1250	41.9	0.000657	3.73
1150	35.9	0.000703	3.58
1050	28.4	0.000756	3.35

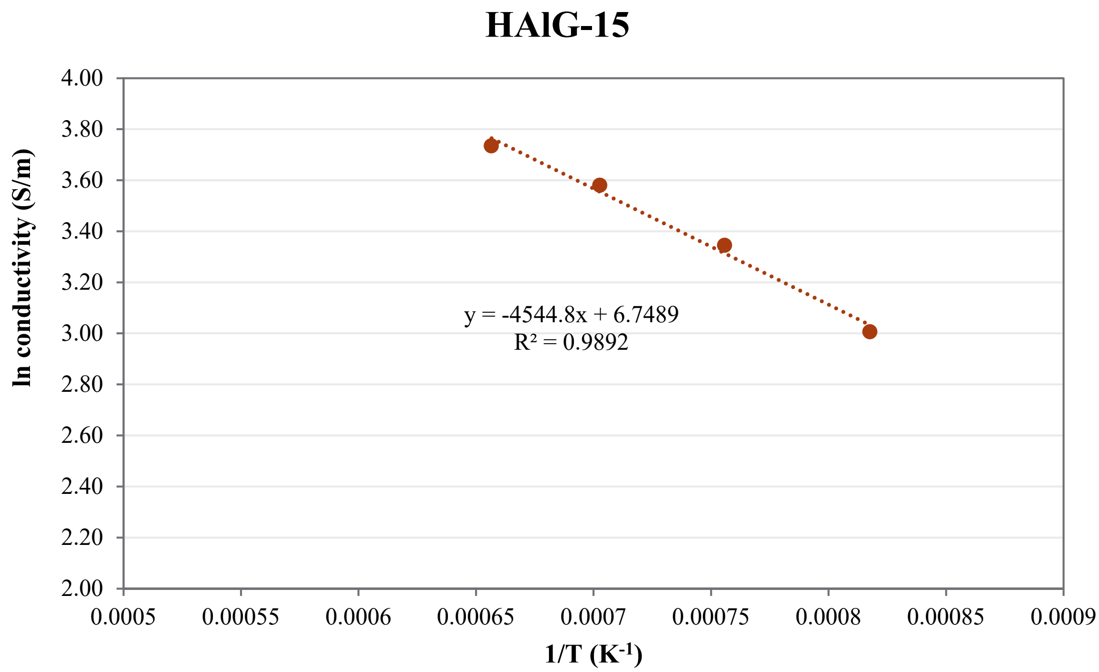

Figure G.14. Electrical Conductivity-Temperature Data with Arrhenius Equation Fit for Glass HAlG-15

G.15 Glass HAlG-16 Electrical Conductivity Data

Table G.15. Electrical Conductivity Data for Glass HAlG-16

Temperature, °C	Conductivity, S/m	1/T, K^{-1}	ln ε, S/m
950	28.9	0.000818	3.37
1250	61.9	0.000657	4.13
1150	51.6	0.000703	3.94
1050	40.7	0.000756	3.71

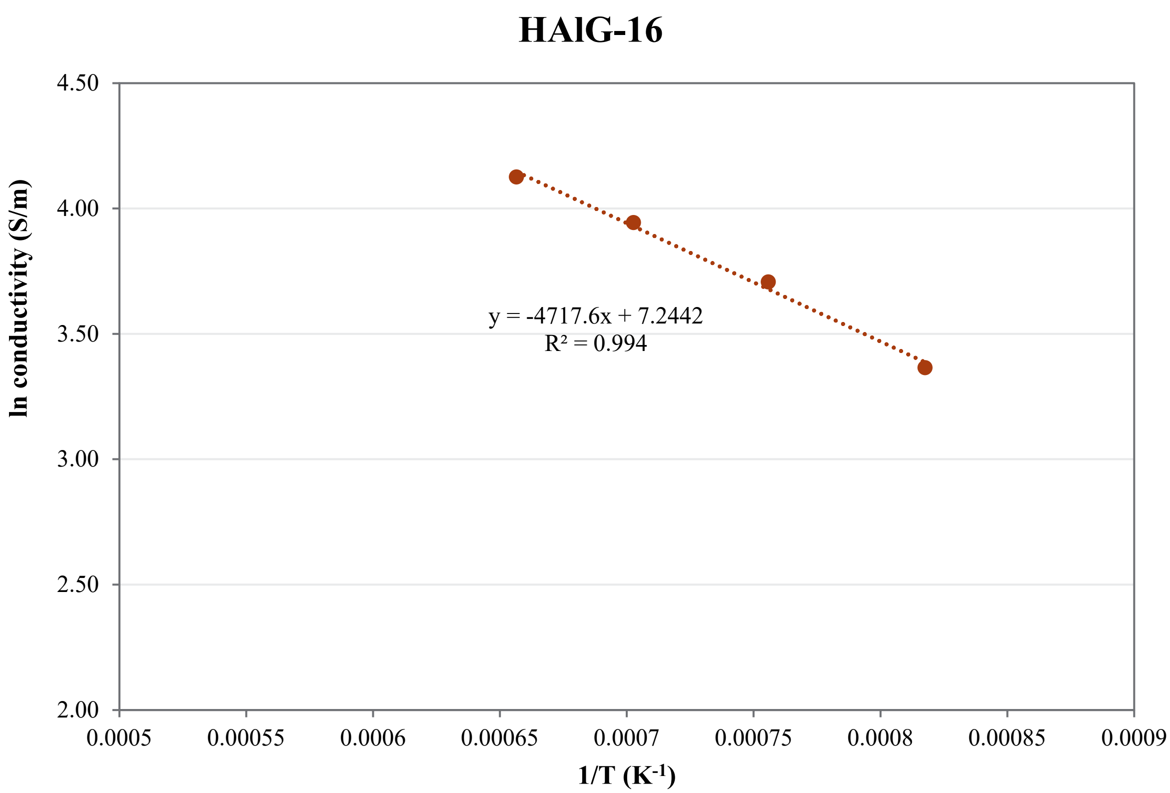

Figure G.15. Electrical Conductivity-Temperature Data with Arrhenius Equation Fit for Glass HAlG-16

G.16 Glass HAlG-17 Electrical Conductivity Data

Table G.16. Electrical Conductivity Data for Glass HAlG-17

Temperature, °C	Conductivity, S/m	1/T, K^{-1}	ln ε, S/m
950	22.4	0.000818	3.11
1250	52.5	0.000657	3.96
1150	42.5	0.000703	3.75
1050	33.1	0.000756	3.50

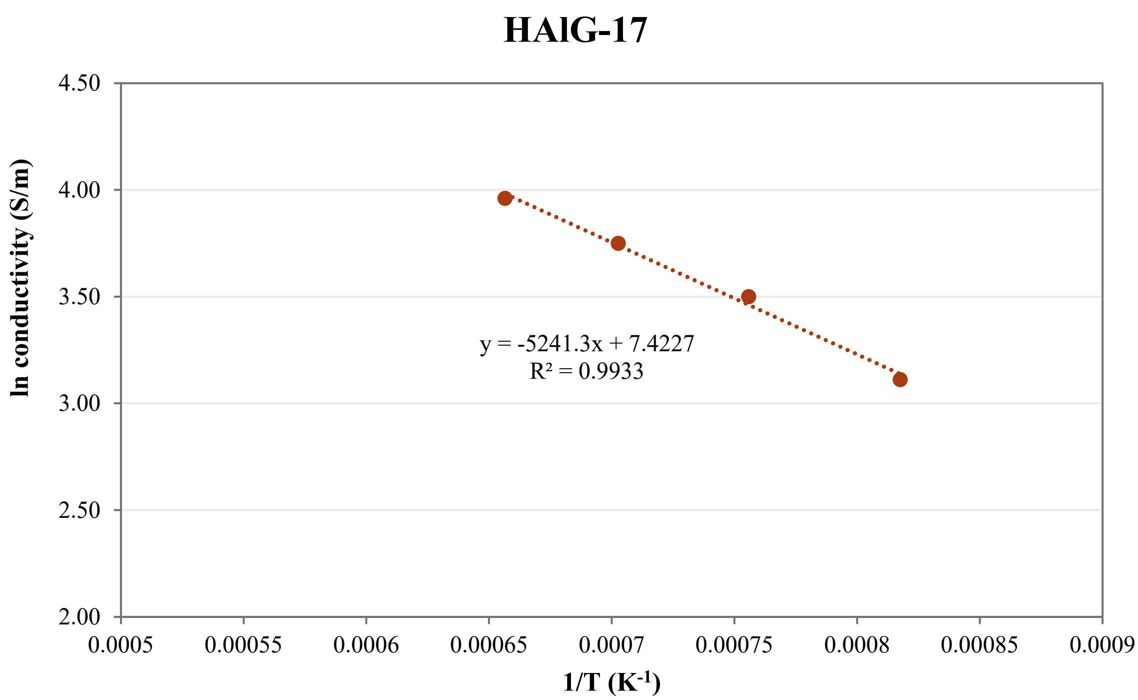

Figure G.16. Electrical Conductivity-Temperature Data with Arrhenius Equation Fit for Glass HAlG-17

G.17 Glass HAlG-18 Electrical Conductivity Data

Table G.17. Electrical Conductivity Data for Glass HAlG-18

Temperature, °C	Conductivity, S/m	1/T, K^{-1}	ln ε, S/m
950	37.9	0.000818	3.64
1250	72.3	0.000657	4.28
1150	63.4	0.000703	4.15
1050	51.6	0.000756	3.94

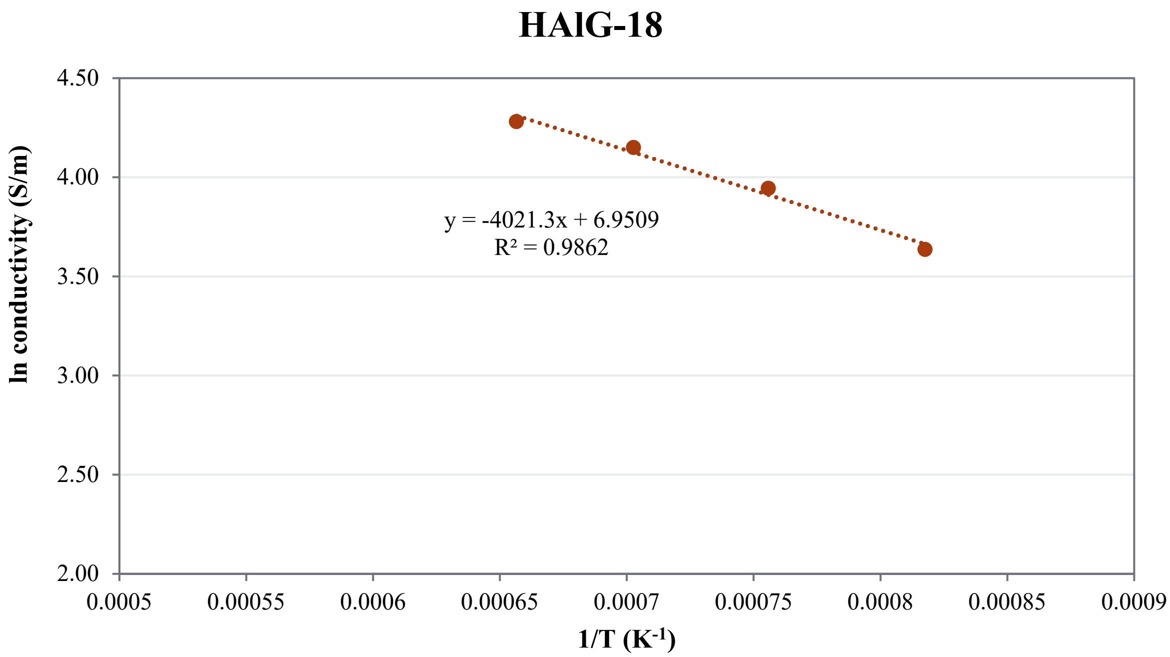

Figure G.17. Electrical Conductivity-Temperature Data with Arrhenius Equation Fit for Glass HAlG-18

G.18 Glass HAlG-19 Electrical Conductivity Data

Table G.18. Electrical Conductivity Data for Glass HAlG-19

Temperature, °C	Conductivity, S/m	1/T, K^{-1}	ln ε, S/m
950	103.6	0.000818	4.64
1050	119.3	0.000756	4.78

G.19 Glass HAlG-20 Electrical Conductivity Data

Table G.19. Electrical Conductivity Data for Glass HAlG-20

Temperature, °C	Conductivity, S/m	1/T, K^{-1}	ln ε, S/m
950	18.3	0.000818	2.91
1250	46.5	0.000657	3.84
1150	37.8	0.000703	3.63
1050	28.5	0.000756	3.35

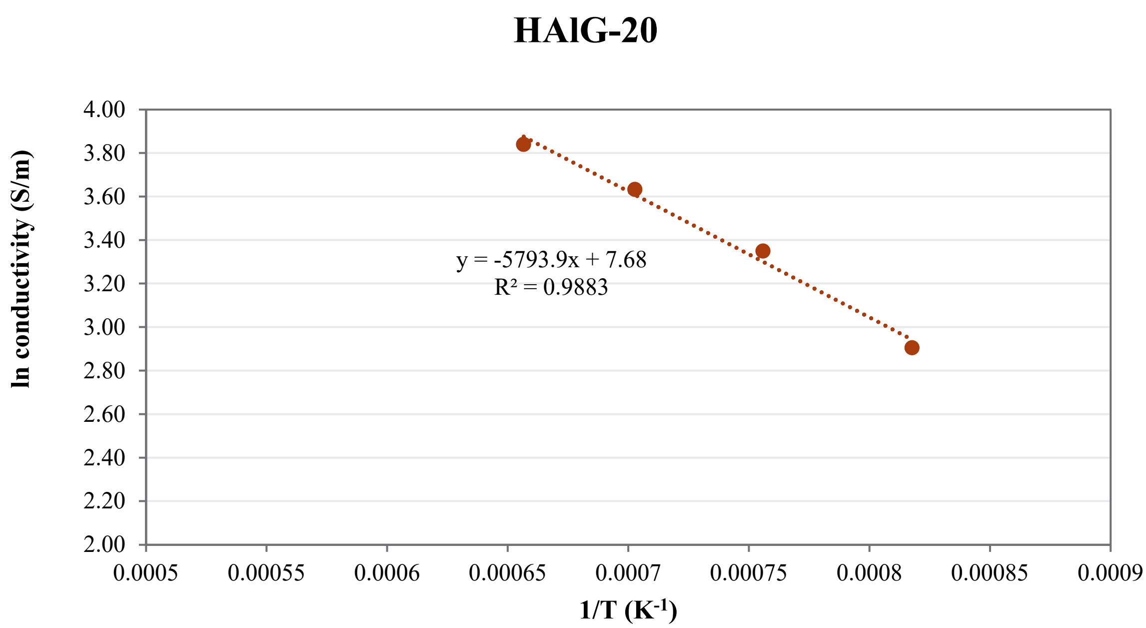

Figure G.18. Electrical Conductivity-Temperature Data with Arrhenius Equation Fit for Glass HAlG-20

G.20 Glass HAlG-21 Electrical Conductivity Data

Table G.20. Electrical Conductivity Data for Glass HAlG-21

Temperature, °C	Conductivity, S/m	1/T, K^{-1}	ln ε, S/m
950	31.6	0.000818	3.45
1250	67.5	0.000657	4.21
1150	56.5	0.000703	4.03
1050	44.3	0.000756	3.79

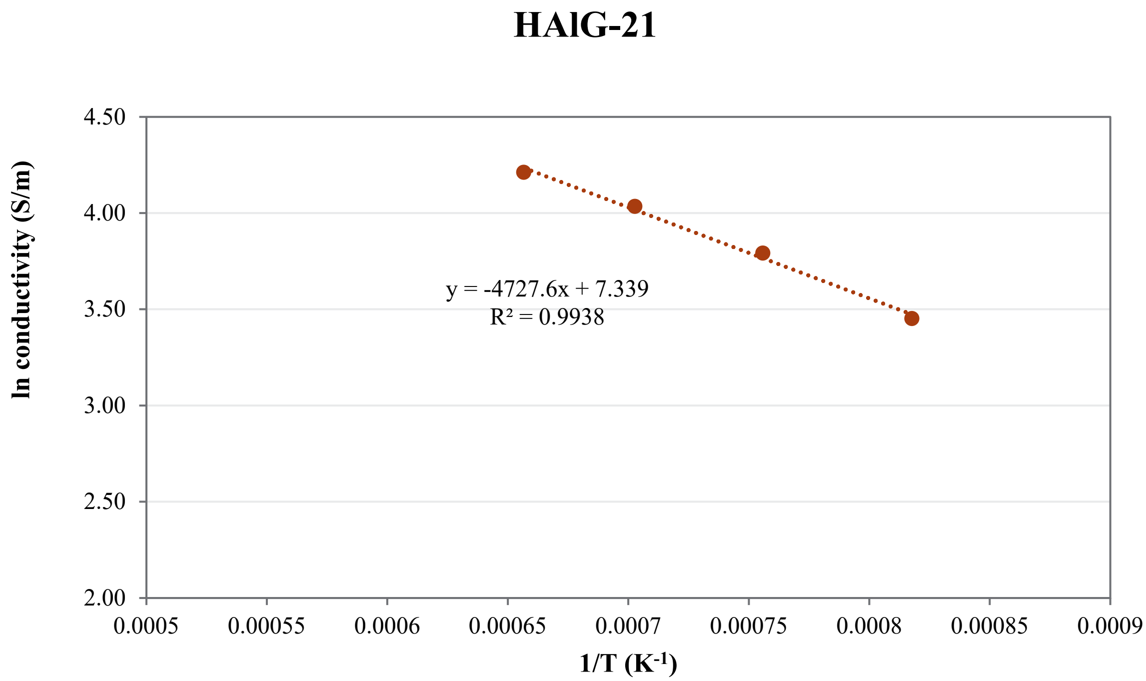

Figure G.19. Electrical Conductivity-Temperature Data with Arrhenius Equation Fit for Glass HAlG-21

G.21 Glass HAlG-22 Electrical Conductivity Data

Table G.21. Electrical Conductivity Data for Glass HAlG-22

Temperature, °C	Conductivity, S/m	1/T, K^{-1}	ln ε, S/m
950	13.9	0.000818	2.63
1250	37.2	0.000657	3.62
1150	29.5	0.000703	3.38
1050	21.4	0.000756	3.06

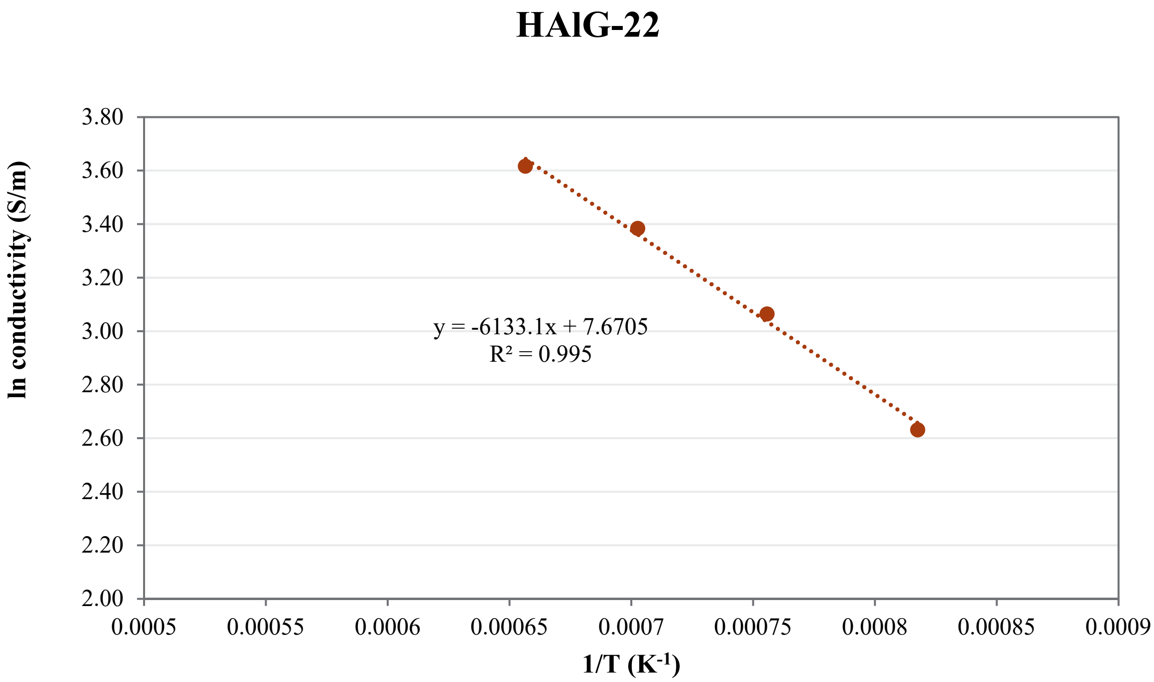

Figure G.20. Electrical Conductivity-Temperature Data with Arrhenius Equation Fit for Glass HAlG-22

G.22 Glass HAlG-23 Electrical Conductivity Data

Table G.22. Electrical Conductivity Data for Glass HAlG-23

Temperature, °C	Conductivity, S/m	1/T, K^{-1}	ln ε, S/m
950	24.9	0.000818	3.21
1250	57.7	0.000657	4.06
1150	48.0	0.000703	3.87
1050	36.7	0.000756	3.60

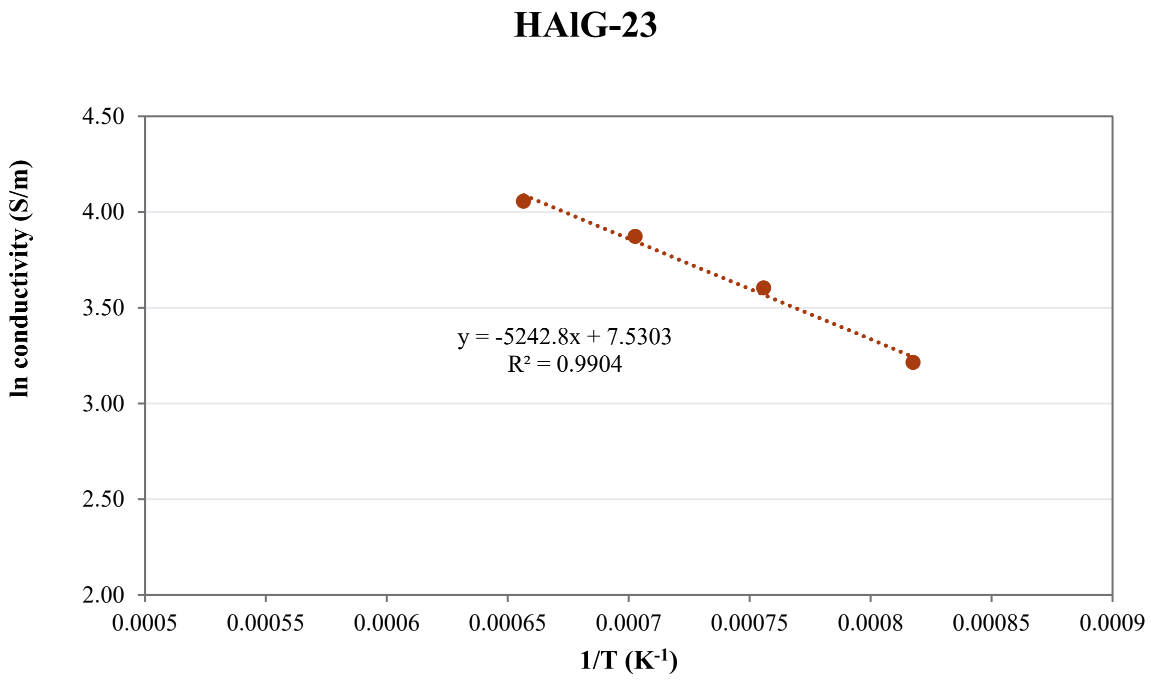

Figure G.21. Electrical Conductivity-Temperature Data with Arrhenius Equation Fit for Glass HAlG-23

G.23 Glass HAlG-24 Electrical Conductivity Data

Table G.23. Electrical Conductivity Data for Glass HAlG-24

Temperature, °C	Conductivity, S/m	1/T, K^{-1}	ln ε, S/m
950	19.4	0.000818	2.97
1250	53.1	0.000657	3.97
1150	41.3	0.000703	3.72
1050	30.1	0.000756	3.40

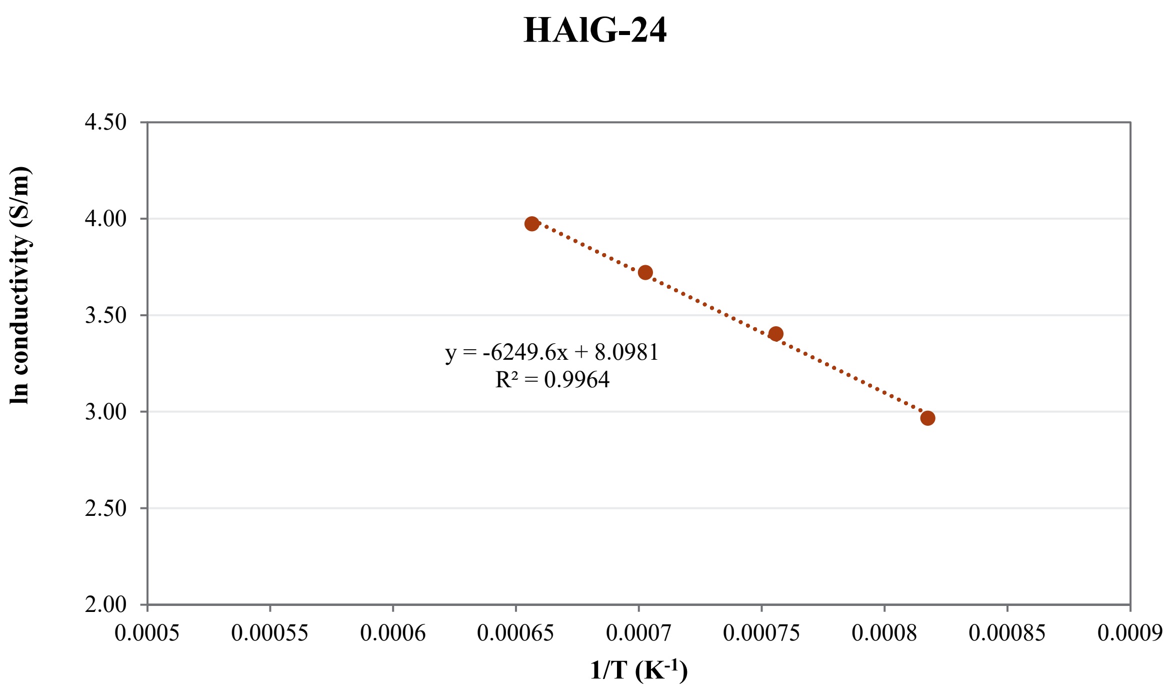

Figure G.22. Electrical Conductivity-Temperature Data with Arrhenius Equation Fit for Glass HAlG-24

G.24 Glass HAlG-25 Electrical Conductivity Data

Table G.24. Electrical Conductivity Data for Glass HAlG-25

Temperature, °C	Conductivity, S/m	1/T, K^{-1}	ln ε, S/m
950	19.5	0.000818	2.97
1250	47.1	0.000657	3.85
1150	38.1	0.000703	3.64
1050	28.2	0.000756	3.34

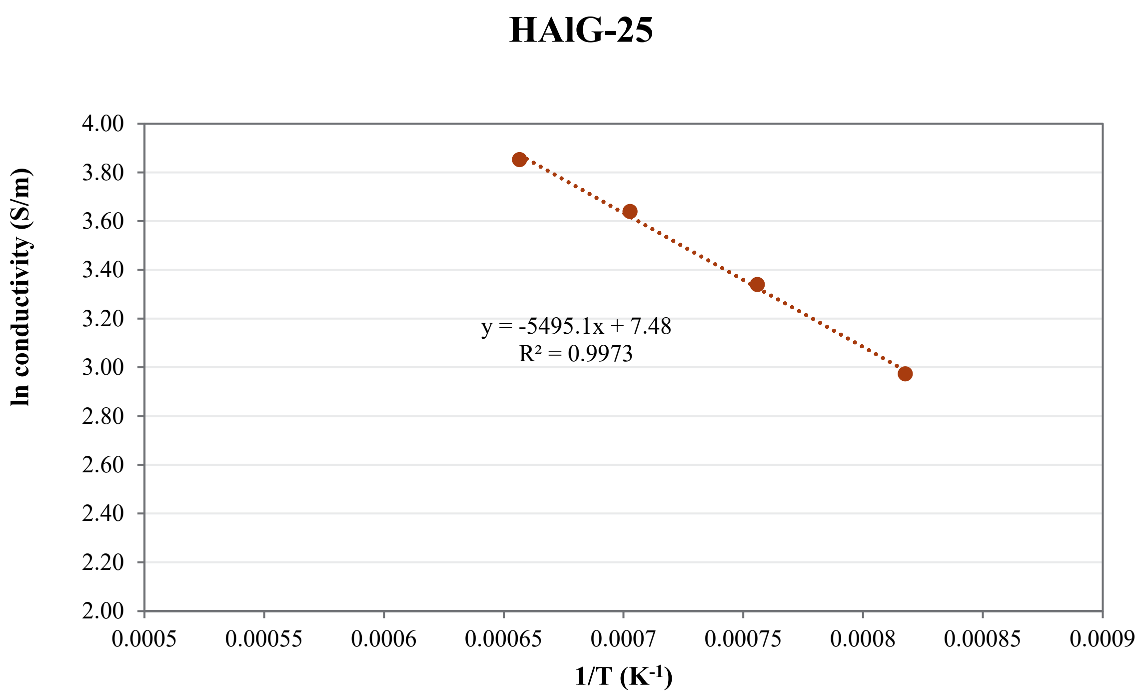

Figure G.23. Electrical Conductivity-Temperature Data with Arrhenius Equation Fit for Glass HAlG-25

Appendix H – Crystal Fraction of Heat-Treated Glasses Photographs

This appendix presents photos of glasses showing how their response to being heat-treated at 950 °C for 24 h and 850 °C for 48 h.

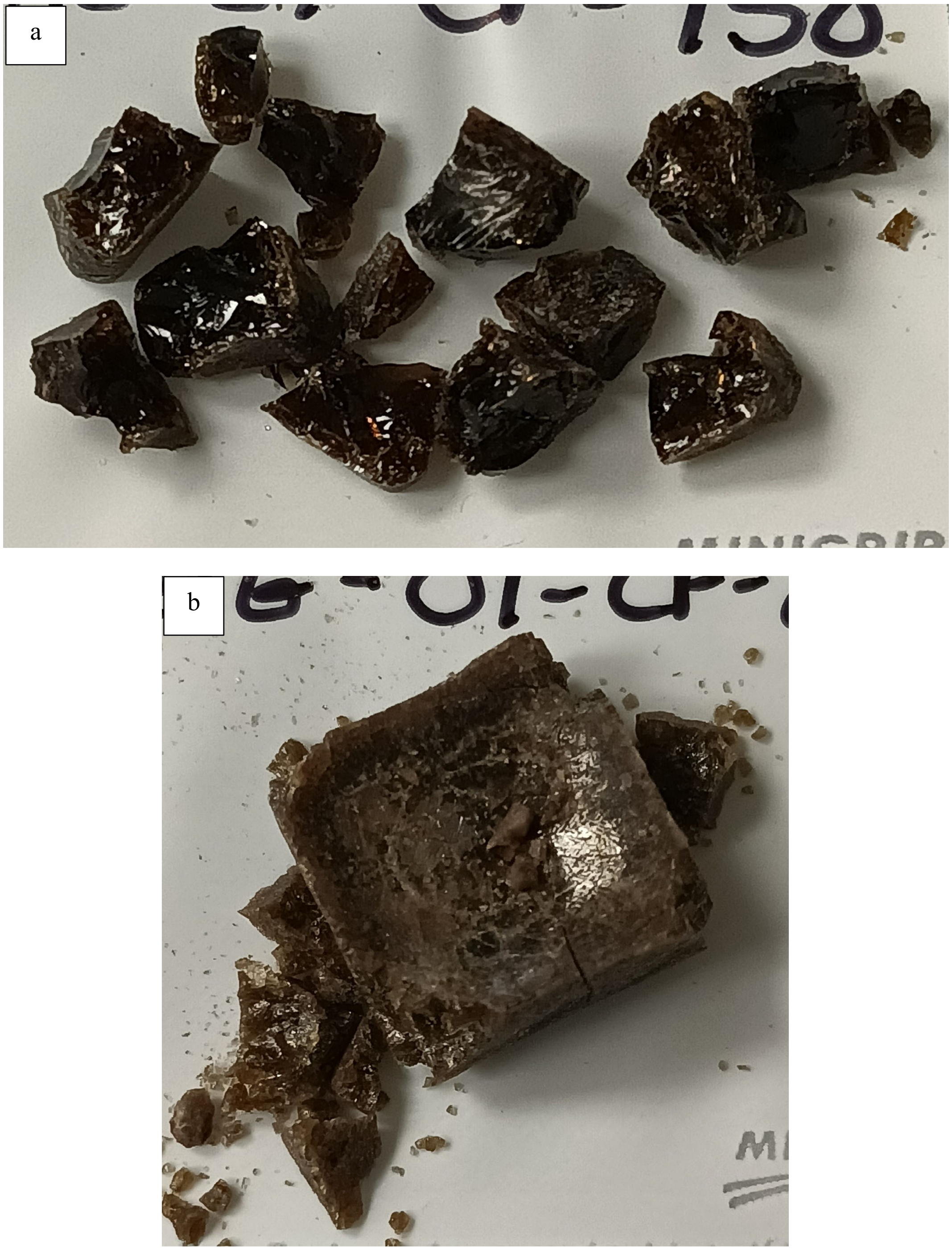

Figure H.1. Glass HAlG-01 after crystal fraction (CF) Heat Treatment at a) 950 °C for 24 h and b) 850 °C for 48 h

Figure H.2. Glass HAlG-02 after CF Heat Treatment at a) 950 °C for 24 h and b) 850 °C for 48 h

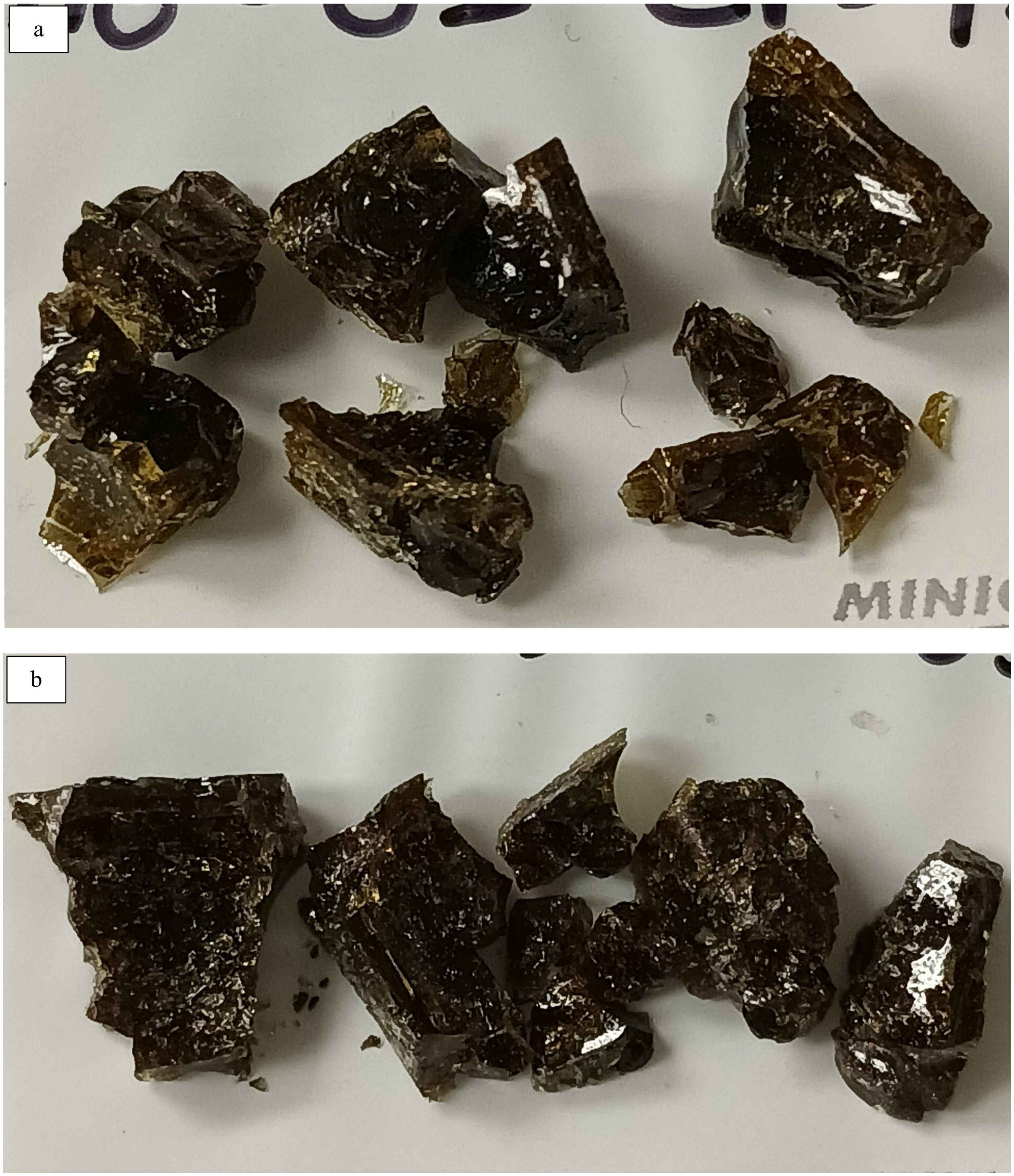

Figure H.3. Glass HAlG-03 after CF Heat Treatment at a) 950 °C for 24 h and b) 850 °C for 48 h

Figure H.4. Glass HAlG-04 after CF Heat Treatment at a) 950 °C for 24 h and b) 850 °C for 48 h

Figure H.5. Glass HAlG-05 after CF Heat Treatment at a) 950 °C for 24 h and b) 850 °C for 48 h

Figure H.6. Glass HAlG-06 after CF Heat Treatment at a) 950 °C for 24 h and b) 850 °C for 48 h

Figure H.7. Glass HAlG-07-1 after CF Heat Treatment at a) 950 °C for 24 h and b) 850 °C for 48 h

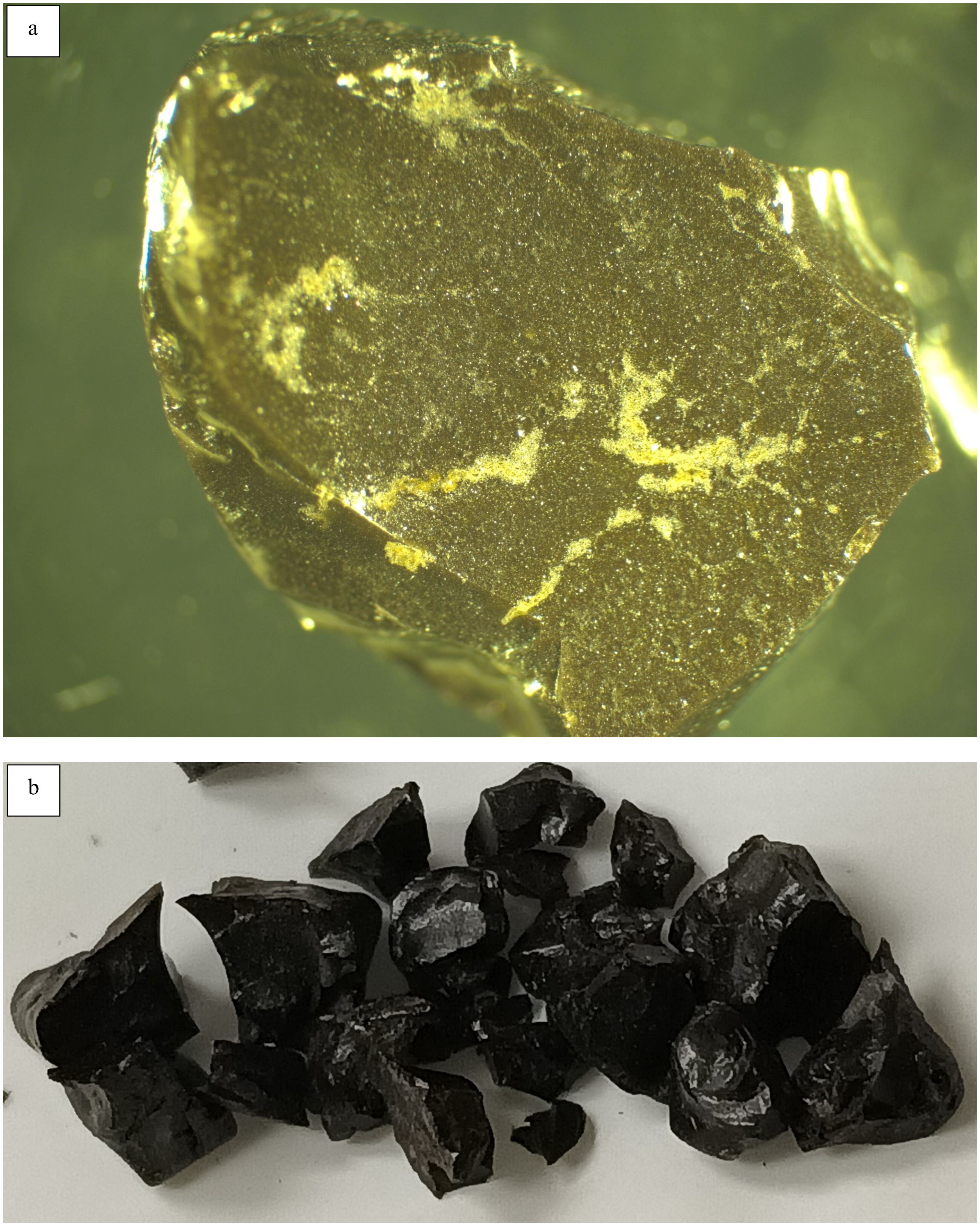

Figure H.8. Glass HAlG-08 after CF Heat Treatment at a) 950 °C for 24 h under microscope and b) 850 °C for 48 h

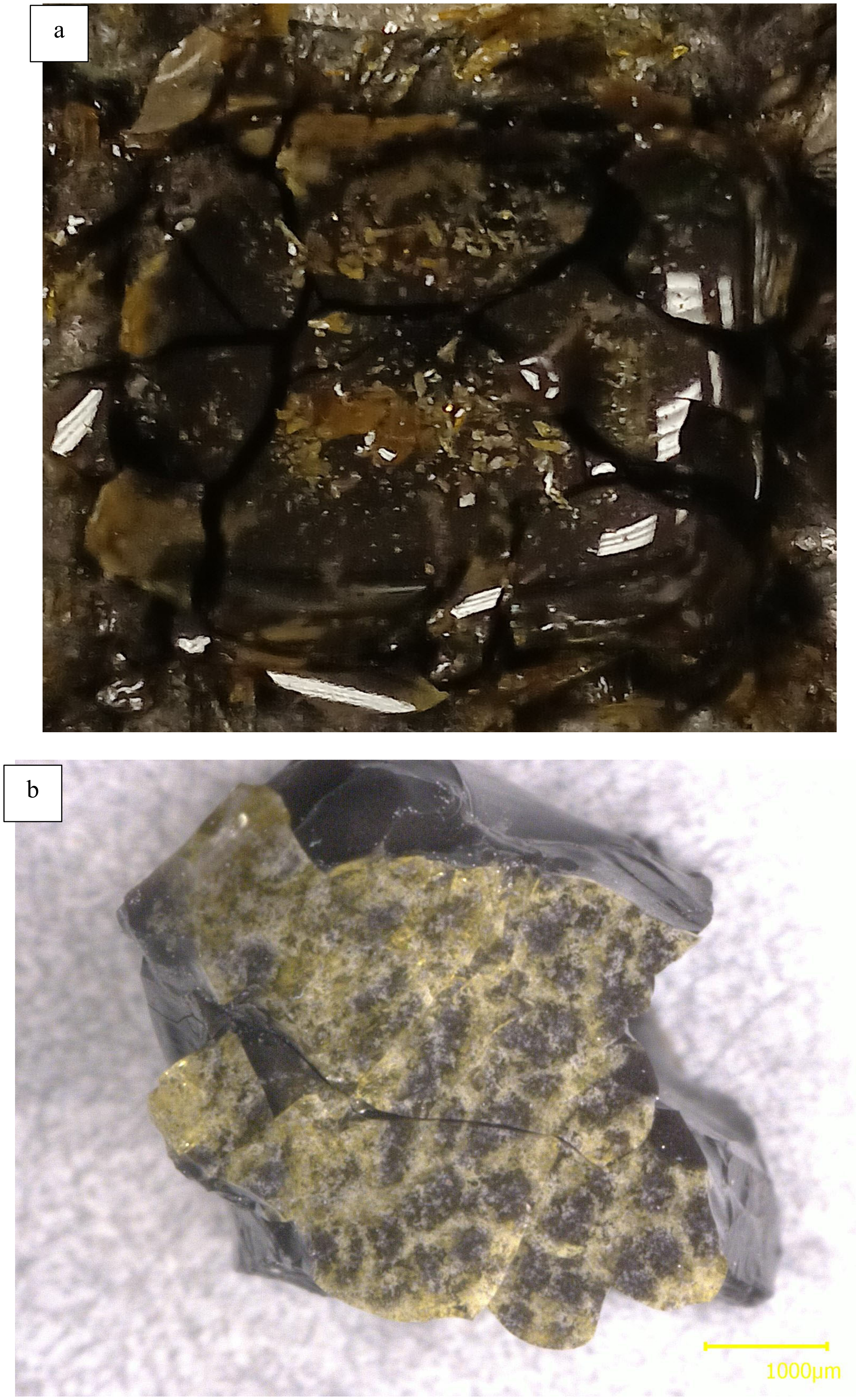

Figure H.9. Glass HAlG-09 after CF Heat Treatment at a) 950 °C for 24 h and b) 850 °C for 48 h at 50X magnification

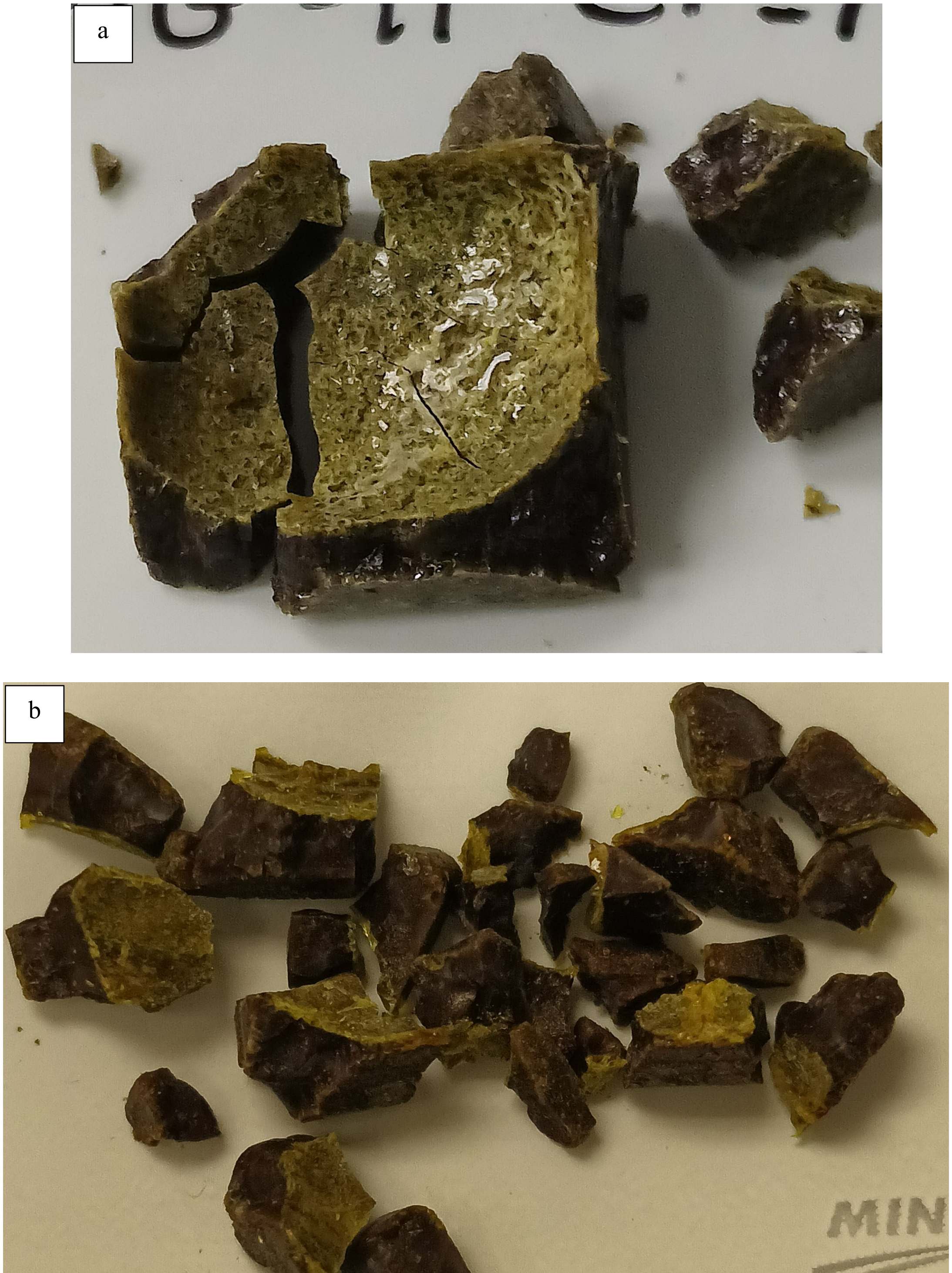

Figure H.10. Glass HAlG-11 after CF Heat Treatment at a) 950 °C for 24 h and b) 850 °C for 48 h

Figure H.11. Glass HAlG-12 after CF Heat Treatment at a) 950 °C for 24 h under the microscope and b) 850 °C for 48 h

Figure H.12. Glass HAlG-13 after CF Heat Treatment at a) 950 °C for 24 h and b) 850 °C for 48 h

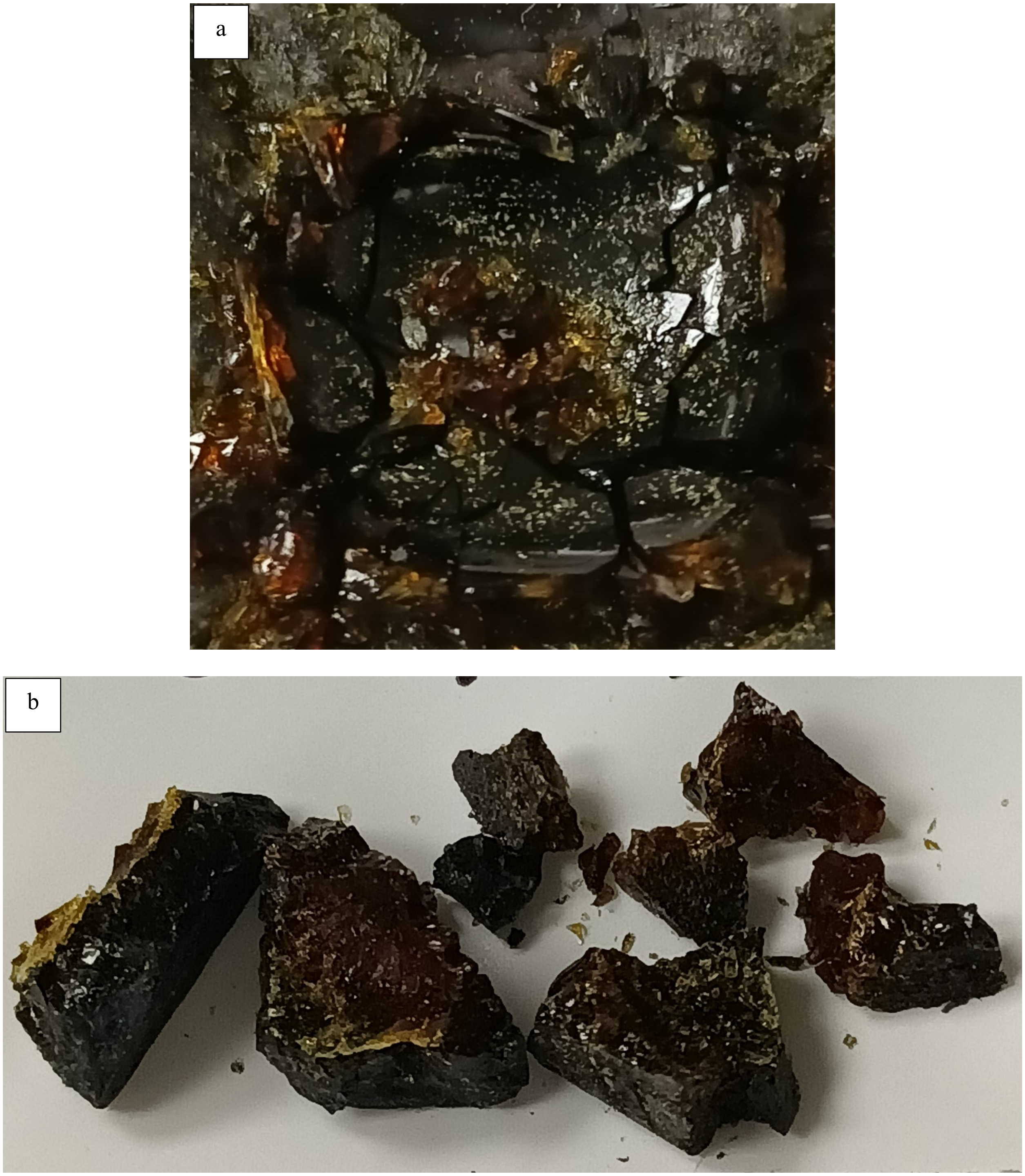

Figure H.13. Glass HAlG-14 after CF Heat Treatment at a) 950 °C for 24 h and b) 850 °C for 48 h

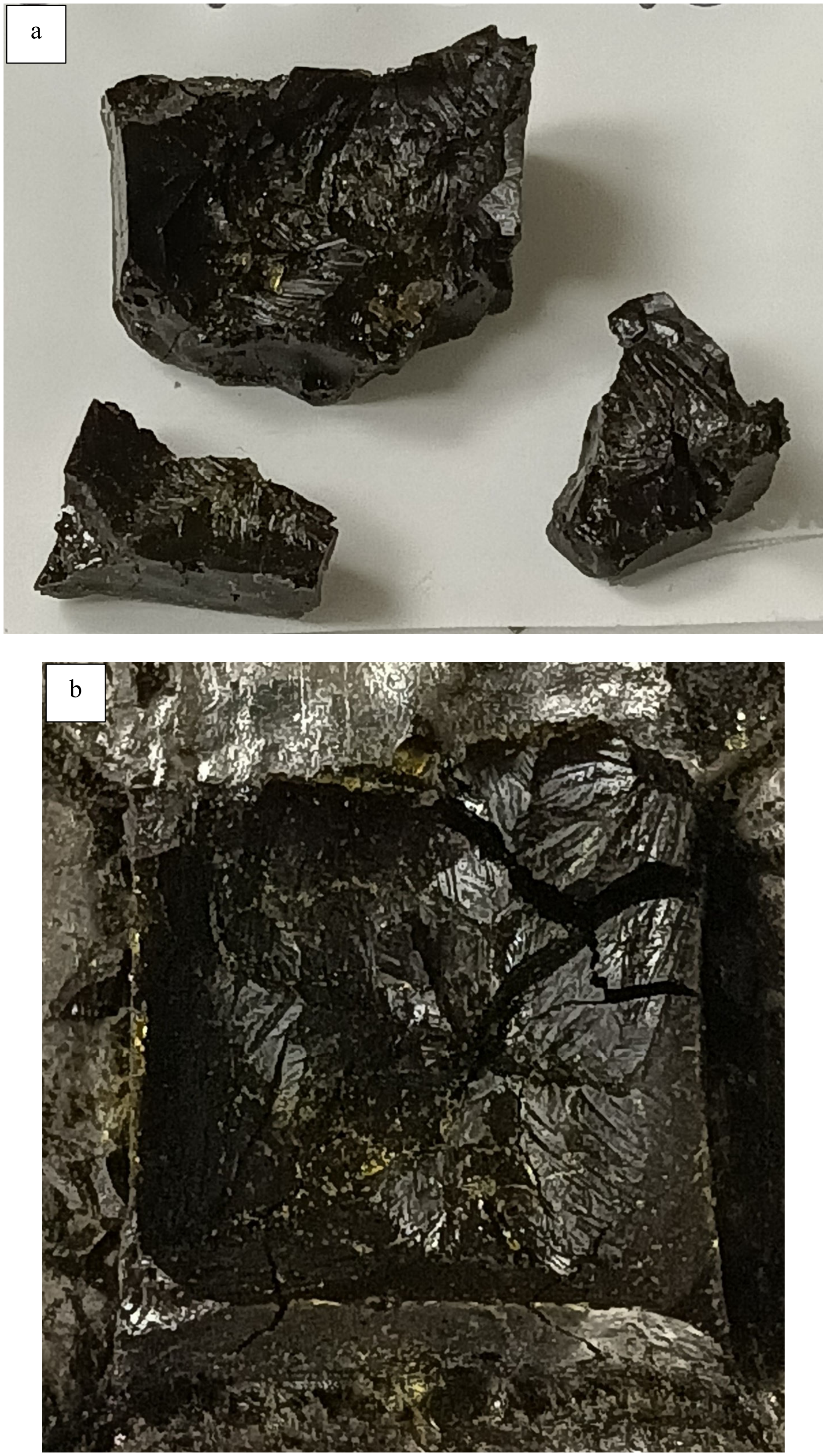

Figure H.14. Glass HAlG-15 after CF Heat Treatment at a) 950 °C for 24 h and b) 850 °C for 48 h

Figure H.15. Glass HAlG-16 after CF Heat Treatment at a) 950 °C for 24 h and b) 850 °C for 48 h

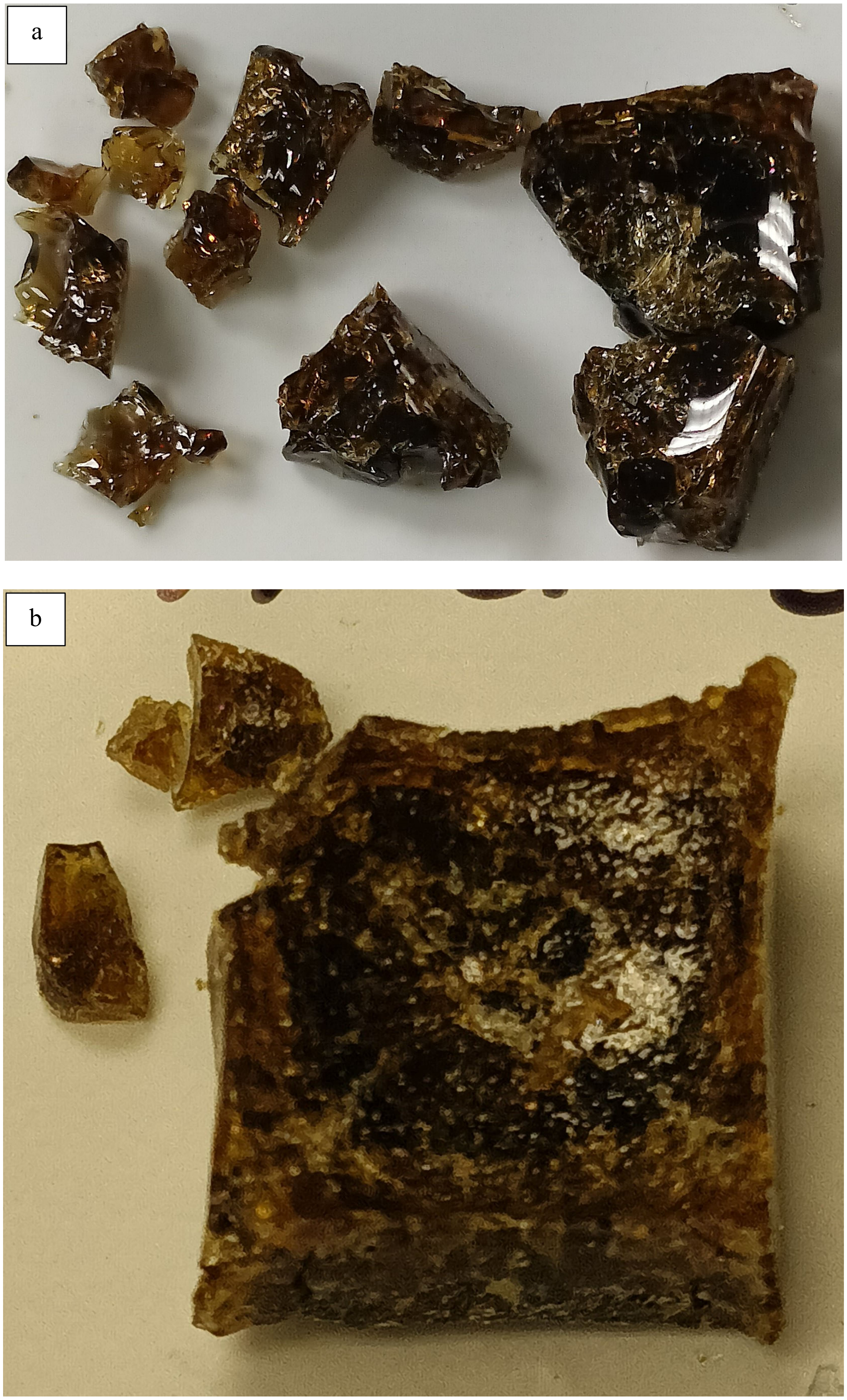

Figure H.16. Glass HAlG-17 after CF Heat Treatment at a) 950 °C for 24 h and b) 850 °C for 48 h

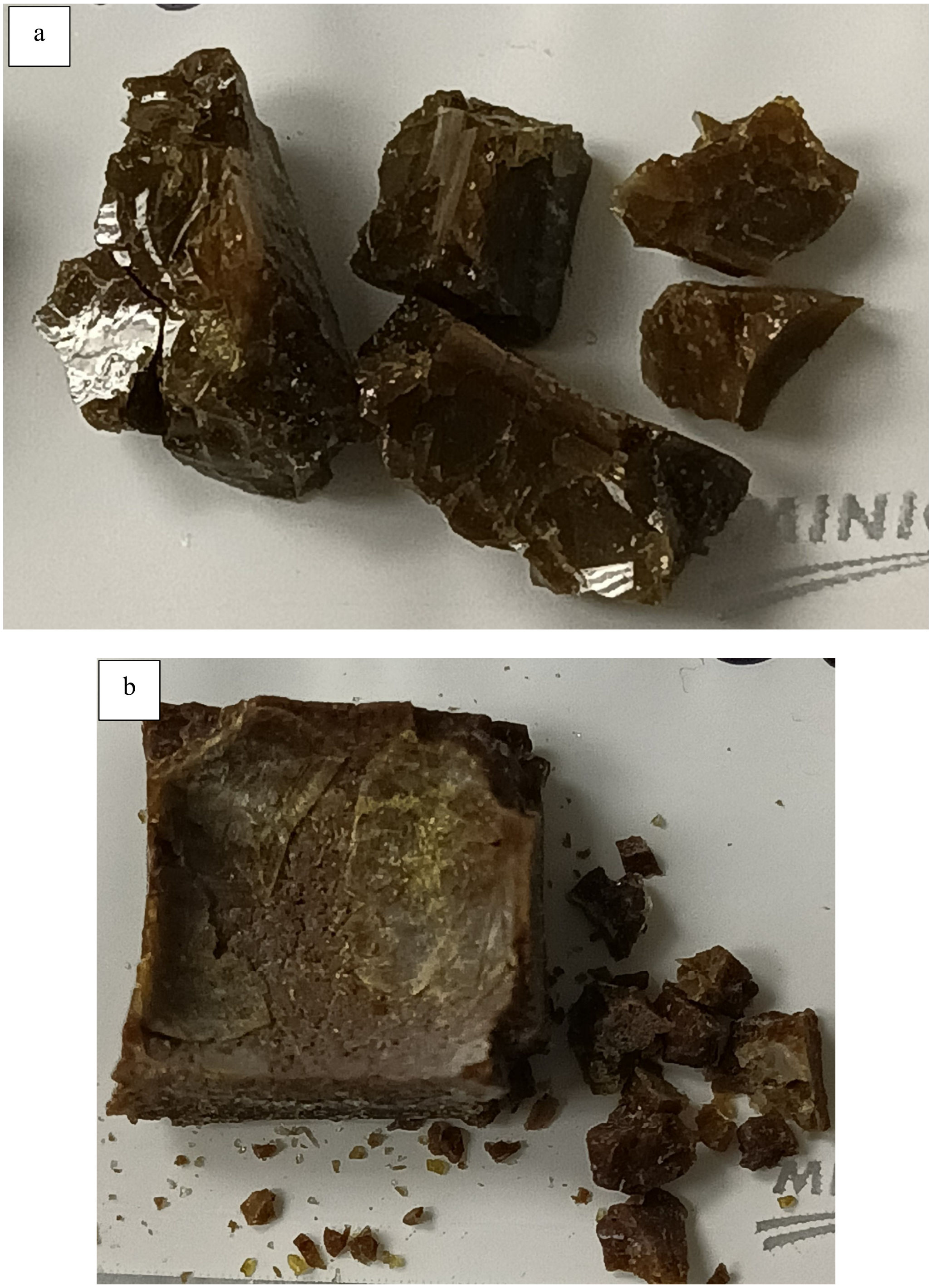

Figure H.17. Glass HAlG-18 after CF Heat Treatment at a) 950 °C for 24 h and b) 850 °C for 48 h

Figure H.18. Glass HAlG-19 after CF Heat Treatment at a) 950 °C for 24 h and b) 850 °C for 48 h

Figure H.19. Glass HAlG-20 after CF Heat Treatment at a) 950 °C for 24 h and b) 850 °C for 48 h

Figure H.20. Glass HAlG-21 after CF Heat Treatment at a) 950 °C for 24 h and b) 850 °C for 48 h

Figure H.21. Glass HAlG-22 after CF Heat Treatment at a) 950 °C for 24 h and b) 850 °C for 48 h

Figure H.22. Glass HAlG-23 after CF Heat Treatment at a) 950 °C for 24 h and b) 850 °C for 48 h

Figure H.23. Glass HAlG-24 after CF Heat Treatment at a) 950 °C for 24 h and b) 850 °C for 48 h

Figure H.24. Glass HAlG-25 after CF Heat Treatment at a) 950 °C for 24 h and b) 850 °C for 48 h

Appendix I – XRD of Crystal Fraction Heat-Treated Glasses

This appendix presents the X-ray diffraction (XRD) plots of several glasses after crystal fraction (CF) heat-treatment at 950 °C for 24 h and 850 °C for 48 h. The majority of the glasses developed crystals, primarily nepheline, spinel, ZrO_2, and Cr_2O_3.

The percentage of crystal content reported in the XRD scans is presented before any adjustments were made from spiking with 5 wt% of high-purity cerium oxide. The data is corrected not only for the amount of cerium oxide introduced into the samples, but also to account for the fact that the cerium oxide used was only 51% crystalline.

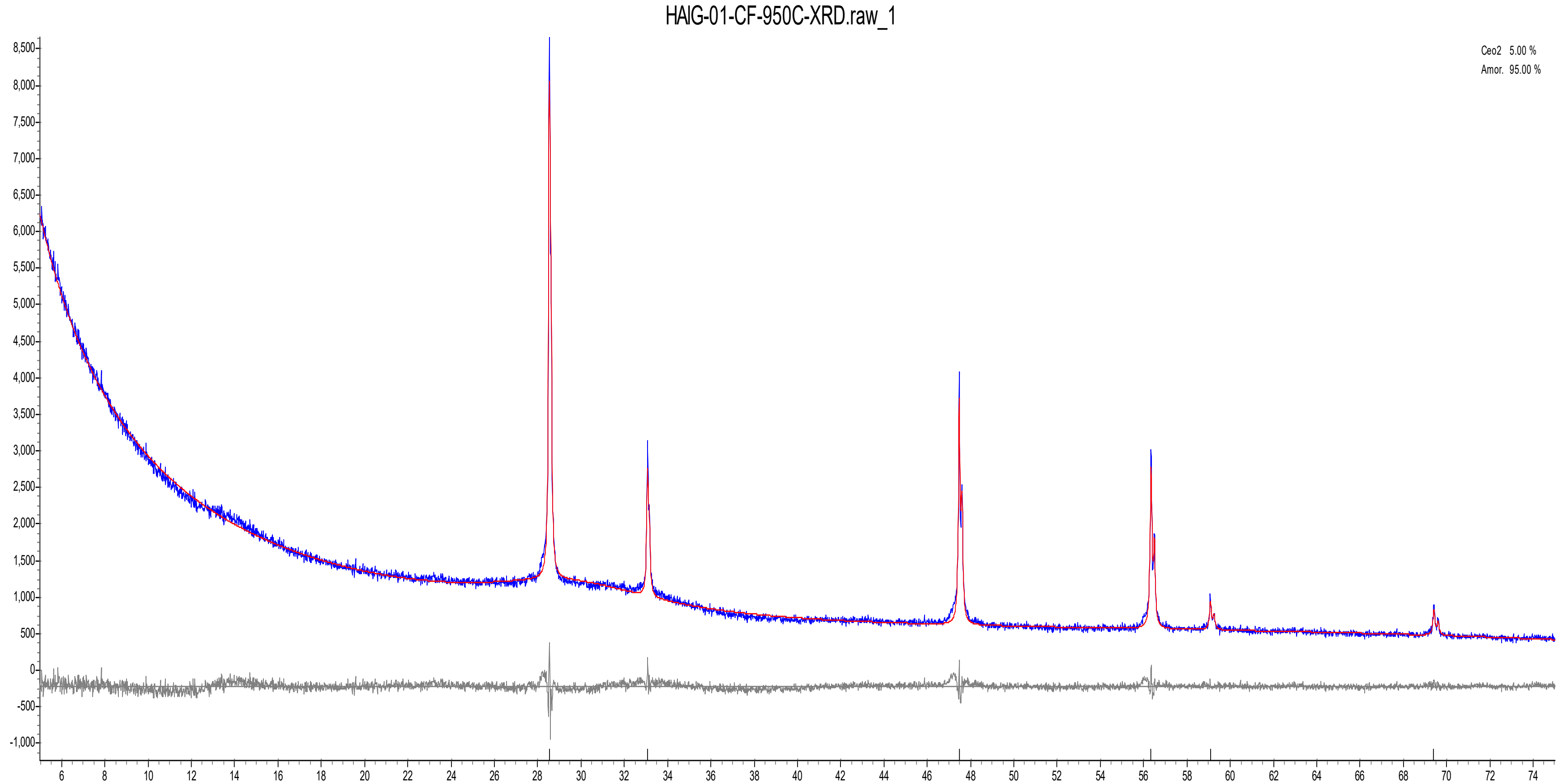

Figure I.1. XRD Spectrum of CF 950 °C Heat-Treated Glass HAlG-01

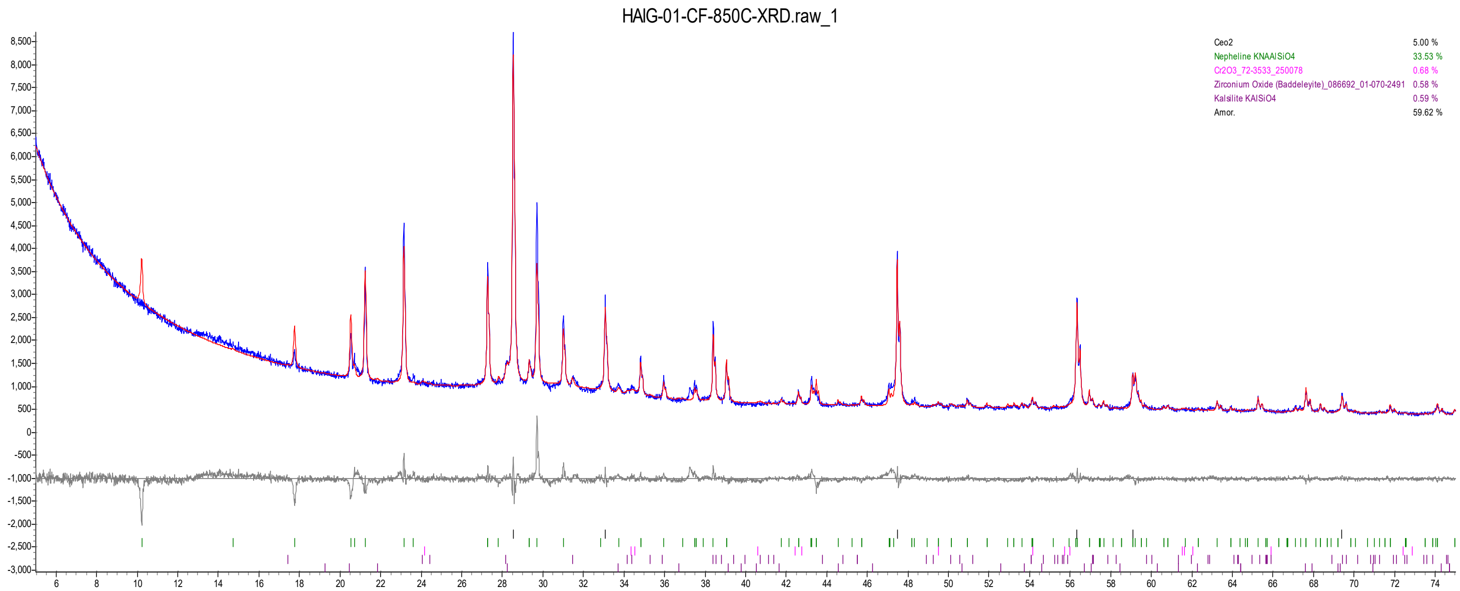

Phase Name	Wt% of Spiked	Wt% in Spiked Sample	Wt% in Original Sample
CeO_2	2.565	2.565	0.000
Nepheline	0.000	19.148	20.157
$KAlSiO_4$	0.000	0.731	0.769
ZrO_2	0.000	0.577	0.608

Figure I.2. XRD Spectrum of CF 850 °C Heat-Treated Glass HAlG-01

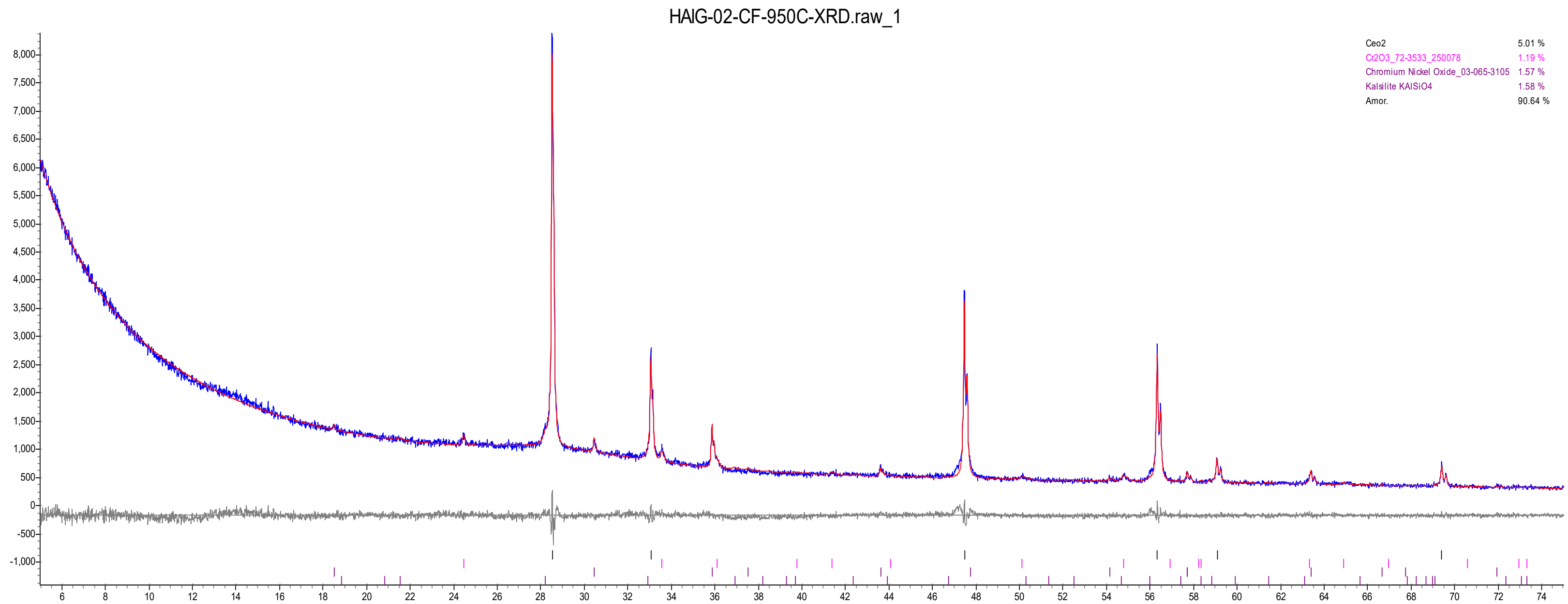

Phase Name	Wt% of Spiked	Wt% in Spiked Sample	Wt% in Original Sample
CeO_2	2.570	2.570	0.000
$KAlSiO_4$	0.000	1.005	1.058
Cr_2O_3	0.000	0.559	0.588
$NiCr_2O_4$ (Spinel)	0.000	0.936	0.986

Figure I.3. XRD Spectrum of CF 950 °C Heat-Treated Glass HAlG-02

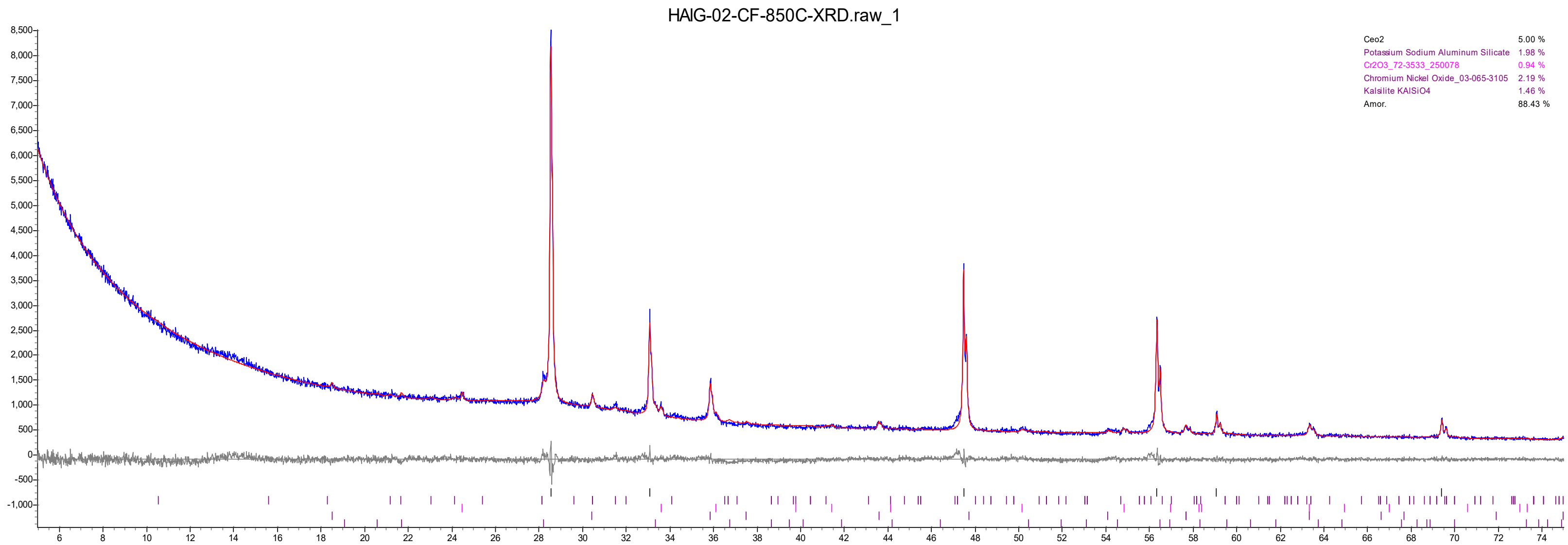

Phase Name	Wt% of Spiked	Wt% in Spiked Sample	Wt% in Original Sample
CeO_2	2.565	2.565	0.000
$KNaAlO_6Si_2$ (Nepheline)	0.000	5.288	5.566
$KAlSiO_4$	0.000	1.335	1.405
Cr_2O_3	0.000	0.606	0.637
$NiCr_2O_4$ (Spinel)	0.000	1.351	1.422

Figure I.4. XRD Spectrum of CF 850 °C Heat-Treated Glass HAlG-02

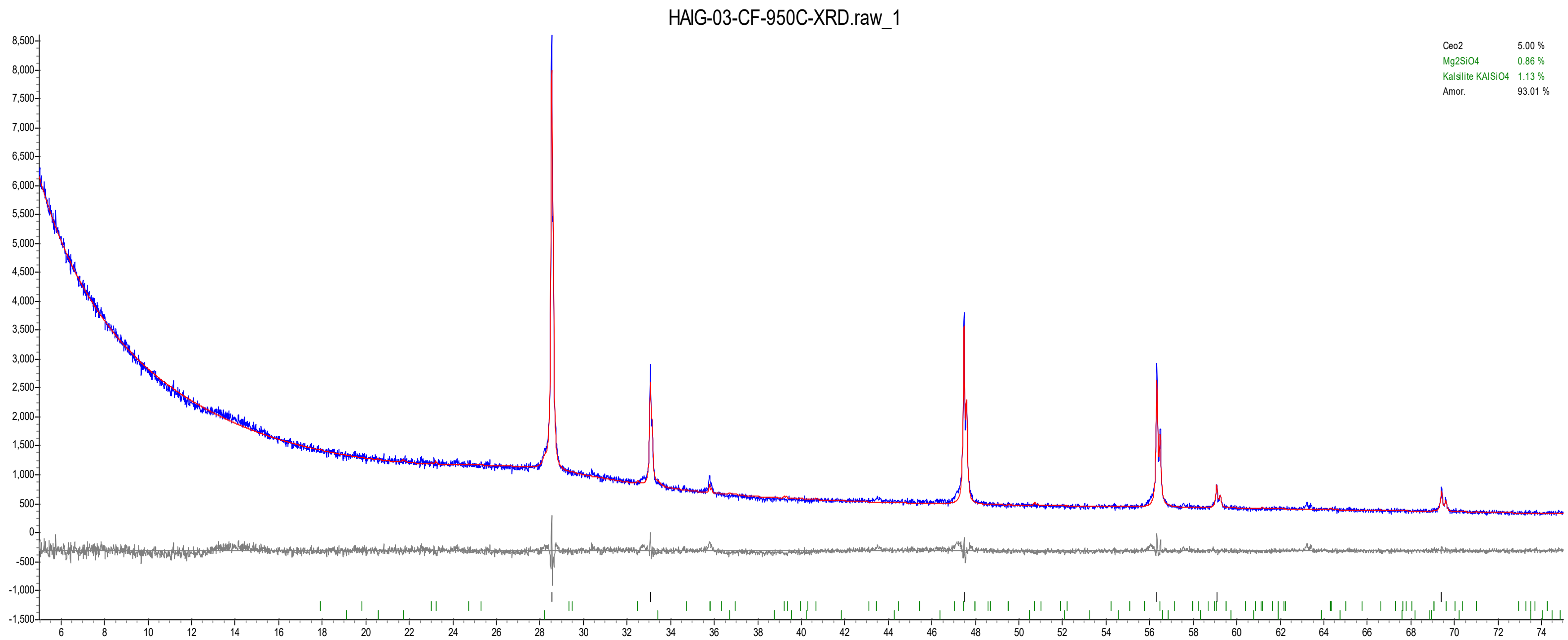

Phase Name	Wt% of Spiked	Wt% in Spiked Sample	Wt% in Original Sample
CeO_2	2.562	2.562	0.000
$KAlSiO_4$	0.000	0.950	1.000
Mg_2SiO_4	0.000	0.638	0.671

Figure I.5. XRD Spectrum of CF 950 °C Heat-Treated Glass HAlG-03

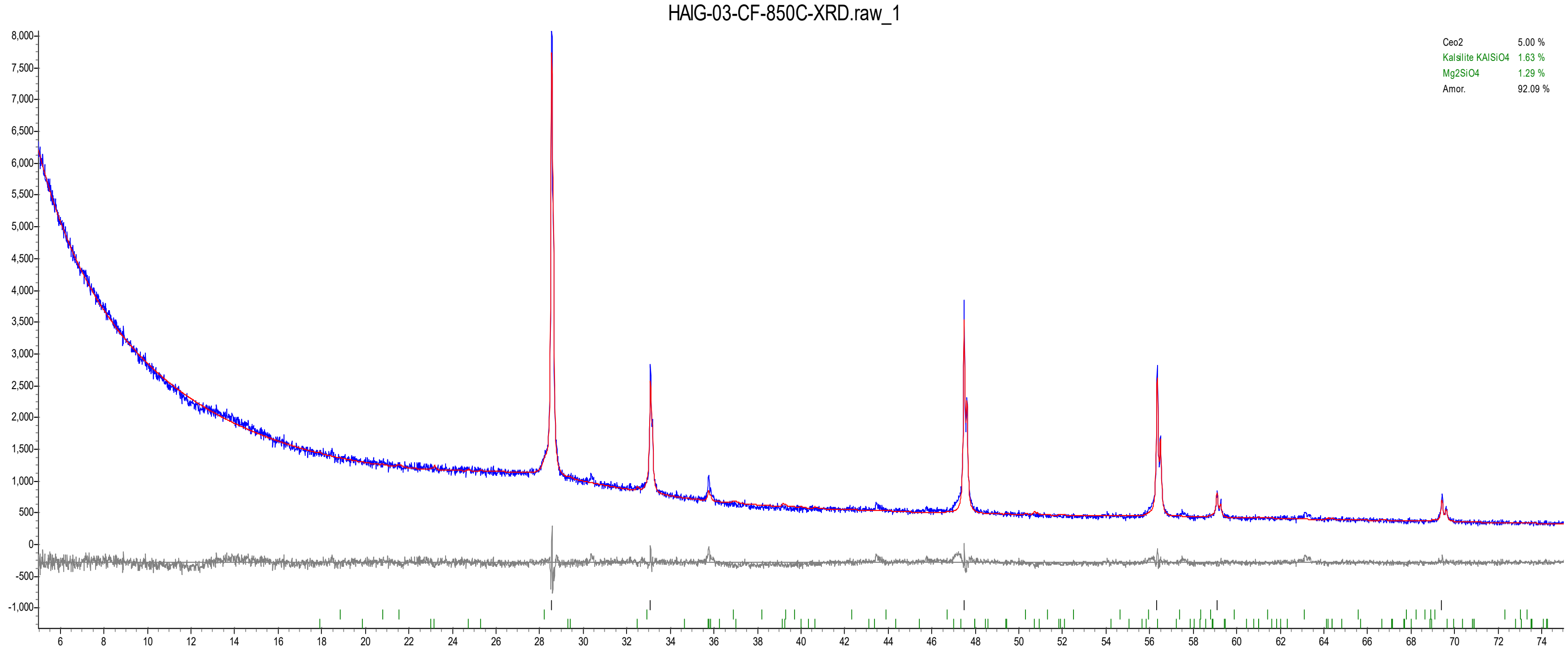

Phase Name	Wt% of Spiked	Wt% in Spiked Sample	Wt% in Original Sample
CeO_2	2.561	2.561	0.000
$KAlSiO_4$	0.000	1.027	1.081
Mg_2SiO_4	0.000	1.019	1.073

Figure I.6. XRD Spectrum of CF 850 °C Heat-Treated Glass HAlG-03

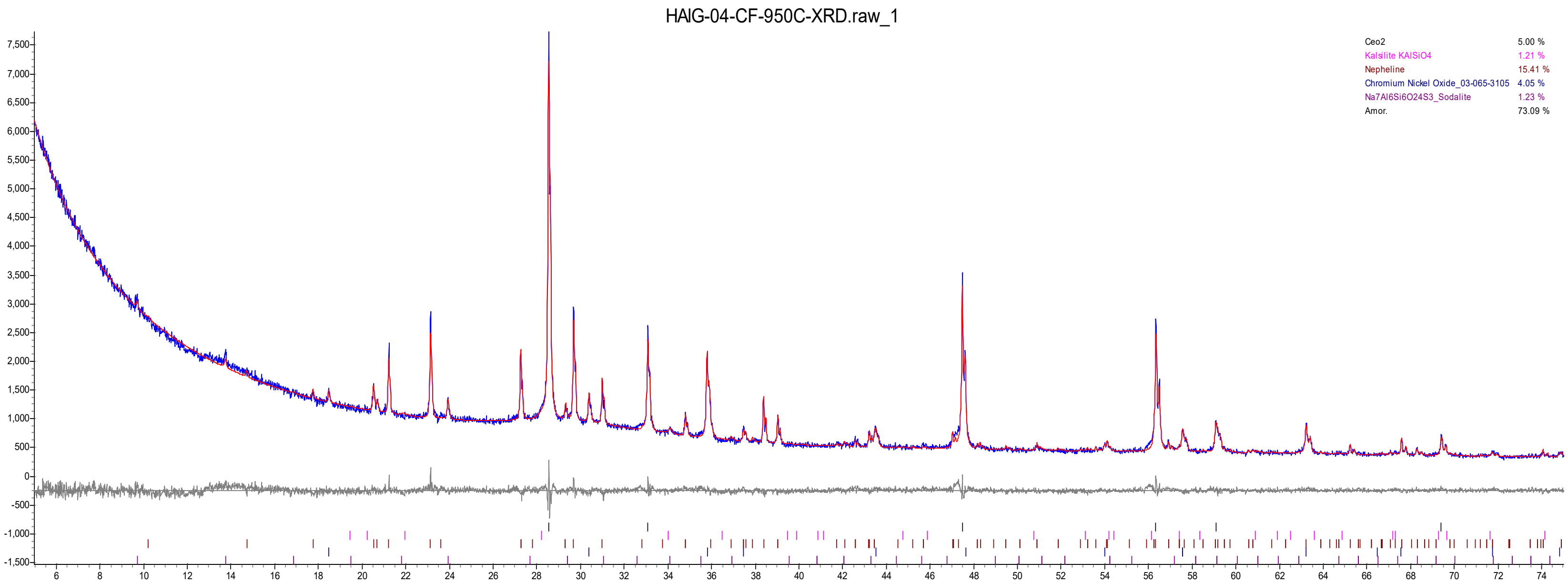

Phase Name	Wt% of Spiked	Wt% in Spiked Sample	Wt% in Original Sample
CeO_2	2.565	2.565	0.000
$KAlSiO_4$	0.000	5.930	6.242
$Na_7Al_6Si_6O_{24}S_3$	0.000	0.704	0.741
$KNaAlSiO_4$ (Nepheline)	0.000	8.743	9.203
$NiCr_2O_4$ (Spinel)	0.000	2.176	2.291

Figure I.7. XRD Spectrum of CF 950 °C Heat-Treated Glass HAlG-04

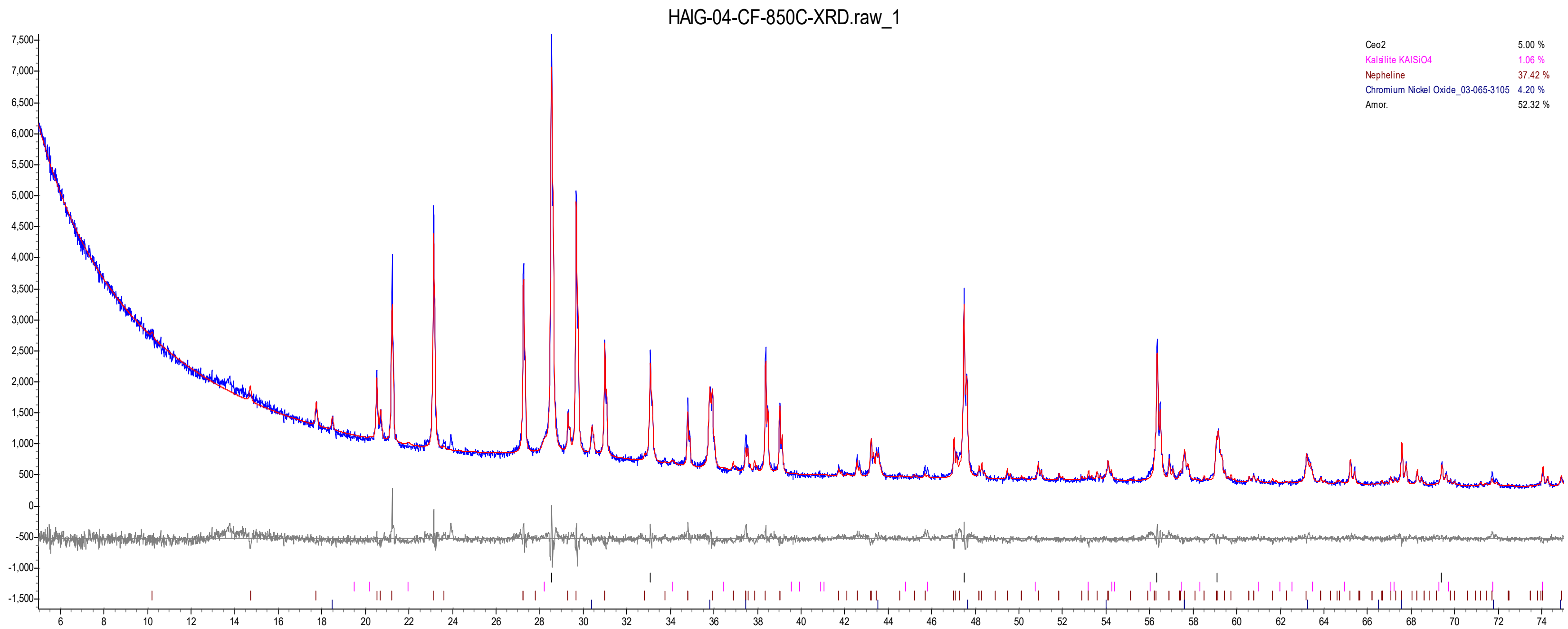

Phase Name	Wt% of Spiked	Wt% in Spiked Sample	Wt% in Original Sample
CeO_2	2.565	2.565	0.000
$KNaAlSiO_4$ (Nepheline)	0.000	19.853	20.898
$NiCr_2O_4$ (Spinel)	0.000	2.025	2.132
$KAlSiO_4$	0.000	1.772	1.866

Figure I.8. XRD Spectrum of CF 850 °C Heat-Treated Glass HAlG-04

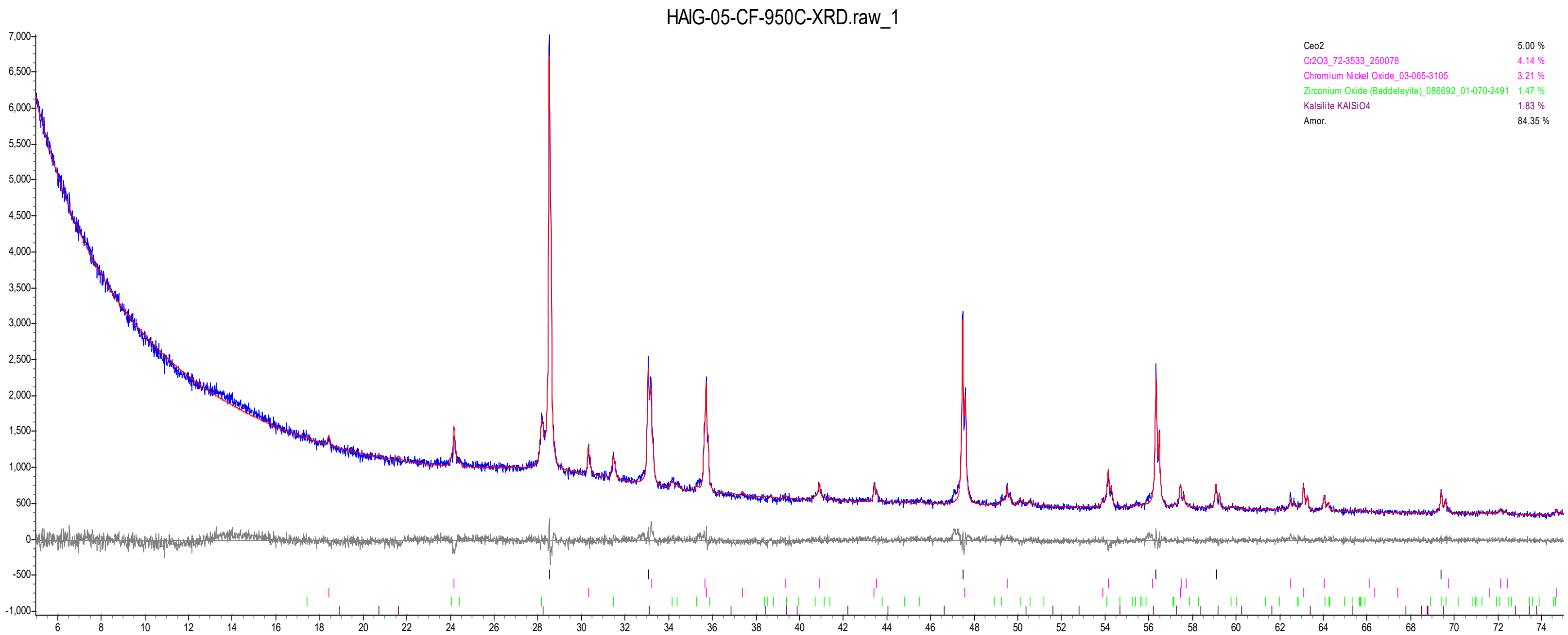

Phase Name	Wt% of Spiked	Wt% in Spiked Sample	Wt% in Original Sample
CeO_2	2.561	2.561	0.000
$KAlSiO_4$	0.000	1.251	1.316
Cr_2O_3	0.000	0.182	0.191
$NiCr_2O_4$ (Spinel)	0.000	2.485	2.616
ZrO_2	0.000	1.029	1.083

Figure I.9. XRD Spectrum of CF 950 °C Heat-Treated Glass HAlG-05

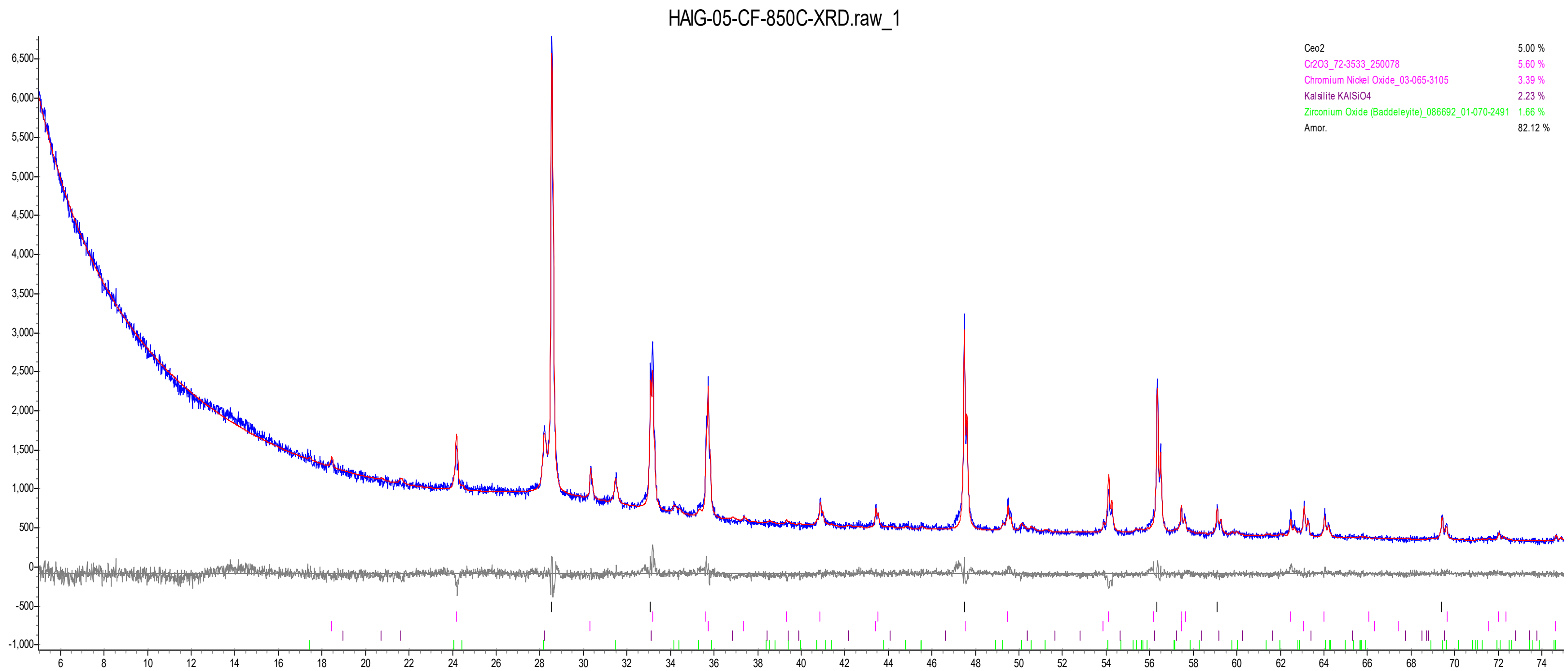

Phase Name	Wt% of Spiked	Wt% in Spiked Sample	Wt% in Original Sample
CeO_2	2.565	2.565	0.000
$KAlSiO_4$	0.000	1.629	1.714
Cr_2O_3	0.000	0.386	0.406
$NiCr_2O_4$ (Spinel)	0.000	2.995	3.152
ZrO_2	0.000	1.058	1.114

Figure I.10. XRD Spectrum of CF 850 °C Heat-Treated Glass HAlG-05

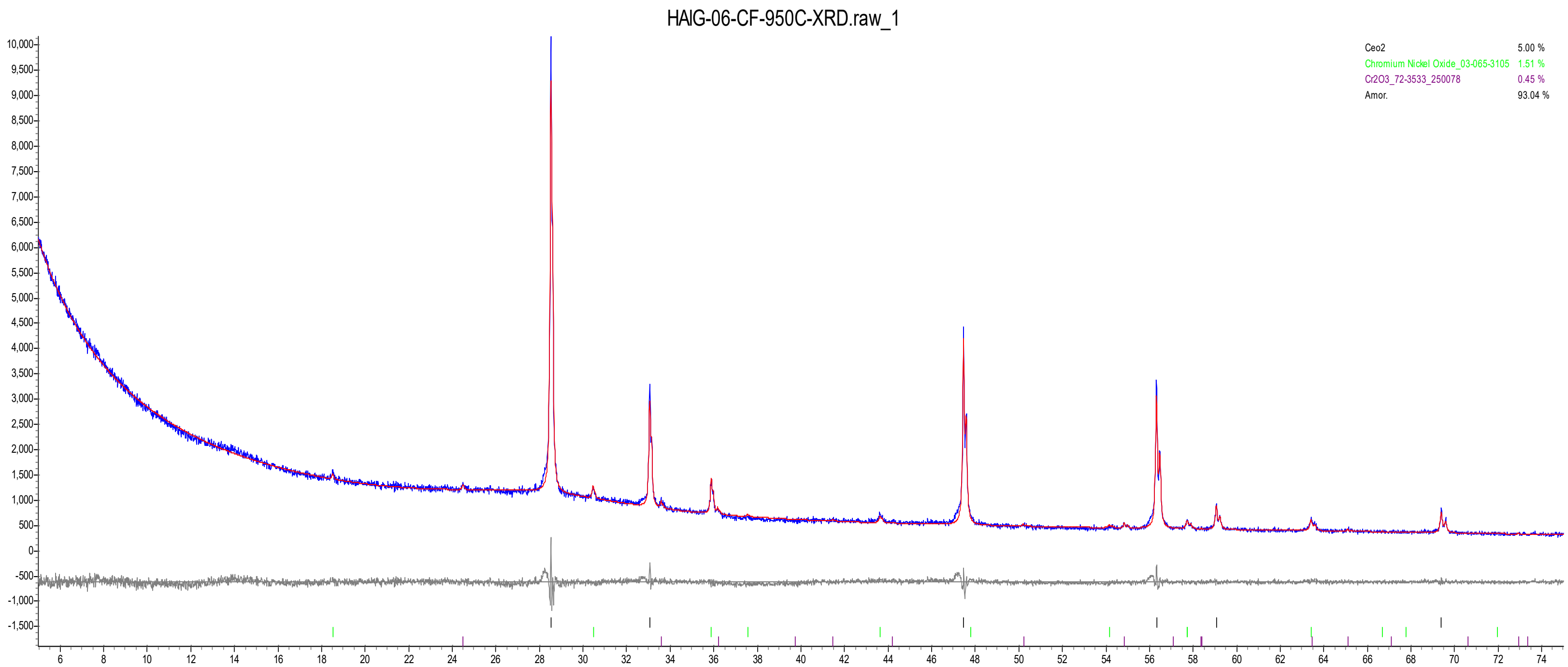

Phase Name	Wt% of Spiked	Wt% in Spiked Sample	Wt% in Original Sample
CeO_2	2.566	2.566	0.000
Cr_2O_3	0.000	0.575	0.606
$NiCr_2O_4$ (Spinel)	0.000	0.819	0.863

Figure I.11. XRD Spectrum of CF 950 °C Heat-Treated Glass HAlG-06

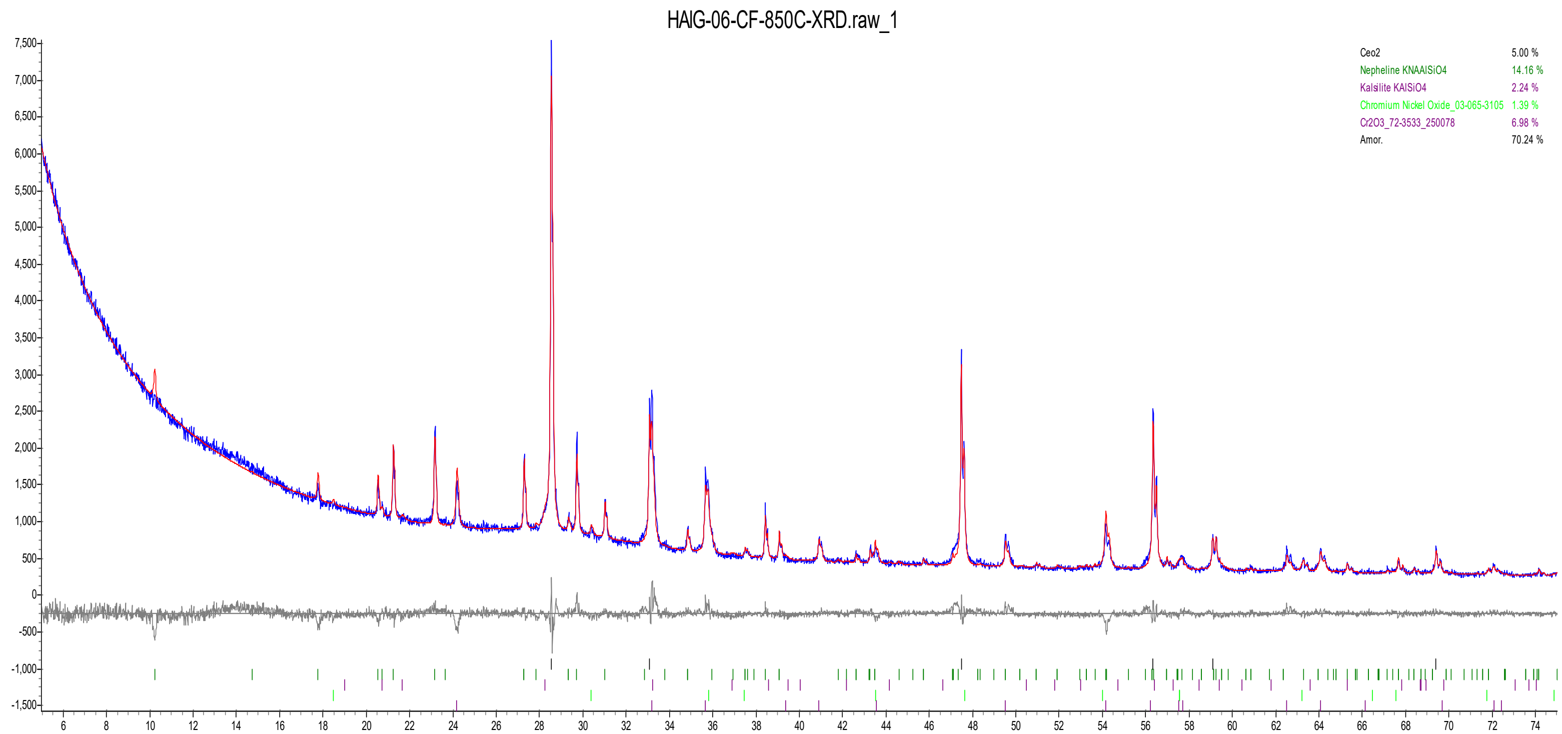

Phase Name	Wt% of Spiked	Wt% in Spiked Sample	Wt% in Original Sample
CeO_2	2.563	2.563	0.000
$KNaAlSiO_4$ (Nepheline)	0.000	8.065	8.489
Cr_2O_3	0.000	0.452	0.476
$KAlSiO_4$	0.000	3.178	3.345
$NiCr_2O_4$ (Spinel)	0.000	2.367	2.491

Figure I.12. XRD Spectrum of CF 850 °C Heat-Treated Glass HAlG-06

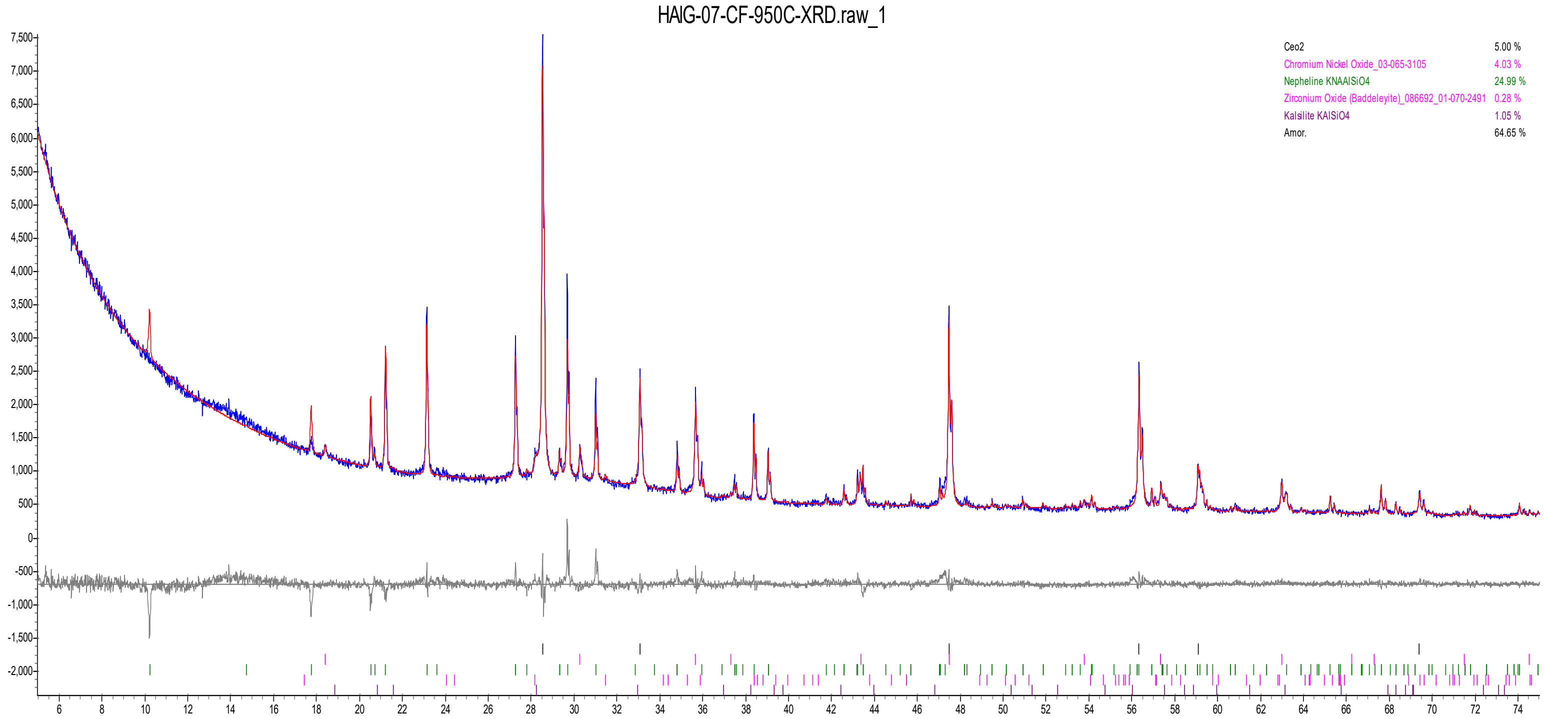

Phase Name	Wt% of Spiked	Wt% in Spiked Sample	Wt% in Original Sample
CeO_2	2.564	2.564	0.000
$KNaAlSiO_4$ (Nepheline)	0.000	12.760	13.431
$NiCr_2O_4$ (Spinel)	0.000	1.907	2.007
$KAlSiO_4$	0.000	1.641	1.728
ZrO_2	0.000	0.453	0.477

Figure I.13. XRD Spectrum of CF 950 °C Heat-Treated Glass HAlG-07

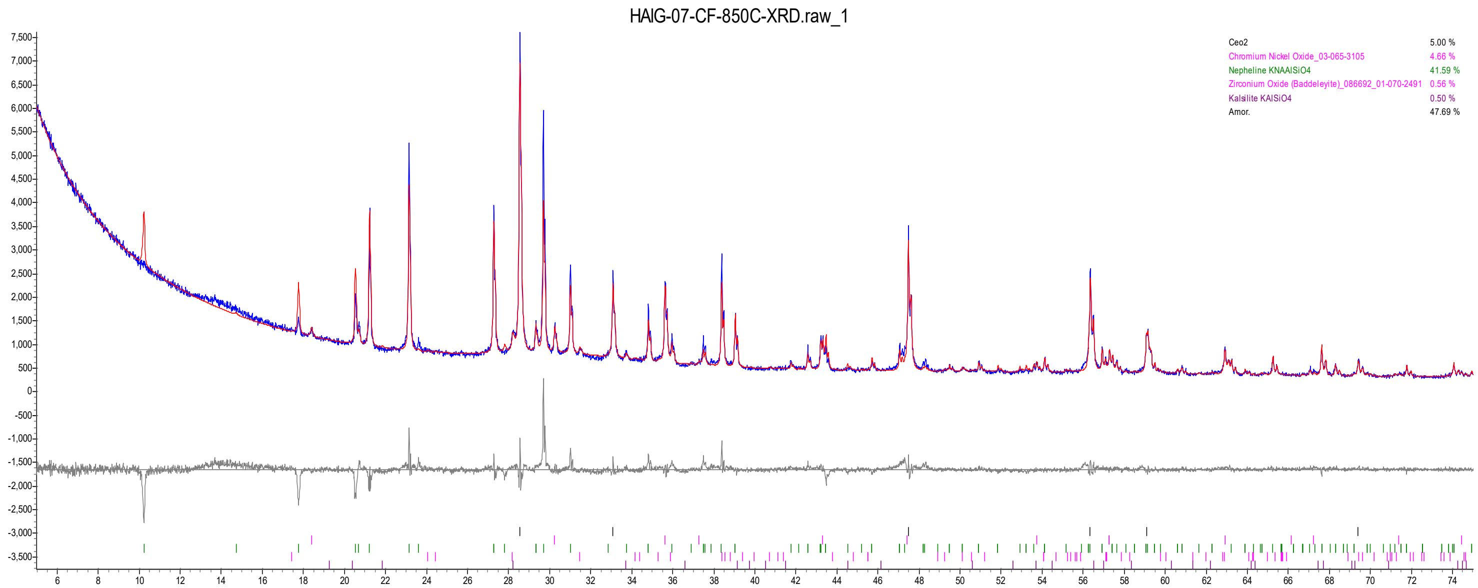

Phase Name	Wt% of Spiked	Wt% in Spiked Sample	Wt% in Original Sample
CeO_2	2.562	2.562	0.000
$KNaAlSiO_4$ (Nepheline)	0.000	23.134	24.350
$NiCr_2O_4$ (Spinel)	0.000	2.529	2.662
ZrO_2	0.000	0.420	0.443
$KAlSiO_4$	0.000	0.237	0.249

Figure I.14. XRD Spectrum of CF 850 °C Heat-Treated Glass HAlG-07

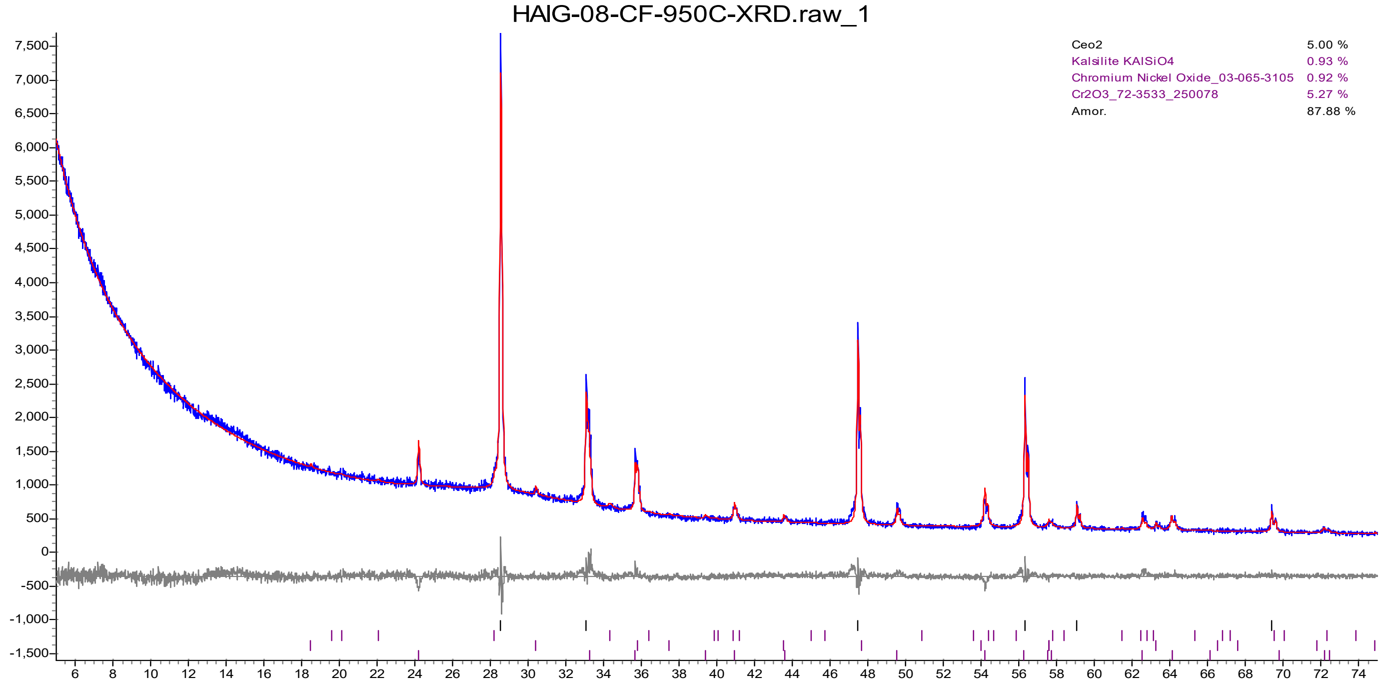

Phase Name	Wt% of Spiked	Wt% in Spiked Sample	Wt% in Original Sample
CeO_2	2.564	2.564	0.000
$KAlSiO_4$	0.000	2.307	2.428
Cr_2O_3	0.000	0.386	0.406
$NiCr_2O_4$ (Spinel)	0.000	1.817	1.912

Figure I.15. XRD Spectrum of CF 950 °C Heat-Treated Glass HAlG-08

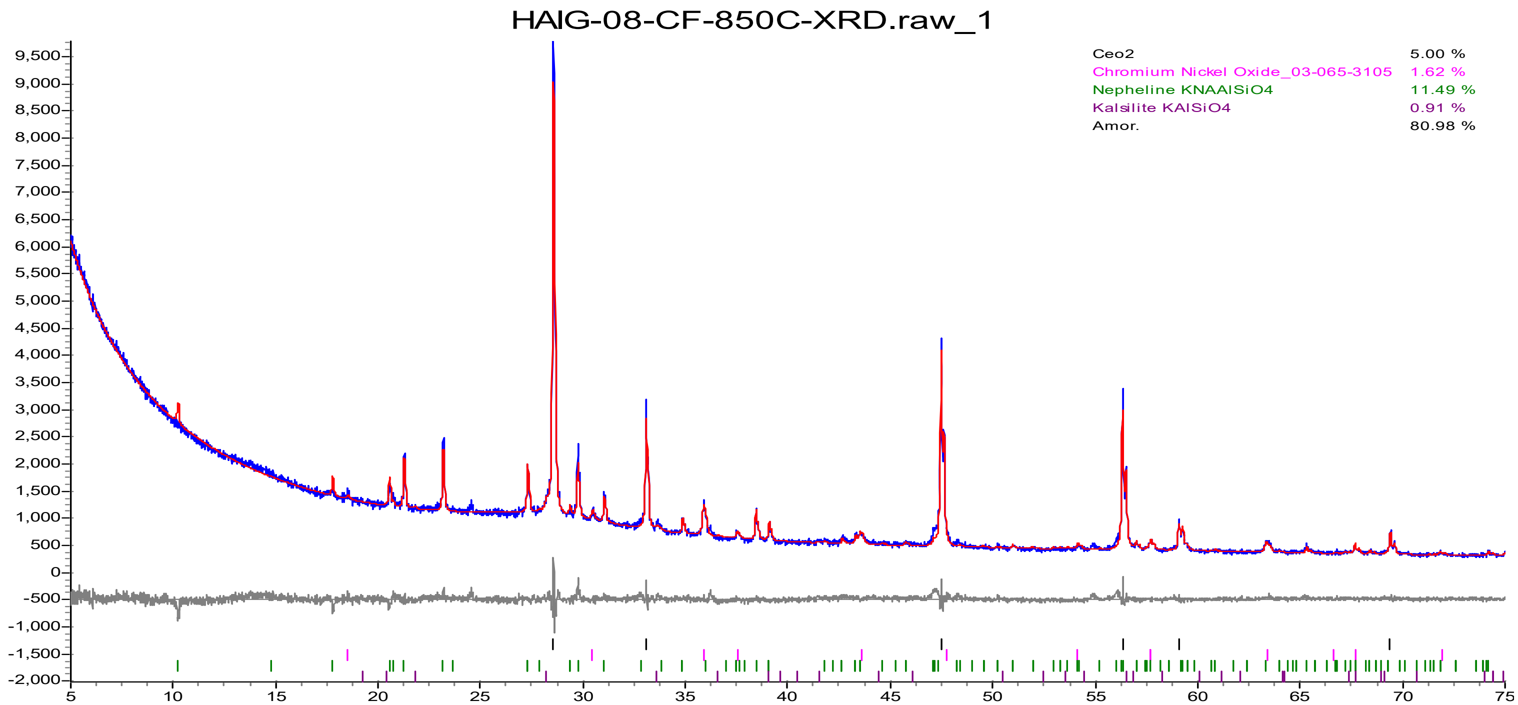

Phase Name	Wt% of Spiked	Wt% in Spiked Sample	Wt% in Original Sample
CeO_2	2.562	2.562	0.000
$KNaAlSiO_4$ (Nepheline)	0.000	6.372	6.707
$NiCr_2O_4$ (Spinel)	0.000	0.943	0.993
$KAlSiO_4$	0.000	0.814	0.857

Figure I.16. XRD Spectrum of CF 850 °C Heat-Treated Glass HAlG-08

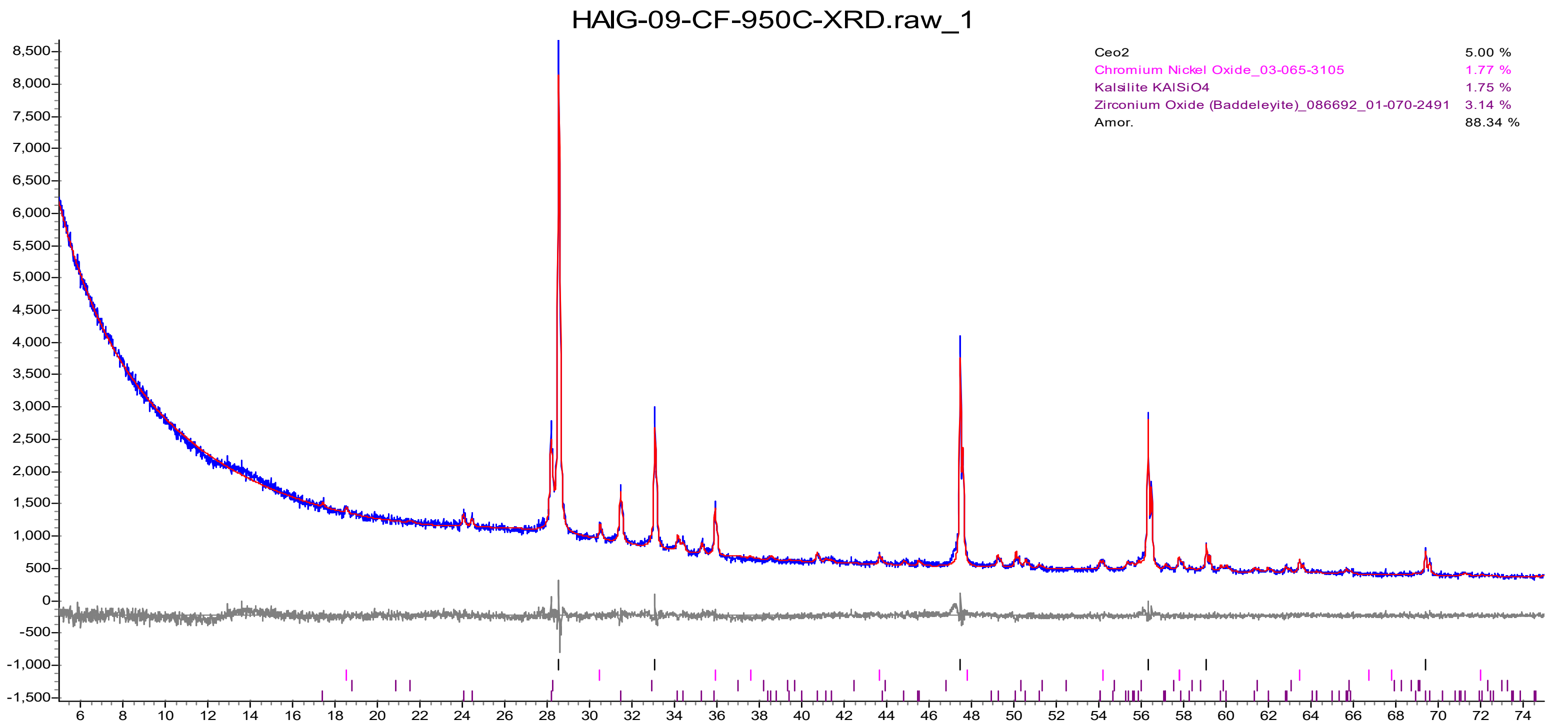

Phase Name	Wt% of Spiked	Wt% in Spiked Sample	Wt% in Original Sample
CeO_2	2.564	2.564	0.000
$NiCr_2O_4$ (Spinel)	0.000	1.014	1.067
$KAlSiO_4$	0.000	1.329	1.399
ZrO_2	0.000	1.712	1.802

Figure I.17. XRD Spectrum of CF 950 °C Heat-Treated Glass HAlG-09

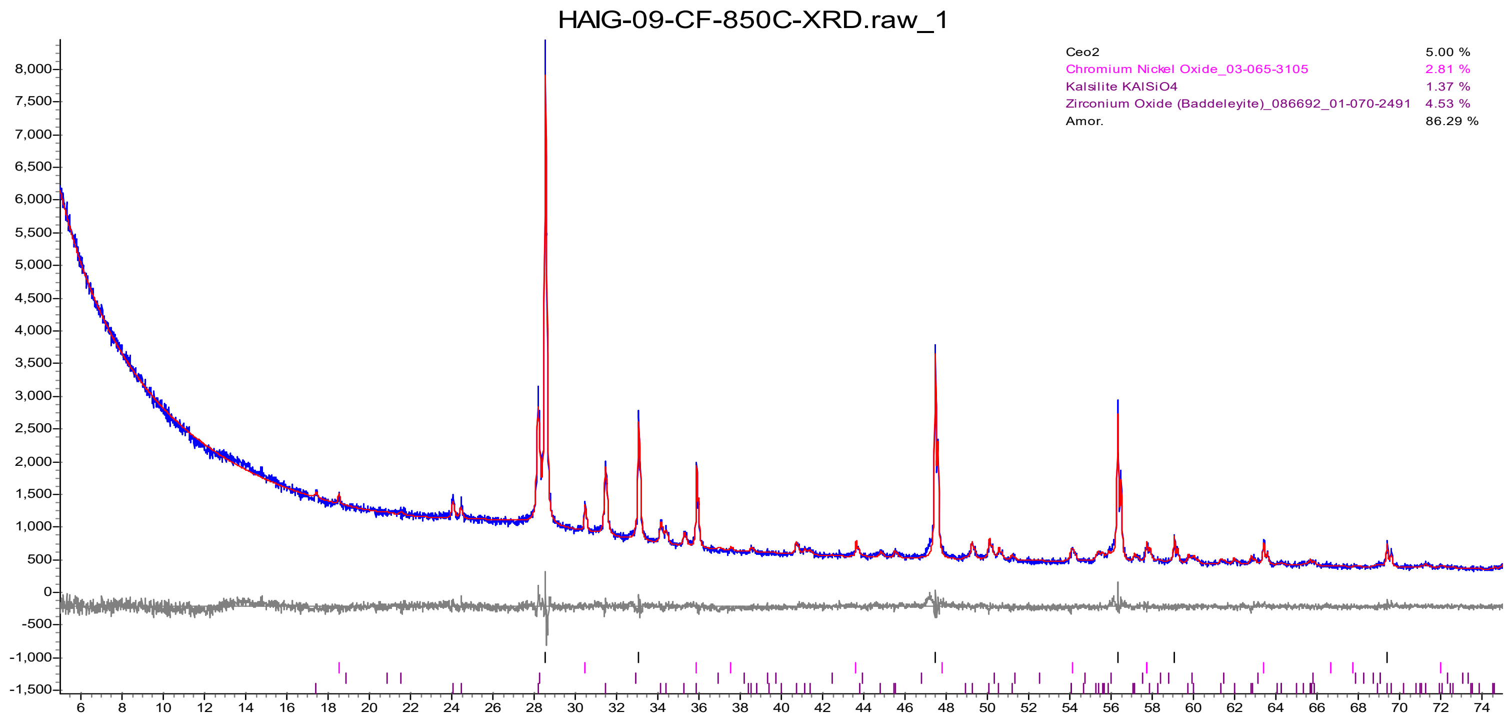

Phase Name	Wt% of Spiked	Wt% in Spiked Sample	Wt% in Original Sample
CeO_2	2.562	2.562	0.000
$NiCr_2O_4$ (Spinel)	0.000	1.589	1.672
$KAlSiO_4$	0.000	1.459	1.536
ZrO_2	0.000	2.534	2.667

Figure I.18. XRD Spectrum of CF 850 °C Heat-Treated Glass HAlG-09

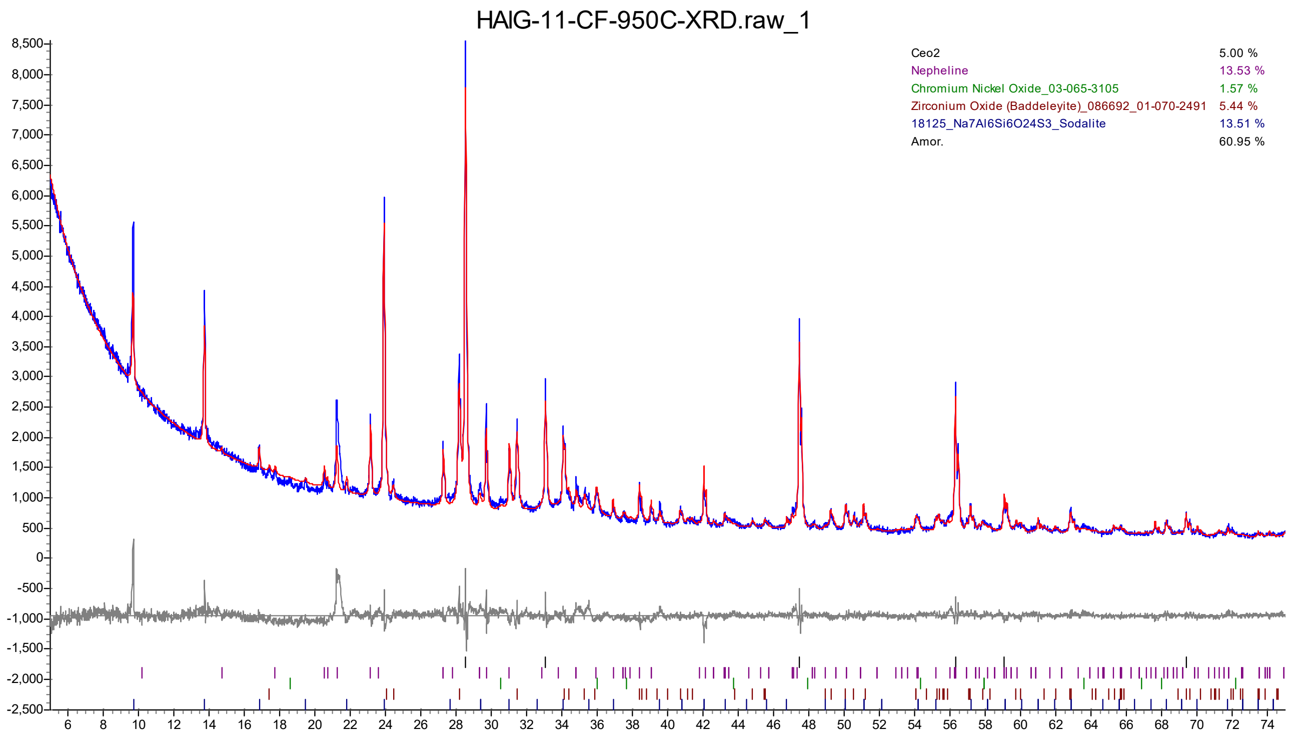

Phase Name	Wt% of Spiked	Wt% in Spiked Sample	Wt% in Original Sample
CeO_2	2.563	2.563	0.000
$Na_7Al_6Si_6O_{24}S_3$	0.000	7.703	8.108
$KNaAlSiO_4$ (Nepheline)	0.000	7.425	7.815
$NiCr_2O_4$ (Spinel)	0.000	0.836	0.880
ZrO_2	0.000	2.686	2.828

Figure I.19. XRD Spectrum of CF 950 °C Heat-Treated Glass HAlG-11

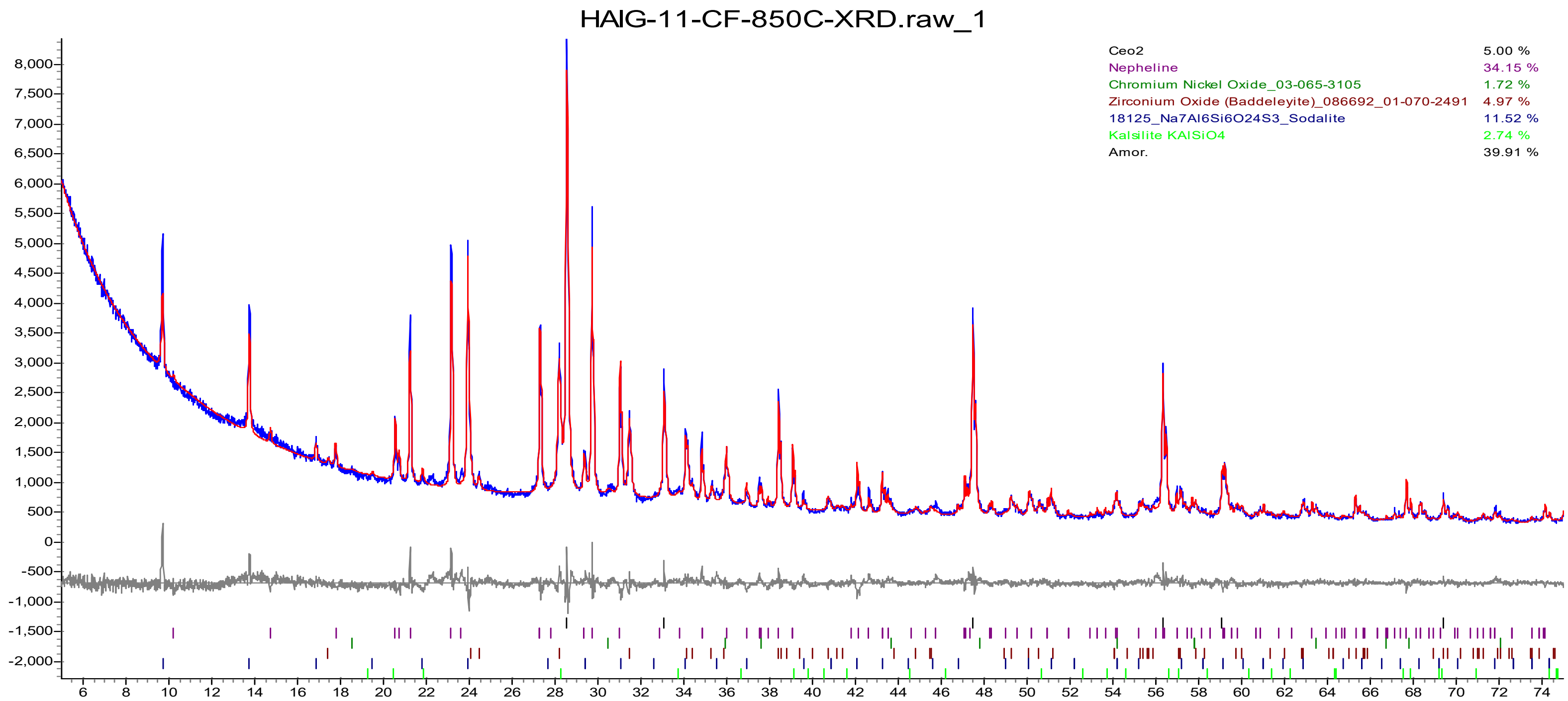

Phase Name	Wt% of Spiked	Wt% in Spiked Sample	Wt% in Original Sample
CeO_2	2.565	2.565	0.000
$KNaAlSiO_4$ (Nepheline)	0.000	18.190	19.147
$Na_7Al_6Si_6O_{24}S_3$	0.000	6.208	6.535
$KAlSiO_4$	0.000	2.031	2.138
$NiCr_2O_4$ (Spinel)	0.000	1.024	1.077
ZrO_2	0.000	2.801	2.949

Figure I.20. XRD Spectrum of CF 850 °C Heat-Treated Glass HAlG-11

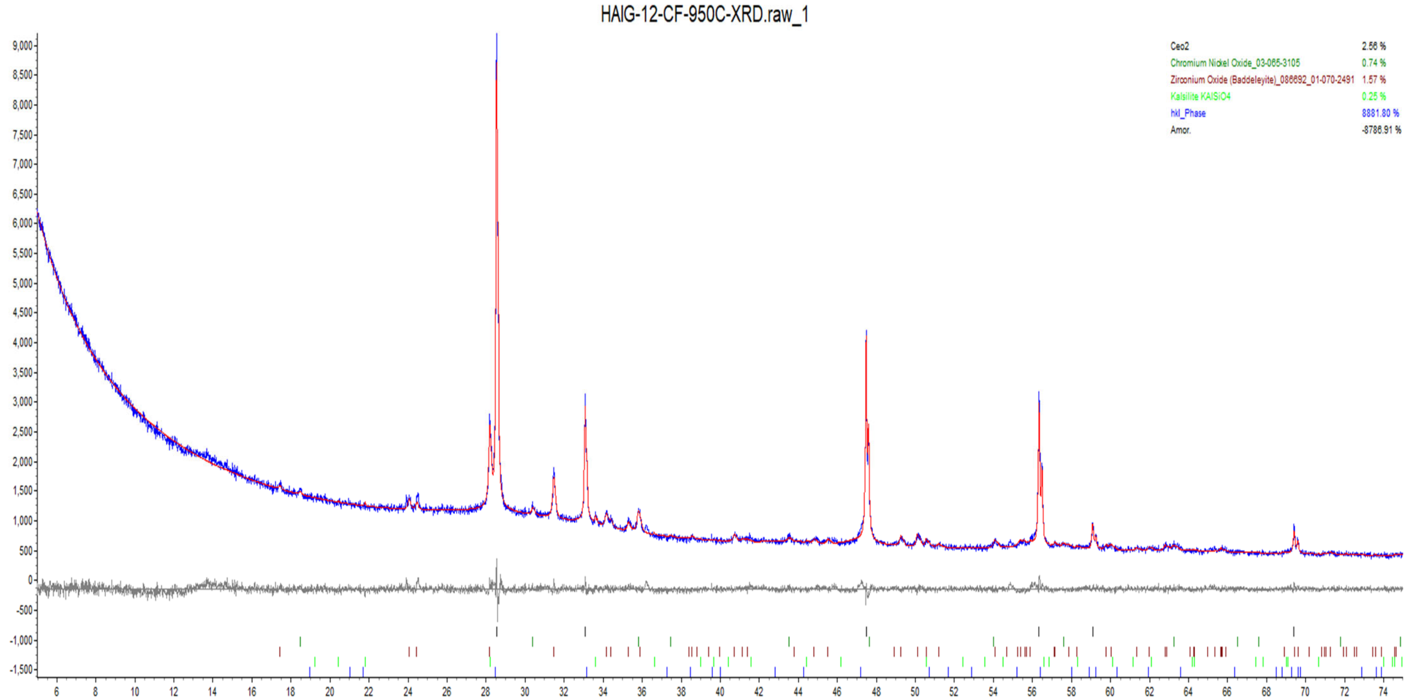

Phase Name	Wt% of Spiked	Wt% in Spiked Sample	Wt% in Original Sample
CeO_2	2.562	2.562	0.000
$KAlSiO_4$	0.000	1.851	1.949
$NiCr_2O_4$ (Spinel)	0.000	0.799	0.841
ZrO_2	0.000	1.570	1.653

Figure I.21. XRD Spectrum of CF 950 °C Heat-Treated Glass HAlG-12

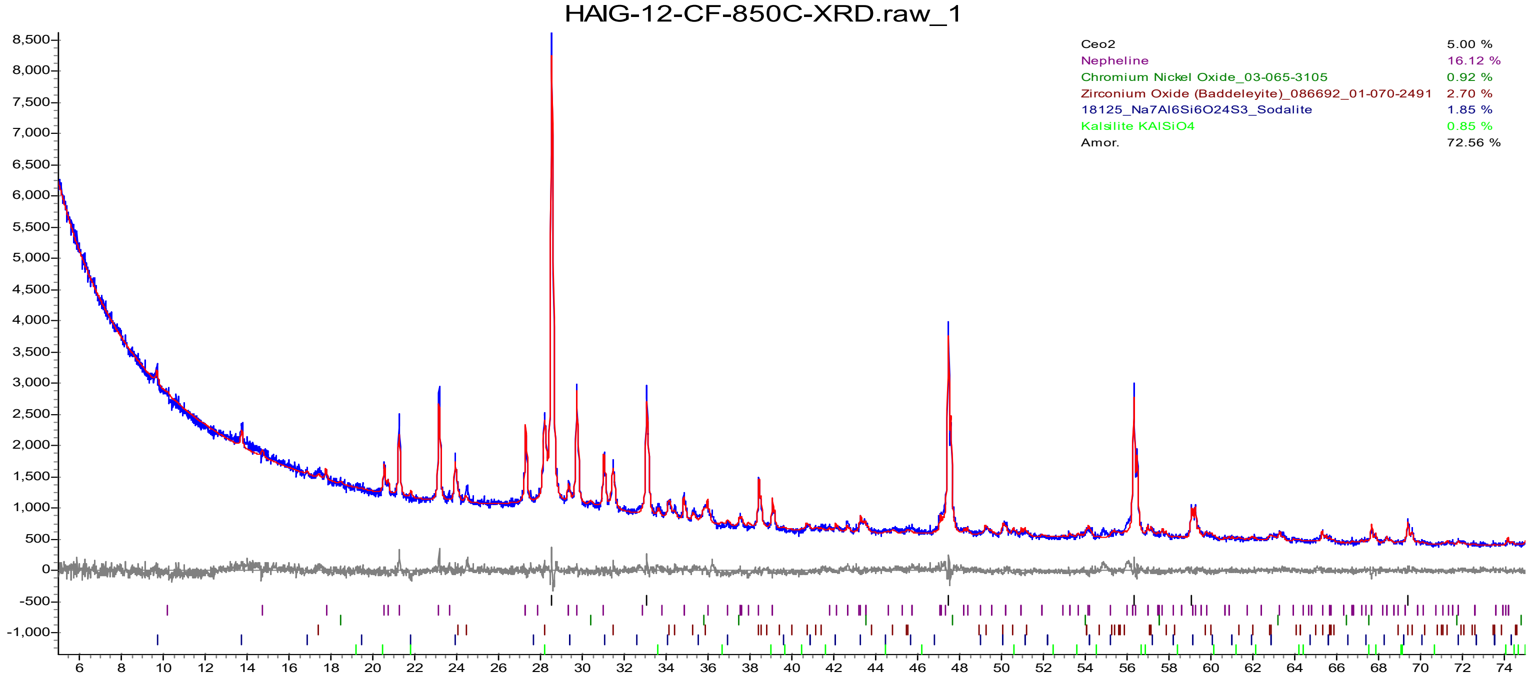

Phase Name	Wt% of Spiked	Wt% in Spiked Sample	Wt% in Original Sample
CeO_2	2.562	2.562	0.000
$KNaAlSiO_4$ (Nepheline)	0.000	9.767	10.280
$Na_7Al_6Si_6O_{24}S_3$	0.000	1.055	1.110
$KAlSiO_4$	0.000	0.953	1.003
$NiCr_2O_4$ (Spinel)	0.000	0.756	0.796
ZrO_2	0.000	1.545	1.626

Figure I.22. XRD Spectrum of CF 850 °C Heat-Treated Glass HAlG-12

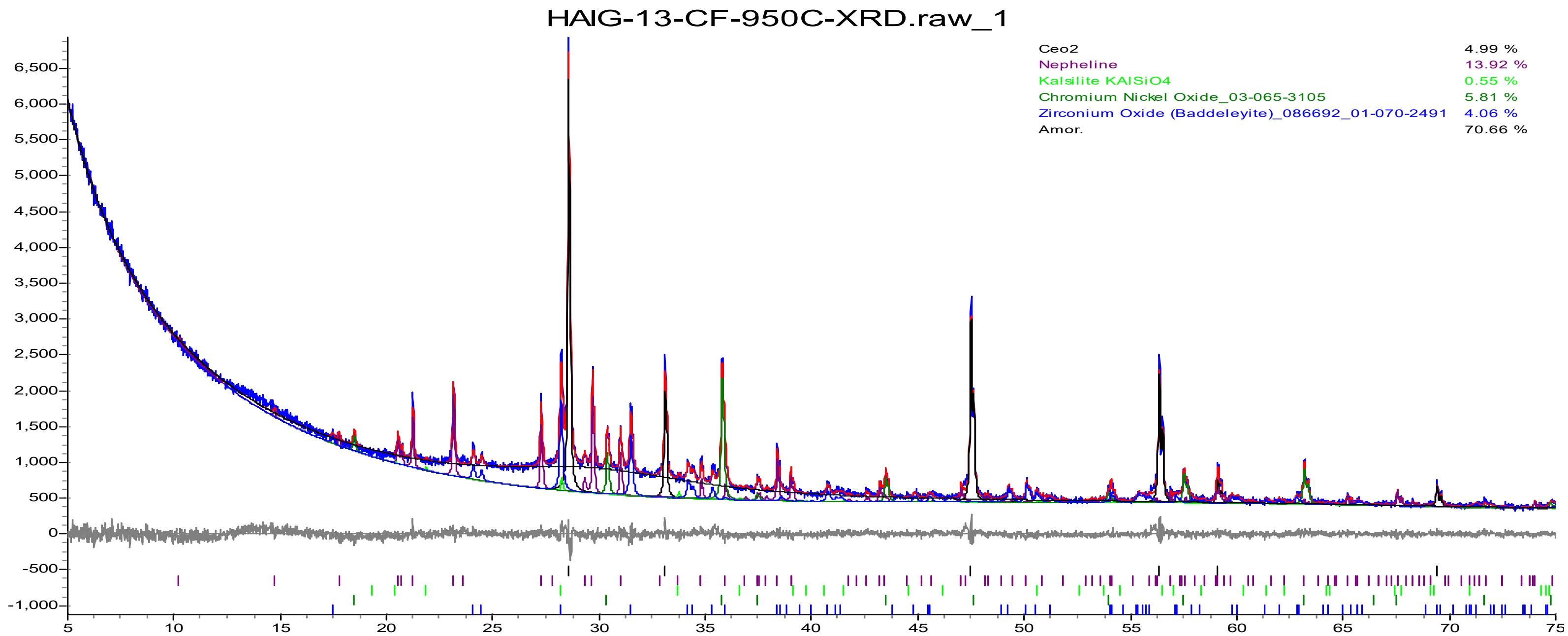

Phase Name	Wt% of Spiked	Wt% in Spiked Sample	Wt% in Original Sample
CeO_2	2.561	2.561	0.000
$KNaAlSiO_4$ (Nepheline)	0.000	7.878	8.293
$NiCr_2O_4$ (Spinel)	0.000	3.125	3.290
ZrO_2	0.000	2.257	2.376
$KAlSiO_4$	0.000	0.436	0.459

Figure I.23. XRD Spectrum of CF 950 °C Heat-Treated Glass HAlG-13

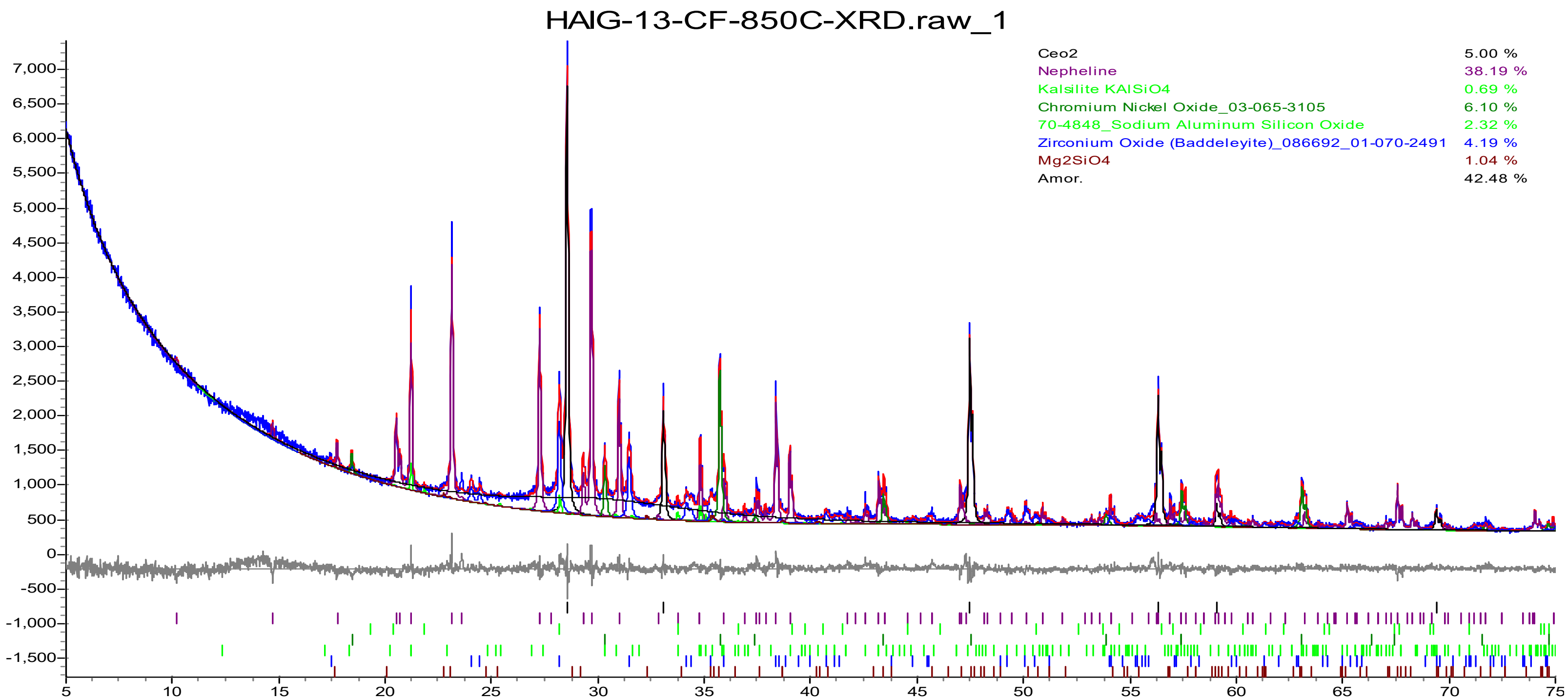

Phase Name	Wt% of Spiked	Wt% in Spiked Sample	Wt% in Original Sample
CeO_2	2.564	2.564	0.000
Nepheline	0.000	21.318	22.440
$NiCr_2O_4$ (Spinel)	0.000	3.119	3.283
ZrO_2	0.000	2.387	2.512
$KAlSiO_4$	0.000	1.639	1.726
Mg_2SiO_4	0.000	0.400	0.422

Figure I.24. XRD Spectrum of CF 850 °C Heat-Treated Glass HAlG-13

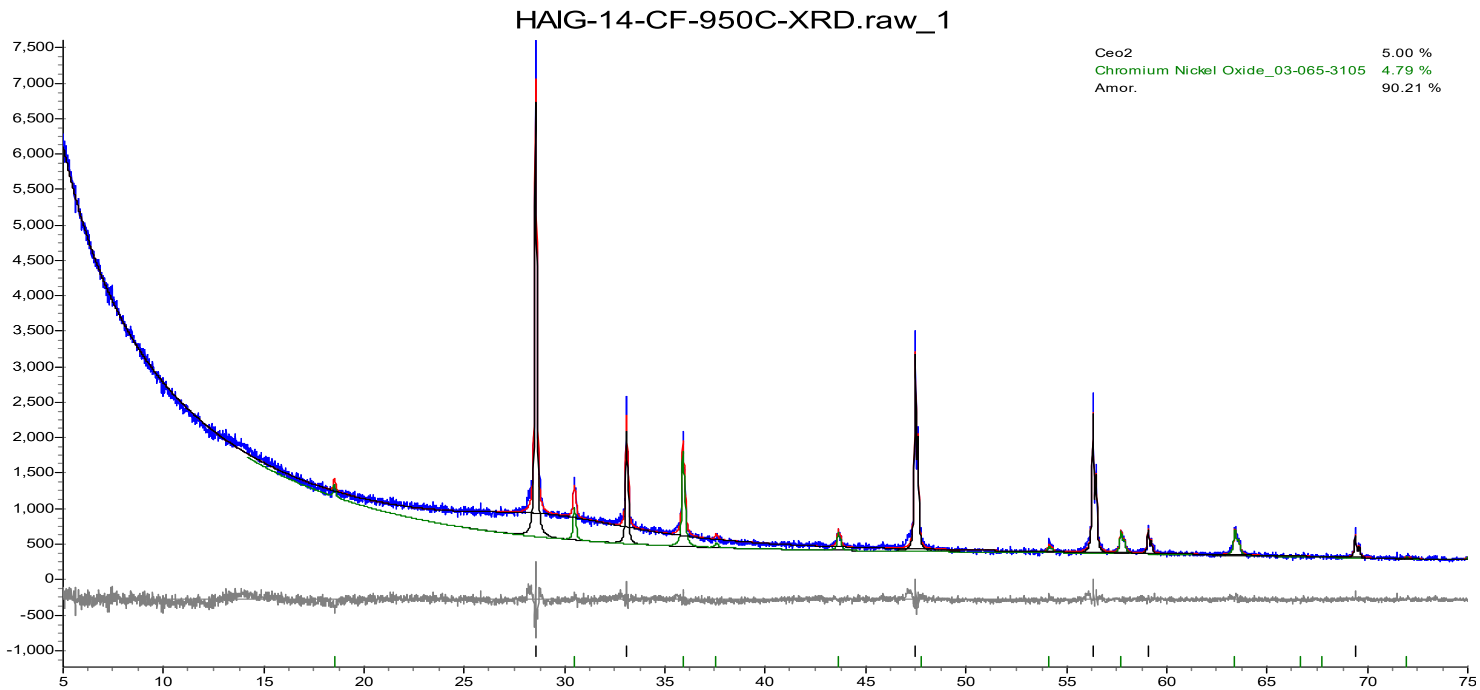

Phase Name	Wt% of Spiked	Wt% in Spiked Sample	Wt% in Original Sample
CeO_2	2.563	2.563	0.000
$NiCr_2O_4$ (Spinel)	0.000	2.619	2.757

Figure I.25. XRD Spectrum of CF 950 °C Heat-Treated Glass HAlG-14

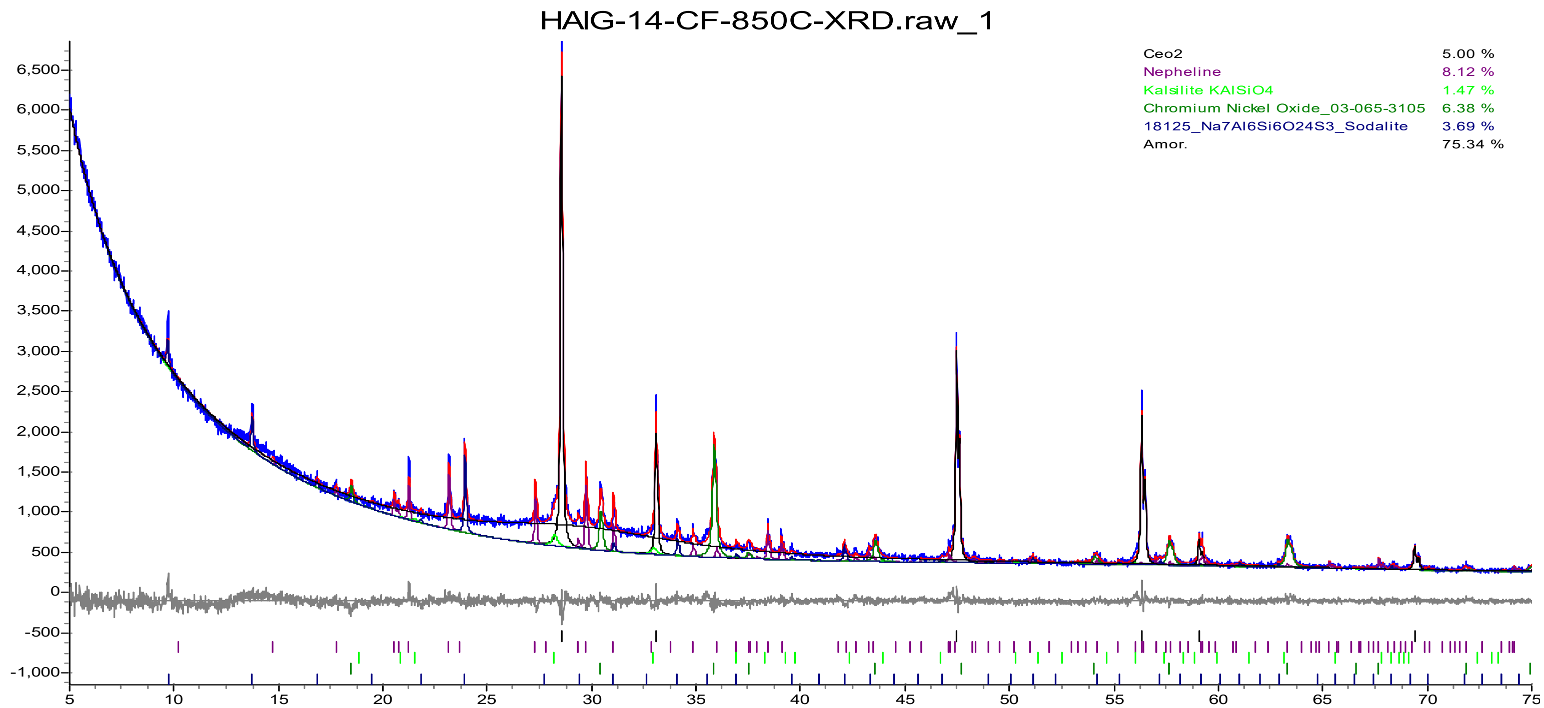

Phase Name	Wt% of Spiked	Wt% in Spiked Sample	Wt% in Original Sample
CeO_2	2.564	2.564	0.000
$KNaAlSiO_4$ (Nepheline)	0.000	4.893	5.150
$NiCr_2O_4$ (Spinel)	0.000	3.437	3.618
$Na_7Al_6Si_6O_{24}S_3$	0.000	1.924	2.025
$KAlSiO_4$	0.000	0.510	0.537

Figure I.26. XRD Spectrum of CF 850 °C Heat-Treated Glass HAlG-14

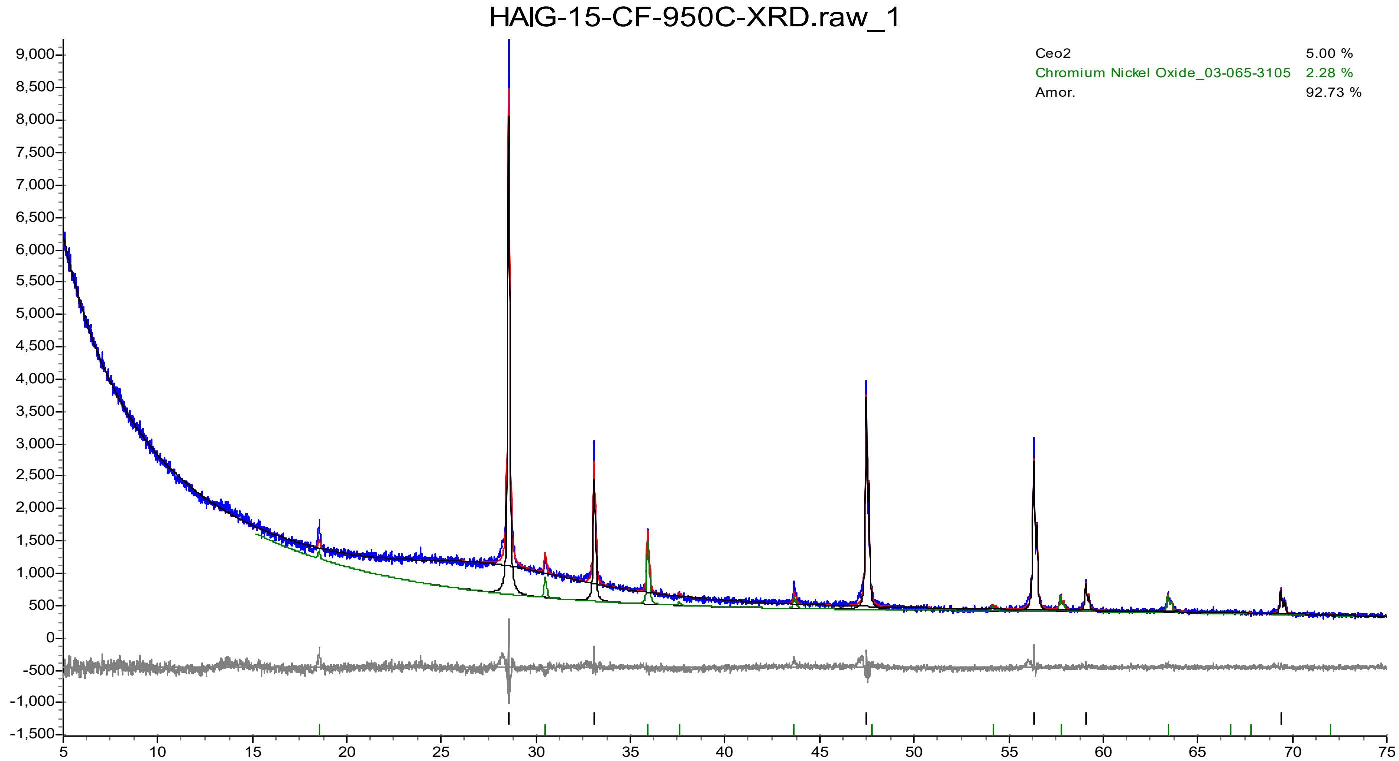

Phase Name	Wt% of Spiked	Wt% in Spiked Sample	Wt% in Original Sample
CeO_2	2.561	2.561	0.000
$NiCr_2O_4$ (Spinel)	0.000	1.268	1.335

Figure I.27. XRD Spectrum of CF 950 °C Heat-Treated Glass HAlG-15

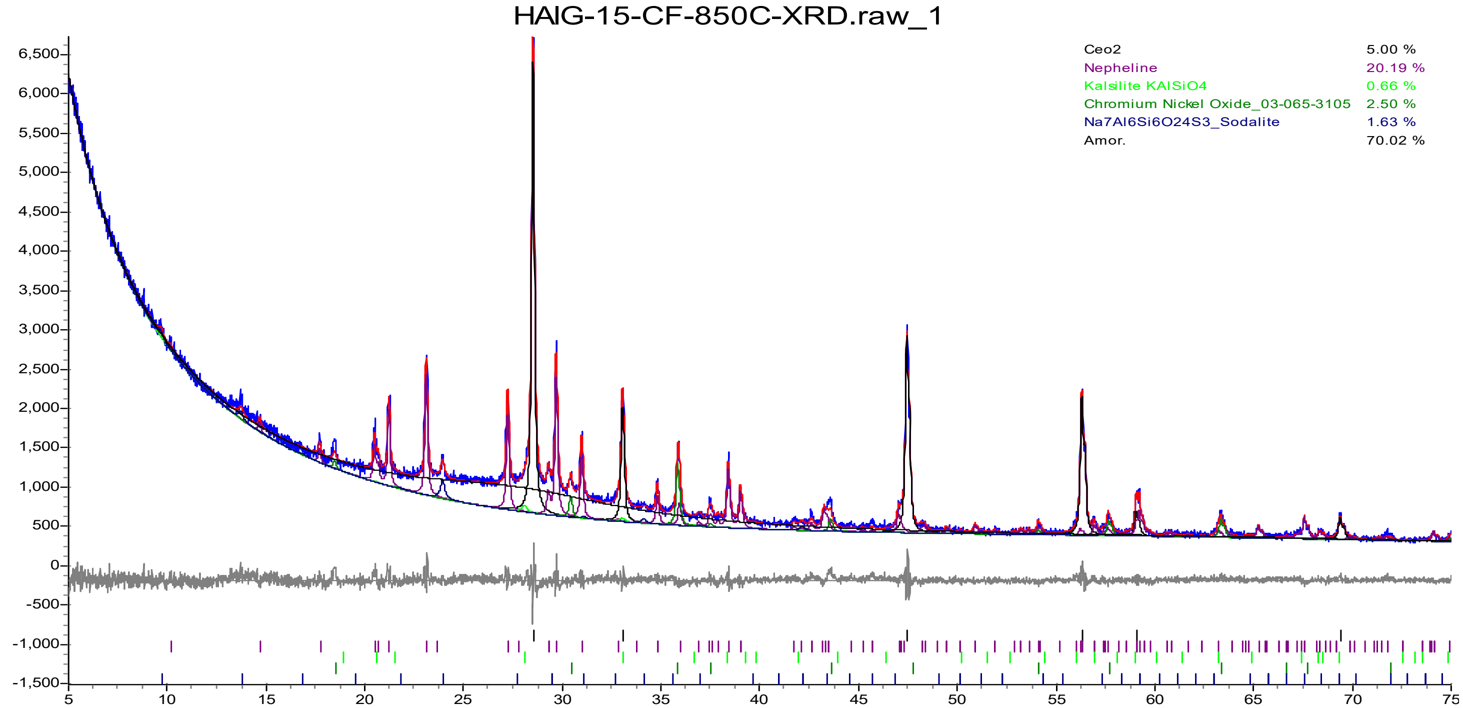

Phase Name	Wt% of Spiked	Wt% in Spiked Sample	Wt% in Original Sample
CeO_2	2.563	2.563	0.000
$KNaAlSiO_4$ (Nepheline)	0.000	11.849	12.473
$NiCr_2O_4$ (Spinel)	0.000	1.404	1.478
$Na_7Al_6Si_6O_{24}S_3$	0.000	0.868	0.913
$KAlSiO_4$	0.000	0.135	0.142

Figure I.28. XRD Spectrum of CF 850 °C Heat-Treated Glass HAlG-15

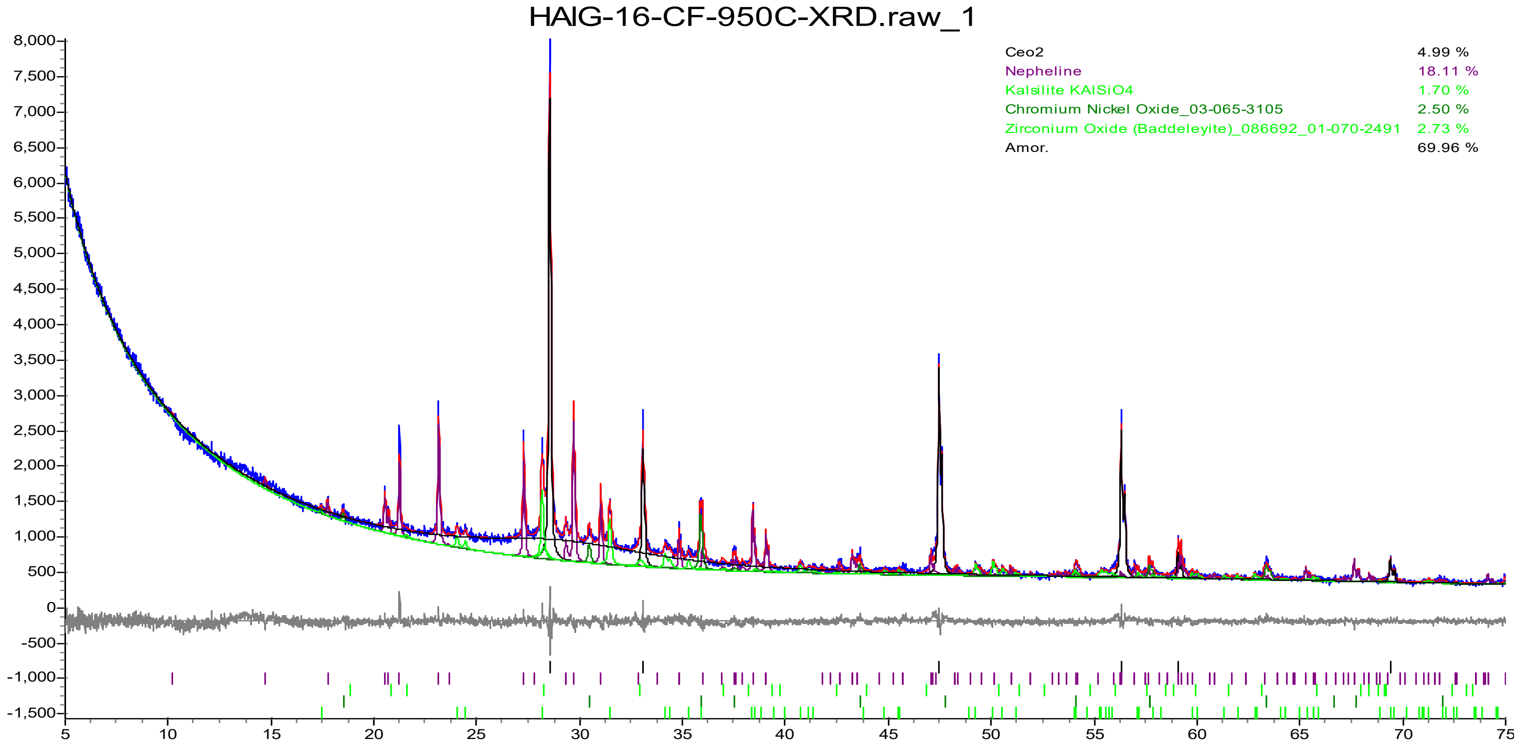

Phase Name	Wt% of Spiked	Wt% in Spiked Sample	Wt% in Original Sample
CeO_2	2.560	2.560	0.000
$KNaAlSiO_4$ (Nepheline)	0.000	10.695	11.257
$NiCr_2O_4$ (Spinel)	0.000	1.414	1.489
$KAlSiO_4$	0.000	0.864	0.909
ZrO_2	0.000	1.443	1.519

Figure I.29. XRD Spectrum of CF 950 °C Heat-Treated Glass HAlG-16

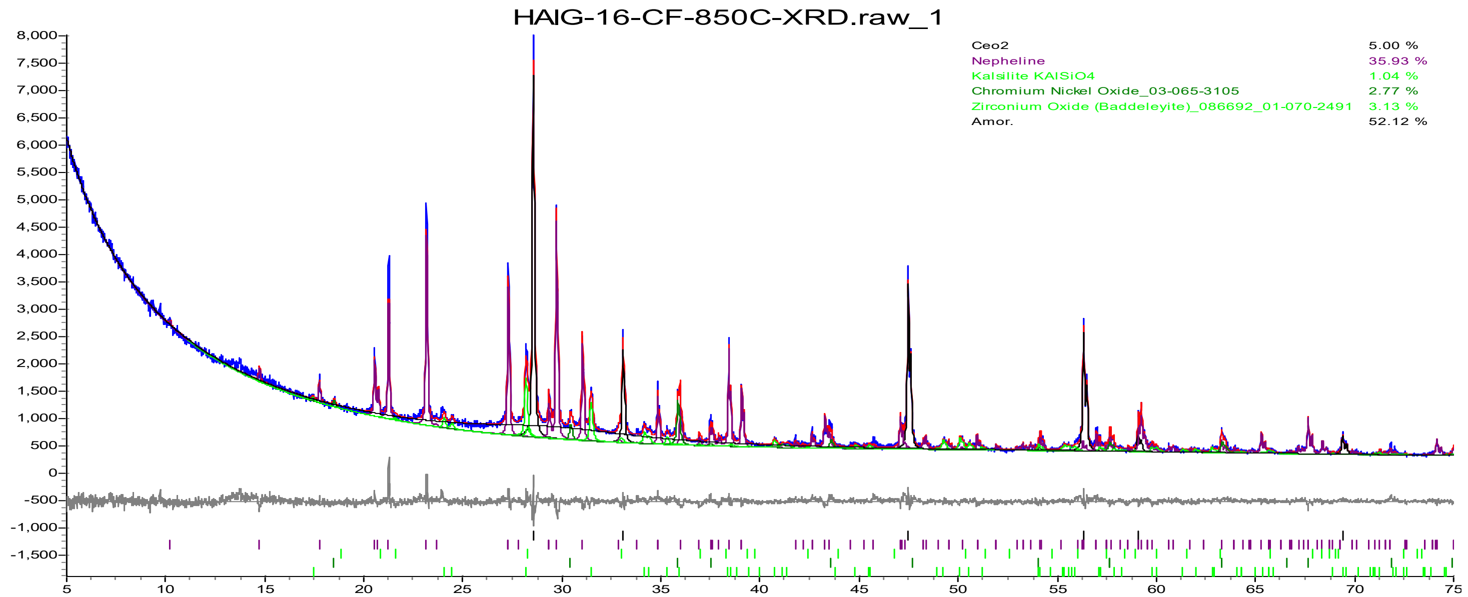

Phase Name	Wt% of Spiked	Wt% in Spiked Sample	Wt% in Original Sample
CeO_2	2.565	2.565	0.000
$KNaAlSiO_4$ (Nepheline)	0.000	19.404	20.426
$NiCr_2O_4$ (Spinel)	0.000	1.319	1.388
$KAlSiO_4$	0.000	1.334	1.404
ZrO_2	0.000	1.757	1.850

Figure I.30. XRD Spectrum of CF 850 °C Heat-Treated Glass HAlG-16

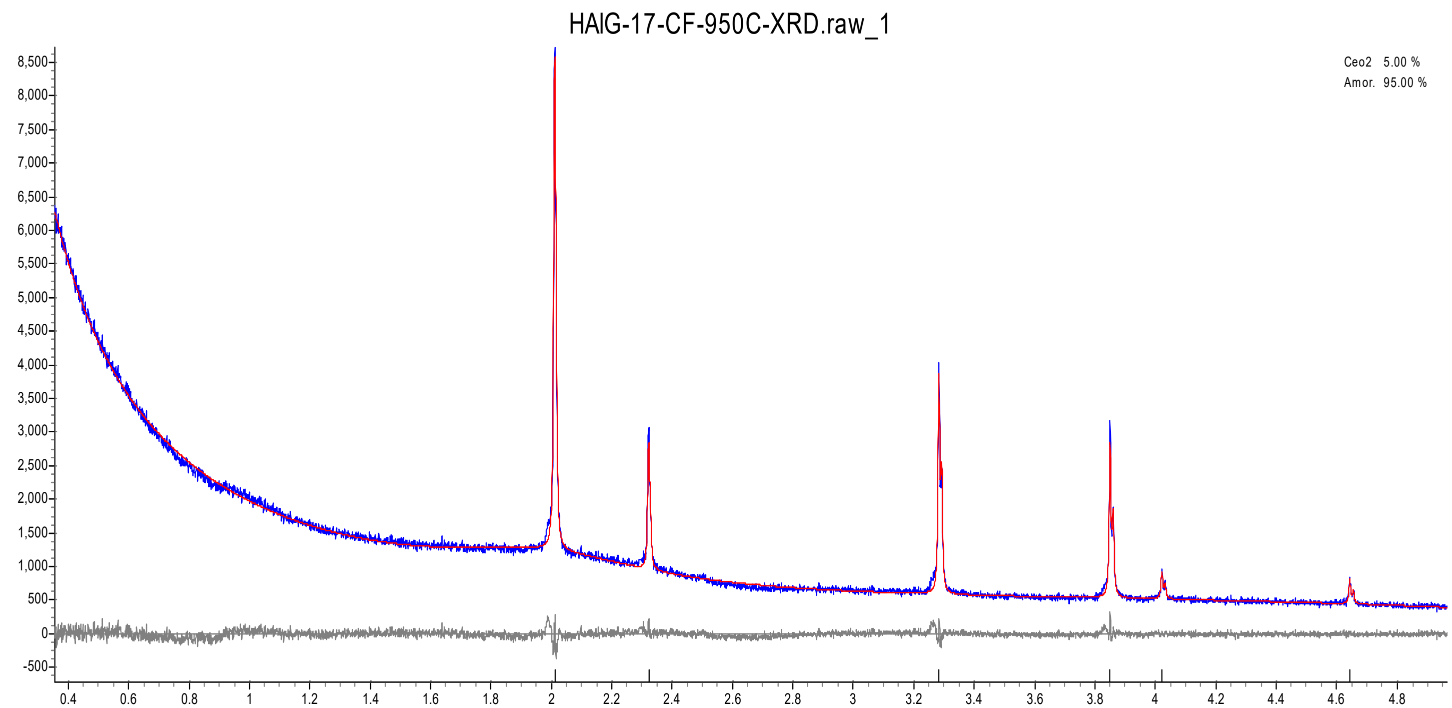

Figure I.31. XRD Spectrum of CF 950 °C Heat-Treated Glass HAlG-17

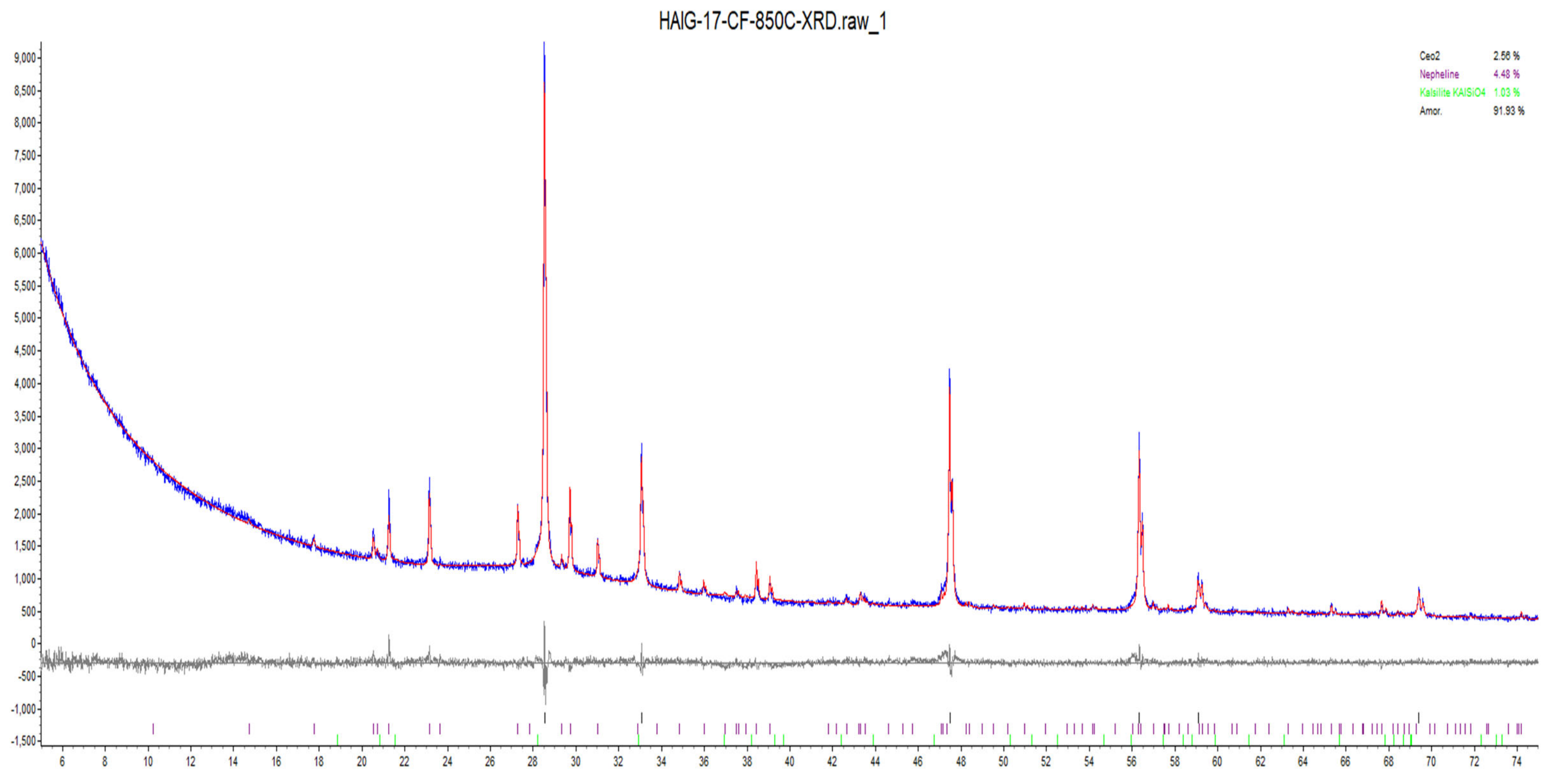

Phase Name	Wt% of Spiked	Wt% in Spiked Sample	Wt% in Original Sample
CeO_2	2.563	2.563	0.000
$KNaAlSiO_4$ (Nepheline)	0.000	5.321	5.601
$KAlSiO_4$	0.000	1.115	1.173

Figure I.32. XRD Spectrum of CF 850 °C Heat-Treated Glass HAlG-17

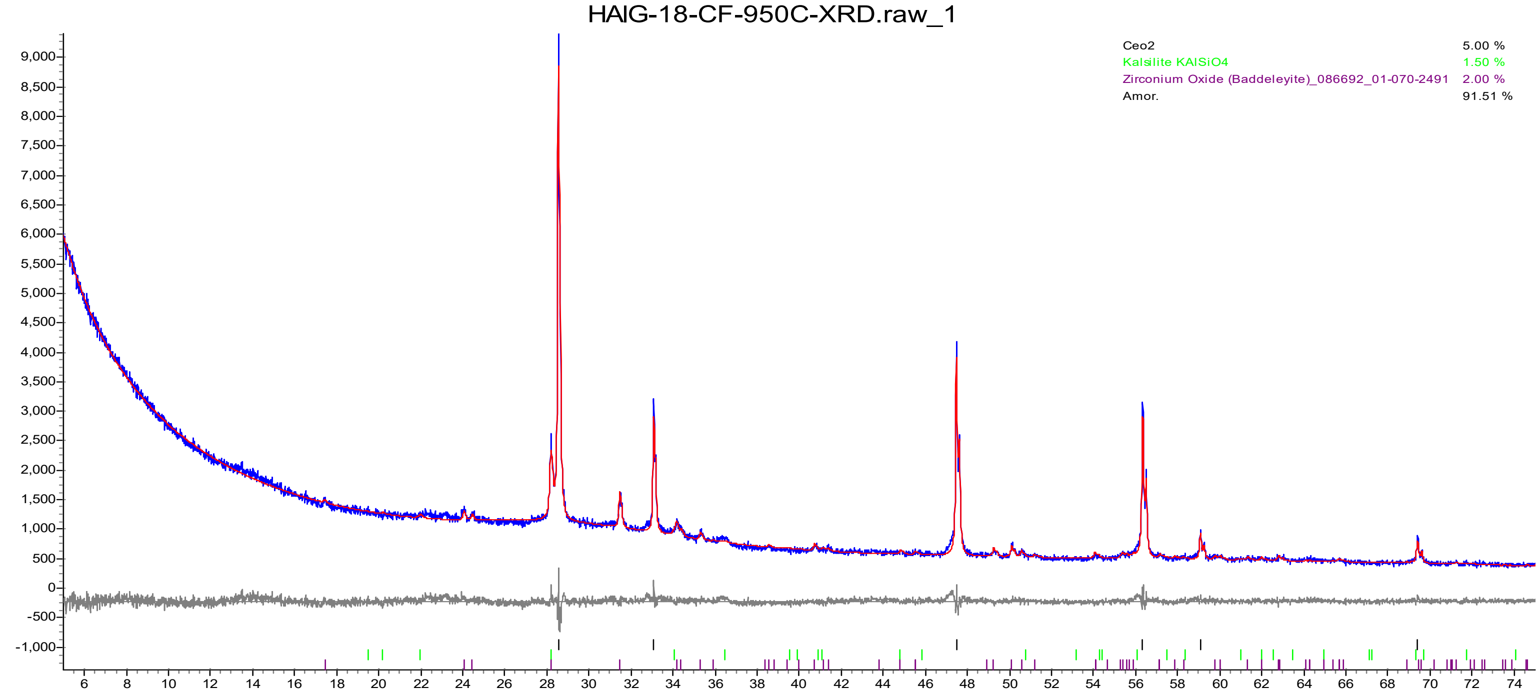

Phase Name	Wt% of Spiked	Wt% in Spiked Sample	Wt% in Original Sample
CeO_2	2.564	2.564	0.000
ZrO_2	0.000	1.283	1.351

Figure I.33. XRD Spectrum of CF 950 °C Heat-Treated Glass HAlG-18

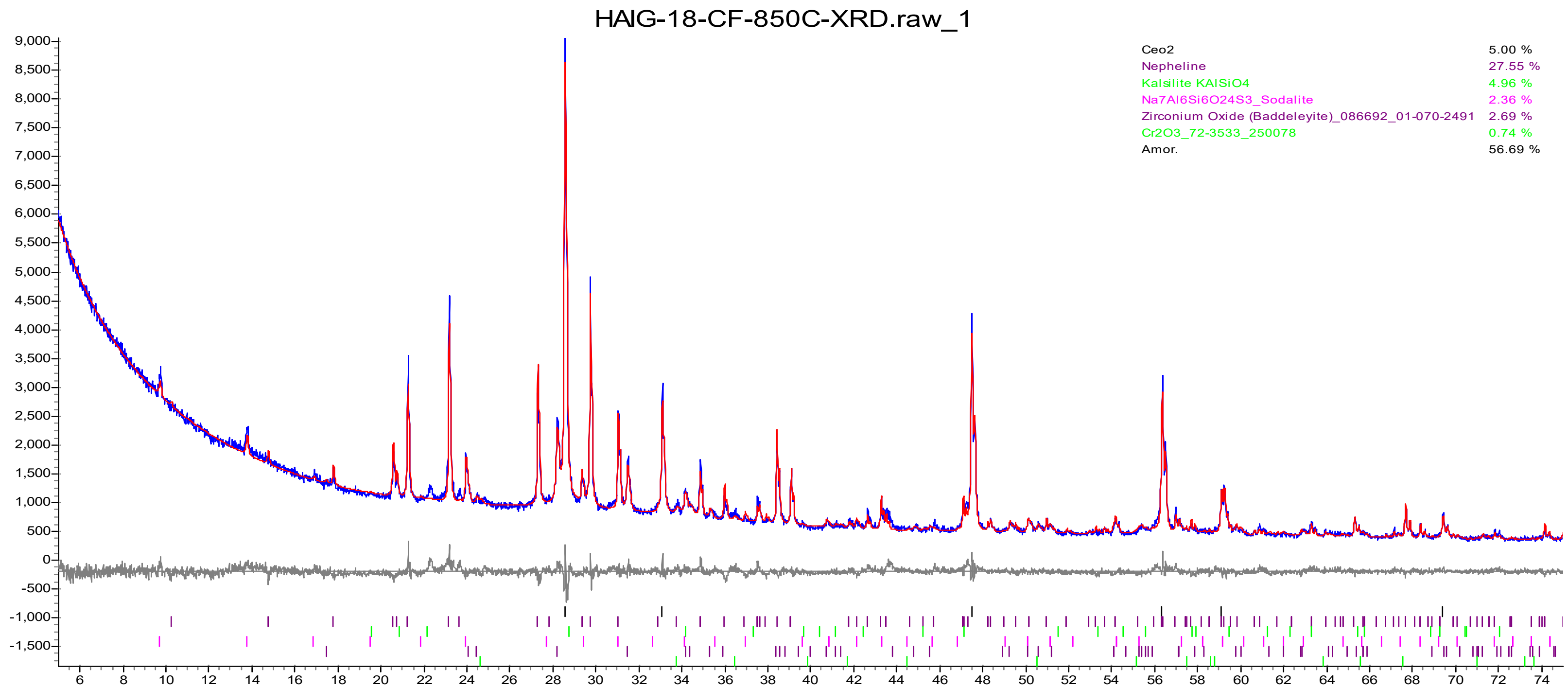

Phase Name	Wt% of Spiked	Wt% in Spiked Sample	Wt% in Original Sample
CeO_2	2.566	2.566	0.000
$KNaAlSiO_4$ (Nepheline)	0.000	15.277	16.082
$Na_7Al_6Si_6O_{24}S_3$	0.000	1.360	1.432
ZrO_2	0.000	1.425	1.500

Figure I.34. XRD Spectrum of CF 850 °C Heat-Treated Glass HAlG-18

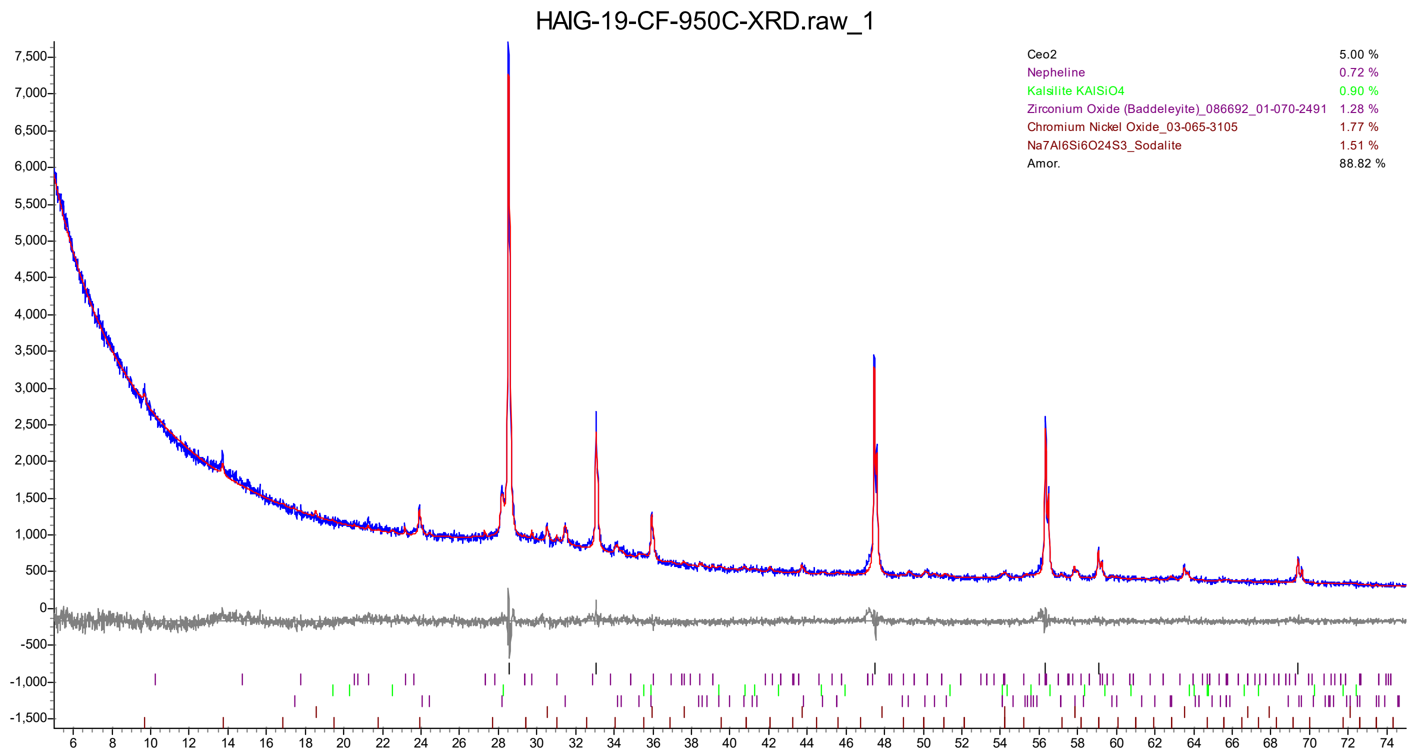

Phase Name	Wt% of Spiked	Wt% in Spiked Sample	Wt% in Original Sample
CeO_2	2.564	2.564	0.000
$Na_7Al_6Si_6O_{24}S_3$	0.000	0.721	0.759
$NiCr_2O_4$ (Spinel)	0.000	1.038	1.093
ZrO_2	0.000	0.845	0.889

Figure I.35. XRD Spectrum of CF 950 °C Heat-Treated Glass HAlG-19

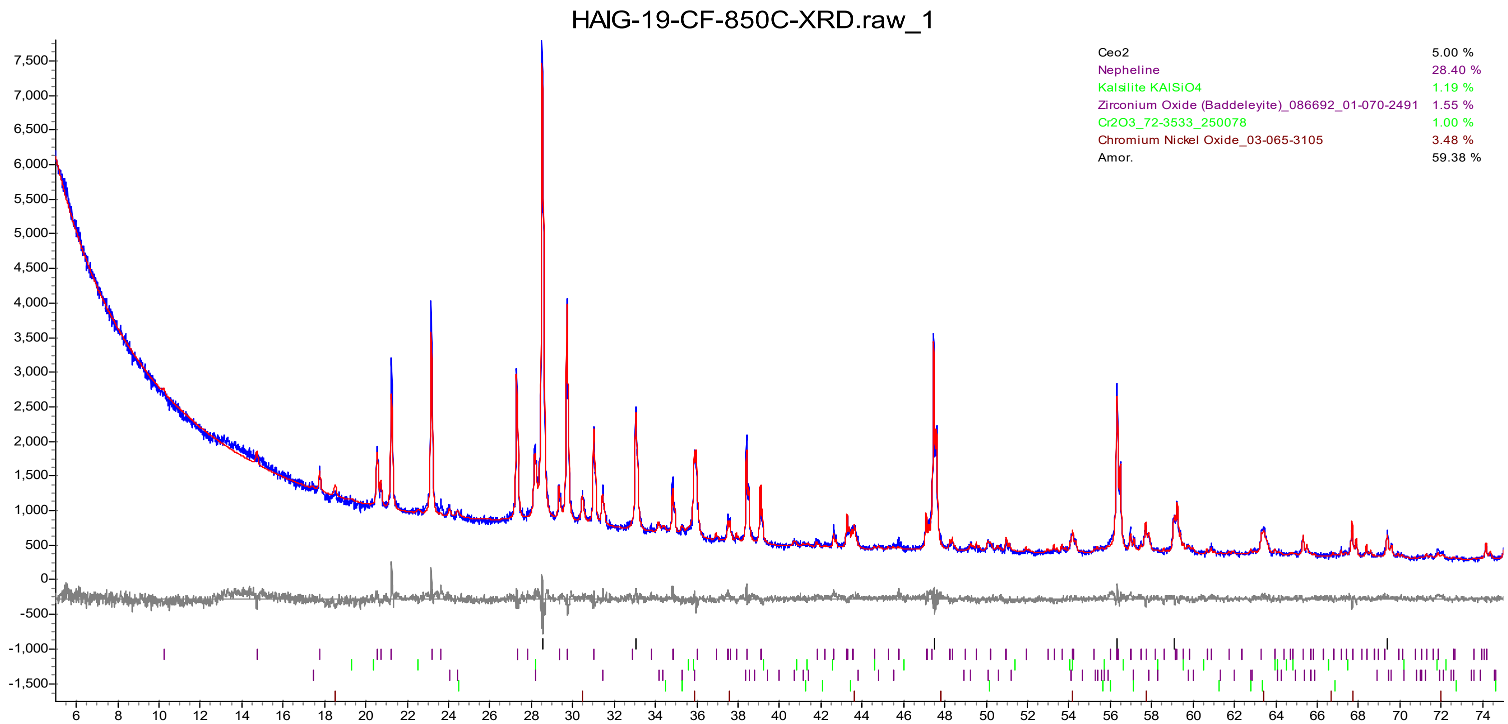

Phase Name	Wt% of Spiked	Wt% in Spiked Sample	Wt% in Original Sample
CeO_2	2.563	2.563	0.000
$KNaAlSiO_4$ (Nepheline)	0.000	16.123	16.971
$NiCr_2O_4$ (Spinel)	0.000	2.108	2.219
ZrO_2	0.000	1.037	1.092

Figure I.36. XRD Spectrum of CF 850 °C Heat-Treated Glass HAlG-19

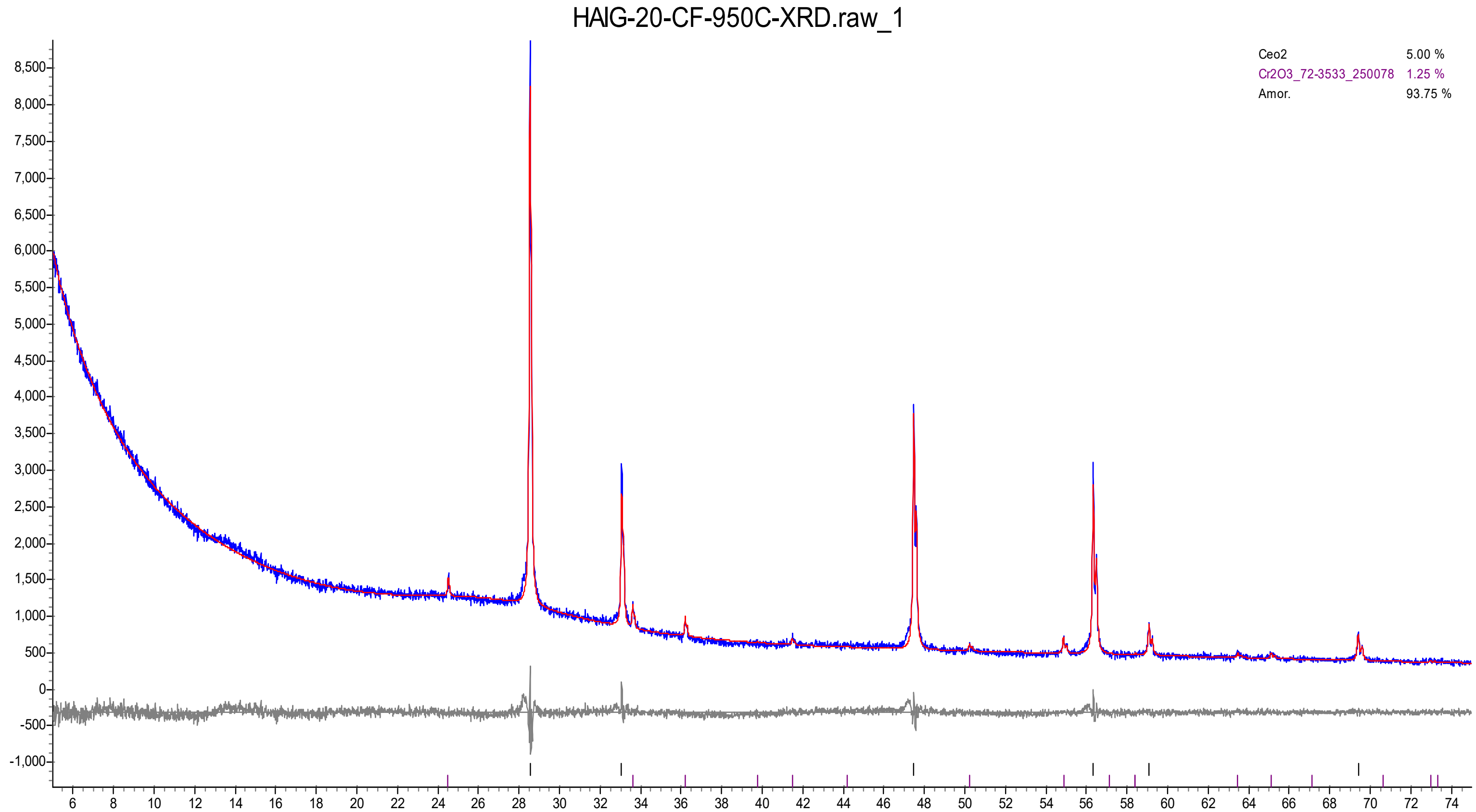

Phase Name	Wt% of Spiked	Wt% in Spiked Sample	Wt% in Original Sample
CeO_2	2.563	2.563	0.000
Cr_2O_3	0.000	0.793	0.835

Figure I.37. XRD Spectrum of CF 950 °C Heat-Treated Glass HAlG-20

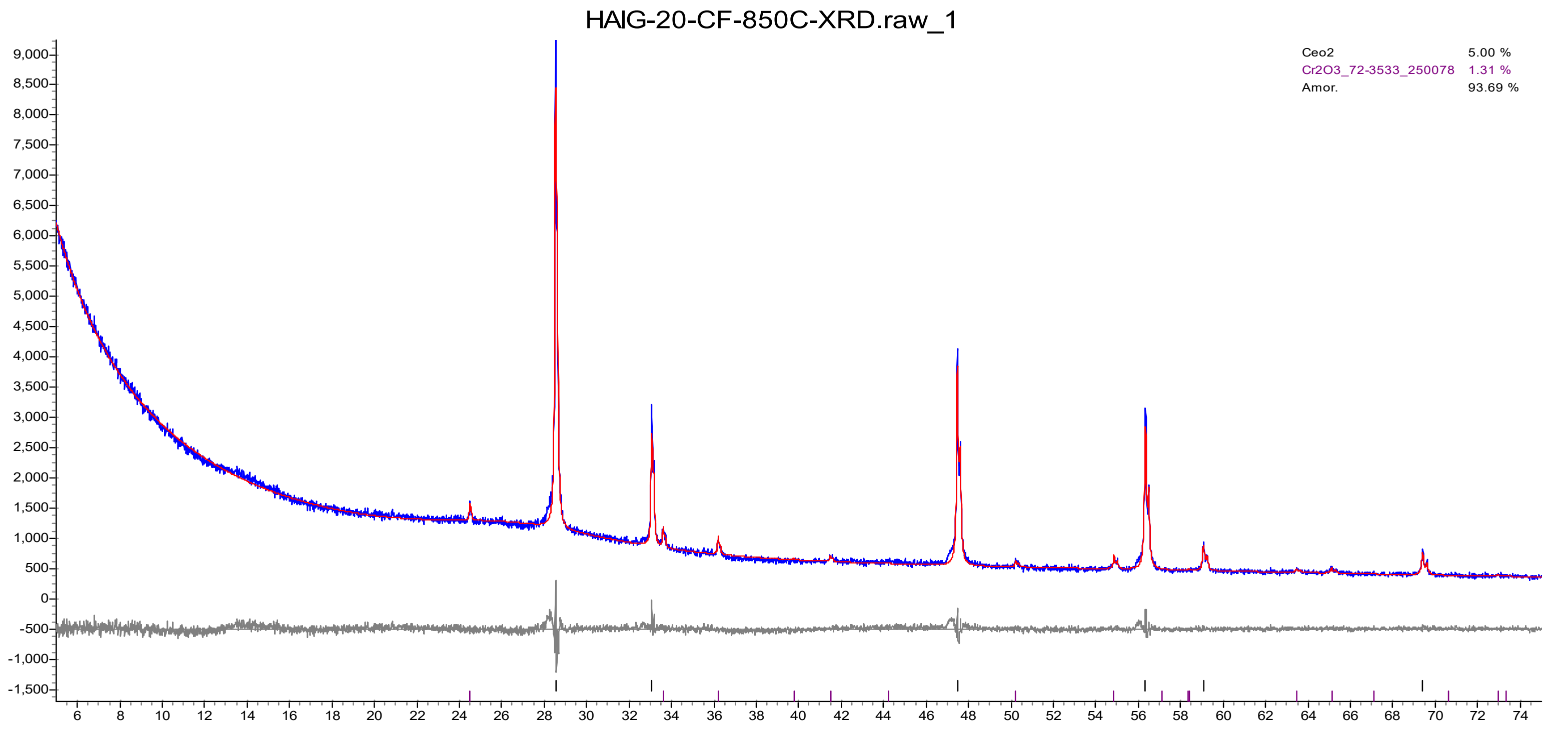

Phase Name	Wt% of Spiked	Wt% in Spiked Sample	Wt% in Original Sample
CeO_2	2.561	2.561	0.000
Cr_2O_3	0.000	0.825	0.868

Figure I.38. XRD Spectrum of CF 850 °C Heat-Treated Glass HAlG-20

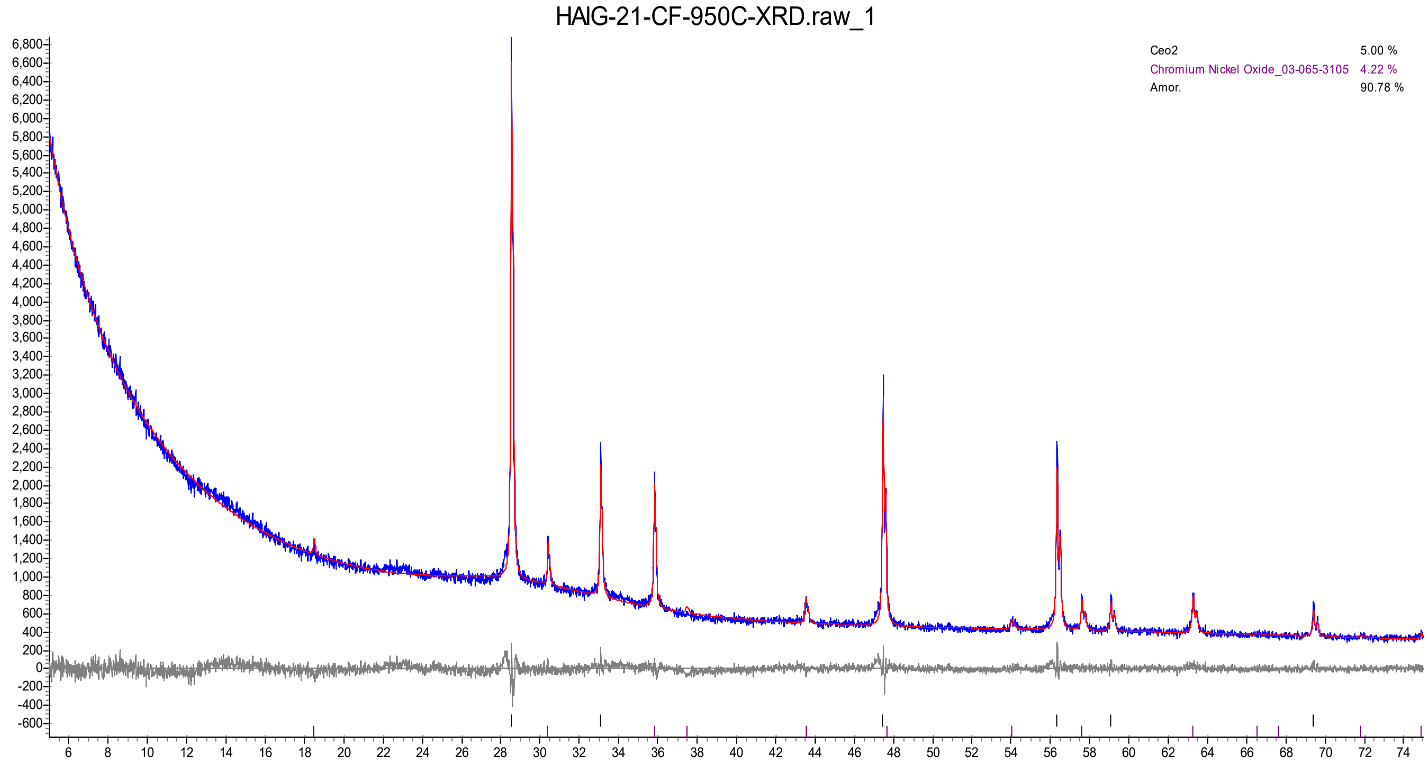

Phase Name	Wt% of Spiked	Wt% in Spiked Sample	Wt% in Original Sample
CeO_2	2.564	2.564	0.000
$NiCr_2O_4$ (Spinel)	0.000	2.300	2.421

Figure I.39. XRD Spectrum of CF 950 °C Heat-Treated Glass HAlG-21

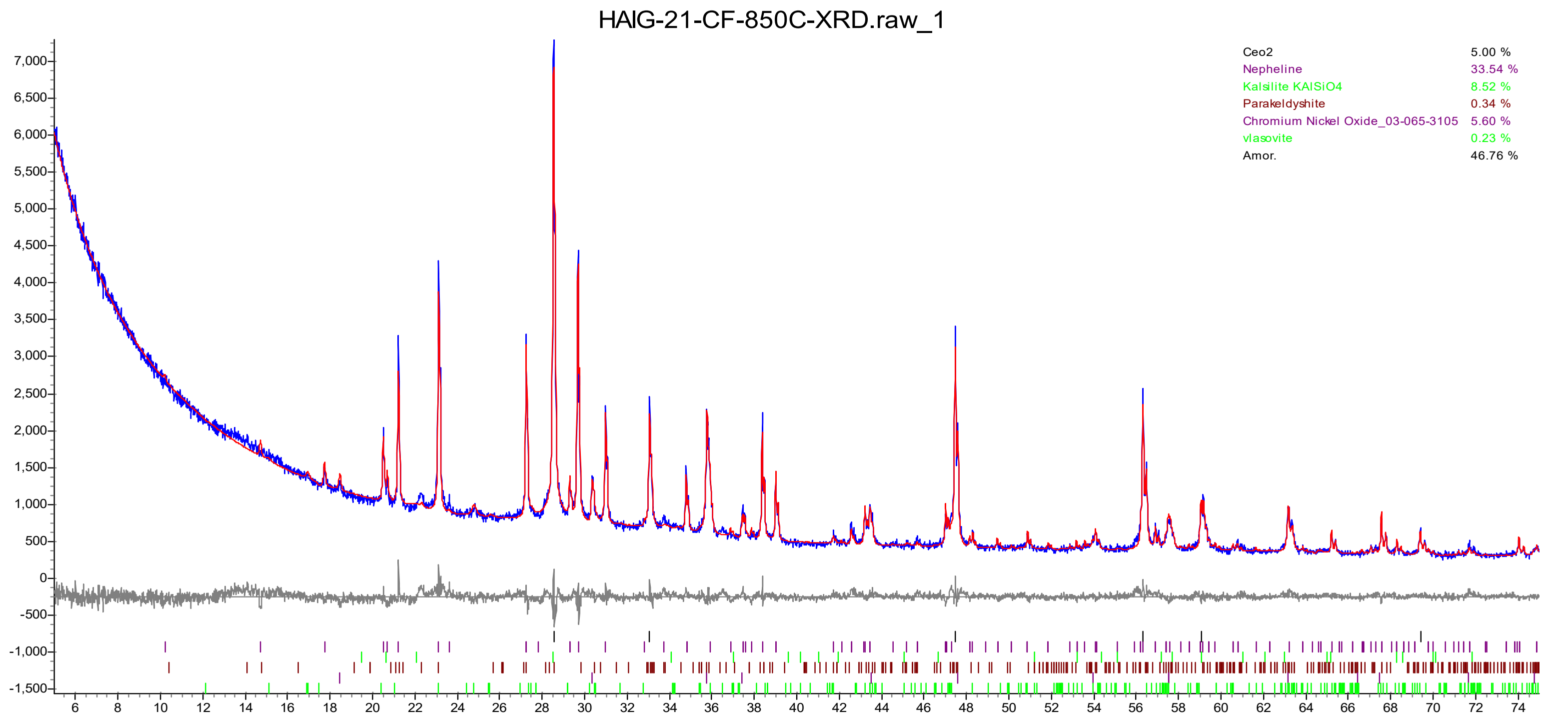

Phase Name	Wt% of Spiked	Wt% in Spiked Sample	Wt% in Original Sample
CeO_2	2.562	2.562	0.000
$KNaAlSiO_4$ (Nepheline)	0.000	18.267	19.228
$NiCr_2O_4$ (Spinel)	0.000	3.004	3.162
Na_2ZrSi_2O	0.000	0.286	0.301

Figure I.40. XRD Spectrum of CF 850 °C Heat-Treated Glass HAlG-21

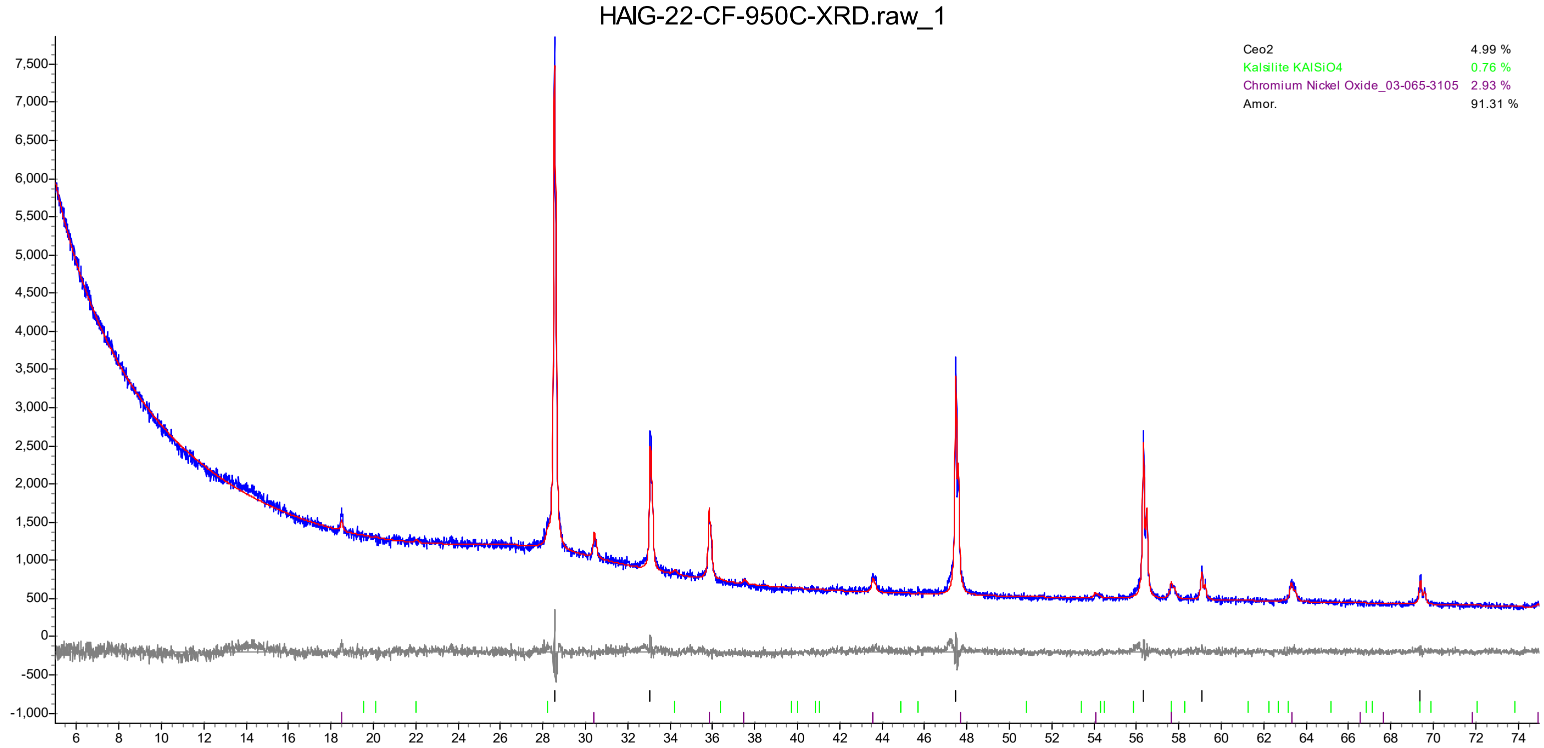

Phase Name	Wt% of Spiked	Wt% in Spiked Sample	Wt% in Original Sample
CeO_2	2.560	2.560	0.000
$NiCr_2O_4$ (Spinel)	0.000	1.707	1.797
$KAlSiO_4$	0.000	1.130	1.189

Figure I.41. XRD Spectrum of CF 950 °C Heat-Treated Glass HAlG-22

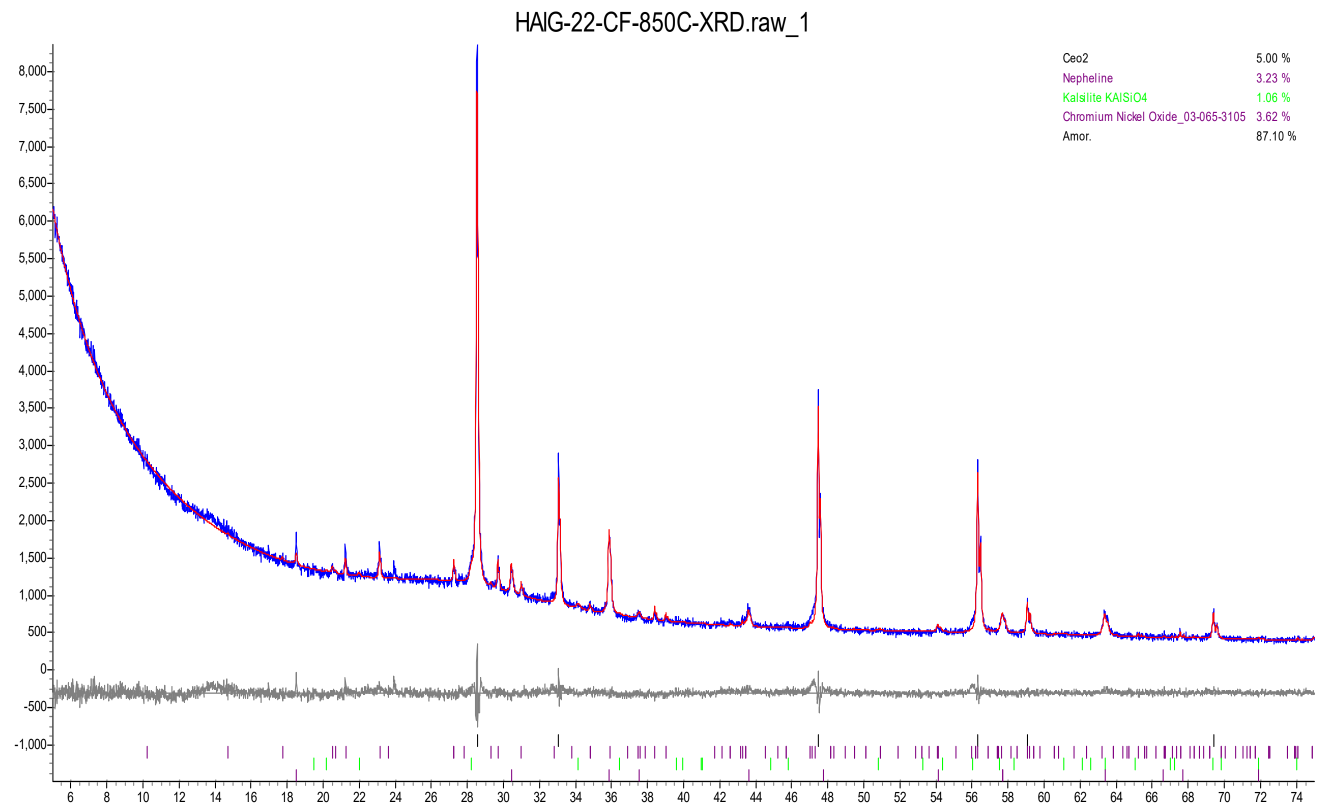

Phase Name	Wt% of Spiked	Wt% in Spiked Sample	Wt% in Original Sample
CeO_2	2.562	2.562	0.000
$NiCr_2O_4$ (Spinel)	0.000	2.086	2.196
$KAlSiO_4$	0.000	1.025	1.079
$KNaAlSiO_4$ (Nepheline)	0.000	1.926	2.027

Figure I.42. XRD Spectrum of CF 850 °C Heat-Treated Glass HAlG-22

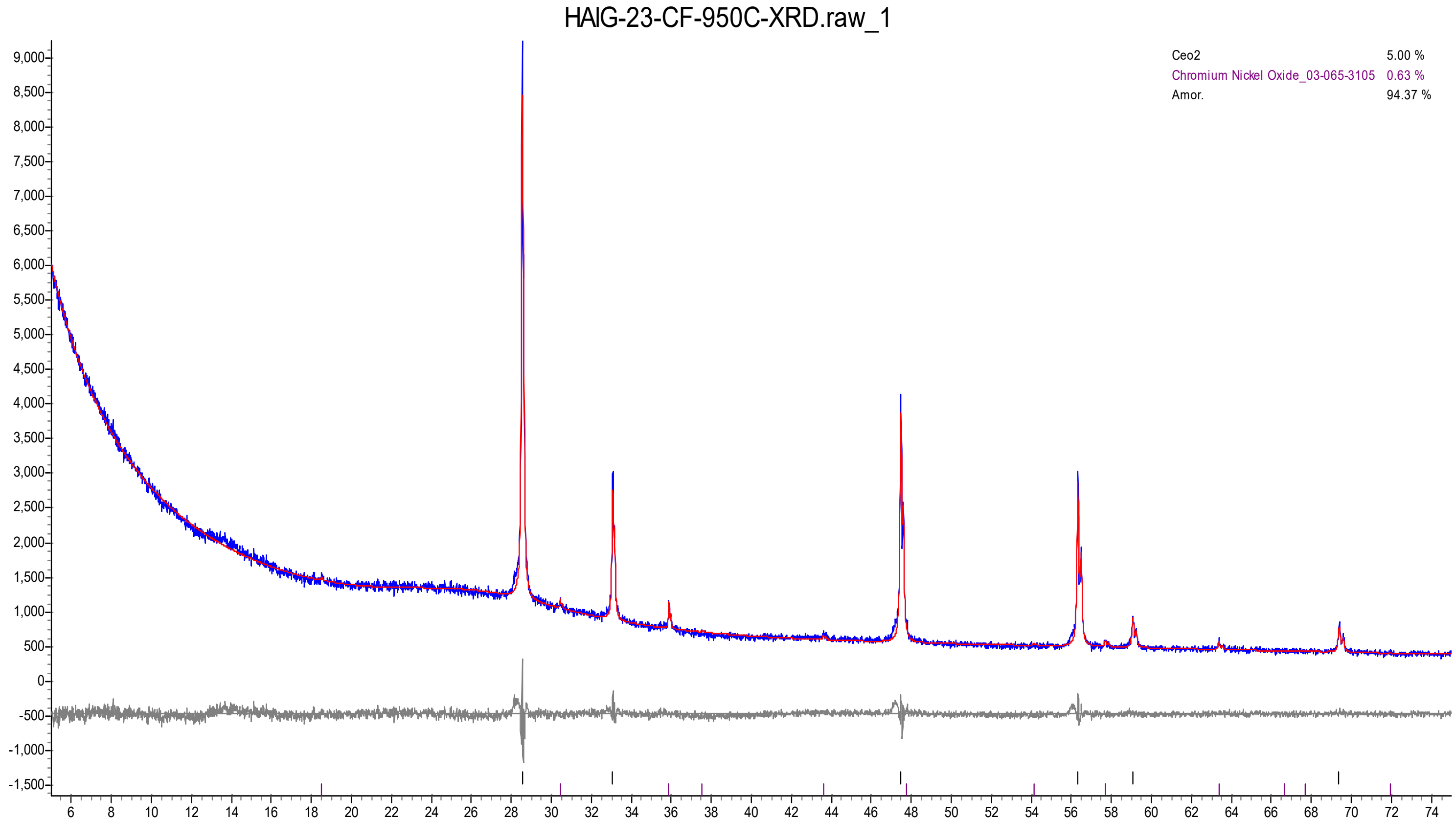

Phase Name	Wt% of Spiked	Wt% in Spiked Sample	Wt% in Original Sample
CeO_2	2.562	2.562	0.000
$NiCr_2O_4$ (Spinel)	0.000	0.378	0.398

Figure I.43. XRD Spectrum of CF 950 °C Heat-Treated Glass HAlG-23

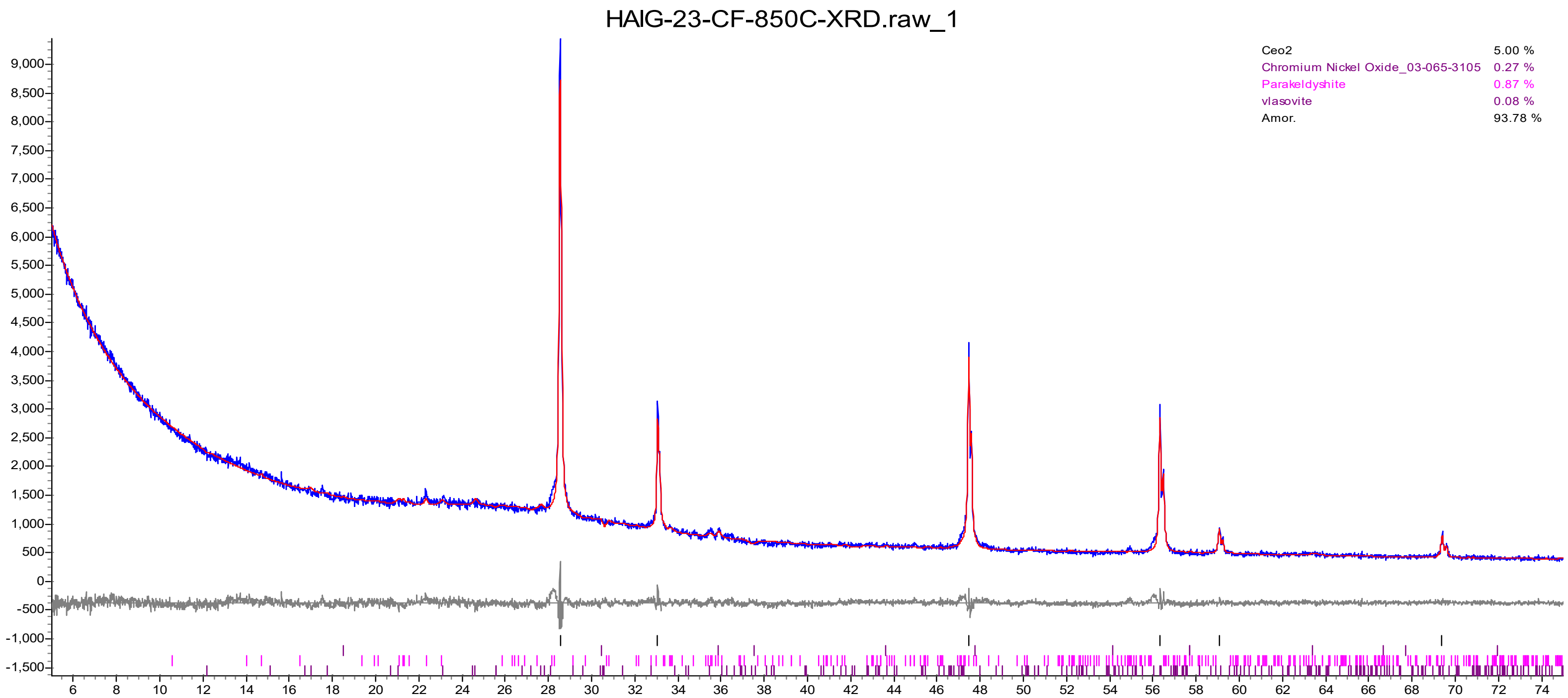

Phase Name	Wt% of Spiked	Wt% in Spiked Sample	Wt% in Original Sample
CeO_2	2.563	2.563	0.000
$NiCr_2O_4$ (Spinel)	0.000	0.595	0.626
Na_2ZrSi_2O	0.000	0.244	0.256

Figure I.44. XRD Spectrum of CF 850 °C Heat-Treated Glass HAlG-23

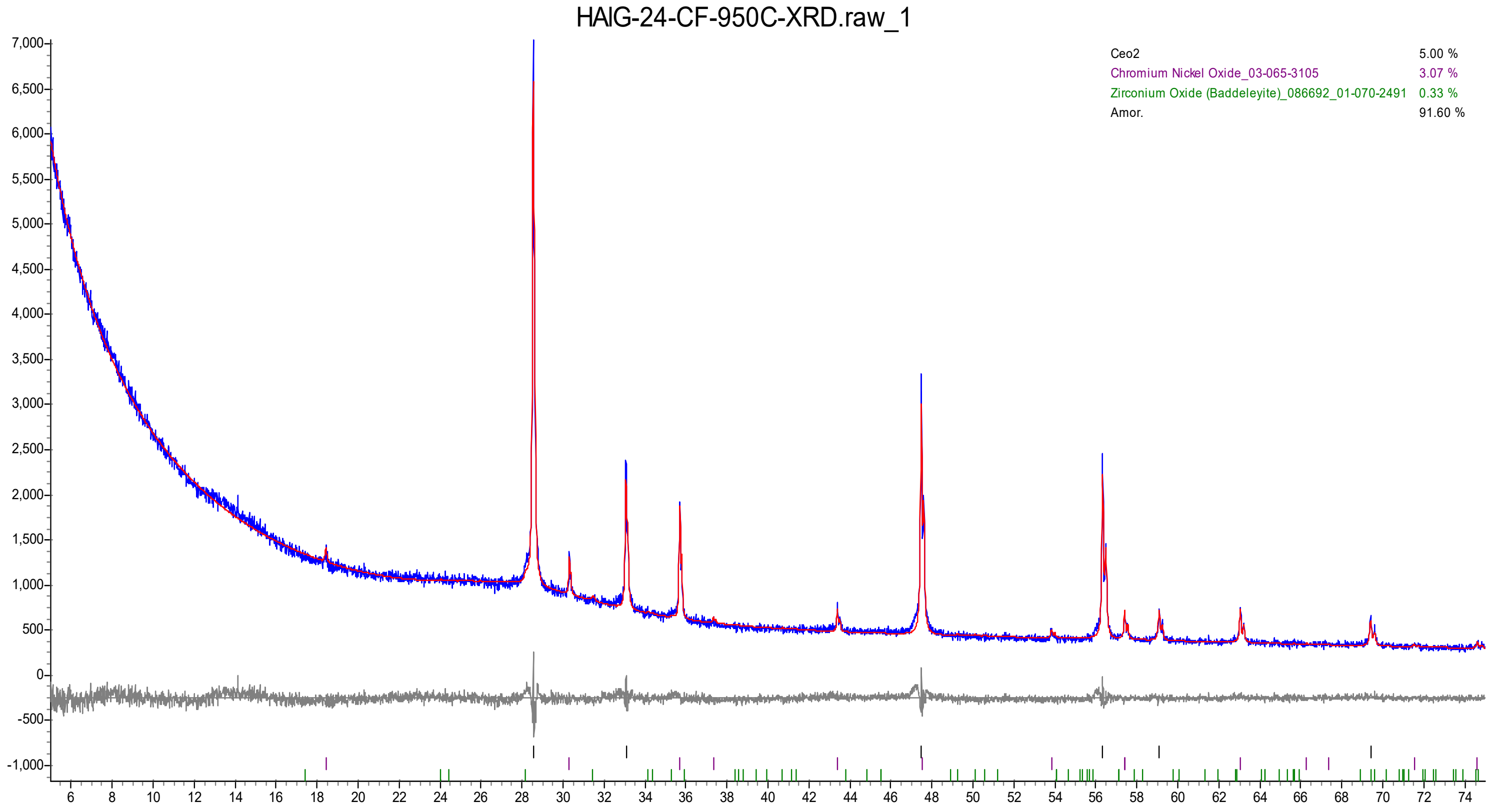

Phase Name	Wt% of Spiked	Wt% in Spiked Sample	Wt% in Original Sample
CeO_2	2.565	2.565	0.000
$NiCr_2O_4$ (Spinel)	0.000	1.712	1.802
ZrO_2	0.000	0.239	0.252

Figure I.45. XRD Spectrum of CF 950 °C Heat-Treated Glass HAlG-24

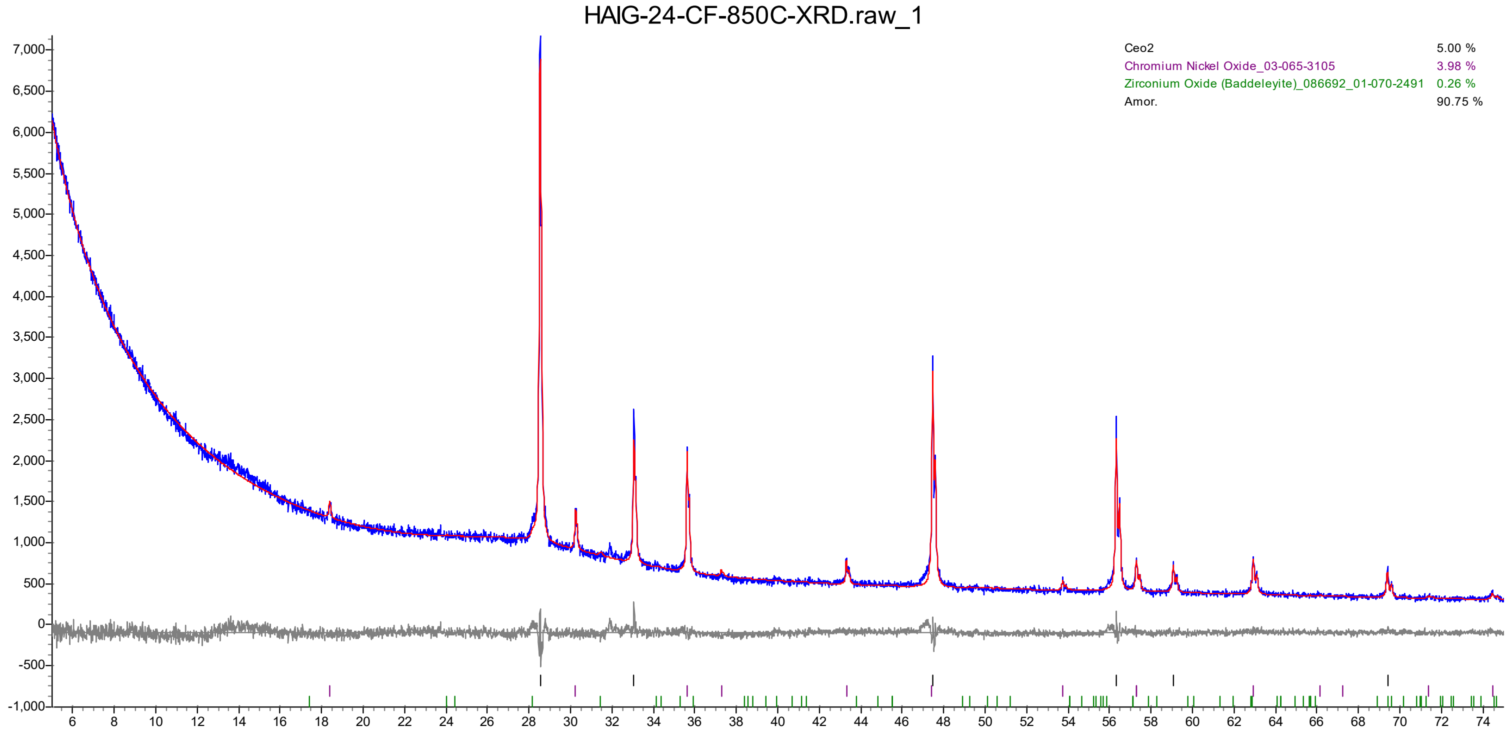

Phase Name	Wt% of Spiked	Wt% in Spiked Sample	Wt% in Original Sample
CeO_2	2.564	2.564	0.000
$NiCr_2O_4$ (Spinel)	0.000	2.224	2.342
ZrO_2	0.000	0.485	0.511

Figure I.46. XRD Spectrum of CF 850 °C Heat-Treated Glass HAlG-24

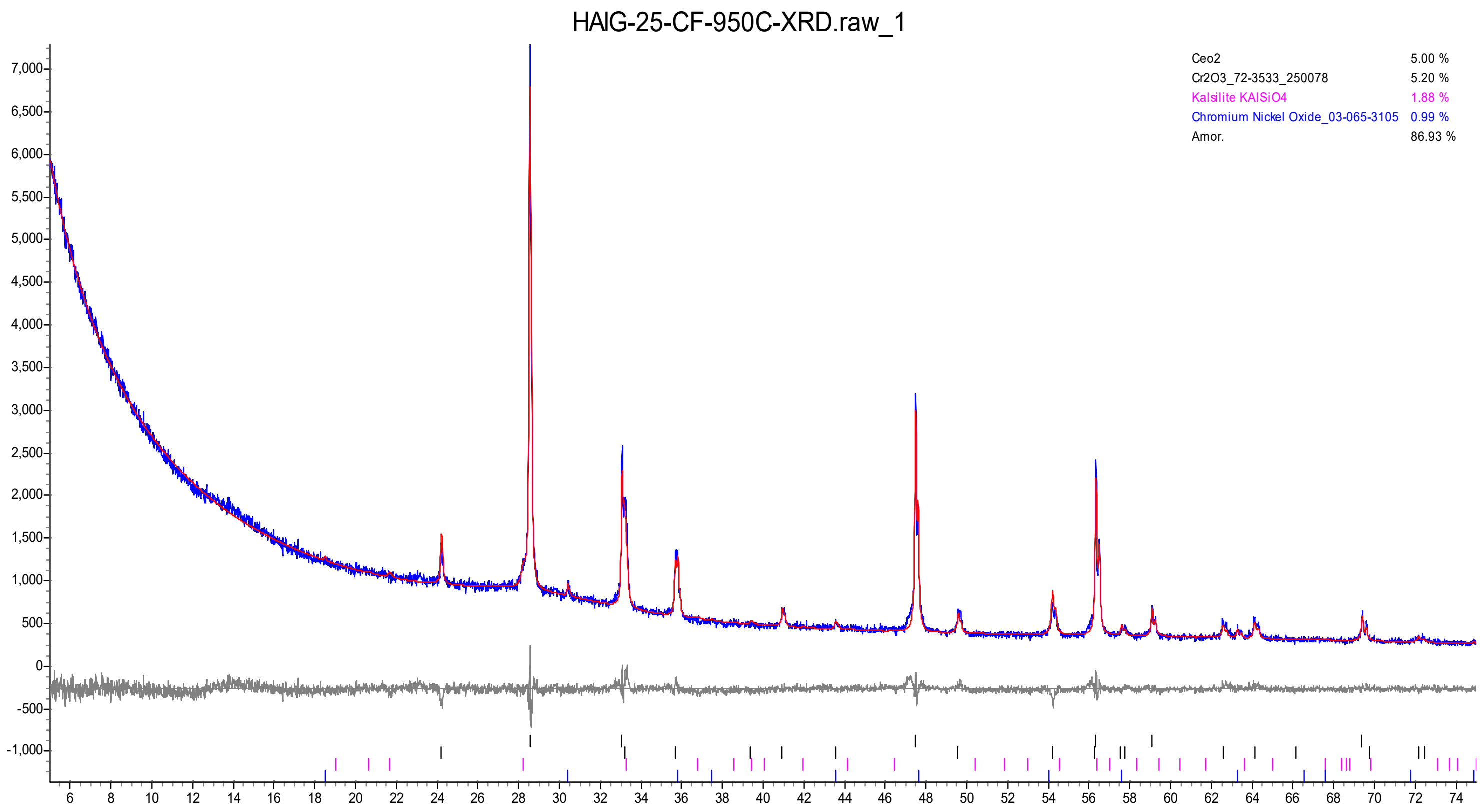

Phase Name	Wt% of Spiked	Wt% in Spiked Sample	Wt% in Original Sample
CeO_2	2.563	2.563	0.000
$NiCr_2O_4$ (Spinel)	0.000	0.480	0.505
Fe_2O_3	0.000	2.614	2.751

Figure I.47. XRD Spectrum of CF 950 °C Heat-Treated Glass HAlG-25

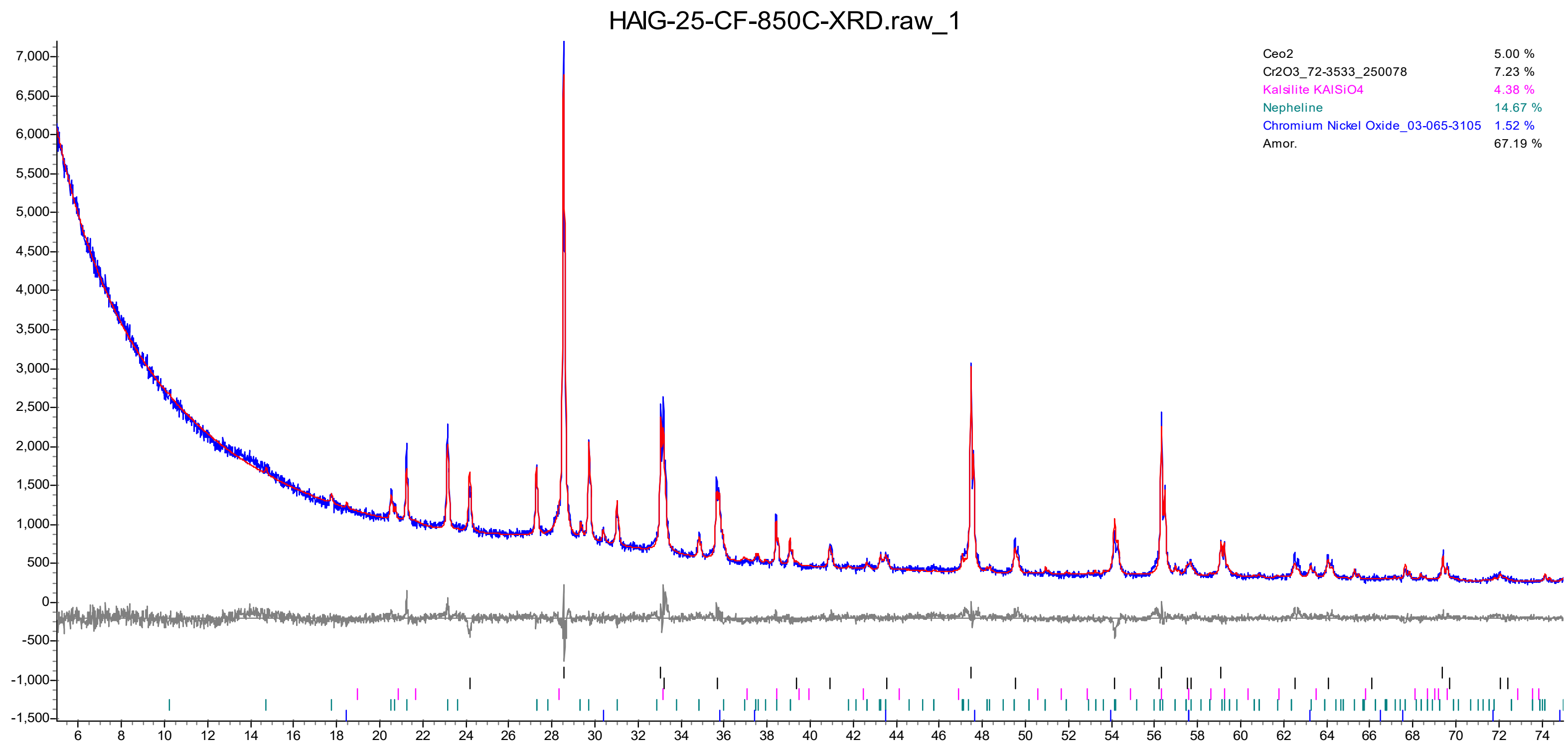

Phase Name	Wt% of Spiked	Wt% in Spiked Sample	Wt% in Original Sample
CeO_2	2.564	2.564	0.000
$KNaAlSiO_4$ (Nepheline)	0.000	8.458	8.904
$NiCr_2O_4$ (Spinel)	0.000	0.894	0.941
Fe_2O_3	0.000	3.335	3.511

Figure I.48. XRD Spectrum of CF 850 °C Heat-Treated Glass HAlG-25

Appendix J – Analyses for Baseline and Sulfur Saturated Glasses and Sulfur Wash Solutions

This appendix presents and compares the normalized compositional analyses of the baseline and sulfur-saturated glasses and wash solutions using inductively coupled plasma – optical emissions spectroscopy and ion chromatography. This shows how much sulfur was retained in the glass as well as what was lost from the glass.

Table J.1. Normalized Measured Compositions (mass fractions) for Baseline and Sulfur-Saturated Versions of the High-Aluminum Waste Glasses

	Glass ID											
	HAlG-01			HAlG-02			HAlG-03			HAlG-04		
Components	Measured Baseline	Sulfur-saturated	% Diff	Measured Baseline	Sulfur-saturated	% Diff	Measured Baseline	Sulfur-saturated	% Diff	Measured Baseline	Sulfur-saturated	% Diff
Al_2O_3	20.2	20.45	1.24	23.3	23.62	1.37	19.6	19.05	-2.81	20.3	20.03	-1.33
B_2O_3	9.18	9.32	1.55	19.2	19.16	-0.21	15.1	14.65	-2.98	9.97	9.59	-3.84
Bi_2O_3	0.679	0.723	6.51	0.137	0.134	-2.12	0.204	0.200	-1.91	0.606	0.599	-1.12
CaO	1.47	1.45	-1.50	0.317	0.290	-8.64	0.446	0.412	-7.69	1.21	1.21	-0.08
CdO	0.128	0.132	3.05	<0.0286	<0.0286	NA	0.038	0.038	-1.56	0.115	0.113	-1.65
Cr_2O_3	<0.365	<0.365	NA	1.12	1.13	1.07	0.174	0.135	-22.24	1.08	0.782	-27.56
F	0.737	0.554	-24.83	0.120	0.091	-23.92	0.184	0.128	-30.27	0.707	0.472	-33.24
Fe_2O_3	1.29	1.37	6.12	4.62	4.57	-1.13	5.41	5.48	1.35	6.75	6.86	1.61
K_2O	1.99	2.06	3.67	0.441	0.494	12.06	0.623	0.663	6.44	1.82	1.66	-8.85
Li_2O	0.545	0.435	-20.11	1.20	0.923	-23.13	0.857	0.654	-23.70	0.524	<0.278	NA
MgO	0.700	0.713	1.93	0.147	0.148	0.88	0.208	0.214	3.03	0.620	0.610	-1.65
MnO	0.0862	0.090	4.41	0.025	0.025	1.01	0.035	0.035	0.95	0.085	0.085	0.41
Na_2O	19.1	20.2	5.71	19.3	20.05	3.89	16.0	17.49	9.31	19.4	19.14	-1.34
NiO	1.08	1.12	3.43	0.213	0.218	2.16	0.324	0.320	-1.11	0.934	0.955	2.22
P_2O_5	3.87	3.61	-6.74	3.28	3.42	4.27	2.81	2.92	3.99	0.356	0.358	0.56
SiO_2	31.9	33.2	4.11	22.4	23.26	3.84	33.0	32.6	-1.21	33.1	33.69	1.78
SO_3	0.400	0.830	107.4	<0.125	0.965	NA	<0.129	0.813	NA	0.390	0.663	69.97
SrO	0.114	0.127	10.96	<0.0591	<0.0591	NA	<0.0591	<0.0591	NA	0.102	0.105	2.75
TiO_2	0.286	0.296	3.67	<0.0848	<0.0848	NA	0.105	0.104	-0.48	0.287	0.281	-2.06
ZnO	0.241	0.249	3.44	<0.0622	<0.0622	NA	0.073	0.072	-1.53	0.221	0.208	-5.79
ZrO_2	4.27	4.30	0.68	1.94	1.96	1.13	1.85	1.91	3.14	0.591	0.593	0.34
Total	98.3	101.3	3.05	98.1	100.7	2.65	97.2	97.98	0.80	99.2	98.28	-0.93

Table J.1 (cont)

	Glass ID											
	HAlG-05			HAlG-06			HAlG-07-1			HAlG-08		
Components	Measured Baseline	Sulfur-saturated	% Diff	Measured Baseline	Sulfur-saturated	% Diff	Measured Baseline	Sulfur-saturated	% Diff	Measured Baseline	Sulfur-saturated	% Diff
Al_2O_3	19.9	19.25	-3.27	27.3	26.5	-2.93	23.6	23.43	-0.72	23.9	23.34	-2.34
B_2O_3	20.5	19.87	-3.07	18.8	18.23	-3.03	11.0	10.9	-0.91	14.4	13.88	-3.61
Bi_2O_3	0.399	0.386	-3.33	0.178	0.176	-1.18	0.586	0.579	-1.13	<0.111	<0.111	NA
CaO	0.822	0.819	-0.38	0.402	0.363	-9.60	1.16	1.18	1.72	0.219	0.199	-9.13
CdO	0.078	0.078	0.13	0.033	0.032	-3.99	0.111	0.107	-3.51	<0.0286	<0.0286	NA
Cr_2O_3	0.635	0.573	-9.72	1.15	1.01	-11.91	0.079	0.044	-44.14	0.774	0.536	-30.75
F	0.397	0.274	-31.11	0.163	0.115	-29.45	0.567	0.441	-22.31	0.087	0.065	-25.68
Fe_2O_3	10.4	10.72	3.08	1.46	1.46	-0.34	8.84	9.21	4.23	10.4	10.63	2.21
K_2O	1.21	1.20	-0.66	0.560	0.631	12.66	1.74	1.54	-11.72	0.302	0.345	14.37
Li_2O	0.449	0.350	-22.09	0.346	<0.273	NA	<0.219	<0.215	NA	1.86	1.85	-0.70
MgO	0.414	0.417	0.75	0.187	0.187	0.21	0.599	0.600	0.15	0.109	0.104	-4.50
MnO	0.066	0.068	1.65	0.0241	0.0238	-1.29	0.087	0.088	1.63	0.030	0.030	0.13
Na_2O	14.8	17.12	15.68	19.6	20.59	5.05	19.7	20.73	5.23	17.7	19.34	9.27
NiO	0.630	0.627	-0.43	0.283	0.275	-2.86	0.865	0.886	2.46	0.210	0.147	-29.86
P_2O_5	0.831	0.754	-9.22	1.97	2.00	1.52	1.86	1.88	1.18	3.86	3.88	0.62
SiO_2	22.0	21.93	-0.32	25.1	25.3	0.80	25.0	25.62	2.48	25.9	24.6	-5.02
SO_3	0.240	0.800	233.17	<0.125	0.798	NA	0.378	0.612	61.83	<0.125	0.845	NA
SrO	0.067	0.070	4.80	<0.0591	<0.0591	NA	0.098	0.103	5.01	<0.0591	<0.0591	NA
TiO_2	0.201	0.204	1.24	0.125	0.123	-1.36	0.268	0.264	-1.34	0.088	0.085	-3.83
ZnO	0.142	0.141	-0.70	0.093	<0.063	NA	0.209	0.203	-2.92	<0.0622	<0.0622	NA
ZrO_2	2.87	2.93	2.02	0.228	0.228	-0.18	1.82	1.86	2.42	<0.135	<0.135	NA
Total	97.0	98.58	1.63	98.2	98.44	0.24	98.8	100.5	1.72	100.0	100.3	0.30

Table J.1 (cont)

	Glass ID											
	HAlG-09			HAlG-11			HAlG-12			HAlG-13		
Components	Measured Baseline	Sulfur-saturated	% Diff	Measured Baseline	Sulfur-saturated	% Diff	Measured Baseline	Sulfur-saturated	% Diff	Measured Baseline	Sulfur-saturated	% Diff
Al_2O_3	20.7	19.89	-3.91	24.2	25.51	5.41	21.1	21.4	1.42	20.4	19.98	-2.06
B_2O_3	21.2	20.04	-5.47	8.41	7.78	-7.54	15.6	15.91	1.99	7.87	7.78	-1.09
Bi_2O_3	0.152	0.133	-12.37	0.305	0.310	1.51	0.433	0.442	1.96	0.533	0.524	-1.65
CaO	0.375	0.307	-18.19	0.704	0.650	-7.68	0.891	0.902	1.25	1.09	1.11	2.20
CdO	<0.0286	<0.0286	NA	0.054	0.054	1.04	0.079	0.082	3.35	0.099	0.098	-1.13
Cr_2O_3	0.948	0.704	-25.73	1.77	0.38	-78.51	1.31	1.04	-20.23	0.338	0.082	-75.63
F	0.132	0.098	-26.00	0.288	0.196	-31.84	0.416	0.298	-28.25	0.580	0.459	-20.81
Fe_2O_3	4.74	4.68	-1.22	1.72	1.79	4.30	0.196	0.217	10.71	8.26	8.45	2.25
K_2O	0.469	0.487	3.84	0.916	0.840	-8.28	1.34	1.31	-2.09	1.55	1.33	-14.13
Li_2O	5.61	4.91	-12.41	4.44	4.38	-1.33	0.755	0.623	-17.44	4.88	4.49	-7.91
MgO	0.175	0.156	-10.97	0.321	0.332	3.46	0.471	0.463	-1.76	0.571	0.554	-2.99
MnO	0.027	0.026	-3.16	0.041	0.042	2.01	0.053	0.067	25.73	0.080	0.081	1.35
Na_2O	13.6	14.63	7.57	19.7	18.8	-4.57	19.3	19.92	3.21	15.9	16.92	6.42
NiO	0.240	0.226	-5.75	0.498	0.497	-0.16	0.661	0.701	6.07	0.899	0.852	-5.27
P_2O_5	1.33	1.19	-10.68	3.40	3.33	-2.12	1.11	1.02	-8.11	0.728	0.605	-16.91
SiO_2	23.3	22.94	-1.55	25.9	28.02	8.19	28.9	30.22	4.57	28.2	28.61	1.45
SO_3	<0.125	1.23	NA	0.165	0.564	242.0	0.26	0.760	192.4	0.319	0.963	201.9
SrO	<0.0591	<0.0591	NA	<0.0591	<0.0591	NA	0.075	0.077	3.16	0.092	0.097	6.02
TiO_2	0.124	0.106	-14.35	0.173	0.174	0.75	0.224	0.229	2.19	0.262	0.266	1.37
ZnO	<0.0695	<0.0622	NA	0.120	0.110	-8.50	0.149	0.153	2.55	0.191	0.191	0.21
ZrO_2	5.34	5.31	-0.58	4.93	5.51	11.66	5.70	5.88	3.14	5.29	5.29	0.04
Total	98.7	97.21	-1.51	98.1	99.33	1.25	99.1	101.7	2.62	98.2	98.75	0.56

Table J.1 (cont)

	Glass ID											
	HAlG-14			HAlG-15			HAlG-16			HAlG-17		
Components	Measured Baseline	Sulfur-saturated	% Diff	Measured Baseline	Sulfur-saturated	% Diff	Measured Baseline	Sulfur-saturated	% Diff	Measured Baseline	Sulfur-saturated	% Diff
Al_2O_3	22.4	22.77	1.65	22.1	22.58	2.17	21.4	21.21	-0.89	20.4	20.69	1.42
B_2O_3	16.1	16.29	1.18	8.47	8.48	0.07	9.77	9.84	0.69	12.8	12.72	-0.63
Bi_2O_3	<0.111	<0.111	NA	0.294	0.280	-4.63	0.203	0.217	6.95	0.288	0.293	1.70
CaO	0.183	0.186	1.48	0.629	0.586	-6.85	0.456	0.451	-1.12	0.620	0.605	-2.50
CdO	<0.0286	<0.0286	NA	0.054	0.052	-4.51	0.033	0.038	14.05	0.054	0.055	1.69
Cr_2O_3	1.86	0.922	-50.46	1.85	1.39	-24.70	1.59	1.08	-32.08	0.122	0.089	-27.01
F	0.082	0.062	-23.84	0.315	0.217	-31.02	0.199	0.156	-21.86	0.302	0.216	-28.48
Fe_2O_3	9.46	9.99	5.64	1.26	1.26	0.00	4.11	4.21	2.36	0.748	0.763	2.01
K_2O	0.252	0.350	38.85	0.90	0892	-0.89	0.665	0.730	9.77	0.916	0.973	6.19
Li_2O	5.50	5.03	-8.60	6.01	5.63	-6.32	2.42	2.38	-1.57	2.74	2.41	-12.19
MgO	0.088	0.098	11.84	0.302	0.299	-1.16	0.231	0.234	1.39	0.320	0.316	-1.28
MnO	0.027	0.028	4.48	0.037	0.037	-1.10	0.031	0.034	8.85	0.038	0.040	5.03
Na_2O	17.5	19.18	9.60	14.6	15.37	5.27	18.9	19.18	1.48	17.5	18.7	6.86
NiO	0.204	0.134	-34.36	0.464	0.0449	-3.13	0.308	0.338	9.81	0.462	0.468	1.36
P_2O_5	0.769	0.674	-12.39	<0.290	0.253	NA	2.16	1.91	-11.71	0.977	0.957	-2.08
SiO_2	22.2	23.26	4.77	40.3	42.04	4.32	30.6	31.39	2.58	36.7	37.76	2.89
SO_3	<0.125	0.978	NA	0.174	0.933	436.0	<0.125	0.712	NA	0.211	0.886	319.8
SrO	<0.0591	<0.0591	NA	<0.0591	<0.0591	NA	<0.0591	<0.0591	NA	<0.0591	<0.0591	NA
TiO_2	<0.0834	<0.0834	NA	0.166	0.160	-3.61	0.129	0.139	7.44	0.171	0.168	-1.58
ZnO	<0.0622	<0.0622	NA	0.109	0.101	-7.71	0.075	0.076	1.45	0.104	0.103	-1.06
ZrO_2	0.635	0.597	-5.92	1.04	1.08	3.56	4.64	4.89	5.39	3.96	4.12	4.12
Total	97.8	100.9	3.17	99.4	102.1	2.72	98.1	99.27	1.19	99.4	102.4	3.02

Table J.1 (cont)

	Glass ID											
	HAlG-18			HAlG-19			HAlG-20			HAlG-21		
Components	Measured Baseline	Sulfur-saturated	% Diff	Measured Baseline	Sulfur-saturated	% Diff	Measured Baseline	Sulfur-saturated	% Diff	Measured Baseline	Sulfur-saturated	% Diff
Al_2O_3	28.5	26.12	-8.35	27.4	26.59	-2.96	21.2	20.03	-5.52	21.9	21.87	-0.14
B_2O_3	10.9	8.62	-20.91	7.92	7.49	-5.38	19.4	18.76	-3.30	11.4	10.31	-9.56
Bi_2O_3	0.346	0.332	-4.08	0.131	0.121	-7.86	0.210	0.197	-6.19	0.430	0.443	2.93
CaO	0.725	0.687	-5.19	0.283	0.275	-2.86	0.456	0.417	-8.55	0.873	0.902	3.38
CdO	0.064	0.061	-4.66	0.0238	<0.0286	NA	0.040	0.038	-2.91	0.083	0.084	1.61
Cr_2O_3	0.700	0.260	-62.89	0.797	0.292	-63.41	1.36	1.11	-18.38	0.427	0.268	-37.28
F	0.353	0.224	-36.54	0.129	0.102	-21.09	0.204	0.146	-28.43	0.462	0.319	-30.84
Fe_2O_3	0.499	0.484	-3.09	5.97	6.04	1.12	0.711	0.725	1.90	7.74	8.11	4.78
K_2O	1.06	0.775	-26.87	0.394	0.358	-9.19	0.664	0.615	-7.35	1.33	1.19	-10.60
Li_2O	5.66	5.02	-11.27	5.6	5.16	-7.82	3.41	3.12	-8.62	4.71	4.18	-11.32
MgO	0.358	0.345	-3.66	0.139	0.141	1.73	0.218	0.217	-0.37	0.438	0.461	5.34
MnO	0.043	0.042	-3.16	0.027	0.027	0.26	0.027	0.026	-3.75	0.065	0.070	6.47
Na_2O	17.8	16.58	-6.85	19.7	19.51	-0.96	14.3	15.67	9.58	15.3	16.41	7.25
NiO	0.548	0.526	-3.98	0.204	0.202	-1.13	0.400	0.328	-18.08	0.690	0.708	2.62
P_2O_5	3.28	3.45	5.30	1.56	1.39	-11.22	3.91	3.96	1.23	3.47	3.92	13.08
SiO_2	23.1	22.57	-2.29	26.3	26.15	-0.57	29.3	29.09	-0.72	25.2	25.62	1.67
SO_3	0.234	0.913	290.0	<0.125	0.874	NA	<0.129	1.159	NA	0.295	0.934	216.8
SrO	<0.0591	0.060	NA	0.023	<0.0591	NA	<0.0591	<0.0591	NA	0.072	0.078	8.39
TiO_2	0.173	0.159	-8.32	0.106	0.107	0.47	0.095	0.093	-2.10	0.193	0.197	1.97
ZnO	0.122	0.118	-3.61	<0.0622	<0.0622	NA	0.0824	0.0714	-13.36	0.155	0.157	1.61
ZrO_2	3.02	3.06	1.42	2.55	2.61	2.24	2.82	2.89	2.62	1.00	1.12	11.70
Total	97.5	90.4	-7.26	99.5	97.59	-1.92	98.9	98.72	-0.18	96.2	97.35	1.20

Table J.1 (cont)

	Glass ID											
	HAlG-22			HAlG-23			HAlG-24			HAlG-25		
Components	Measured Baseline	Sulfur-saturated	% Diff	Measured Baseline	Sulfur-saturated	% Diff	Measured Baseline	Sulfur-saturated	% Diff	Measured Baseline	Sulfur-saturated	% Diff
Al_2O_3	20.2	20.03	-0.84	20.6	20.5	-0.49	21.5	20.64	-4.00	24.1	23.19	-3.78
B_2O_3	8.96	8.84	-1.35	16.9	16.98	0.47	15.1	14.43	-4.44	14.3	13.99	-2.17
Bi_2O_3	0.640	0.651	1.64	0.380	0.374	-1.50	0.981	0.962	-1.90	<0.111	<0.111	NA
CaO	1.48	1.29	-12.50	0.793	0.762	-3.88	3.47	3.45	-0.69	0.215	0.200	-6.93
CdO	0.121	0.123	1.24	0.071	0.070	-1.35	0.089	0.090	2.12	<0.0286	<0.0286	NA
Cr_2O_3	1.74	1.31	-24.94	0.822	0.711	-13.45	0.701	0.654	-6.75	0.616	0.543	-11.92
F	0.722	0.512	-29.11	0.415	0.277	-33.25	0.253	0.180	-28.85	0.086	0.062	-27.53
Fe_2O_3	1.11	1.16	4.23	0.204	0.212	3.73	5.29	5.49	3.78	10.5	10.32	-1.71
K_2O	1.98	1.76	-11.01	1.23	1.24	0.73	0.683	0.761	11.42	0.308	0.436	41.69
Li_2O	4.40	3.92	-10.82	5.52	5.37	-2.79	3.11	2.53	-18.65	1.88	1.79	-4.95
MgO	0.683	0.663	-2.88	0.404	0.386	-4.36	0.498	0.509	2.15	0.102	0.104	1.76
MnO	0.081	0.081	0.14	0.048	0.047	-1.54	0.931	0.965	3.71	0.031	0.031	-1.29
Na_2O	13.3	14.39	8.20	11.3	12.79	13.19	11.5	13.47	17.13	17.7	18.57	4.92
NiO	1.01	1.02	1.49	0.592	0.595	0.54	0.368	0.380	3.32	0.144	0.148	2.71
P_2O_5	2.19	2.38	8.54	2.99	3.07	2.68	0.718	0.871	21.27	3.86	3.87	0.31
SiO_2	37.3	37.65	0.94	33.5	34.76	3.76	31.5	31.23	-0.86	24.8	24.87	0.28
SO_3	0.406	0.991	144.0	0.255	1.28	403.9	0.275	1.09	294.9	<0.125	0.853	NA
SrO	0.108	0.109	0.83	0.065	0.066	1.78	0.099	0.096	-2.67	<0.0591	<0.0591	NA
TiO_2	0.286	0.287	0.31	0.173	0.164	-5.03	<0.0834	<0.0834	NA	0.085	<0.0854	NA
ZnO	0.228	0.222	-2.81	0.136	0.130	-4.12	<0.0622	<0.0622	NA	<0.0622	<0.0622	NA
ZrO_2	2.04	2.06	0.98	1.90	2.03	6.63	0.945	0.930	-1.54	<0.135	<0.135	NA
Total	99.0	99.45	0.45	98.2	101.8	3.67	98.2	98.88	0.69	99.2	99.46	0.26

Table J.2. Measured Compositions for the High-Aluminum Glass Wash Solutions (mg/L)

Component	HAlG-01	HAlG-02	HAlG-03	HAlG-04	HAlG-05	HAlG-06	HAlG-07	HAlG-08	HAlG-09	HAlG-11
Al	2.76	9.26	2.77	1.98	1.54	11.0	5.22	2.40	9.70	32.4
B	14.6	25.4	9.68	19.1	20.4	26.1	15.1	13.3	27.2	161
Ca	1.07	<1.04	3.04	8.40	5.76	1.29	2.96	<1.00	<1.00	<1.00
Cr	3.97	53.9	10.5	94.9	12.8	38.9	11.2	26.8	61.4	416
Fe	<1.00	<1.00	<1.00	<1.00	<1.00	<1.00	<1.00	<1.00	<1.00	<1.00
K	104	15.1	14.4	111	39.2	17.2	102	9.23	16.9	85.5
Li	4.20	11.1	7.77	5.83	5.20	4.19	2.24	15.5	61.6	69.1
Mn	<1.00	<1.00	<1.00	<1.00	<1.00	<1.00	<1.00	<1.00	<1.00	<1.00
Na	1130	821	627	1080	546	728	1050	636	553	1610
P	65.9	14.7	11.4	5.53	<1.00	9.88	16.0	12.2	12.2	28.9
S	674	502	427	684	372	457	710	437	411	691
Si	2.65	1.98	1.92	2.21	<1.00	2.31	1.95	<1.00	2.77	4.33
Zn	<1.00	<1.00	<1.00	<1.00	<1.00	<1.00	<1.00	<1.00	<1.00	<1.00
Zr	<1.00	<1.00	<1.00	<1.00	<1.00	<1.00	<1.00	<1.00	<1.00	<1.00
F	26.9	<5.00	<5.00	25.8	<5.00	<5.00	17.4	<5.00	<5.00	34.0
PO_4	<10.0	40.7	29.9	15.3	<10.0	25.7	42.7	32.4	32.4	89.6
SO_4	2080	1520	1250	2130	1170	1410	2100	1290	1270	2050

Table J.2 (cont.)

Component	HAlG-12	HAlG-13	HAlG-14	HAlG-15	HAlG-16	HAlG-17	HAlG-18	HAlG-19	HAlG-20	HAlG-21
Al	3.02	4.00	14.9	2.73	4.40	3.11	12.5	12.4	4.70	14.2
B	18.7	8.57	38.8	14.6	11.5	18.9	217	11.3	13.9	76.0
Ca	4.50	1.87	<1.00	2.43	2.38	2.83	<1.00	<1.00	3.91	6.92
Cr	123	53.4	224	140	178	12.6	129	165	26.2	51.7
Fe	<1.00	<1.00	<1.00	<1.00	<1.00	<1.00	<1.00	<1.35	<1.00	<1.00
K	60.7	109	17.6	51.4	31.8	36.7	95.8	28.5	16.1	74.4
Li	7.68	37.5	60.9	69.9	17.6	28.7	72.7	36.3	39.7	42.2
Mn	<1.00	<1.00	<1.00	<1.00	<1.00	<1.00	<1.00	<1.00	<1.00	<1.00
Na	1040	911	917	810	1060	751	1350	1050	554	947
P	10.9	13.0	16.0	5.06	22.5	13.2	6.17	31.9	21.2	4.96
S	626	641	544	597	626	521	578	618	444	622
Si	1.36	2.58	3.30	3.87	3.13	3.15	1.61	5.14	2.71	2.18
Zn	<1.00	<1.00	<1.00	<1.00	<1.00	<1.00	<1.00	<1.00	<1.00	<1.00
Zr	<1.00	<1.00	<1.00	<1.00	<1.00	<1.00	<1.00	<1.00	<1.00	<1.00
F	11.3	28.4	<5.00	13.8	7.81	9.07	35.6	7.40	<5.00	23.9
PO_4	28.4	32.5	42.1	12.0	64.8	35.6	14.7	103	60.2	12.9
SO_4	1890	1920	1680	1780	1890	1670	1820	1860	1280	1850

Table J.2 (cont.)

Component	HAlG-22	HAlG-23	HAlG-24	HAlG-25
Al	1.38	3.02	<1.09	5.00
B	8.20	12.4	7.56	12.0
Ca	14.3	4.09	32.8	<1.00
Cr	92.1	30.2	18.7	27.7
Fe	<1.00	<1.00	<1.00	<1.01
K	87.9	29.2	25.3	9.43
Li	49.4	56.1	40.0	16.8
Mn	<1.00	<1.00	<1.00	<1.00
Na	754	382	481	660
P	5.78	15.7	1.42	13.0
S	566	356	444	436
Si	1.69	2.66	1.16	2.06
Zn	<1.00	<1.00	<1.00	<1.00
Zr	<1.00	<1.00	<1.00	<1.00
F	31.2	8.58	<5.00	<5.00
PO_4	15.3	43.7	<10.0	33.5
SO_4	1800	1040	1320	1340

PNNL-38071, Rev 0
EWG-RPT-045, Rev 0

Pacific Northwest National Laboratory

902 Battelle Boulevard
P.O. Box 999
Richland, WA 99354
1-888-375-PNNL (7665)

www.pnnl.gov